

University of Montana

ScholarWorks at University of Montana

Graduate Student Theses, Dissertations, &
Professional Papers

Graduate School

2006

Synthesis of novel 6-nitroquipazine analogs for imaging the serotonin transporter by positron emission tomography

David B. Bolstad
The University of Montana

Follow this and additional works at: <https://scholarworks.umt.edu/etd>

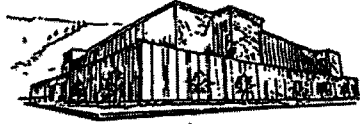
Let us know how access to this document benefits you.

Recommended Citation

Bolstad, David B., "Synthesis of novel 6-nitroquipazine analogs for imaging the serotonin transporter by positron emission tomography" (2006). *Graduate Student Theses, Dissertations, & Professional Papers*. 9590.

<https://scholarworks.umt.edu/etd/9590>

This Dissertation is brought to you for free and open access by the Graduate School at ScholarWorks at University of Montana. It has been accepted for inclusion in Graduate Student Theses, Dissertations, & Professional Papers by an authorized administrator of ScholarWorks at University of Montana. For more information, please contact scholarworks@mso.umt.edu.



**Maureen and Mike
MANSFIELD LIBRARY**

The University of
Montana

Permission is granted by the author to reproduce this material in its entirety, provided that this material is used for scholarly purposes and is properly cited in published works and reports.

****Please check "Yes" or "No" and provide signature****

Yes, I grant permission

 X

No, I do not grant permission

Author's Signature:

 David O. Bahrt

Date:

 07/06/06

Any copying for commercial purposes or financial gain may be undertaken only with the author's explicit consent.

SYNTHESIS OF NOVEL 6-NITROQUIPAZINE ANALOGS FOR IMAGING THE
SEROTONIN TRANSPORTER BY POSITRON EMISSION TOMOGRAPHY

by

David B. Bolstad

B.S. Chemistry, Central Washington University, 2001

B.A. Biology, Central Washington University, 2001

Presented in partial fulfillment of the requirements

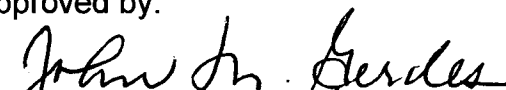
for the degree of


Doctor of Philosophy

The University of Montana

July 2006

Approved by:


Chairperson


Dean, Graduate School

7-6-06
Date

UMI Number: 3228603

Copyright 2006 by
Bolstad, David B.

All rights reserved.

INFORMATION TO USERS

The quality of this reproduction is dependent upon the quality of the copy submitted. Broken or indistinct print, colored or poor quality illustrations and photographs, print bleed-through, substandard margins, and improper alignment can adversely affect reproduction.

In the unlikely event that the author did not send a complete manuscript and there are missing pages, these will be noted. Also, if unauthorized copyright material had to be removed, a note will indicate the deletion.

UMI[®]


UMI Microform 3228603

Copyright 2006 by ProQuest Information and Learning Company.

All rights reserved. This microform edition is protected against unauthorized copying under Title 17, United States Code.

ProQuest Information and Learning Company
300 North Zeeb Road
P.O. Box 1346
Ann Arbor, MI 48106-1346

Synthesis of Novel 6-Nitroquipazine Analogs for Imaging the Serotonin Transporter by Positron Emission Tomography

Chairperson: John M. Gerdes 

A positron emission tomography (PET) imaging agent that can effectively quantify the serotonin transporter (SERT) in brain regions with moderate to low densities of SERT has yet to be identified. The recent literature has suggested that the need for such an agent may be filled by a selective, high affinity SERT ligand that displays extended *in vivo* kinetic profiles, concurrent with a reduction of *in vivo* nonspecific binding. Recently, our group has identified 2'-alkyl-6-nitroquipazine analogs as novel SERT ligands displaying very high affinity for SERT (picomolar concentration range). We have utilized the 6-nitroquipazine molecular construct for the development of new SERT PET imaging agents, by generating a series of racemic 2'-alkyl-6-nitroquipazine analogs that can incorporate the carbon-11 or the longer-lived fluorine-18 radionuclides. We expect that the increased SERT affinity of our new ligands will afford more efficacious SERT PET agents that can effectively quantify low density SERT regions in living brain.

A large focus of the present study was to expand our initial racemic lead agents by synthesizing each of them in enantiomerically pure form. Our synthetic strategy utilized an efficient asymmetric synthesis of the piperazine head-group from amino acid starting materials. The syntheses afforded non-radiolabelled target ligands and the appropriate radioligand precursors in good yields. Preliminary pharmacological data suggests a marked difference in binding affinity between the enantiomers of our agents. Furthermore, using racemic amino acids and the same asymmetric synthetic strategy, we were also able to generate novel 2'-aryl-6-nitroquipazine analogs that were not synthetically accessible using our derived methods for the 2'-alkyl agents.

The racemic radiotracer [^{18}F]2'-(3-fluoropropoxymethyl)-6-nitroquipazine agent was synthesized and evaluated in rat for initial radiotracer distribution. The studies in rat have demonstrated favorable accumulation of the tracer in the brain indicating efficient passage through the blood brain barrier. Furthermore, these studies indicate the greatest concentration of radiotracer in regions of the brain with known SERT density. The studies of the initial, racemic tracer have shown that [^{18}F]2'-(3-fluoropropoxymethyl)-6-nitroquipazine demonstrates potential as a new SERT PET imaging agent.

ACKNOWLEDGEMENTS

I am eternally grateful to Dr. John Gerdes for the enlightening introduction to organic synthesis he provided me as an undergraduate researcher. This experience was the seminal influence that led me to pursue organic chemistry and profoundly altered my current life's direction. My abilities as a scientist and researcher have developed as a result of his expert guidance and attention to detail. For the many years you've served as a mentor and a friend, I give my most gracious thanks.

To all of the current and former members of the Gerdes research group I give thanks for all of their support and friendship over the years. Of course, Brian Kusche probably deserves his name on this work too and the last six years have shown just what a fantastic lab partner and tremendous friend he has been. I couldn't have completed this journey without him.

The fantastic scientists of the Lawrence Berkeley National Lab also deserve praise for their contributions toward the completion of this work. Without the radiochemical abilities of Dr. Jim O'Neil, my dissertation would only tell a partial story. We are indebted to Dr. O'Neil for the current and future successes of this project. To Dr. Andy Gibbs I say thanks for the assistance with certain experiments, but mostly for being a great friend.

I must also recognize the members of my committee who have provided advice and support over the past few years. Dr's Ed Waali, Don Kiely, Sean Esslinger and Michael Kavanaugh have my gratitude for their participation in my

graduate education and their continued kindness throughout my time at the University of Montana.

I must also thank my family who has provided constant encouragement throughout my seemingly endless years of education. My accomplishments are a result of their continuous support and I am forever grateful for their love and motivation. To all of my friends in Montana and Washington, I thank you for the countless hours of fun and excitement that have helped me to maintain my sanity and made the last few years of my life the most rewarding yet. It has been an exciting ride and one that I hope continues.

Most importantly, I must give thanks to my wife, Erin S. Davis Bolstad, whose unwavering love, support and encouragement has maintained my inspiration and allowed me to succeed in life and in my education. Without her love, I would not have accomplished all that I have and I would not be the person that I have become. Thank you for being my best friend.

TABLE OF CONTENTS

LIST OF FIGURES.....	VI
LIST OF TABLES.....	X
LIST OF SCHEMES.....	XI
LIST OF ABBREVIATIONS.....	XIII
1. INTRODUCTION, BACKGROUND AND PURPOSE	1
1.1 Serotonin Biology.....	1
1.2 The Serotonin Transporter.....	4
1.3 The Serotonin Transporter and Disease	6
1.4 Positron Emission Tomography Imaging	9
1.5 Imaging of the Serotonin Transporter with SPECT and PET.....	13
1.6 6-Nitroquipazine Analogs: Previous Work from Our Lab and Others.....	16
1.7 Focus of the Investigation.....	23
2. SYNTHESIS OF RACEMIC TARGETS	25
2.1 Introduction.....	25
2.2 Generation of N-Boc-2'-Hydroxymethyl-6-Nitroquipazine.....	27
2.3 Synthesis of (rac)-MeProF and a Tosylate Precursor for the Radiosynthesis of [¹⁸ F](rac)-MeProF.....	36
2.4 Synthesis of 2'-(2-Methoxyethyl)-6-nitroquipazine: EtOMe-NQP.....	42
2.5 Gilman Quinoline Coupling Mechanistic Considerations	47
2.6 The Boron Tribromide Dealkylation: Reaction Complications and Inconsistencies.....	51
2.7 Radiochemical synthesis of [¹¹ C]MOM-NQP and [¹⁸ F]MeProF-NQP	53
3. ASYMMETRIC SYNTHESSES	57
3.1 Introduction.....	57
3.2 Synthesis of the Enantiomers of MOM-NQP	64
3.3 Synthesis of the Enantiomers of MeProF-NQP	75
3.4 The Synthesis of Enantiomeric Radiolabelling Precursors	82
4. OTHER ASYMMETRIC-LIKE SYNTHESSES.....	87
4.1 Introduction for the 2'-Aryl-6-Nitroquipazines	87
4.2 Synthesis of 2'-Aryl-6-nitroquipazines.....	94
4.3 The Alternate Assymmetric-Like synthesis of 2'-EtOMe-NQP.....	110
5. BIOLOGICAL DATA	115
5.1 Serotonin Transporter Binding Affinity of Target Ligands	115
5.2 Preliminary in vivo Evaluation of Racemic PET Agent [¹⁸ F]MeProF-NQP ..	122
6. CONCLUSIONS AND FUTURE WORK.....	128
7. EXPERIMENTAL.....	132
7.1 General Methods.....	132
7.2 Experimentals.....	134
APPENDIX:.....	208
LITERATURE CITED	216

LIST OF FIGURES

Figure 1.1: The biosynthesis of serotonin.	1
Figure 1.2: A general representation of a serotonergic synapse.	2
Figure 1.3: A collection of known SERT ligands; the tricyclic antidepressants (4 and 5) and the modern selective serotonin reuptake inhibitors (SSRI's, 6 – 9).....	9
Figure 1.4: Sample PET images (bottom) from a study in baboon, displaying the accumulation of SERT tracer [¹¹ C]AFM 14 in the midbrain and thalamus. The corresponding MRI image of the brain is displayed above the PET images. (Image from ref. 51).	10
Figure 1.5: First generation SPECT imaging agent for SERT.	13
Figure 1.6: Next generation PET imaging agents for SERT.	14
Figure 1.7: SERT imaging agents derived from 6-nitroquipazine.	15
Figure 1.8: 6-Nitroquipazine and a description of ring numbering in the quipazine series.	16
Figure 1.9: Investigational compounds from our initial SAR study. ⁶⁴	17
Figure 1.10: Training set ligands utilized in the generation of our SERT pharmacophore.	18
Figure 1.11: Our derived SERT pharmacophore model, illustrated as a superposition overlay of select conformations of training set ligands. (Image from ref. 66).	19
Figure 1.12: Walker's synthesis of 2'-methoxymethyl-6-nitroquipazine (MOM-NQP). ⁶⁷ ..	20
Figure 1.13: Example ligands from the SAR studies performed by Chi et al. The K _i values are determined with rat brain homogenate ² and [³ H]citalopram.....	22
Figure 2.1: Attempted route toward the generation of 2'-fluoromethyl-6-nitroquipazine..	25
Figure 2.2: Summary of the route used by Kusche ⁷⁴ to obtain ProF-NQP. For 49, the protecting group (PG) was N-formyl or N- <i>tert</i> -butoxycarbonyl (N-Boc).....	26
Figure 2.3: Synthetic strategy devised for the synthesis of [¹¹ C]MOM-NQP.	28
Figure 2.4: Failed, previously attempted route for acquiring an alcohol intermediate.	28
Figure 2.5: TMS-I promoted dealkylation reaction attempted by Walker. ⁶⁷	29
Figure 2.6: ¹ H NMR spectra of N-Boc protected alcohol 58 (top) and amino alcohol 55 (bottom) demonstrating the line broadening observed as a result of the introduction of the N-Boc protecting group. The scale is in δ ppm.....	34

Figure 2.7: ^{13}C NMR spectra of N-Boc protected alcohol 58 (top) and amino alcohol 55 (bottom) demonstrating the line broadening observed as a result of the introduction of the N-Boc protecting group. The scale is in δ ppm.....	35
Figure 2.8: a) [^{18}F]ProF-NQP; b) Alkylation strategy to afford fluoroalkyl ethers.....	37
Figure 2.9: Attempted Boc deprotection conditions for the formation of fluoromethyl target 59.	37
Figure 2.10: ^1H NMR of MeProF-NQP 61, with the fluorine-coupled hydrogen resonances indicated. The scale is in δ ppm.	40
Figure 2.11: Methyl, ethyl and propyl side chain quipazines to study the Ar2 region SAR.	42
Figure 2.12: The elimination-addition Gilman coupling mechanism proposed by Walker, ⁶⁷ demonstrated with a general N-trityl protected piperazine.....	48
Figure 2.13: Alternate mechanistic explanation for the extra 50 mol% of lithium amide.	49
Figure 2.14: Proposed dipolar character of 2,3-pyridynes as an explanation for Gilman coupling regioselectivity for substitution at the 2-position of quinoline.....	50
Figure 2.15: Nucleophilic aromatic substitution ($\text{S}_{\text{N}}\text{Ar}$) mechanism for the Gilman coupling reaction.	51
Figure 3.1: Examples of enantiomers that elicit different biological responses.....	57
Figure 3.2: Hypothetical ligand-receptor model to demonstrate a plausible enantiomeric discrimination of a ligand. The general receptor binding site consists of amine, aromatic and side chain binding regions (panel a). When (<i>R</i>)-MOM-NQP binds to the receptor (panel b), ligand contact with each receptor binding region is made. When (<i>S</i>)-MOM-NQP binds (panels c and d), ligand contact with each binding region cannot be made since the side chain is positioned far from the binding region (panel c) or extends well below that region (panel d).	59
Figure 3.3: Synthesis of (<i>R</i>)-2'-methyl-6-nitroquipazine. The (<i>S</i>)-isomer is similarly prepared.	60
Figure 3.4: Failed resolution strategy attempted by Kusche to isolate stereochemically pure piperazine intermediates.....	61
Figure 3.5: Key intermediate alcohol described by Naylor as a precursor for the enantiomers of MOM-NQP and MeProF-NQP.	62
Figure 3.6: The mechanism of ACE-Cl dealkylation.....	71
Figure 3.7: Intermediate benzyl alcohol (<i>S</i>)-122 to generate both asymmetric targets... ..	78

Figure 3.8: Intermediate N-benzyl alcohol (<i>S</i>)-122 as a plausible precursor for all assymmetric targets.	83
Figure 3.9: Reaction of (<i>S</i>)-MeProF with Mosher's reagent. The trifluoromethyl group can be analyzed by ¹⁹ F NMR to quantify enantiomeric excess.	86
Figure 4.1: Our 2'-aryl target ligands: 2'-phenyl- and 2'-benzyl-6-nitroquipazine.	87
Figure 4.2: Compound structures from the study of Plenge, 1985, 1991. ^{123,124}	88
Figure 4.3: Compound structures from the study of Plenge, 1997. ¹²⁵	89
Figure 4.4: Compound structures from the study of Chang, 1999. ¹²⁶	90
Figure 4.5: Compound structures from the study of Weller, 2002. ¹²⁷	91
Figure 4.6: Compound structures from the study of Griffin, 1999. ¹²⁹	91
Figure 4.7: Two pharmaceutical agents with reduced incidence of sexual dysfunction side effects.	92
Figure 4.8: Refined lead agent MOM-NQP, and new dual aromatic ring ligands Phen- NQP and Ben-NQP.	94
Figure 4.9: Various strategies for piperazine synthesis and our design for obtaining a phenyl piperazine.	95
Figure 4.10: Lee's reported thermal coupling to form 6-nitroquipazine.	101
Figure 4.11: Reduction in amine nucleophilicity as a result of inductive effects from the formyl protecting group.	107
Figure 4.12: The peptide cyclization step showing the opportunities for two isomeric products.	112
Figure 5.1: Sample binding curve from a radioligand displacement binding assay. No error bars are indicated. The dotted lines demonstrate an estimation of the IC50 value.	117
Figure 5.2: New ligands from this study that remain to be tested for activity at SERT. The 2'-aryl agents also need to be evaluated for affinity modulation properties. ...	121
Figure 5.3: Whole body rat tracer distribution data with [¹⁸ F]MeProF. Data is reported as an average of three measurements. The brain study (boxed) was expanded to include brain sub-regions (Figure 5.4)	124
Figure 5.4: Rat tracer distribution data for discrete brain regions. Data is reported as an average of three measurements.	125
Figure 6.1: New SERT PET agent [¹⁸ F](<i>rac</i>)-MeProF-NQP and current standard ligands DASB 15 and [¹¹ C]AFM 16.	128

Figure 6.2: Intermediate N-benzyl alcohol (S)-122 as a precursor for all asymmetric targets.	129
Figure 6.3: Summary new SERT agents synthesized using the methodology of Naylor, with different amino acid starting materials. Although not indicated, the compounds from Kusche, 2006 were synthesized in non-racemic form.	130
Figure 6.4: New SERT ligands from this study and their determined SERT binding affinity.	131

LIST OF TABLES

Table 1.1: A table of known serotonin receptors, their functional class, location in the vertebrate/invertebrate body and associated functions.	4
Table 1.2: Relative SERT densities in discrete brain regions.....	7
Table 1.3: Preliminary SAR data from the Gerdes laboratory.	21
Table 4.1: Summary of the thermal coupling experiments. For the amine substrate, Ar denotes the side chain aromatic functionality and PG denotes the nitrogen protecting group used for that entry. Mol% indicates amount of amine substrate relative to quinoline 159 (100 mol%). For trityl and formyl protecting groups, standard acidic deprotection conditions were used as described earlier in Chapters 2 and 3.	103
Table 5.1: Comprehensive SERT binding affinity data for all racemic compounds from our lab that have been tested. The entries above the dotted line were also shown in Table 1.3.....	118
Table 5.2: SERT binding data for the non-racemic ligands.	120

LIST OF SCHEMES

Scheme 2.1: Boron tribromide mediated demethylation of MOM-NQP.	30
Scheme 2.2: Formation of N-trityl protected alcohol.	31
Scheme 2.3: 'Cold' radiochemical synthesis of MOM-NQP from the N-trityl protected alcohol.	31
Scheme 2.4: Synthesis of key intermediate 58, HOM-BOC-NQP.	33
Scheme 2.5: 'Cold' radiosynthesis of MOM-NQP using the N-Boc protected alcohol.	36
Scheme 2.6: Synthesis of racemic MeProF-NQP.	39
Scheme 2.7: Attempted 'short-cut' alkylations to obtain intermediates in the synthesis of MeProF-NQP.	41
Scheme 2.8: Control reactions to evaluate the ability of methoxide ion to evoke S _N 2 substitution on our 'short-cut' electrophiles.	41
Scheme 2.9: Synthesis of EtOMe-NQP that was modeled after Walker's ⁶⁷ synthesis of MOM-NQP 35 (Figure 1.12).	43
Scheme 2.10: Synthesis of N-Boc protected ethyl alcohol.	46
Scheme 2.11: Another coupling, facilitated by the Gilman conditions, that is unable to proceed under benzyne-type conditions.	50
Scheme 2.12: Radiochemical synthesis of [¹¹ C](rac)-MOM-NQP.	54
Scheme 2.13: Radiochemical synthesis of [¹⁸ F](rac)-MeProF-NQP.	55
Scheme 3.1: Our synthesis of key amino alcohol (S)-94 using D-serine. Naylor's reported yields are in parentheses. ¹¹¹	64
Scheme 3.2: Synthesis of N-Boc-N-Benzyl glycine.	65
Scheme 3.3: Attempted O-methylation sequence using N-Boc as the protecting group.	66
Scheme 3.4: Failed attempt to selectively introduce a methyl group to the alcohol.	67
Scheme 3.5: Successful alkylation strategy using N-formamide as a protecting group.	68
Scheme 3.6: Formation of N-Bn-MOM-quipazine with the Gilman coupling.	69
Scheme 3.7: Debenzylation reaction giving side product formation from ring-reduction.	70
Scheme 3.8: Refinement of the ACE-Cl mediated debenzylation reaction.	73
Scheme 3.9: The complete synthesis of (S)-MOM-NQP; the (R)- stereoisomer was similarly prepared.	75
Scheme 3.10: Facile production of benzyl protected quipazine alcohol (S)-122 using the OTHP group for alcohol protection.	77

Scheme 3.11: Synthesis of the fluoropropyl side chain from the key alcohol intermediate (S)-122 using two distinct fluorination strategies.	78
Scheme 3.12: The complete synthesis of (S)-MeProF-NQP; the (R)- stereoisomer was similarly prepared.	81
Scheme 3.13: Synthesis of enantiomeric radiolabelling precursors (boxed). Only the (S)-intermediates are shown.	82
Scheme 3.14: Synthesis of Boc alcohol radiochemical precursor (R)-58 from the key intermediate N-benzyl alcohol (R)-122.	84
Scheme 3.15: Attempted debenylation of the nitrobenzyl intermediate.	84
Scheme 4.1: Initial synthesis of 2'-phenylquipiazine.	96
Scheme 4.2: Nitration attempt with 100 mol% of nitric acid forming a complex product mixture.	97
Scheme 4.3: Synthesis of 2-chloro-6-nitroquinoline.	98
Scheme 4.4: Gilman coupling attempts with 2-chloro-6-nitroquinoline.	98
Scheme 4.5: Synthesis of the N-benzyl aryl piperazines using the 'assymetric' methodology described in Chapter 3.	100
Scheme 4.6: Synthesis of N-formyl protected aryl piperazines.	100
Scheme 4.7: Synthesis of N-benzyl protected benzyl piperazine.	101
Scheme 4.8: Isolation of 3'-phenyl-6-nitroquipazine.	104
Scheme 4.9: Complete, optimized synthesis of the 2'-aryl-6-nitroquipazine targets. The thermal coupling step was optimized as detailed in Table 4.1.	110
Scheme 4.10: Synthesis of the racemic aspartyl dipeptide.	111
Scheme 4.11: Complete synthesis of 2'-methoxyethyl-6-nitroquipazine using dimethyl aspartate amenable for asymmetric preparations.	113

LIST OF ABBREVIATIONS

¹³ C NMR	carbon nuclear magnetic resonance spectrum
¹ H NMR	proton nuclear magnetic resonance spectrum
2-Cl-q	2-chloroquinoline
5-HT	5-hydroxytryptamine/serotonin
6-NQP	6-nitroquipazine
9-BBN	9-borabicyclo[3.3.1]nonane
Ac ₂ O	acetic anhydride
ACE-Cl	1-chloroethyl chloroformate
ACN	acetonitrile/CH ₃ CN
AFM	2-[2-(dimethylaminomethyl)phenylthio]-5-(fluoromethyl)phenylamine
Af-M	affinity modulation
Ar	aromatic group
BBr ₃	boron tribromide
β-CIT	2-β-carbomethoxy-3-β-(4-iodophenyl)tropane
Ben-NQP	2'-benzyl-6-nitroquipazine
Bn	benzyl
Boc	<i>t</i> -butoxycarbonyl
Boc ₂ O	di- <i>tert</i> -butyldicarbonate
br	broad
calcd.	calculated
cat.	catalytic amount
CCl ₄	carbon tetrachloride
CFT	2-β-carbomethoxy-3-β-(4-fluorophenyl)tropane
CH ₂ Cl ₂	dichloromethane/DCM
CH ₃ CN	acetonitrile/ACN
CH ₃ -I	methyl iodide
CHCl ₃	chloroform
CHO	formyl
Cl-Ben	chlorobenzene
CNS	central nervous system
d	doublet
δ	chemical shifts in parts per million (ppm)
Δ	delta: difference
DASB	N,N-dimethyl-2-(2-amino-4-cyanophenylthio)benzylamine
DAST	(diethylamino)sulfur trifluoride
DAT	dopamine transporter
DBEDA	N,N-dibenzylethylene diamine
dc	decay corrected
DCE	1,2-dichloroethane
DCM	dichloromethane
dd	doublet of doublets
DDQ	2,3-dichloro-5,6-dicyano-1,4-benzoquinone
DHP	dihydropyran
DMAP	4-dimethylaminopyridine
DME	1,2-dimethoxyethane
DMF	N,N-dimethylformamide
DMSO	dimethylsulfoxide
EDC.HCl	1-[3-(dimethylaminopropyl]-3-ethylcarbodiimide hydrochloride
ee	enantiomeric excess
EI	electron impact
EOB	end of bombardment
eq	equivalent

ESI	electro-spray ionization
Et	ethyl
Et₂O	diethyl ether
Et₃N	triethylamine
EtOAc	ethyl acetate
EtOMe-NQP	2'-(2-methoxyethyl)-6-nitroquipazine
g	gram(s)
GC/MS	gas chromatography/mass spectroscopy
GlpT	glycerol-3-phosphate transporter
GUT	grand unification theory
h	hour(s)
H₂	hydrogen gas
H₂O₂	hydrogen peroxide
H₂SO₄	sulfuric acid
HBr	hydrobromic acid
HCl	hydrochloric acid - hydrogen chloride
HCO₂H	formic acid
HNO₃	nitric acid
HOM-BOC	4'- <i>tert</i> -butoxycarbonyl-2'-hydroxymethyl-6-nitroquipazine
HOM-NQP	2'-hydroxymethyl-6-nitroquipazine
HPLC	high pressure/performance/price liquid chromatography
HRMS	high resolution mass spectrum
Hz	Hertz
<i>i</i>-PrOH	isopropyl alcohol
<i>J</i>	coupling constant
K₂CO₃	potassium carbonate
K_i	inhibition binding constant; binding affinity
KOH	potassium hydroxide
LacY	lactose permease
LBNL	The Lawrence Berkeley National Laboratory
LC	liquid chromatography
LiAlH₄	lithium aluminum hydride
logP	log of partition coefficient
m	multiplet
μ	micro
M	molar, moles per liter
m/z	mass to charge ratio
MAO	monoamine oxidase
McN5652	trans-1,2,3,5,6,10b-Hexahydro-6-(4-(methylthio)-phenyl)pyrrolo-(2,1-a)-isoquinoline
Me	methyl
MeOH	methyl alcohol, methanol
MeProF-NQP	2'-(3-fluoroproxy)methyl-6-nitroquipazine
MFS	major facilitator superfamily
mg	milligram
MgSO₄	magnesium sulfate
MHz	megahertz
min	minute(s)
mL	milliliter
mmol	millimol
mol%	amount of reagent as a percentage of another reagent (100 mol% = 1 eq.)
MOM-NQP	2'-methoxymethyl-6-nitroquipazine
Na₂SO₄	sodium sulfate
NaH	sodium hydride
NaHCO₃	sodium bicarbonate
NaOH	sodium hydroxide
<i>n</i>-BuLi	<i>n</i> -butyllithium

NET	norepinephrine transporter
NH₄Cl	ammonium chloride
NH₄OH	ammonium hydroxide
NMDA	N-methyl-D-aspartate
NMR	nuclear magnetic resonance
NQP	6-nitroquipazine
NSB	nonspecific binding
OSD	original scholar diggers
OTHP	tetrahydropyranyl ether
Pd/C	palladium on carbon
PET	positron emission tomography
PFP	pentafluorophenol
PG	protecting group
Phen-NQP	2'-phenyl-6-nitroquipazine
pKa	-log of the acid dissociation equilibrium constant
POCl₃	phosphorus oxychloride
ppm	parts per million
ProF-NQP	2'-(3-fluoropropyl)-6-nitroquipazine
Prom-NQP	2'-(3-methoxypropyl)-6-nitroquipazine
Prop-NQP	2'- <i>n</i> -propyl-6-nitroquipazine
p-TsOH	p-toluene sulfonic acid
PVD	Paul van Dyk
rac	racemic
rcy	radiochemical yield
R_f	retention factor
s	singlet
SAR	structure activity relationship
SD	sexual dysfunction
SERT	serotonin transporter
SNF	sodium/neurotransmitter symporter family
SOCl₂	thionyl chloride
SPECT	single photon emission computed tomography
SSRI	selective serotonin reuptake inhibitors
t	triplet
t_{1/2}	half life
TBAF	tetrabutylammonium fluoride
TBAOH	tetrabutylammonium hydroxide
td	triplet of doublets
TEA	triethylamine
TFA	trifluoroacetic acid
THF	tetrahydrofuran
THP	tetrahydropyran/yl
TLC	thin layer chromatography
TMD	transmembrane α -helical domain
TMS	trimethylsilyl
TOF-MS	time-of-flight mass spectroscopy
Trit	triphenylmethyl
trityl	triphenylmethyl
Ts	p-toluenesulfonyl
TsOH	p-toluenesulfonic acid
UV	ultraviolet/light

CHAPTER 1

INTRODUCTION, BACKGROUND AND PURPOSE

1.1 Serotonin Biology

Serotonin (5-hydroxytryptamine, 5-HT) **1** is a biogenic indolamine neurotransmitter that is present in the central nervous system (CNS) and peripheral regions of both vertebrates and invertebrates. Within living systems, serotonin is synthesized from L-tryptophan **2** in two steps (Figure 1.1). Step one is an aromatic hydroxylation facilitated by tryptophan hydroxylase to provide 5-hydroxytryptophan **3** that undergoes decarboxylation by amino acid decarboxylase to provide 5-HT **1**.¹

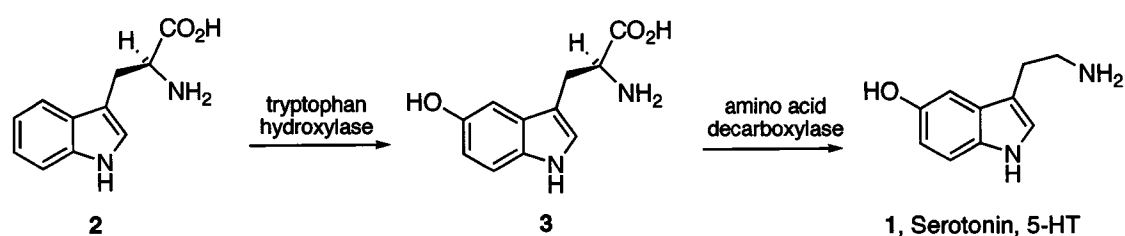


Figure 1.1: The biosynthesis of serotonin.

Within the mammalian CNS, the serotonergic neurons are located primarily in the raphe that is located within the brain stem. Neuronal projections from the raphe extend to the cerebral cortex, hippocampus, hypothalamus and thalamus thereby providing high densities of serotonergic neurons in these regions.² Interneuronal signaling with 5-HT occurs primarily at the synapse. The

synapse is a junction between an axon terminal of one neuron (presynaptic neuron) and the dendrite of another (postsynaptic neuron) (Figure 1.2).

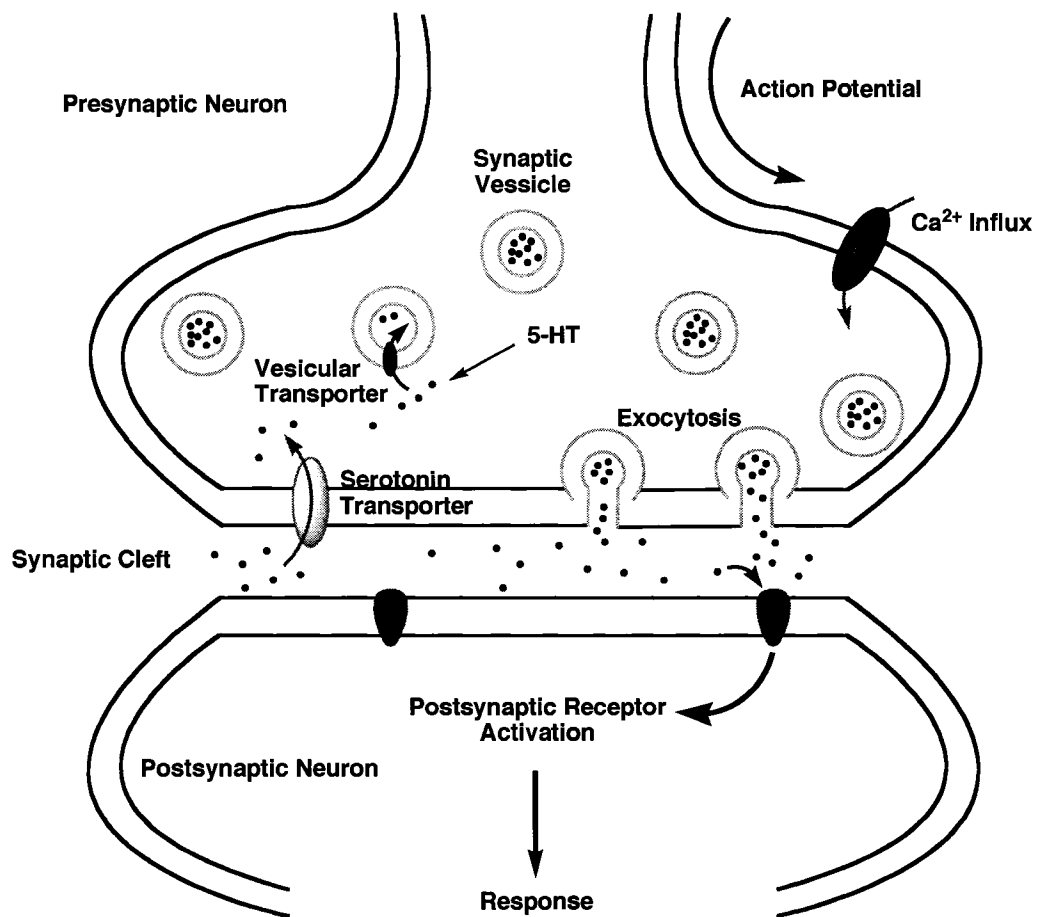


Figure 1.2: A general representation of a serotonergic synapse.

The space between the neurons is approximately 20 nm and is called the synaptic cleft. When an action potential traveling along the presynaptic neuron reaches the axon terminal, voltage-gated Ca²⁺ channels in the membrane open allowing for an influx of Ca²⁺ ions. The influx of calcium ions causes the synaptic vesicles to fuse with the cellular membrane and release their neurotransmitter contents (e.g. 5-HT, 1) into the synaptic cleft through the process of exocytosis.

Once in the synaptic cleft, the neurotransmitters reach the postsynaptic neuron through diffusion, and a response is afforded through activation of postsynaptic receptor proteins.³ Following neurotransmission, transport proteins located within the presynaptic membrane clear neurotransmitter from the synaptic cleft. For 5-HT, the transport protein is the serotonin transporter (SERT, see Section 1.2 for a more detailed discussion). Once transported, 1 is packaged back into vesicles through the action of a vesicular transporter. Additional removal of 1 from the synaptic cleft is facilitated by the oxidative degradation of 1 by monoamine oxidase (MAO).¹

A wide variety of serotonergic receptors exist in the CNS and in the periphery. Currently there are fourteen serotonin receptors that have been identified and characterized to various extents.⁴ These receptors are grouped into families based on their similar biochemical characteristics (primary structure, genes), pharmacology and signaling mechanisms.⁴ Currently three functional classes of serotonin receptors are known. Most of the receptors (twelve of fourteen) are G protein-coupled receptors, one is a ligand-gated ion-channel and the last is the serotonin transporter (SERT). These receptors and a brief listing of their known function(s) are summarized in Table 1.1.^{2, 4-6} In peripheral regions, serotonin receptors are found in blood platelets,⁷ the smooth muscle of the digestive tract⁸ and circulatory system⁹ and on peripheral neurons where 5-HT has been shown to have a role in pain signaling and analgesia following tissue injury.¹⁰

Table 1.1: A table of known serotonin receptors, their functional class, location in the vertebrate/invertebrate body and associated functions.

Receptor	Type	Location	Functions
5-HT _{1A}	G-protein	CNS-per	Sleep, anxiety, thermoregulation, depression
5-HT _{1B}	G-protein	CNS-per	Migraine, vaso., aggression, bipolar disorder, gastric motility
5-HT _{1D}	G-protein	CNS-per	Migraine
5-HT _{1E}	G-protein	CNS	Largely unknown
5-HT _{1F}	G-protein	CNS-per	Migraine, vaso.
5-HT _{2A}	G-protein	CNS-per	Schizophrenia, anxiety
5-HT _{2B}	G-protein	CNS-per	Migraine, gastric motility, vaso., appetite
5-HT _{2C}	G-protein	CNS	Depression, anxiety, obesity, cognition, schizophrenia
5-HT ₃	Ion Chan.	CNS-per	IBS, emesis, cognition
5-HT ₄	G-protein	CNS-per	IBS, gastric motility
5-HT ₅	G-protein	CNS	Largely unknown
5-HT ₆	G-protein	CNS	Bipolar disorder, Parkinson's, Alzheimer's, learning, seizures, appetite
5-HT ₇	G-protein	CNS-per	Sleep, migraine, depression, cognition, schizophrenia, IBS
SERT	transporter	CNS-per	Uptake of 5-HT into cells

Key: G-Protein = G Protein-coupled receptor, ion chan. = ligand-gated ion channel, CNS = central nervous system, per = periphery, vaso. = vasocon-striction, IBS = irritable bowel syndrome

1.2 The Serotonin Transporter

The serotonin transporter (SERT) is a member of the sodium/neurotransmitter symporter protein family (SNF). The SNF proteins utilize the co-transport of sodium and chloride ions down a concentration gradient to provide the energy for transport of substrate.¹¹ Other transport proteins in the SNF family include those for the other biogenic amine neurotransmitters; dopamine (dopamine transporter, DAT) and norepinephrine (norepinephrine transporter, NET). Hydropathy analysis of the primary amino acid sequences of the biogenic amine transport proteins predicts a common tertiary structure with twelve transmembrane α -helical domains (TMD's). The SNF transporters are

membrane bound and have their carboxy and amino terminals on the intracellular (cytoplasmic) side of the membrane. The human SERT (hSERT) contains 630 amino acids.¹²

To date, a high-resolution molecular structure determination (e.g. x-ray crystal structure) of SERT, or the other biogenic amine transporters, has yet to be put forward. The majority of knowledge about SERT structure as it relates to function comes from mutation studies probing the biochemical changes in receptor function as a result of amino acid substitutions or deletions.¹³⁻¹⁸ Several studies have used these results to model the transport binding region of SERT to suggest the relative arrangements of the TMD's.^{11, 15}

Recently, the structures of two major facilitator superfamily (MFS) transport proteins, the glycerol-3-phosphate transporter (GlpT) and the lactose permease (LacY), have been reported.^{19, 20} Proteins of the MFS are related to the SNF transporters structurally (12 TMD's, intracellular amino and carboxi termini) and functionally (ion coupled membrane transport proteins) and both belong to the larger group of secondary transporters. Because of the structural similarities between the MFS and SNF transporter families, the LacY tertiary structure was recently utilized as a template to generate a refined three-dimensional model of SERT.²¹

More recently, a prokaryotic homolog of the biogenic amine transporters was crystallized and a structural determination made.²² The bacterial protein, called LeuT_{Aa}, is a sodium dependent transport protein that is responsible for the movement of leucine into bacterial cells. LeuT_{Aa} is suggested as a better

template for modeling SERT, relative to GlpT and LacY, because of its corresponding dependence on sodium ions for transport of substrate. However, no refined SERT protein models, that utilize LeuT_{Aa} as a design template, have yet come forward in the literature.

Developing a cogent understanding of the three-dimensional structure of SERT will provide insight into functional aspects of the protein and also provide a tool for the design and synthesis of new SERT ligands.

1.3 The Serotonin Transporter and Disease

Serotonin **1** has been well documented as having a key role in the pathology of certain CNS related disorders.^{23, 24} It has been suggested that the amount (density) of cell-surface expressed SERT may serve as an indicator of the overall integrity of serotonergic terminals in the CNS.²⁵ The distribution of SERT in the CNS in healthy human brains has been determined from postmortem studies²⁶⁻²⁹ and a summary of relative (high, medium, low) SERT distributions in different brain regions is given in Table 1.2. The role of SERT in neuropsychiatric disorders (depression, dependence, bipolar disorder, obsessive compulsive disorder, among others) and neurological disease (Parkinson's disease, Wilson's disease, Stroke, Tourette's syndrome, among others) is still poorly understood. Studies in postmortem and living brain have demonstrated significant changes in SERT density (increases and decreases) for these diseased states, relative to healthy controls.

Table 1.2: Relative SERT densities in discrete brain regions.

Relative amount of cell surface expressed SERT	Brain Regions
High	MIDBRAIN AND DIENCEPHALON: Medial and dorsal raphe, thalamus, hypothalamus, striatum
Medium	LIMBIC SYSTEM: Hippocampus, parahippocampal gyrus, amygdala and cingulate cortex
Low	Neopallium and cerebellum

Additionally, regional cerebral changes in SERT density have been noted for age differences (decreased availability with increasing age) and seasonal variation (decreased in autumn and winter) in healthy patients. Detailed summaries of these studies have recently been reported.^{23, 24} The results from these studies have provided conflicting correlations. For example, in two separate studies of depression, children and adolescents have shown increased ($p < 0.02$) SERT in the midbrain regions relative to controls³⁰ while adults demonstrate significant ($p = 0.02$) decreases in SERT within the same region.³¹ Similar conflicting correlations for other diseased states have been documented.^{23, 24} Clearly there are discrepancies observed in the current body of research that has been devoted to understanding the role of SERT in neuropsychiatric disorders and neurological disease. It is suggested that an enhanced understanding of the SERT role in these disorders will be assisted by the development of better *in vivo* pharmacological tools, such as new positron emission tomography (PET) and/or single photon emission computed tomography (SPECT) imaging agents.²³

Of the conditions mentioned above, depression, anxiety and OCD have seen significant therapeutic benefit from serotonin reuptake inhibitors. These drugs bind to SERT and competitively inhibit (block) the uptake of 5-HT. It is hypothesized that a resultant increase of 5-HT in the synaptic cleft affords increased transmission of signal and an amelioration of symptoms.³²

The earliest SERT inhibitors, introduced in the 1950's, were the tricyclic antidepressants (for example **4** and **5**, Figure 1.3). Although these had a profound effect at reducing depressive conditions, they also promoted adverse side effects such as cardiotoxicity, sedation and weight gain.¹ A new generation of a SERT inhibitors, the selective serotonin reuptake inhibitors (SSRI's, for example **6** – **9**, Figure 1.3), were introduced in the late 1970's. The most prolific and well known SSRI, Fluoxetine (Prozac, **6**), was the first to receive Food and Drug Administration (FDA) approval for the treatment of depression in 1987.^{1, 33} The SSRI's interact selectively with SERT to provide their therapeutic effect and have demonstrated a reduction in adverse side effects relative to the tricyclic antidepressant counterparts.¹

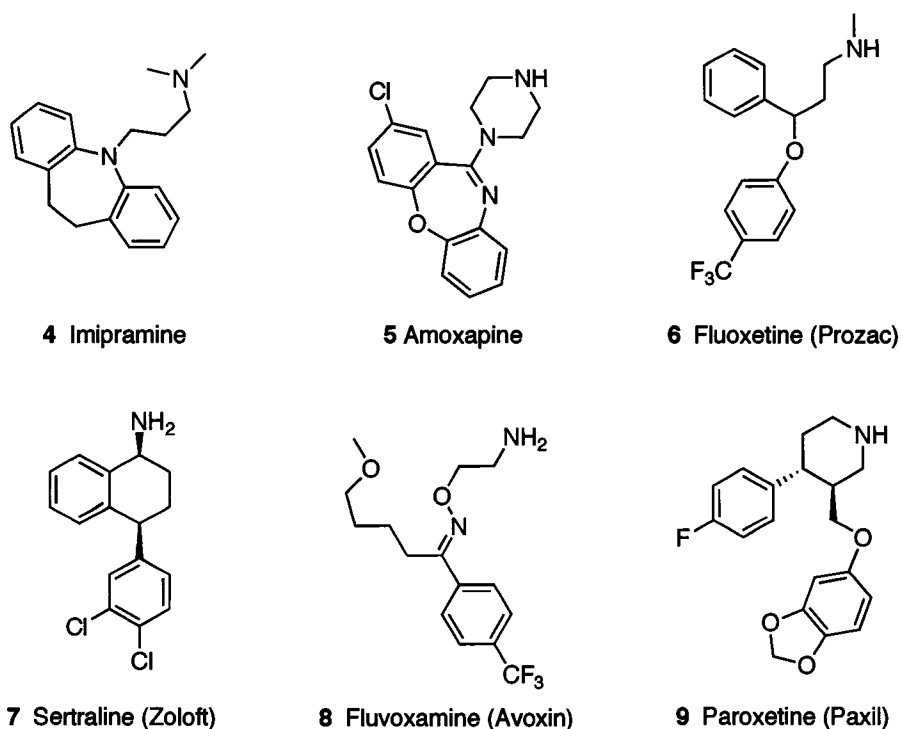


Figure 1.3: A collection of known SERT ligands; the tricyclic antidepressants (4 and 5) and the modern selective serotonin reuptake inhibitors (SSRI's, 6 – 9).

1.4 Positron Emission Tomography Imaging

Positron Emission Tomography (PET) is a medical imaging technique that utilizes radioactive probes (tracers, radioligands) to visualize and quantitate biochemical processes within living tissues. These tracers possess positron emitting radionuclides that undergo decay *in vivo*, thereby providing the necessary signal for quantifying the biochemical process of interest.³⁴ The most commonly utilized radionuclides are fluorine-18, carbon-11, nitrogen-13 and oxygen-15.³⁵ Another radionuclide that is often used with CNS ligand tracers, is bromine-76.³⁶ These positron radionuclides undergo beta plus (β^+) decay and emit a positron that travels a few millimeters or less before colliding with an electron. The annihilation event produces two high-energy photons that are

emitted 180° apart along a line of decay response. Using precision detection instrumentation, the origin of the photons in three-dimensional (3D) space can be determined thereby providing the *in vivo* location of the decay event. Resultant 3D maps of radionuclide decay can be created that allow for the quantitative measurement of radiotracer accumulation and/or localization in the tissue or region of interest. Anatomical correlation of the 3D PET decay images with high-resolution nuclear magnetic resonance images (MRI) allows for the discrete identification of target tissues and the anatomical volume associated with tracer accumulation.³⁷ Provided that the radiotracers are selective for their *in vivo* target, PET imaging allows for the non-invasive measurement of the associated biochemical processes.³⁴ A sample PET image is shown in Figure 1.4.

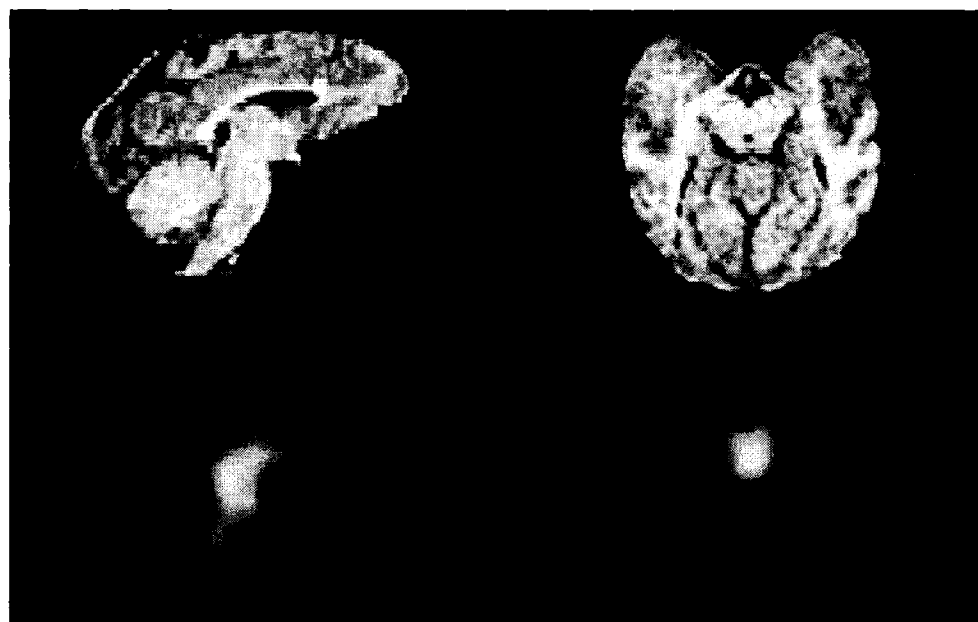


Figure 1.4: Sample PET images (bottom) from a study in baboon, displaying the accumulation of SERT tracer [¹¹C]AFM 14 in the midbrain and thalamus. The corresponding MRI image of the brain is displayed above the PET images. (Image from ref. 51).

To afford efficacious PET imaging agents for the CNS, prospective PET ligands must meet certain criteria. These criteria have been recently detailed³⁸⁻⁴¹ and are summarized below.

-Synthetic Criteria – Radioligand planning and synthesis – The position of radionuclide introduction into a prospective ligand can have profound implications on tracer development. The modification of a parent compound to accommodate a radionuclide may grossly change the ligands properties (lipophilicity, binding affinity for target, metabolic fate), relative to the parent, and affect the tracers performance. Target agents should be rigorously characterized, in non-radioactive form, for the appropriate *in vitro* characteristics (see below). Radiochemical syntheses are desired where the yield of target ligand at the end of synthesis (e.g. incorporation of radionuclide, removal of protecting groups, purification and preparation of injectate) is usually greater than 10%. Furthermore, the radiosynthesis should afford the target tracer with specific activity (amount of radioactivity per mole or gram of ligand) that is sufficient for adequate PET data acquisition (usually >500 Ci/mmol). Additionally, radiosynthesis time needs to be minimized so PET experiments can be completed in the useable lifetime of the radionuclide (usually 4-5 half-lives). For certain radionuclides, especially carbon-11 ($t_{1/2} = 20.3$ min), this criterion is of timely importance.

-In vitro pharmacological profiles – The competitive binding affinity (K_i) of the tracer for its target protein in the CNS should typically be at low nanomolar concentrations or below, so that the target can be adequately quantitated given

the low doses (< 1 mg) of ligand typically administered for PET imaging studies. The radioligand should display at least a 100 fold preference for its target over other sites that it may interact with. This selectivity helps minimize complications that arise from non-specific (non-target) binding interactions during the *in vivo* PET experiments. To achieve adequate brain penetration by passage through the blood-brain barrier (BBB) the lipophilicity of the compounds (partition coefficient, logP) needs to be considered. More lipophilic (logP > 3.5) qualities can sometimes lead to increased nonspecific binding *in vivo*⁴⁰ and management of the tracer lipophilic qualities should be considered as additional *synthetic criteria*.

-In vivo pharmacological profiles – The uptake of the radioligand into the brain should occur quickly following injection. The nonspecific binding interactions should washout of the tissues rapidly, so target specific binding can be quantified on a timescale appropriate for the radionuclide. The target specific binding interactions should be reversible on the experiment time scale so kinetic tracer analyses can be performed. Radioligands should show minimal metabolic activity in the CNS since radiolabeled metabolites may have distinct *in vivo* properties that could complicate the tracer target evaluation.

-Additional considerations – Ligand toxicity is of minimal concern since the injected mass of radioligand is well below a therapeutic dose; that is usually less than 10 µg. The dose of radiation administered in an experiment is also a concern, yet is minimal based on the low tracer dose as a function of radioligand specific activity.

Other specific tracer considerations can be made based on the needs of the system under study. Additional criteria for the *in vivo* imaging of the SERT target within the CNS are provided in the next section.

1.5 Imaging of the Serotonin Transporter with SPECT and PET

Studies toward efficacious imaging agents for SERT have been ongoing now for approximately fifteen years. The first successful imaging agent developed for SERT was the cocaine analog (single photon emission computed tomography (SPECT) agent [^{123}I] β -CIT **10** (Figure 1.5).⁴²

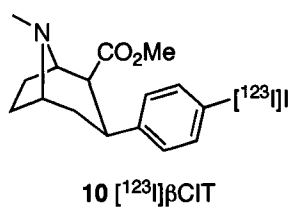


Figure 1.5: First generation SPECT imaging agent for SERT.

Ligand **10** however, is not selective for SERT, and has also found use as an imaging agent for the dopamine transporter (DAT). The inability of **10** to quantify SERT in regions where DAT was coexpressed proved to be a significant limitation to the efficacy of this tracer, and has limited its use in imaging medium to low density SERT regions.⁴³ The synthesis of novel ligands that are selective for SERT, relative to the other biogenic amine transporters (DAT and NET), remains an ongoing challenge in the development of new SERT imaging agents.

Next generation SERT PET imaging agents have largely been derived from two structural classes (Figure 1.6, with references); the pyrroloisoquinolines (**11** and **12**) derived from (+)-McN5652 **26** and the diaryl sulfides (**13** – **15**).

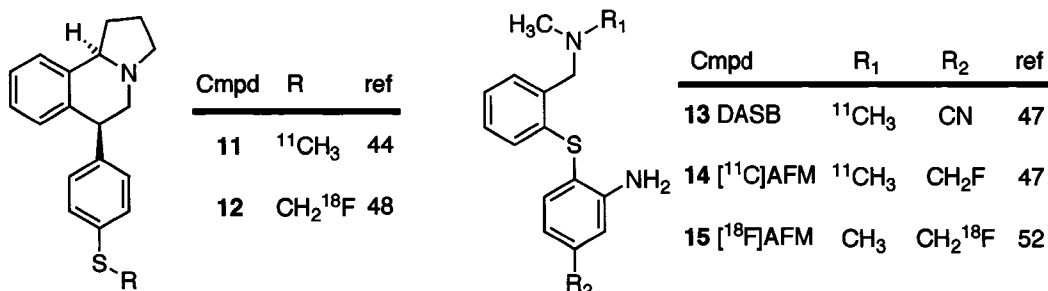


Figure 1.6: Next generation PET imaging agents for SERT.

The first tracer to find use as a *selective in vivo imaging agent* for human SERT was **11**.⁴⁴ Although **11** has been utilized successfully in human studies of depression⁴⁵ and drug abuse,⁴⁶ it has been shown to be an inferior tracer to ligands from the diarylsulfide series (particularly **13** and **14**, Figure 1.6).⁴⁷ The fluorine-18, fluoromethyl analog **12** has demonstrated superior *in vivo* properties (40% higher specific binding, reduced metabolism, faster kinetics) relative to carbon-11 variant **11**.⁴⁸ Additionally, the longer-lived fluorine-18 radionuclide provides an opportunity for off-site imaging applications. However, the successful imaging of brain tissues with low SERT density may fail as a result of high NSB in non-target regions (i.e. cerebellum).⁴⁹

Of the diaryl sulfides that have been developed, DASB **13** and [^{11}C]AFM **14** have emerged as lead SERT imaging agents (Figure 1.6).⁴⁷ Although **13** has been one of the most widely used ligands for the *in vivo* imaging of SERT in humans,^{46, 50} it still does not allow for a reliable quantification of low-density

SERT regions.⁴³ It has been suggested that the use of [¹¹C]AFM **14** (with greater target to non-target ratios) may allow for the quantification of low-density SERT regions.^{43, 47, 51} A recently developed fluorine-18 ligand, [¹⁸F]AFM **15**, shares the high specific binding qualities of carbon-11 analog **14** as demonstrated in rat.⁵² Given the longer lifetime of the fluorine-18 radionuclide, and the possibility for off-site imaging applications, **15** may emerge as a superior ligand to both **13** and **14**. Studies of ligand **15** in non-human primates, to substantiate the early rodent findings have yet to be put forward. To date, diaryl sulfide ligands **13** and **14** have been established as the most efficacious ligands for the *in vivo* imaging of SERT.^{43, 47, 53} However, there still exists a need for ligands that can quantify SERT in brain regions displaying low-density expression of the receptor.⁴³

Six 6-nitroquipazine analogs have been advanced as plausible SERT tracers since the early 1990's (Figure 1.7, with references). These tracers have all largely failed to provide the *in vivo* qualities necessary for efficacious SERT imaging agents. Compound **16** suffers from metabolic defluorination and an apparent lack of selectivity for SERT in blocking studies.⁵⁴

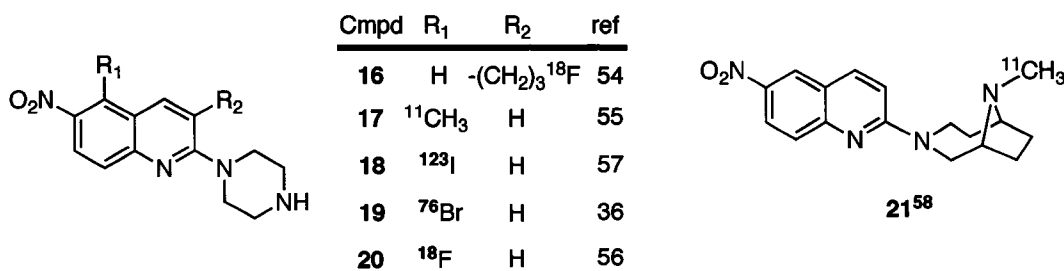


Figure 1.7: SERT imaging agents derived from 6-nitroquipazine.

Compounds **17**, **19** and **20** all showed poor thalamus to cerebellum (high to low SERT density; target to non-target) ratios.^{36, 55, 56} Compound **17** also displayed slow binding kinetics (equilibrium not reached at 90 min) that was not amenable to the lifetime of the carbon-11 radionuclide. SPECT agent **18** has demonstrated good target to non-target ratios (> 2) in primate brain but the use of this compound has been limited due to metabolic dehalogenation generating free iodine-123 that obscures experimental images.^{55, 57} PET agent **21** has recently been described.⁵⁸ However, in a comparison study with DASB **13**, **21** was shown to be an inferior PET ligand.⁵⁹ Collectively, these 6-nitroquipazine agents have not proven as efficacious at imaging SERT as diaryl sulfides **13** and **14**.

1.6 6-Nitroquipazine Analogs: Previous Work from Our Lab and Others

Our group has been interested in the development of novel SERT tracers derived from the known SERT inhibitor 6-nitroquipazine (6-NQP, **22**) (Figure 1.8).

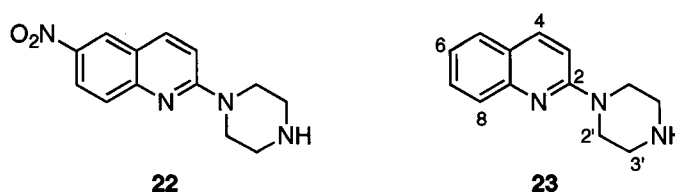


Figure 1.8: 6-Nitroquipazine and a description of ring numbering in the quipazine series.

The IUPAC name for **22** is 6-nitro-2-(piperazin-1-yl)quinoline. However, the term 'quipazine' is typically used when referring to compounds in this series. The parent compound, quipazine **23**, is also shown in Figure 1.8 and the numbering scheme for the rings is indicated. Substituents on the piperazine ring

are indicated with a 'prime' after the position number to differentiate them from substituents on the quinoline ring.

Compound **22** was first described in the early 1980's under the trade name DU 24565 and its selectivity for SERT over the other biogenic amine transporters (NET and DAT) was high (10^3 fold).⁶⁰ A tritiated ($[^3\text{H}]$) variant of **22** was generated⁶¹ and the *in vitro* and *in vivo* characterization of $[^3\text{H}]\mathbf{22}$ further demonstrated the potency and selectivity of **22** for SERT.^{62, 63}

Our group performed a structure activity relationship (SAR) study to evaluate the effects of methyl group introduction to quipazine **22** at the 2'- and 3'-positions (Figure 1.9).⁶⁴

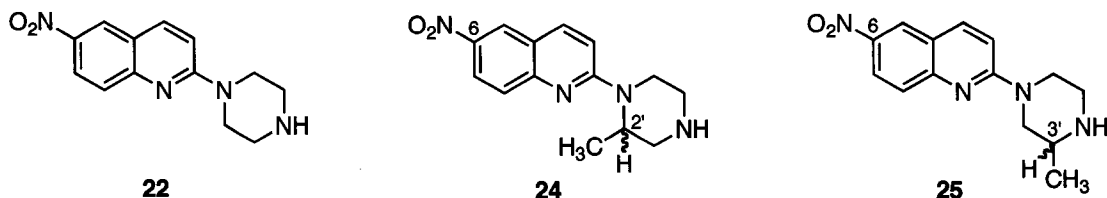


Figure 1.9: Investigational compounds from our initial SAR study.⁶⁴

We observed a marked increase in SERT affinity with 2'-methyl agent **24** ($K_i = 0.08$ nM) relative to **22** ($K_i = 0.16$ nM) and a competitive binding decrease with the 3'-methyl analog **25** ($K_i = 4.56$ nM). The selectivity of these compounds for SERT has not yet been evaluated through comparison binding studies at NET and DAT. However, it is conjectured to be high, based on the selectivity of parent compound **22**.

Concurrent with this SAR study, our group was generating an inhibitor-based pharmacophore of the SERT binding site using SERT inhibitors of known

efficacy.^{65, 66} The training set ligands used in this computational study are shown in Figure 1.10 with their key structural similarities identified.

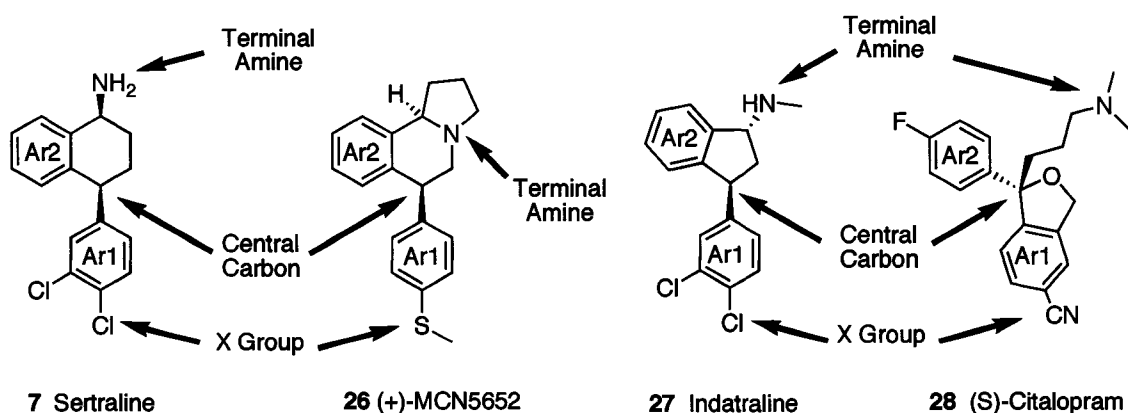


Figure 1.10: Training set ligands utilized in the generation of our SERT pharmacophore.

These computational studies used rigorous conformational searching and scoring functions to identify conformations of each molecule (**7**, **26** – **28**) that are most like each other in three-dimensional (3D) space relative to their key structural similarities. The key points of similarity, the terminal amine group, both aromatic rings (Ar_1 , distal to amine group; Ar_2 proximal to amine group) and the X group (Shown in Figure 1.10) were used as points of comparison in this study. The resultant pharmacophore model is shown in Figure 1.11 as a superposition overlay of select conformations of the training set ligands. The similarities in the alignments of the key structural elements are detailed in Figure 1.11 where the regions are indicated with arrows.

When 2'-methyl quipazine analog **24** was fit into the pharmacophore, it was observed that the methyl group provided a contact into the Ar_2 region of the model. It is thought that this simple alkyl group may be a suitable replacement

for the Ar2 moiety. The 3'-methyl analog **25** fit less optimally into this region, placing the methyl group into a region of the 3D model that was undefined. The decreased affinity of **25** might result from steric interactions that occur within this undefined region of our model.

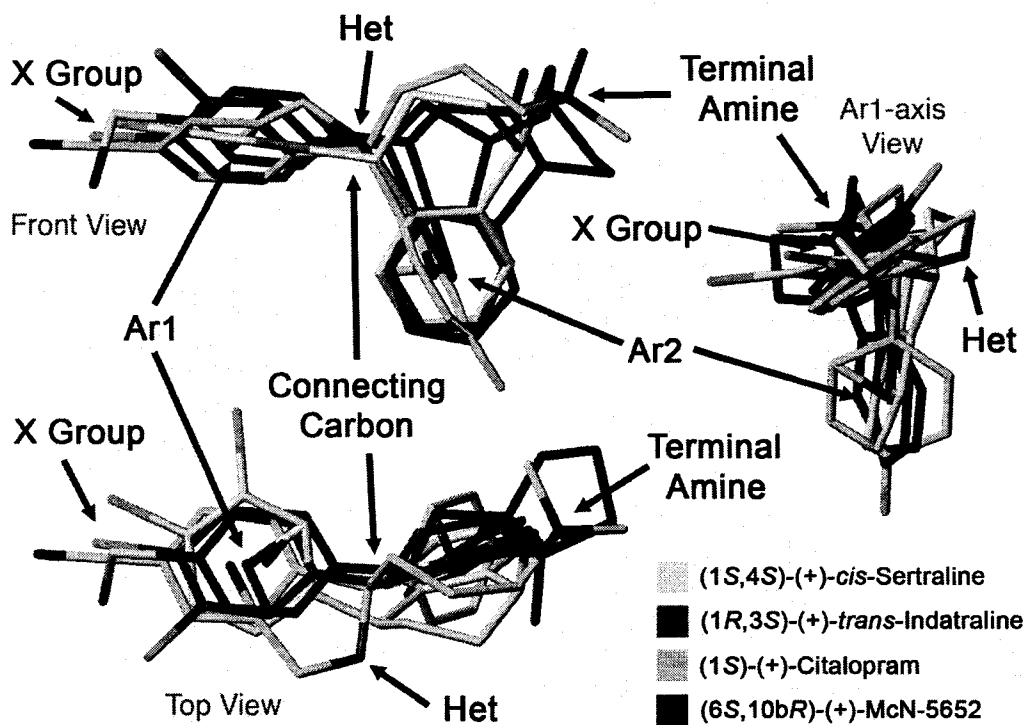


Figure 1.11: Our derived SERT pharmacophore model, illustrated as a superposition overlay of select conformations of training set ligands. (Image from ref. 66).

With quipazine **24** identified as a new lead agent, subsequent studies sought to refine the SAR of this initial lead. Our computational efforts corroborated our initial SAR findings and suggested the abandonment of the 3'-substituted-6-nitroquipazine analogs (like **25**). Former group member Mark Walker initiated these studies with his synthesis of 2'-methoxymethyl-6-nitroquipazine (MOM-NQP, **35**, Figure 1.12).⁶⁷ Briefly, the Walker synthesis began from known dibenzylpiperzine ester **29**⁶⁸ that was reduced to alcohol **30**

with LiAlH_4 in ether. Alkylation of **30** with NaH and CH_3I in THF, followed by dihydrochloride formation gave **31**. Hydrogenolysis of the benzyl groups with Pd/C in ethanol gave piperazine **32** that was protected with trityl chloride in DCM to give **33**.

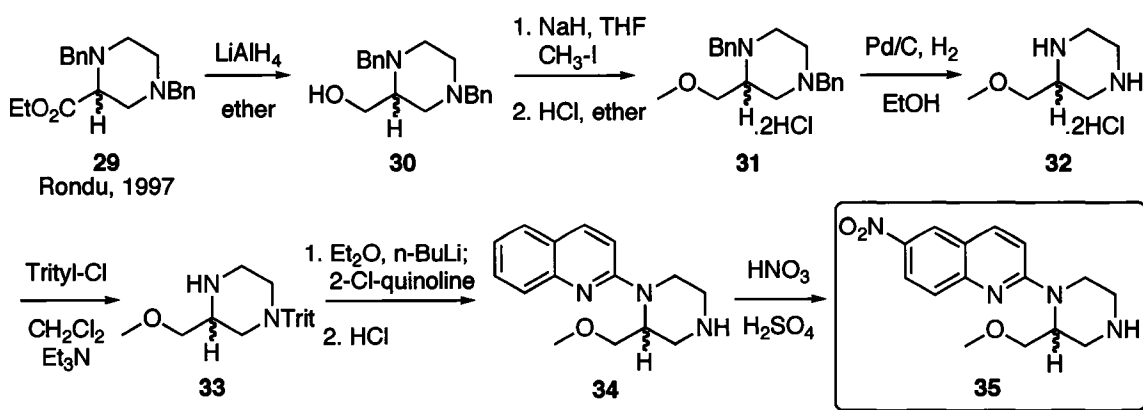
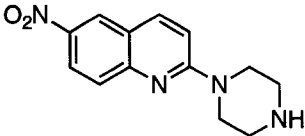
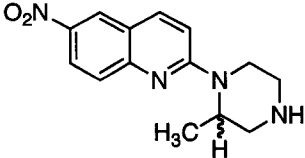
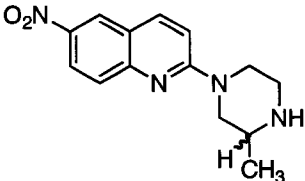
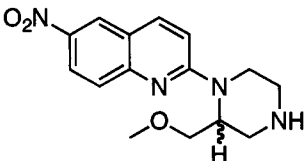


Figure 1.12: Walker's synthesis of 2'-methoxymethyl-6-nitroquipazine (MOM-NQP).⁶⁷

Compound **33** was coupled to 2-chloroquinoline using the method of Gilman⁶⁹ to provide quipazine **34** following deprotection. Nitration of **34** provided the target, MOM-NQP **35**.⁶⁷

Compound **35** displayed very high binding affinity for SERT, and is one of the most potent SERT inhibitors known to date.⁷⁰ It displayed a 65-fold increase in potency over parent compound **22** and a 32-fold increase over our initial lead agent **24**. The MOM-NQP ligand **35**, like the 2'-methyl analog **24**, still needs to be evaluated for its SERT selectivity relative to DAT and NET. A summary of the initial SAR data is detailed in Table 1.3, in comparison to parent compound 6-NQP **22**. The radioligand displacement binding assay used to acquire the SERT binding data is detailed in Chapter 5.

Table 1.3: Preliminary SAR data from the Gerdes laboratory.

Compound	Structure	Binding affinity ($K_i \pm$ sd) nM
22⁶⁴		0.163 ± 0.053
24⁶⁴		0.081 ± 0.061
25⁶⁴		4.56 ± 2.4
35⁷⁰		0.0025 ± 0.0003

Other structure activity studies of 6-NQP analogs at SERT have been ongoing by other researchers and their work has focused primarily on quinoline ring substituted analogs.^{54, 71-73} A few representative targets from their work are shown in Figure 1.13. Many of the compounds produced by Chi and coworkers have displayed good SERT affinity in the low to sub-nanomolar concentration range (i.e. compounds **36**, **38** and **40** and others). Additionally, they have successfully demonstrated that groups of moderate size are well tolerated at the 3- and 4- positions of the quinoline ring (i.e. **37**, **38** and **40**).

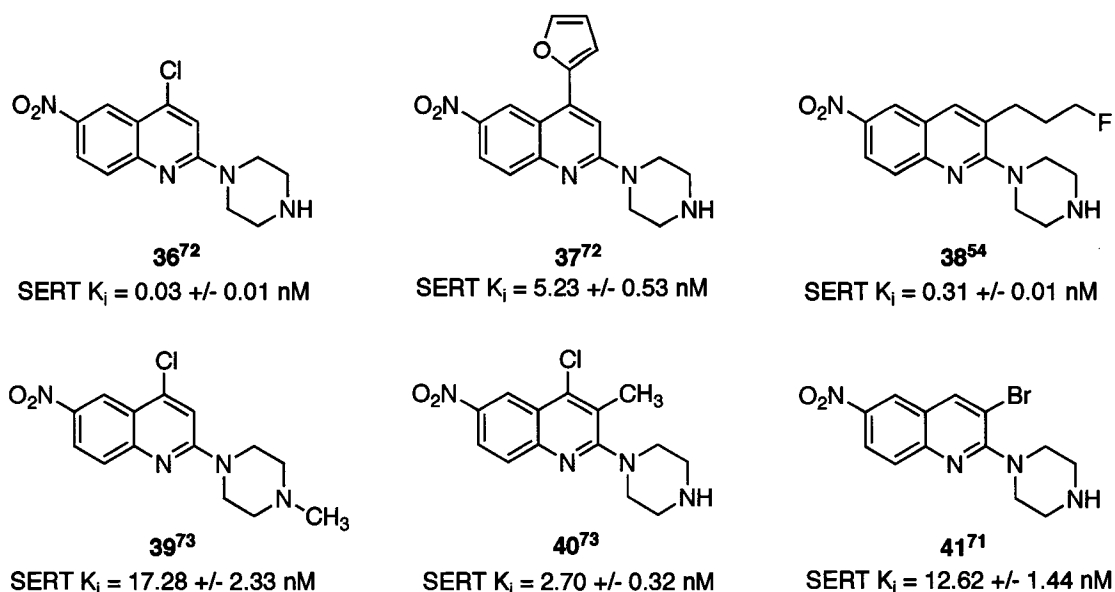


Figure 1.13: Example ligands from the SAR studies performed by Chi et al. The K_i values are determined with rat brain homogenate² and [³H]citalopram.

The addition of a methyl group to the terminal amine was not well tolerated, and a 570 fold decrease in SERT affinity was demonstrated for the conversion of **36** to **39**.

To date, compound **38** is the only ligand from Chi and co-workers that has been advanced as a PET imaging tracer. This agent however displayed significant *in vivo* metabolic defluorination as evidenced by the accumulation of radioactivity in bone. Additionally, the *in vivo* challenge of [¹⁸F]**38** with selective SERT blocking agents (fluoxetine and paroxetine) only reduced the binding of [¹⁸F]**39** by 11-31% in the frontal cortex signifying that *in vivo* nonspecific binding of this tracer is high.⁵⁴ These results suggest that [¹⁸F]**38** may not be a suitable tracer for imaging SERT.

1.7 Focus of the Investigation

Following the successes of our initial SAR investigations, attention was turned toward the development of 6-nitroquipazine analogs as new SERT PET imaging agents. As discussed earlier, recent reports of new PET agents for SERT have suggested that a need still exists for tracers that can quantitatively measure SERT in brain regions with medium to low SERT density.^{43,47} A tracer that can meet these demands must demonstrate the *in vivo* properties that promote accurate *in vivo* SERT measurements; including, the disappearance of nonspecific binding within a timeframe that is within four half-lives of the radionuclide and appropriate signal-to-noise ratios that permit reproducible quantification of moderate to low SERT density regions. Given the very high affinity of our new 2'-substituted-6-nitroquipazine analogs (compounds **24** and **35**, as per Table 1.3) and the known SERT selectivity of 6-nitroquipazine **22**,⁶⁰ we felt that select analogs may offer significant improvements in tracer performance relative to the established 6-NQP SERT imaging agents (Figure 1.7).

With the new goal of obtaining novel PET imaging agents that could reproducibly image brain regions with moderate and low densities of SERT, we set out to establish synthetic protocols for obtaining these agents from our initial lead agents MOM-NQP **35** and 2'-methyl-NQP **24**. The investigation described within, details our discovery of new SERT PET imaging agents, with an emphasis on the synthetic methods utilized to obtain our targets in non-racemic form.

Chapter Two of this dissertation discusses the initial racemic syntheses of our new targets and the preliminary radiochemical studies that produced our target fluorine-18 and carbon-11 SERT PET tracers. The asymmetric synthetic methods developed to obtain our non-racemic targets will be discussed in Chapter Three. The discussion of the asymmetric method is extended in Chapter Four, as it is applied to the synthesis of novel 2'-aryl-6-nitroquipazine analogs. The biological evaluation of our new SERT ligands is provided in chapter five, and a summary of the study closes out this work in chapter six. Finally, full experimental details are afforded in Chapter Seven.

CHAPTER 2

SYNTHESIS OF RACEMIC TARGETS

2.1 Introduction

Preliminary studies from our laboratory aimed at acquiring a SERT PET imaging agent have been focused on the generation of a fluorinated target ligand derived from the initial lead agent 2'-methyl-6-nitroquipazine **24**. The fluorinated target ligand **42** was never synthesized, even in non-radioactive 'cold' form and efforts to acquire it were abandoned (Figure 2.1).

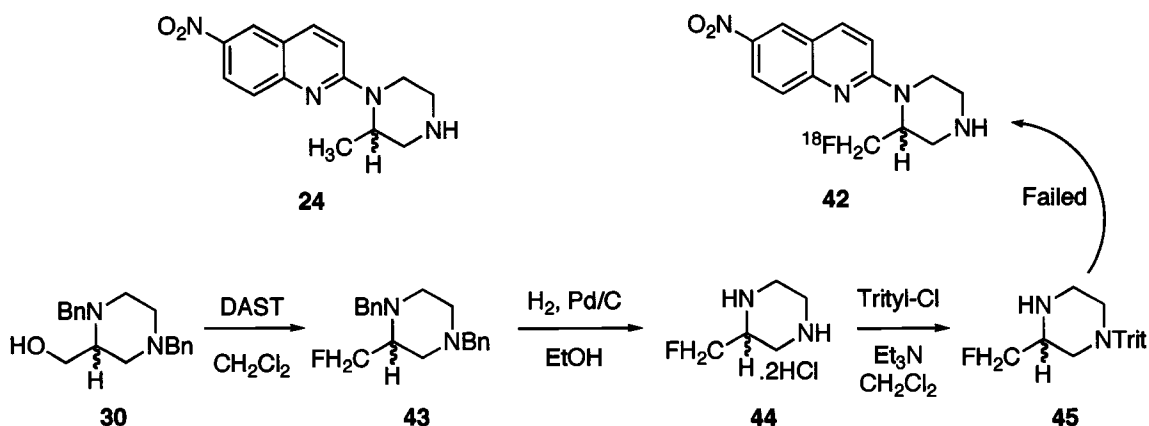


Figure 2.1: Attempted route toward the generation of 2'-fluoromethyl-6-nitroquipazine.

These synthetic failures resulted largely from the instability of the fluorine atom to the alkyllithium coupling conditions (discussed later) used to form **42** from piperazine **45** and 2-chloroquinoline. A control reaction confirmed that the fluorine atom was undergoing elimination (HF) since an analysis of the product mixture by GC/MS showed a decrease in mass ($m/z \Delta 20$) of the trityl protected

material **45** consistent with the loss of HF. This was unfortunate since piperazine **45** could be synthesized easily from the dibenzyl alcohol substituted **30** (Figure 2.1). Additionally, attempts at generating a tosylate leaving group from the alcohol **30** and another alcohol intermediate **58** (HOM-BOC, shown later) failed. Thus, a radiochemical precursor could not be generated. The introductions of other sulfonate leaving groups (mesylate, triflate) were never attempted since our radiochemical collaborators preferred to have the tosylate leaving group chromophore as an experimental tool for observing its displacement by radioactive [^{18}F]fluoride ion.

Given these failures at generating fluoromethyl agent **42**, our group next sought to extend the piperazine side chain to 3-fluoropropyl in the hope that a fluorinated agent might be generated. These efforts were successful, and the formation of compound **50** was partially the focus of another research group member, Brian Kusche.⁷⁴ The synthesis of target ProF-NQP **50** is briefly summarized below (Figure 2.2).

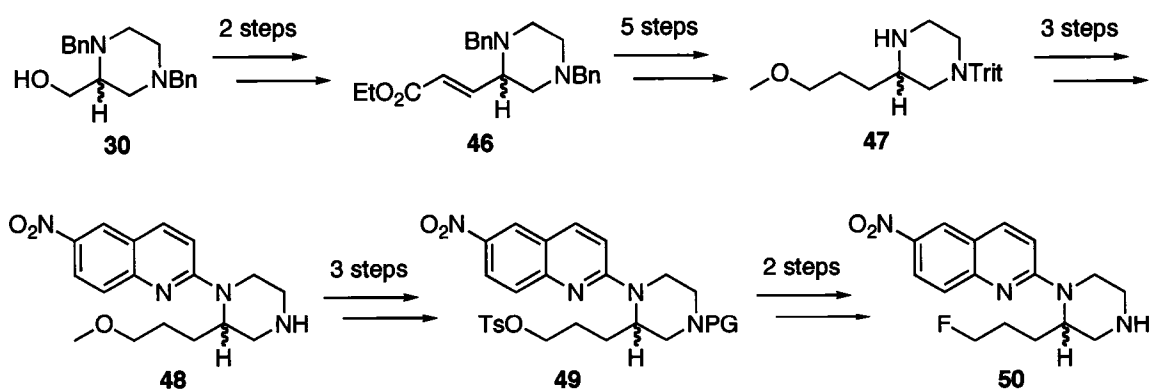


Figure 2.2: Summary of the route used by Kusche⁷⁴ to obtain ProF-NQP. For **49**, the protecting group (PG) was N-formyl or N-*tert*-butoxycarbonyl (N-Boc).

The side chain extension was accomplished through a Swern-oxidation/Horner-Emmons homologation sequence using alcohol **30**, to afford unsaturated ester **46**. The conversion of **46** to protected piperazine **47** was accomplished in five steps and the coupling of **47** to 2-chloroquinoline afforded 2'-(3-methoxy-1-propyl)-6-nitroquipazine (PrOM-NQP) **48** following deprotection and nitration. With the extended side chain, the introduction of the tosylate leaving group proceeded smoothly and precursor **49** for radiolabelling was generated in 3 steps from **48**. Depending on the method of synthesis, an *N*-*tert*-butoxycarbonyl (N-Boc) or *N*-Formyl protecting group (PG) was utilized. The conversion of **49** to 2'-(3-fluoro-1-propyl)-6-nitroquipazine (ProF-NQP) **50** was accomplished using nucleophilic fluoride ion from tetrabutylammonium fluoride (TBAF) in THF. Radiochemical studies with the compound are ongoing and an optimization of the synthesis to obtain a fluorine-18 radiotracer is forthcoming.⁷⁴

The synthetic studies described herein detail the efforts to generate SERT PET agents from our refined lead agent MOM-NQP **35**.

2.2 Generation of N-Boc-2'-Hydroxymethyl-6-Nitroquipazine

To afford plausible radiotracers, the synthetic plans must meet certain criteria. Mainly, because of the short half-life of the carbon-11 and fluorine-18 atoms, the radionuclide group must be introduced very late in the synthesis, ideally as a last step. This is a necessary criterion since the short half-lives of the radionuclides ($[^{18}\text{F}] t_{1/2} = 110 \text{ min}$; $[^{11}\text{C}] t_{1/2} = 20.4 \text{ min}$) require that the formation of the radioactive atom, synthesis of the radiochemical tracer and PET

experiment all be accomplished in a short period of time (4 – 5 half-lives of the respective radionuclide). The subsequent removal of any protecting groups should also be fast and the purifications uncomplicated so reaction times can be minimized. To fulfill these criteria, an alkylation strategy was considered whereby a [^{11}C]-methyl group could be introduced on the side chain using routine synthetic protocols, followed by removal of an appropriate nitrogen protecting group (PG) to afford the desired radiotracer [^{11}C]35 (Figure 2.3).

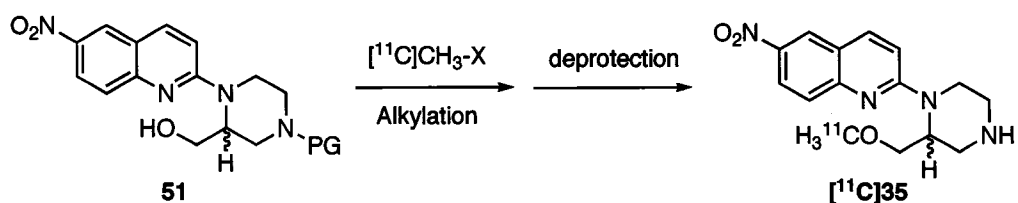


Figure 2.3: Synthetic strategy devised for the synthesis of [^{11}C]MOM-NQP.

Initial studies from our laboratory aimed at generating a protected hydroxymethyl-nitroquinoline **51** met with only mediocre success. For example, attempts at generating ethyl 2'-carboxylate-6-nitroquipazine **53** that could be reduced to alcohol **51** were unsuccessful (Figure 2.4, unpublished results). Thus, alternate methods were investigated that began from lead compound **35** and necessitated O-dealkylation technologies.

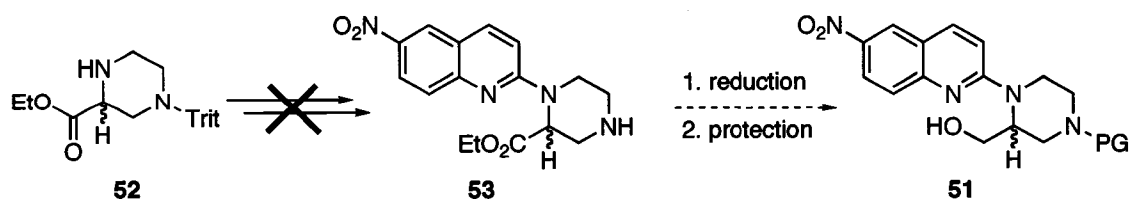


Figure 2.4: Failed, previously attempted route for acquiring an alcohol intermediate.

Trimethylsilyl iodide (TMS-I) is a reagent well characterized in its ability to afford O-dealkylation under generally mild conditions.^{75, 76} TMS-I is commercially available, but it can also be generated *in situ* through the reaction of TMS-Cl with NaI in toluene.⁷⁷ In our hands however, this reagent gave unsatisfactory results (yields < 20%) with unnitrated quipazine **34** yielding only a poor yield of alcohol **54** (Figure 2.5).⁶⁷ In hindsight, the poor yields may have resulted from the lack of a protecting group on the secondary nitrogen. However, this notion has yet to be fully investigated and alternate methods have been considered.

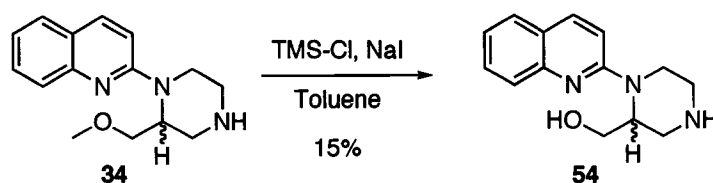
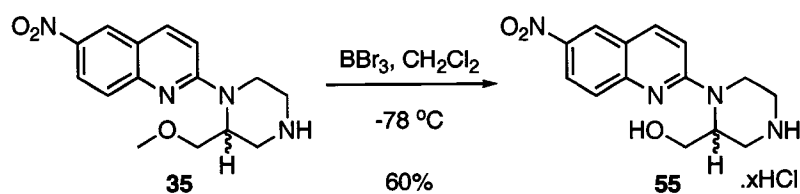


Figure 2.5: TMS-I promoted dealkylation reaction attempted by Walker.⁶⁷

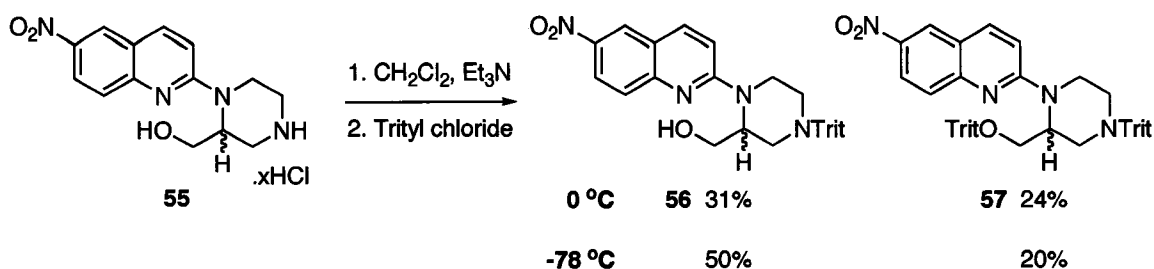
Boron tribromide (BBr₃) is another common O-dealkylation reagent and it is most commonly utilized for the demethylation of phenols.^{78, 79} However, there are reports in the literature of BBr₃ use for the demethylation of aliphatic ethers, which provided good yields of target alcohols.⁸⁰ A BBr₃ dealkylation was attempted with MOM-NQP **35** using 400 mol% of BBr₃ (1 M in CH₂Cl₂) in CH₂Cl₂ (DCM) at -78 °C. Excess BBr₃ was used so that coordination of the reagent to the other electron donors would not inhibit reactivity with the methyl ether.⁷⁸



Scheme 2.1: Boron tribromide mediated demethylation of MOM-NQP.

These conditions resulted in good conversion to alcohol **55** and the product was isolated as a hydrochloride salt through a forced crystallization from EtOH/HCl_(g) with ether. Product identity was assigned based on the disappearance of the methyl singlet and a TLC profile that showed a more polar material (as the free base) relative to starting material (R_f of 0.04 vs. 0.15; MeOH:DCM, 1:9). With the alcohol in hand, it was now necessary to choose a nitrogen protecting group that could easily be removed and would withstand the conditions necessary for O-alkylation (base and electrophile, CH₃-X).

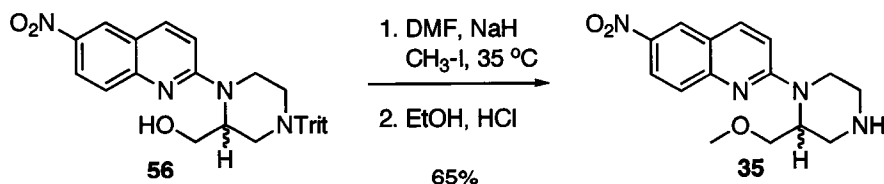
The triphenylmethyl (trityl) protecting group was chosen initially because it met these general criteria and was a reagent with which we were familiar from previous work in our lab (e.g. Figure 1.12).⁶⁷ The nitrogen protection was attempted using the method of Rondu⁶⁸ which employed trityl chloride in DCM with triethylamine at 0 °C. These reaction conditions provided a poor yield of the desired N-trityl protected alcohol **56** because of a competing reaction with the primary alcohol to provide di-protected product **57** (Scheme 2.2). Products **56** and **57** were easily separated (column chromatography) and their ¹H NMR spectra clearly indicated the presence of a single protecting group and two protecting groups, respectively.



Scheme 2.2: Formation of N-trityl protected alcohol.

An attempt to minimize the alcohol reactivity by lowering the temperature to $-78\text{ }^\circ\text{C}$ only improved the yield of desired product slightly, providing milligram quantities of **56** in 50% yield.

With N-trityl alcohol **56** generated, it was time to attempt our cold radiosynthetic strategy (Figure 2.3) to reintroduce the methyl group and remove the trityl protecting group. The alkylation of **56** was first attempted in tetrahydrofuran (THF) with NaH as the base followed by the addition of methyl iodide at $35\text{ }^\circ\text{C}$. Although conversion to the methyl ether occurred, the reaction was slow and required an overnight stir to reach completion. Another attempt was made using DMF as a solvent with excess NaH (3000 mol%) and methyl iodide (800 mol%) (Scheme 2.3).⁸¹



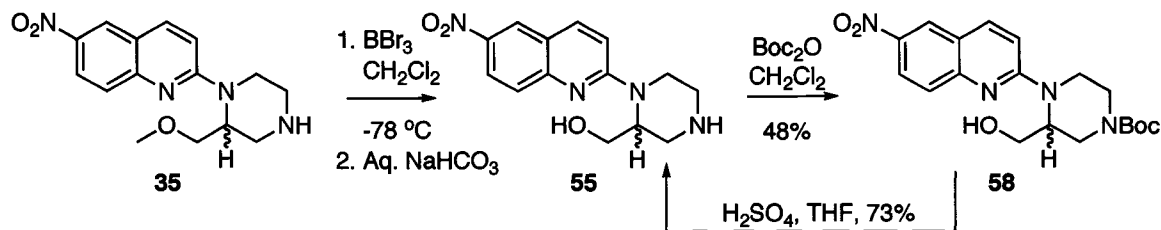
Scheme 2.3: 'Cold' radiochemical synthesis of MOM-NQP from the N-trityl protected alcohol.

Following the addition of reagents, the reaction was heated (35 °C) briefly and a check by TLC after five minutes showed that the starting material had been consumed, and the alkylated product had formed. After work-up, the crude reaction mixture was immediately subjected to deprotection conditions (EtOH, HCl, 10 min) to remove the trityl group. Work-up and chromatography provided lead agent MOM-NQP **35** in 65% yield (Scheme 2.3). The ¹H NMR spectrum of **35** was identical to that produced according to Walker as described in Chapter 1.⁶⁷

This synthesis validated our radiosynthetic strategy for the generation of [¹¹C]**35**. Furthermore, the transformations were accomplished quickly, with reaction times being less than ten minutes. However, we were still disadvantaged by the lack of regioselectivity in our N-trityl protection that provided only a modest chemical yield of protected target **56**. At this time other efforts within our laboratory demonstrated the usefulness of the *tert*-butylcarbamate (Boc) group for the protection of the secondary amine functionality in our quipazine compounds. The introduction of this group proceeded smoothly using di-*tert*-butyldicarbonate (Boc₂O) in DCM followed by concentration of the reaction mixture and chromatography of the residue.⁸² This was an attractive alternative sequence to the trityl synthesis since Boc groups are well known for their tolerance of aqueous environments⁸³ and they could likely be introduced in the workup of the boron tribromide demethylation reaction. Additionally, the Boc deprotection products (CO₂ and isobutylene) are gaseous

and easily removed from the reaction mixture, simplifying the purification process for target **35**.

The initial attempt of this reaction sequence using 500 mol% BBr₃ (1 M solution in DCM) and 180 mol% of di-*tert*-butyldicarbonate provided a modest yield of N-Boc protected product **58** (Scheme 2.4).



Scheme 2.4: Synthesis of key intermediate **58**, HOM-BOC-NQP.

Pure, free-base form, amino alcohol **55** can be isolated by deprotection of the Boc group with 4 M sulfuric acid in THF. The identity of **58** was confirmed primarily from LC/TOF-MS data, which provided a molecular weight of 388, that was consistent target molecule **58**. Analysis by ¹H NMR was problematic since the incorporation of the *tert*-butylcarbamate protecting group had a profound broadening effect on the piperazine hydrogen signals, and to a lesser extent on the aromatic signals. However, the absence of a methyl singlet (expected at 3.2 – 3.7 ppm) and the presence of the *tert*-butyl group singlet (~1.5 ppm) accompanied with all of the quinoline resonances was enough for us to proceed with confidence that compound **58** had been formed.

The ¹H NMR spectra of **58** in comparison to the deprotected amino alcohol **55** are shown in Figure 2.6, where line broadening of the Boc-intermediate (upper panel) is shown.

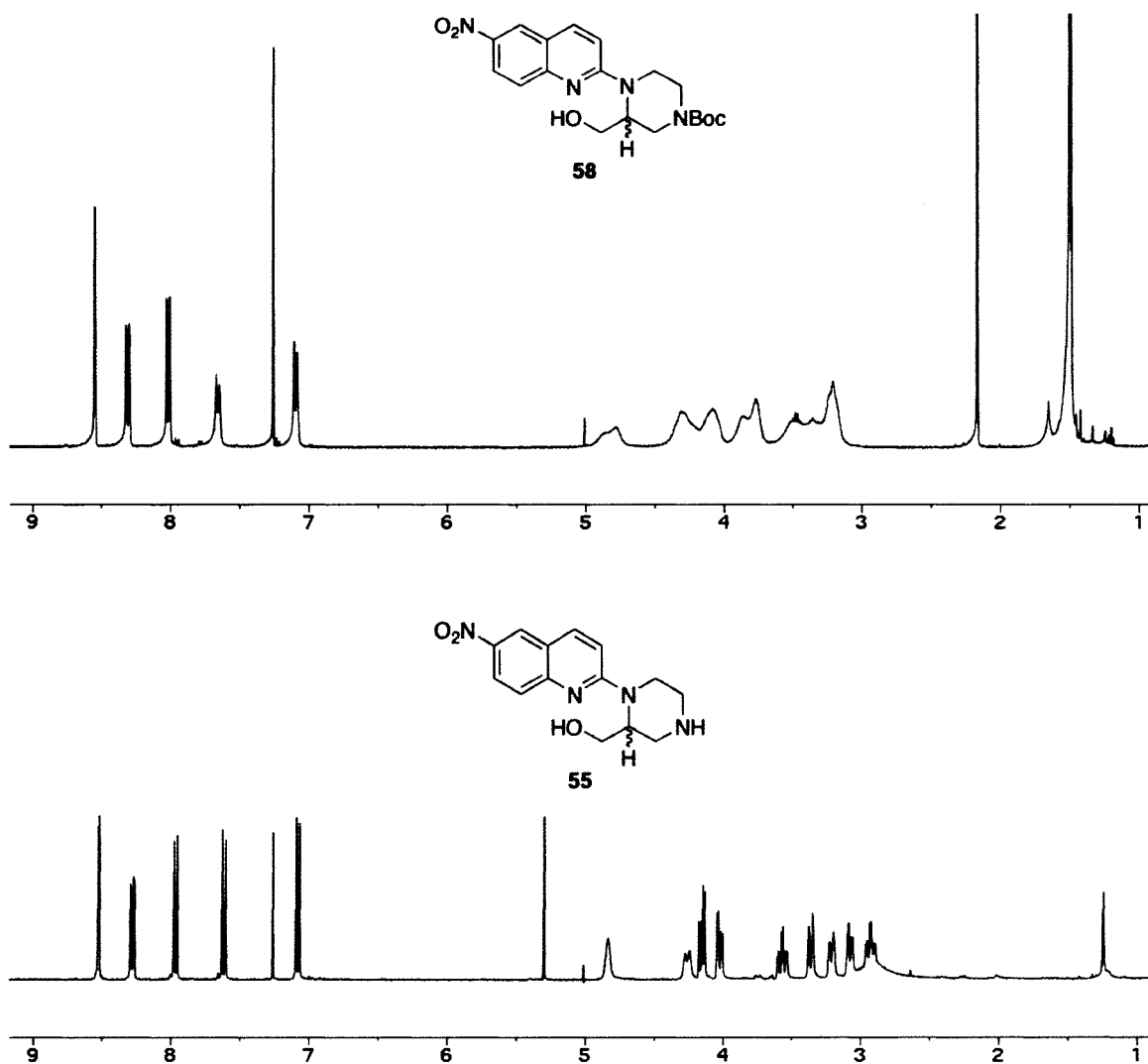


Figure 2.6: ¹H NMR spectra of N-Boc protected alcohol **58** (top) and amino alcohol **55** (bottom) demonstrating the line broadening observed as a result of the introduction of the N-Boc protecting group. The scale is in δ ppm.

The differences in the resolution of the piperazine protons is clearly observed and this broadening has been consistent across all Boc protected compounds in the quipazine series. This broadening effect is also transferred to the carbon atoms and a similar comparison can be made with the ¹³C NMR spectra of the same compounds (Figure 2.7).

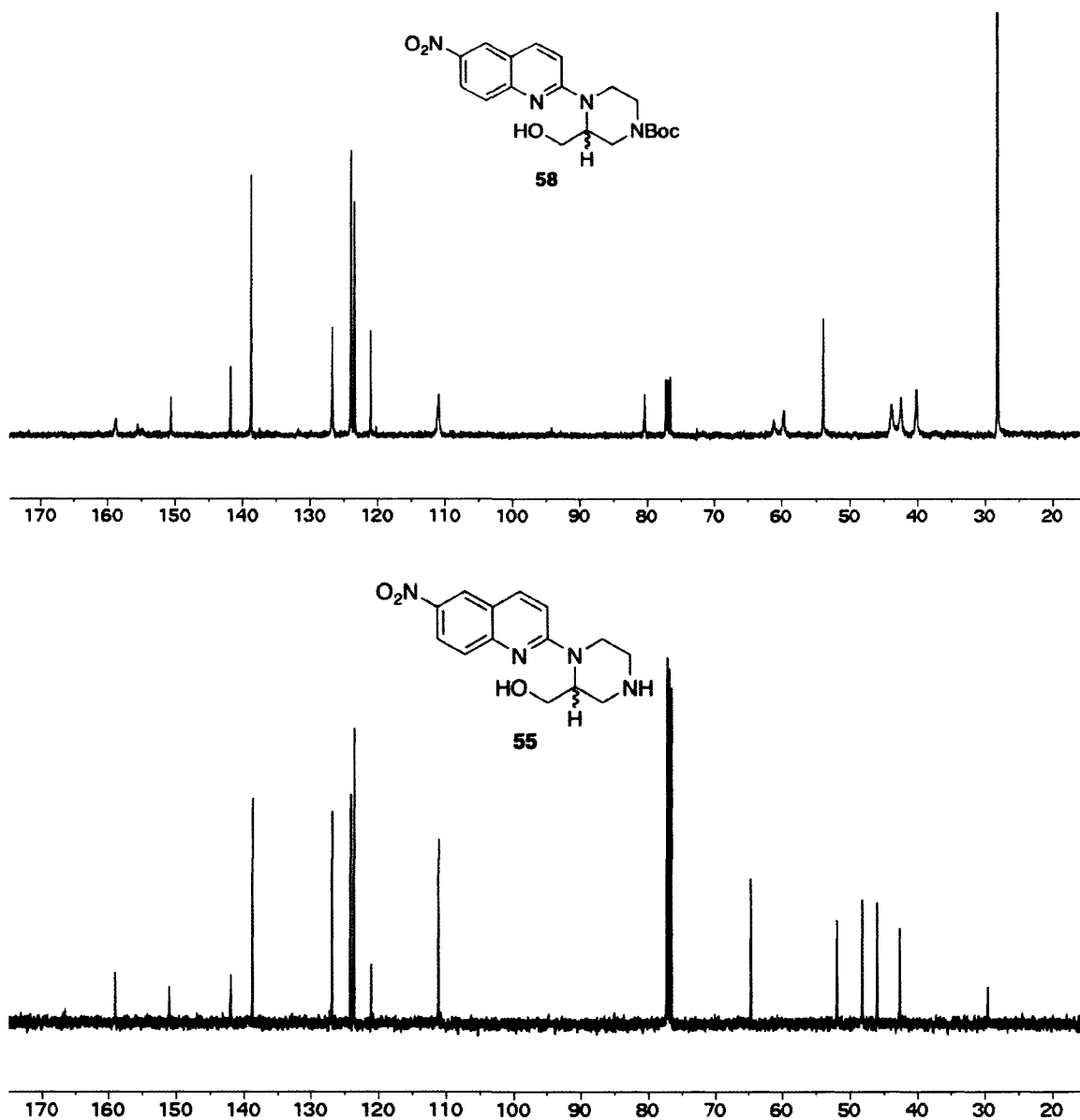
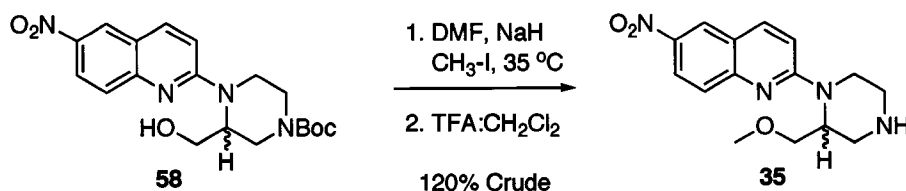


Figure 2.7: ¹³C NMR spectra of N-Boc protected alcohol **58** (top) and amino alcohol **55** (bottom) demonstrating the line broadening observed as a result of the introduction of the N-Boc protecting group. The scale is in δ ppm.

Ultimately, the confirmation of product identity came from the independent synthesis of the methyl ether to form **35** using the same strategy that was employed for the N-trityl protected alcohol **56**. A clean conversion to the methyl ether was accomplished using 250 mol% NaH, and ~600 mol% CH₃-I in DMF

(reduced quantities vs. N-Trityl reaction). The crude Boc protected intermediate (not shown) was treated with trifluoroacetic acid (TFA in DCM, 1:1)⁸⁴ at ambient temperature until complete conversion to the secondary amine (more polar) was observed by TLC (~1 h). A basic workup provided the crude material that was unambiguously identified as desired target **35** by ¹H NMR (Scheme 2.5).



Scheme 2.5: 'Cold' radiosynthesis of MOM-NQP using the N-Boc protected alcohol.

This experiment was evidence enough that we had developed a methodology that could be adapted to the synthesis of [¹¹C]**35**. Adequate quantities of radiolabelling precursor **58** could be generated so that radiochemical experiments by collaborators at the Lawrence Berkeley National Laboratory (LBNL) could commence. These experiments are detailed in Section 2.7.

2.3 Synthesis of (rac)-MeProF and a Tosylate Precursor for the Radiosynthesis of [¹⁸F](rac)-MeProF

Other concurrent efforts within our laboratory were focused on the synthesis of the fluorine-18 agent [¹⁸F]2'-(3-fluoropropyl)-6-nitroquipazine [¹⁸F]**50** ([¹⁸F]ProF-NQP, shown in Figure 2.8a) as per Figure 2.2. However, preliminary results from our radiochemical collaborators at LBNL indicated some

decomposition and side reaction complications during the radiosynthesis.⁷⁴ Consequently, avenues toward other fluorine-18 ligands were considered.

We decided to append a fluoroalkyl side chain onto the primary alcohol of our N-Boc intermediate **58**. In this way we had the opportunity to gain multiple agents **59** – **61** from a common intermediate (Figure 2.8b).

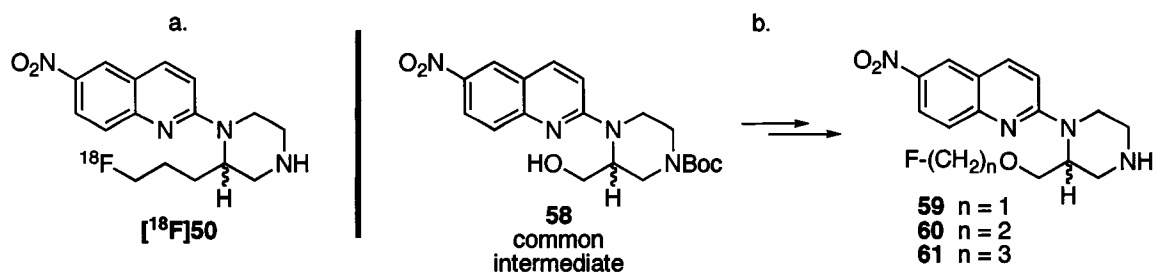


Figure 2.8: a) [¹⁸F]ProF-NQP; b) Alkylation strategy to afford fluoroalkyl ethers.

Thus far, these routes have proven quite unsuccessful. The Boc protected fluoromethyl ether ($n = 1$, **62**) was readily formed in a reaction of **58** with FCH₂Cl in DMF with NaH as the base. However, the ether side chain did not survive the Boc deprotection step under a number of different conditions (Figure 2.9).

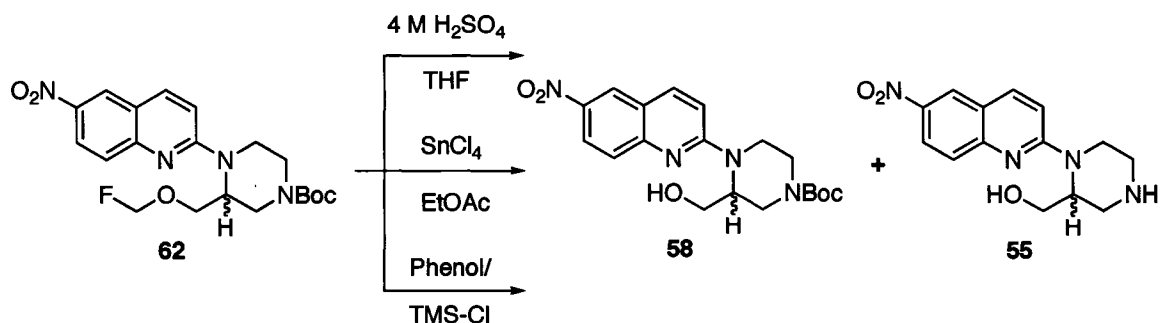
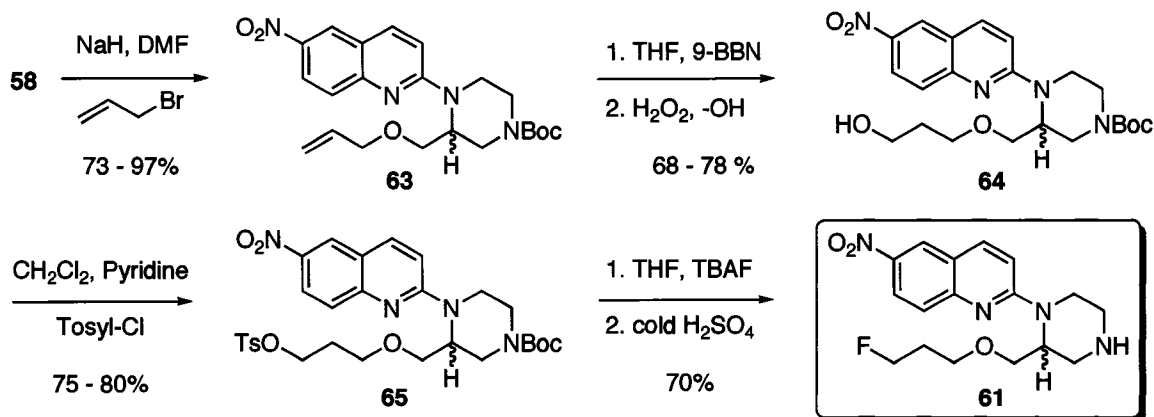


Figure 2.9: Attempted Boc deprotection conditions for the formation of fluoromethyl target **59**.

The conditions included; 4 M H₂SO₄ in THF at 50 °C and 0 °C, SnCl₄ in EtOAc⁸⁵ and TMS-Cl/Phenol⁸⁶. Under all of these conditions, the fluoromethyl ether cleaved in preference to removal of the Boc group to give intermediate **58** and/or amino alcohol **55**. With these results, we abandoned our efforts at generating fluoromethyl ether **59**. Attempts to alkylate the N-trityl protected alcohol **56** with bromofluoroethane (n =2) under DMF/NaH and THF/NaH conditions failed for unknown reasons, resulting with the generation of multiple side products as observed by TLC. Since these reactions were attempted on a small scale (< 10 mg), characterizations of the reaction products were not attempted. Efforts to alkylate Boc alcohol **58** with bromofluoroethane to generate compound **60** are currently underway at LBNL with our collaborator Dr. Andy Gibbs. The reaction of **58** with bromofluoropropane in DMF with NaH failed to produce the Boc protected fluoropropyl ether (structure not shown), and only recovered starting material was obtained. Although it was never investigated in detail, it is suspected that lack of conversion to the propyl ether resulted from the alkoxide acting as a base rather than a nucleophile.

Since these alkylation attempts were not efficacious, a new synthetic strategy was devised which would afford the fluoropropyl target, 2'-(3-fluoropropoxymethyl)-6-nitroquipazine (MeProF-NQP, **61**). Key to this new approach was the use of allyl bromide in the alkylation step which reduced the possibility of elimination reactions competing with substitution. Importantly, this synthesis generated Boc-Tosylate **65** that later served as the precursor for radiofluorination and the generation of [¹⁸F]MeProF-NQP [¹⁸F]**61** (Scheme 2.6).

Alkylation of Boc alcohol **58** with allyl bromide provided allyl ether **63** in good to almost quantitative yields following chromatography.



Scheme 2.6: Synthesis of racemic MeProF-NQP.

Hydroboration of the terminal alkene with 9-borabicyclo[3.3.1]nonane (9-BBN),⁸⁷ followed by alkaline peroxide oxidation provided primary alcohol **64**. Conversion of **64** to tosylate **65** was accomplished with tosyl chloride and pyridine in DCM in good yield. Displacement of the tosylate with nucleophilic fluoride ion was accomplished with 150 mol% of tetrabutylammonium fluoride (TBAF) in THF at 60 °C.⁸⁸ After chromatography, the Boc protected fluoroalkyl intermediate (structure not shown) was deprotected to provide target compound **61** in 70% yield. Incorporation of the fluorine atom was very efficient, and no detectible traces of alkene were observed (¹H NMR) as a result of fluoride promoted elimination which has been characterized as a common side reaction in nucleophilic fluoride transformations.⁸⁹ Side chain identity was confirmed based on the ¹H NMR spectrum of **61** which shows doublet of triplet and doublet of pentet hydrogen signals that were split by the fluorine for the geminal and

vicinal (relative to fluorine) hydrogens, respectively, indicating that the fluorine atom was at the end of the propyl chain (Figure 2.10).

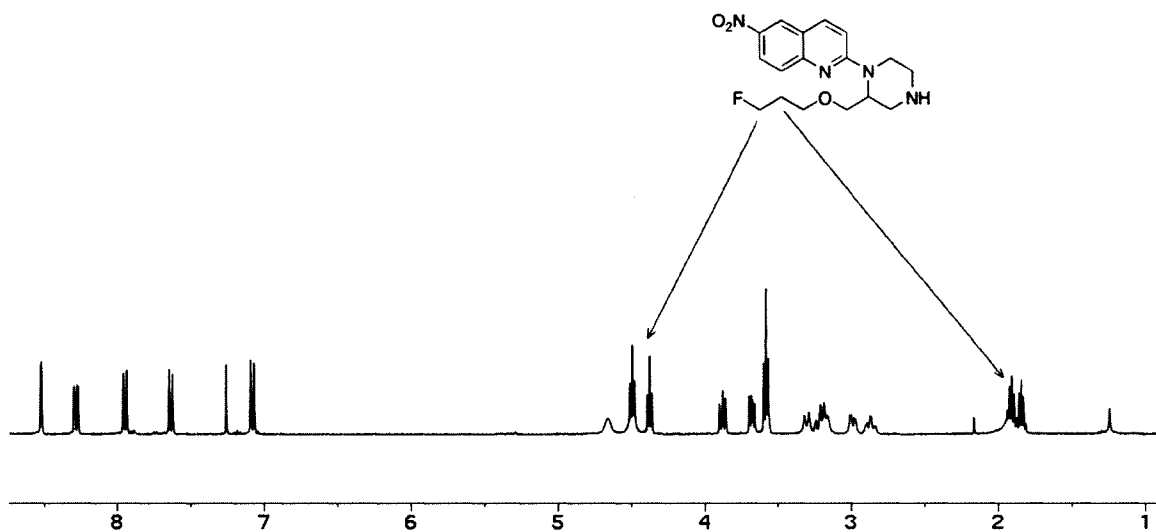
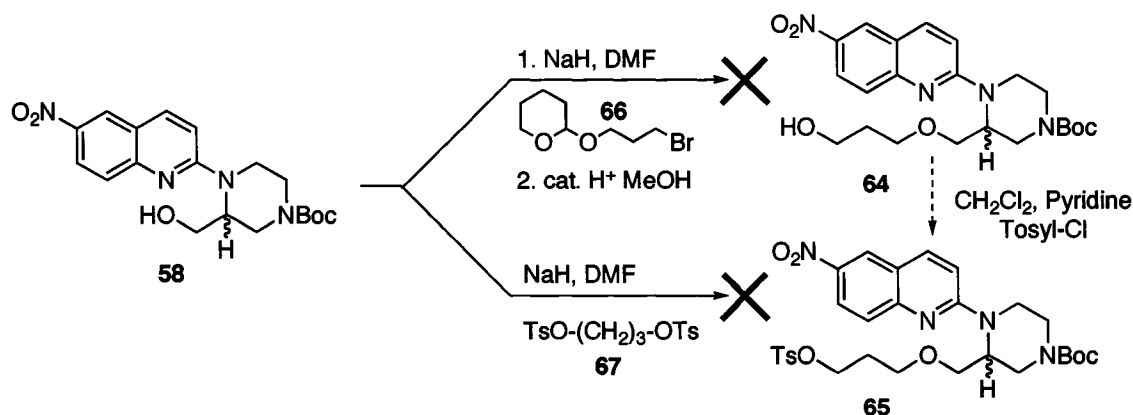


Figure 2.10: ¹H NMR of MeProF-NQP **61**, with the fluorine-coupled hydrogen resonances indicated. The scale is in δ ppm.

For this new synthetic approach, our target ligand MeProF-NQP **61** was synthesized in five steps from intermediate Boc alcohol **58**. The yield for this process on average was 32%. However, given optimal yields for each step, this yield can be as high as 45%,

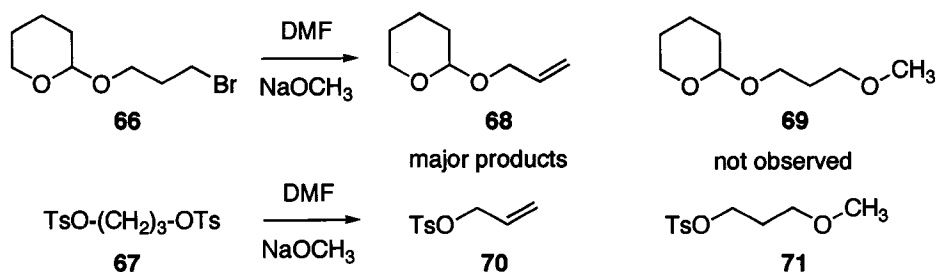
Other alkylation methodologies were attempted to short-cut the approach of Scheme 2.6 by synthesizing propyl alcohol **64** or tosylate **65** directly from protected alcohol **58**. As shown in Scheme 2.7, tetrahydropyranyl (THP) protected 3-bromopropanol **66** and 1,3-propanediol di-p-tosylate **67** were used as alkylating agents in these reactions. Unfortunately, these attempts provided the same poor results that were observed with bromofluoropropane (as per Figure 2.8), with no significant product formation seen. To test our hypothesis that we were seeing a lack of substitution due to competing alkoxide elimination

reactions, control reactions were performed with the more nucleophilic alkoxide, methoxide ion.



Scheme 2.7: Attempted 'short-cut' alkylations to obtain intermediates in the synthesis of MeProF-NQP.

The electrophiles **66** and **67** were added to NaOCH₃ in DMF in an identical manner to the alkylation strategies employed for **58** (as per Scheme 2.7) and the crude reaction mixtures were analyzed by ¹H NMR (Scheme 2.8).



Scheme 2.8: Control reactions to evaluate the ability of methoxide ion to evoke S_N2 substitution on our 'short-cut' electrophiles.

In both cases, the predominate product formed was the alkene (**68** or **70**) and little substitution product (**69** or **71**) was observed, as evidenced by a lack of a strong singlet at 3.0 – 3.5 ppm in the ¹H NMR spectra of the crude reaction mixtures. Based on these results, our original synthetic plan (Scheme 2.6) was

maintained to produce our target, MeProF-NQP **61**. Additionally, intermediate tosylate **65** proved to be an excellent radiochemical precursor for the radiofluorination reactions performed at LBNL. The successes in forming [^{18}F]MeProF as well as its preliminary *in vivo* performance in rat will be detailed in Section 2.7 and Chapter 5, respectively.

2.4 Synthesis of 2'-(2-Methoxyethyl)-6-nitroquipazine: EtOMe-NQP

The synthesis of the methoxyethyl side-chain analog of 6-nitroquipazine was desired as an alternative route to additional PET imaging agents. However, ethyl analog **78** was also desired as a part of a larger structure activity relationship (SAR) study to explore the size of the Ar2 SERT binding region (as per Figure 1.11). The Ar2 region is presumed to accommodate our piperazine side chains (Figure 2.11).⁷⁴

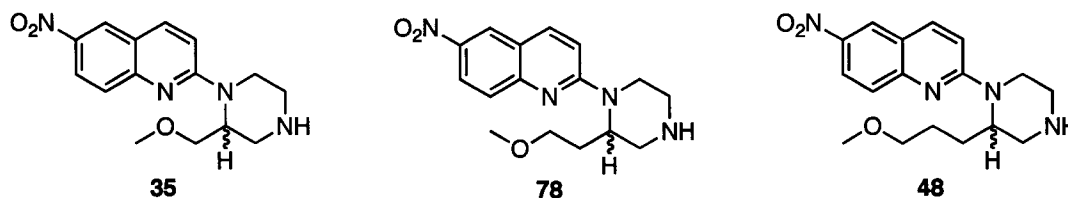
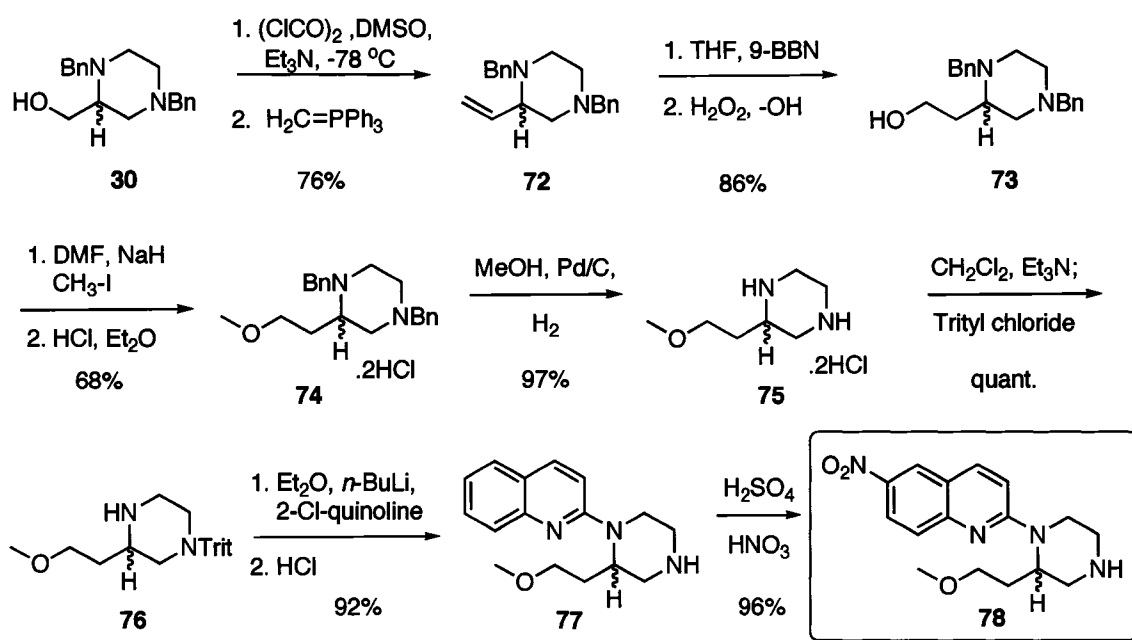


Figure 2.11: Methyl, ethyl and propyl side chain quipazines to study the Ar2 region SAR.

Since the Ar2 region of the SERT pharmacophore is represented by aromatic ring groups in a majority of commercial and non-commercial ligands (as per discussions in Chapter 1), we had hoped to better understand the limits of the Ar2 binding region as our alkyl side chains extend beyond the volume occupied by the more common, aromatic side chains. Additionally, we sought to

better understand the role of the side chain oxygen heteroatom for modulating the binding affinity of our ligands at SERT. The ethyl side chain compound **78** would place the oxygen one atom further away from the piperazine headgroup relative to **35** and may provide us with insight into the subtle SERT binding characteristics of this ligand region.

The synthesis of **78** was modeled on the chemistry utilized to synthesize lead compound **35**, with only minimal changes made to the previous procedure (Scheme 2.9).⁶⁷



Scheme 2.9: Synthesis of EtOMe-NQP that was modeled after Walker's⁶⁷ synthesis of MOM-NQP **35** (Figure 1.12).

An intermediate in the synthesis of **35**, 1,4-dibenzyl-2-hydroxymethylpiperazine **30**,⁹⁰ was the chosen starting material for this sequence, and the addition of a carbon to the side chain was accomplished through an oxidation-homologation sequence. Compound **30** was subjected to

Swern oxidation conditions, according to Kusche,⁷⁴ to generate the intermediate aldehyde (not shown). Following the workup and evaporation of the extraction solvent, the crude aldehyde material was pumped under high vacuum for ~10 minutes then immediately used in a Wittig reaction with 200 mol% of ylide to give alkene **72** in a 76% combined yield. The alkene **72** underwent hydroboration with 9-BBN, and oxidation with alkaline hydrogen peroxide afforded primary alcohol **73** in excellent yield. From here forward, the synthesis parallels the methods used by Walker to form lead agent **35**.⁶⁷ The alkylation of alcohol **73** to provide methyl ether **74** was performed with DMF as a solvent rather than THF as had been utilized previously for the synthesis of **35**. The more polar DMF solvent greatly increased the reaction rate (1 h vs. 16 h) and simplified the work-up. DMF could easily be removed by flooding with two volumes each of water and saturated NaHCO₃, then and extracting the product with ether. Following chromatography, free base form **74** was dissolved in ether and the solution saturated with HCl_(g) to produce dihydrochloride **74**.

The benzyl groups were removed by catalytic hydrogenolysis using 5% Pd/C in MeOH, with balloon pressure of hydrogen to afford **75**. The trityl group was selectively introduced to the 4-position of the piperazine to provide **76** by the reaction of trityl chloride in DCM with Et₃N.⁶⁸ In general, the crude material from the tritylation reactions was usually of sufficient purity for the subsequent quinoline coupling step. However, should these intermediates require purification, the stationary phase must be something other than silica gel, or deprotection of the trityl group will result. Our lab has discovered that using basic

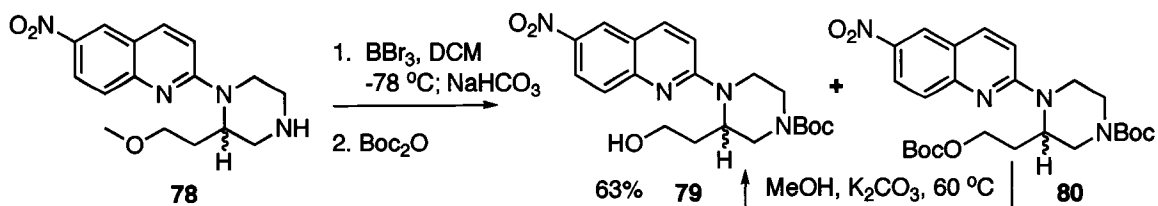
alumina as a stationary phase, with mixtures of chloroform and ethyl acetate as eluent is a suitable replacement, and provides efficient separations of N-trityl protected piperazines.

The coupling of compound **76** to 2-chloroquinoline was performed according to the method of Gilman, who in the 1940's, described an efficient coupling of simple lithium di-alkylamides to 2-chloroquinoline.⁶⁹ A detailed discussion of this reaction follows (Section 2.5). Briefly, a solution of 2-chloroquinoline (100 mol%) in ether was added to an ethereal solution of 150 mol% each of piperazine **76** and *n*-butyllithium at 0 °C. Following the work-up, chromatography, and removal of the trityl protecting group, compound **77** was isolated in 92 % yield. Nitration of this material provided the target quipazine EtOMe-NQP **78** in excellent yield. The overall synthesis of **78** was accomplished in eight steps with an overall yield of 38%.

The protocol used for the removal of the trityl group to form **77** was significantly improved relative to earlier work in our laboratory.⁶⁷ The previous procedure utilized 6 M HCl in ethanol, followed by a base quench and extraction to give the crude product that contained trityl left-overs and required column chromatography for purification. This method worked well, providing yields around 80%. However, the polarity of the deprotected secondary amine made normal phase purification of desired product **77** difficult. Very polar MeOH:DCM solvent mixtures were required to elute the product and excessive tailing of material **77** was observed. The improved procedure used 6 M HCl (6 mL) added to a solution of trityl protected quipazine (structure not shown) in a minimal

amount of acetone (3 – 4 mL). The mixture was swirled or stirred for only a few minutes, then diluted with 20 – 30 mL of 1 M HCl. Washing the acidic, aqueous mixture with DCM removed all traces of the trityl side products and upon returning the aqueous layer to basic pH with 4 N NaOH and saturated NaHCO₃, the pure, deprotected quipazine **77** could be extracted with DCM.

With the synthesis of our ethyl homolog **78** complete, we turned our attention again to the preparation of potential radiolabelling precursors that might afford us new fluorine-18 or carbon-11 PET agents. Compound **78** was converted to the Boc-protected alcohol **79** using the same dealkylation strategy developed for key intermediate **58** and the demethylation reaction with BBr₃ provided an efficient conversion of ether **78** to the primary alcohol (Scheme 2.10).



Scheme 2.10: Synthesis of N-Boc protected ethyl alcohol.

However, unlike the formation of methyl alcohol **58**, the N-Boc protection of the crude ethyl alcohol (structure not shown) was not regioselective for the nitrogen and, in addition to desired target **79**, a di-Boc protected product **80** was also formed. This reactivity is also observed for longer alkyl chains (3 carbons and more).⁷⁴ Presumably the ethyl side chain provides reduced steric influences that hinder attack for the methyl alcohol side chain and limit the formation of a di-

Boc derivative. Both Boc protected compounds (**79** and **80**) were collected together following chromatography and treated with excess K_2CO_3 in MeOH at 60 °C. These conditions resulted in the selective deprotection of the carbonate after ~3 h and provided **79** in 63% yield.

The alkylation of **79** to generate parent methyl ether **78** using the non-radioactive (cold) methods described in Scheme 2.5 has not yet been attempted. Furthermore, no radiochemical studies have been planned with this material to generate a carbon-11 agent. Interestingly, two separate experiments to convert the alcohol into a tosylate-leaving group for fluorination attempts have failed, using the same conditions that readily formed tosylate **65**. No product was ever identified and the starting material was not recovered in any significant quantity. This curious reactivity is still under investigation within our laboratory, and opportunities for undesired intramolecular reactivities are being considered.

2.5 Gilman Quinoline Coupling Mechanistic Considerations

Earlier work in our laboratory⁶⁷ has demonstrated that the Gilman coupling reaction⁶⁹ is highly sensitive to the ratios of reactants. Deviations from the reported ratios (150 mol% each of amine and *n*-BuLi to 100 mol% 2-chloroquinoline **81**) significantly reduced the yield of coupled product. A mechanism was suggested that sought to explain this sensitivity, that also incorporated the formation of a reactive, aryne intermediate specie (Figure 2.12).⁶⁷

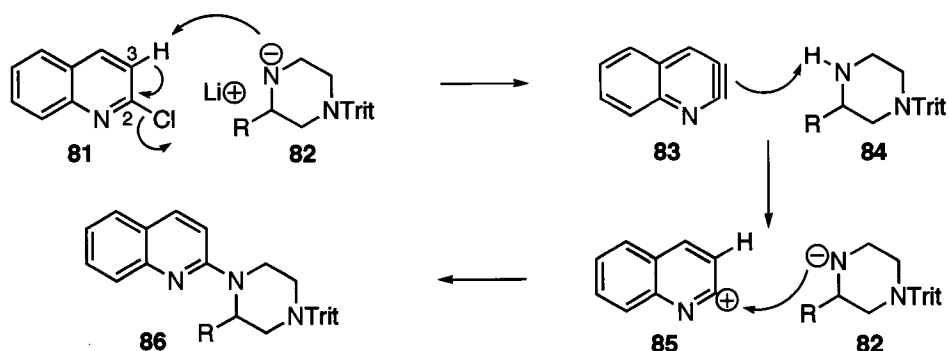


Figure 2.12: The elimination-addition Gilman coupling mechanism proposed by Walker,⁶⁷ demonstrated with a general N-trityl protected piperazine.

The proposed mechanism begins with the removal of the 3-position hydrogen of **81** by lithium amide **82** to eliminate the chlorine atom and form aryne intermediate **83**. Intermediate **83** then undergoes protonation from amine **84** to form charged intermediates **82** and **85** that combine to form the coupled product **86**. Although the mechanism seems plausible, there is nothing to suggest the need for an extra 50 mol% of lithium amide **82** to afford efficient conversion to **86** (as suggested by the strict adherence to reagent ratios). Additionally, it is believed that nucleophilic attack on arynes (like **83**) precedes the protonation step in elimination-addition type mechanisms.⁹¹

An alternate mechanistic explanation (Figure 2.13) addresses these concerns by suggesting a need for excess amide **82** to act as a proton transfer agent in the reaction. Furthermore, the mechanism also provides for a nucleophilic attack on aryne **83** by amide **82**.

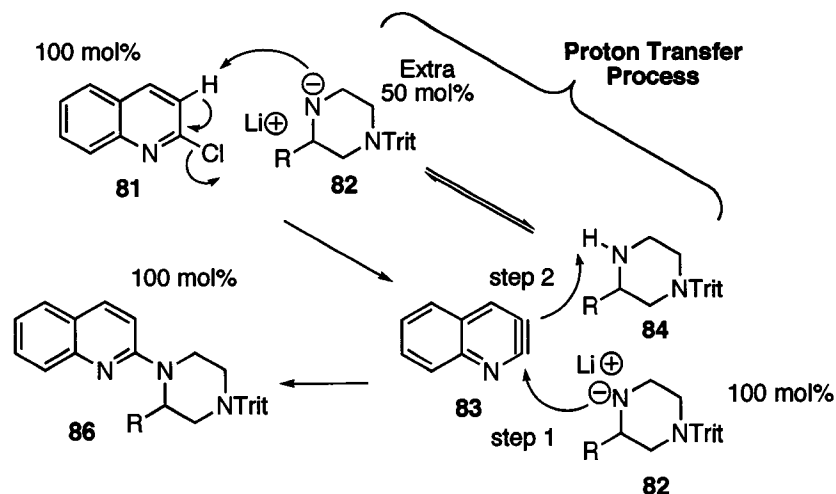


Figure 2.13: Alternate mechanistic explanation for the extra 50 mol% of lithium amide.

For this mechanism, excess amide **82** (extra 50 mol%, top-center) serves as a proton acceptor-donor, initially generating aryne **83**, then protonating (as conjugate acid **84**, step 2) the 3-position of the quinoline ring following nucleophilic attack of amide **82** at the 2-position (step 1). The proposed *proton transfer process* ensures that a nucleophilic specie will attack aryne **83** and also suggests an explanation for the need of excess **82**.

Although the above mechanism may provide a better explanation than Walker's⁶⁷ for the sensitivity of the Gilman coupling to the stoichiometry of the reactants, it does not account for the explicit regioselectivity for substitution at the 2-position of quinoline **81**. It is known that nucleophilic attacks on arynes typically produce two or more regioisomeric products as a result of reactivity at both ends of the triple bond.⁹² This was in fact how the benzyne intermediate was discovered, when attempts at doing nucleophilic substitution reactions on aromatic halides produced multiple regioisomeric products.⁹³ Furthermore, it has

been shown that substituent effects can influence the preferred side of nucleophilic attack. However, the regioselectivity is rarely shown to be high.⁹⁴

Connon and Hagarty have suggested that 2,3-pyridynes **87** may experience bond polarization as the result of the electron withdrawing effect of the ring nitrogen to generate the dipolar specie **87a** (Figure 2.14).⁹⁵ Provided this opportunity, it is reasonable to suggest that a nucleophilic attack on **83** would favor substitution at the 2-position as a result of the dipolar character of **83a** (Figure 2.14). However, the degree to which this may be favored is not clear.

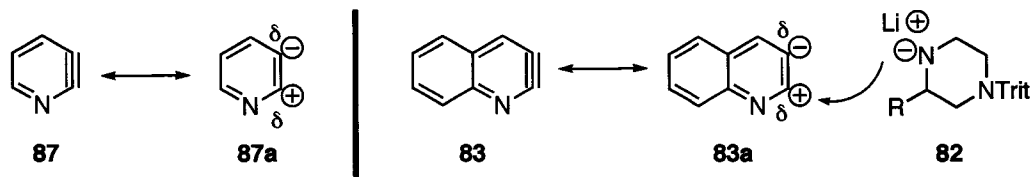
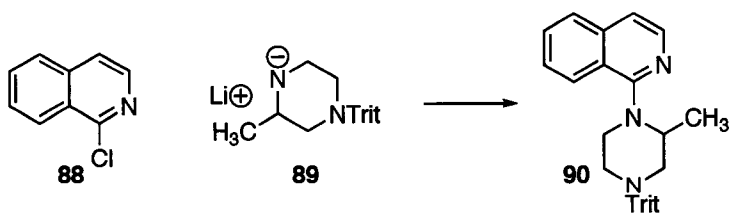


Figure 2.14: Proposed dipolar character of 2,3-pyridynes as an explanation for Gilman coupling regioselectivity for substitution at the 2-position of quinoline.

Another, recent observation from our laboratory was the conversion of 1-chloroisoquinoline **88** and lithium amide **89** to coupled material **90** in excellent yield using the same Gilman conditions as described above (Scheme 2.11).



Scheme 2.11: Another coupling, facilitated by the Gilman conditions, that is unable to proceed under benzyne-type conditions.

Since **88** cannot react in a benzyne-type mechanism, a different mechanism must be operating. Simple nucleophilic aromatic substitution (S_NAr) may be the mechanism operating, and this is also a very plausible mechanism for our Gilman coupling using quinoline **81** (Figure 2.15).

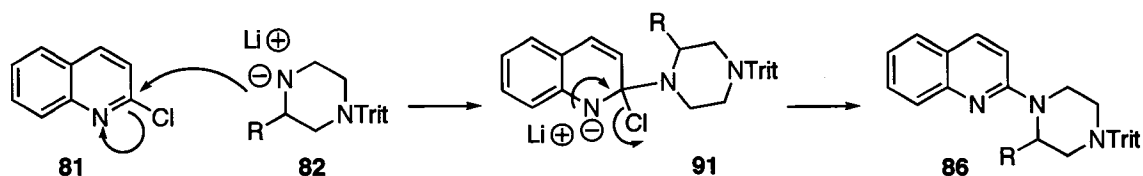


Figure 2.15: Nucleophilic aromatic substitution (S_NAr) mechanism for the Gilman coupling reaction.

However, the S_NAr mechanism still does not explain why the Gilman coupling is highly sensitive to reactant stoichiometry. Clearly, more detailed experiments aimed at discovering the actual mechanistic details are required. Benzyne are known to undergo [4 + 2] cycloadditions^{92, 95} and trapping experiments with furan or other dienes could be performed to detect the formation of aryne intermediate **83**.

2.6 The Boron Tribromide Dealkylation: Reaction Complications and Inconsistencies

The boron tribromide dealkylation reaction (Scheme 2.4 and Scheme 2.10) has led to frustration on a number of occasions because the reaction outcome is not consistent. The conversion has been attempted with a methoxy methyl side chain a total of eighteen times with an average yield of 48% for Boc alcohol **58**. However, across all of these synthetic attempts the range of yields

extends from 0 – 70%. The conditions for this reaction had 500 – 600 mol% of BBr_3 added to a $-78\text{ }^\circ\text{C}$ solution of ether **35** in DCM. The mixture was maintained at $-78\text{ }^\circ\text{C}$ for 3 – 4 h then warmed to ambient temperature and stirred overnight. The reaction was quenched with saturated NH_4Cl solution and made basic with 4 M NaOH. The alcohol was extracted and the Boc group installed to provide **58** (as per Scheme 2.4). This methodology was utilized on eight instances with an average yield of 46% (range, 34 – 58%). Then, for still unknown reasons, yields dropped in two attempts to 0% and 11%. The same trend was observed by another group member, who had similar poor results (yields < 30%) with similar reactions on propyl side chain quipazine analogs.⁷⁴

At this time the reaction quench was changed to saturated NaHCO_3 so that any acid generated as a result of BBr_3 reacting with water would be neutralized. Following this change, product yields increased to the mid 60% range. Ultimately, the most consistent results were observed when the ether starting materials (e.g. **35** or **48**) were purified prior to use using a Biotage purification system with amine-based silica gel. The amine silica allowed for mixtures of EtOAc:Hexanes to be used as eluent rather than the very polar MeOH:DCM or MeOH: CHCl_3 mixtures that had been employed previously. When the Biotage purification method was used in combination with a NaHCO_3 quench, Boc protected product **58** was obtained in an average yield of 60% (49 – 70%, $n = 5$). The average yield for all uses of NaHCO_3 in the quench was 58% (31 – 70%, $n = 8$), and this is marked improvement over the 38% (0 – 58%, $n = 10$) average yield for all NH_4Cl quenched reactions. It is recommended that the

Biotage Purification–NaHCO₃ quench conditions be utilized until a more promising set of conditions emerges.

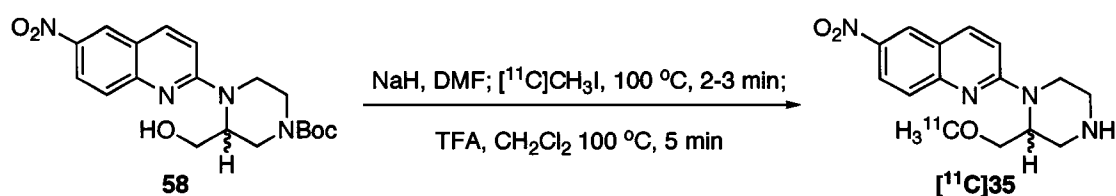
2.7 Radiochemical synthesis of [¹¹C]MOM-NQP and [¹⁸F]MeProF-NQP

The radiochemical syntheses of our PET ligands was accomplished at LBNL in collaboration with scientists specializing in radiopharmaceutical development. Dr. James P. O'Neil is the lead radiochemist in charge of the Cyclotron facility and has been our key liaison for these studies. The Biomedical Isotope Facility at LBNL houses a CTI RDS-111 cyclotron that is used to generate the positron emitting radionuclides.

The synthesis of [¹¹C](*rac*)-MOM-NQP [¹¹C]35 followed the general alkylation approach described earlier for the cold radiochemical synthesis of 35 (Scheme 2.5). Carbon-11 methyl iodide is synthesized from [¹¹C]CO₂ in a gas phase procedure adapted from published methods.^{96, 97} Briefly, carbon-11 CO₂ is generated through the ¹⁴N(p,α)¹¹C nuclear reaction using a 10 MeV proton beam. The [¹¹C]CO₂ is then transferred to a flow reactor where it is reduced to [¹¹C]CH₄ then subjected to a thermal free-radical halogenation reaction with gaseous iodine (I₂) to generate [¹¹C]CH₃-I that is cryogenically (-78 °C) trapped for subsequent reactions.

The two-step alkylation sequence begins with the deprotonation of N-Boc precursor 58 with NaH in DMF (Scheme 2.12). The mixture was cooled to -5 °C and gaseous [¹¹C]CH₃-I was bubbled into the solution. The mixture was then heated at 100 °C for 2-3 min and cooled. The crude reaction mixture was loaded

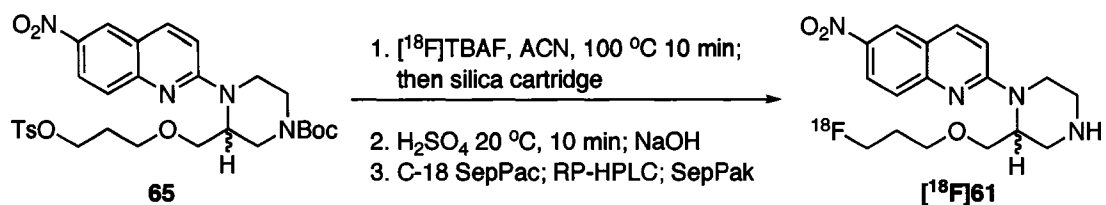
onto a C-18 Sep-Pak cartridge and the crude intermediate (structure not shown) eluted with DCM. Trifluoroacetic acid (TFA) was added in a 1:9 ratio and the solvent was concentrated at 100 °C to provide the crude product [^{11}C]35 that was purified by reversed phase HPLC (radioactivity detection) to afford the target radioligand [^{11}C]35 in 9 – 16% (n = 4) decay corrected (dc) end-of-bombardment (EOB) yield.



Scheme 2.12: Radiochemical synthesis of [^{11}C](rac)-MOM-NQP.

Recent literature evidence⁵⁵ has demonstrated that the *in vivo* equilibration point of binding of 6-NQP derived SERT PET lignds is not achieved until 2-3 hours. Consequently, we have not pursued any *in vivo* studies with this ligand since the experiments could not be performed in the useable lifetime (4 – 5 half-lives) of the radionuclide ([^{11}C] $t_{1/2}$ = 20.4 min). However, radioligand [^{11}C]35 may be of use for examining SERT density in cerebral slice preparations employing *in vitro* autoradiographic techniques.⁹⁸

The synthesis of [^{18}F]MeProF-NQP [^{18}F]61 followed the general procedure developed for the cold synthesis of 61 (Scheme 2.6) but with modifications necessary for radiochemical synthesis (Scheme 2.13).



Scheme 2.13: Radiochemical synthesis of [¹⁸F](*rac*)-MeProF-NQP.

Briefly, radioactive fluoride ion was generated by irradiating oxygen-18 enriched water (> 94%) with a 10 MeV proton beam in a silver coated target chamber. Following irradiation, the water (containing Ag[¹⁸F]F, 175 μL) and dry acetonitrile (ACN, 300 μL) were added to 2 μL of tetra-*n*-butyl-ammonium hydroxide (TBAOH) in a siliconized vacutainer. The water was removed through azeotropic evaporation of the water/ACN mixture at 100 °C (3 cycles) to afford [¹⁸F]TBAF in > 90% radiochemical yield (rcy). The [¹⁸F]TBAF was then transferred with ACN to a reaction vial containing tosylate **65**. The vial was sealed and heated at 100 °C for 10 min. The crude mixture was pushed through a silica gel cartridge with ACN and evaporation of the solvent at 100 °C provided the crude Boc-protected fluoride (structure not shown) in > 50% dc RCY. The crude material was treated with conc. H₂SO₄ for 10 min at 20 °C to remove the Boc group. After diluting with 0.1 N NaOH, the solution was loaded onto a C-18 Sep-Pak cartridge and rinsed with water. The crude target radiotracer [¹⁸F]**61** was eluted by flushing the cartridge with MeOH. The methanol solution was diluted with water (1 mL) and purified by semi-preparative HPLC (radioactivity detection), and the product fraction was diluted with water and loaded onto a C-18 Sep-Pak cartridge. The purified, [¹⁸F](*rac*)-MeProF [¹⁸F]**61** was obtained in 17.8% dc radiochemical yield by eluting with ethanol. The radiochemical

synthesis takes 90 minutes to complete. Tracer [¹⁸F]61 has undergone initial *in vivo* evaluations in rat and these studies will be discussed further in Chapter 5.

CHAPTER 3

ASYMMETRIC SYNTHESSES

3.1 Introduction

The enantiomers of a wide range of chemical compounds are well known to elicit different biological responses. The enantiomers of the terpene carvone (Figure 3.1) have very distinct fragrances and flavors and are the major components of the essential oils from common spices and herbs.

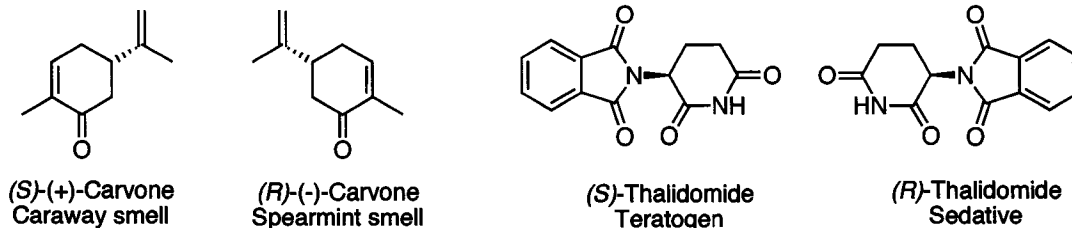


Figure 3.1: Examples of enantiomers that elicit different biological responses.

For carvone, the olfactory receptors in our bodies are able to distinguish between the stereoisomers and the biological effect is a different 'smell' signal that is transmitted to our brains.⁹⁹ Another well-known example is Thalidomide (Figure 3.1). The racemic mixture of this compound was utilized in the 1960's as a sleep-aid and anti-nausea medication for pregnant women. Thalidomide's teratogenic effects at that time were unknown, and unfortunately, around 15,000 pregnancies were affected by the drug's use. The birth defects that resulted left the children deformed and often lead to death in the first years of life. Later, it was found that only the (S)-stereoisomer provided these teratogenic effects and the (R)-antipode was shown to be an effective sedative. Unfortunately, even if

the 'safe' (*R*)-isomer is administered, the compound is metabolically racemized *in vivo* and the teratogenic qualities will still be afforded.¹⁰⁰

The naturally occurring benzomorphan compounds that exert strong pain-relieving qualities through interactions with the opioid receptors (e.g. morphine) are all the levorotatory form. The dextrorotatory isomers (e.g. dextromethorphan) do not show activity at the opioid receptors and often possess activities at other CNS receptors such as NMDA.¹⁰¹ The differences in biological activity are a result of optically active compounds interacting with the optically active biomolecules.

This relationship can be explained simply, although somewhat crudely, as shown in Figure 3.2 for a hypothetical ligand-receptor interaction involving the enantiomers of **35**. The general receptor binding site is shown (panel a.) and consists of amine, aromatic and side chain binding regions. The side chain binding region extends above the other two regions (as indicated by the darkened lines). When (*R*)-**35** is bound to the receptor, the molecule contacts these point nicely with the methoxymethyl side chain extending up into the appropriate side chain binding region (panel b.). However, when (*S*)-**35** is bound with the side chain in the correct 'up-position' it is on the wrong side of the piperazine ring to reach into the side chain binding region (panel c.). If the piperazine ring is rotated 180° around the quinoline bond to move the substituent into the correct position, it will not be extending up into the binding region (panel d.). Instead, it will be positioned significantly below that region, and provide a different binding profile relative to the (*R*)-isomer.

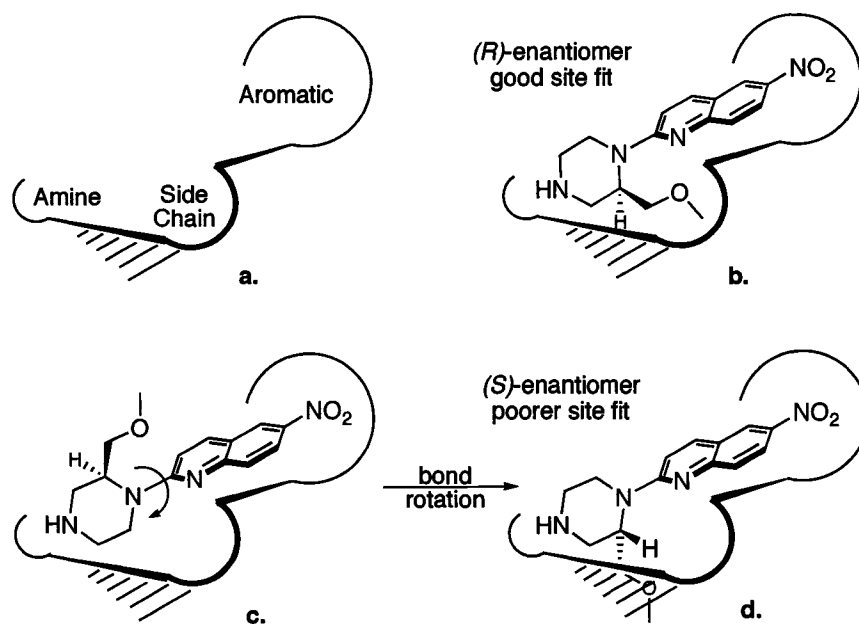


Figure 3.2: Hypothetical ligand-receptor model to demonstrate a plausible enantiomeric discrimination of a ligand. The general receptor binding site consists of amine, aromatic and side chain binding regions (panel a). When (*R*)-MOM-NQP binds to the receptor (panel b), ligand contact with each receptor binding region is made. When (*S*)-MOM-NQP binds (panels c and d), ligand contact with each binding region cannot be made since the side chain is positioned far from the binding region (panel c) or extends well below that region (panel d).

Given this hypothetical example, the enantiomeric binding differential could result in a variety of biological outcomes. These include: 1) The (*S*)-enantiomer may show no activity at this receptor at all; 2) The molecule may have a reduction in activity as a result of less optimal binding and 3) The molecule may show an inverse in activity relative to the (*R*)-isomer (i.e. its antagonist-agonist properties).

The inherent chirality of bio-macromolecules enables the stereochemical discrimination of stereoisomers, and pharmaceutical researchers are trying to take advantage of these differences in their drug design strategies. The use of stereochemically pure pharmaceuticals can improve the therapeutic effect of an

active ingredient, enhancing product marketability. Furthermore, researchers may find that they can extend the profit-life of a molecule by patenting a pure stereoisomer for a 'new' inventive use.¹⁰²

Given the diverse differences that exist between enantiomers within some biological systems, it was desirable for us to isolate and biologically characterize each enantiomer of our final synthetic targets. Additionally, we desired to acquire the radiolabelling precursors so we could also evaluate the enantiomers of our PET agents *in vivo*. The differences in biological activity for the enantiomers of our 6-NQP analogs could result in the identification of a non-racemic radioligand with increased *in vivo* efficacy relative to the racemate, providing a more efficacious candidate PET tracer.

Our laboratory performed an initial SAR study with the enantiomers of 2'-methyl quipazine **24**.¹⁰³ The synthesis of the (*R*)-enantiomer (*R*)-**24** is shown in Figure 3.3.

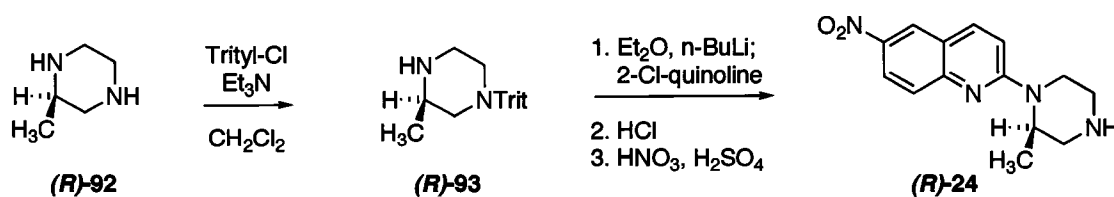


Figure 3.3: Synthesis of (*R*)-2'-methyl-6-nitroquipazine. The (*S*)-isomer is similarly prepared.

The synthesis was accomplished in four steps from commercially available (*R*)- and (*S*)-methylpiperazines, according to the method of Walker.⁶⁷ Unfortunately, when the enantiomers were individually evaluated for their binding affinity at SERT, a significant difference in the affinities was not observed.¹⁰³ We

cautiously attribute the lack of difference to the relatively short methyl side chain, which may not be large enough to evoke stereochemical differences in SERT binding affinity (additional discussion can be found in Chapter 5).

Unfortunately, for our more complex piperazine side chains (for example, with MOM-NQP **35** and MeProF-NQP **61**), commercially available, stereochemically pure piperazine starting materials are either too costly or unavailable. Thus, our initial strategy was to resolve the stereoisomers from racemic intermediates.

Traditional attempts of resolving the stereoisomers through diastereomeric salt formation and fractional crystallization were unsuccessful mainly because crystals never formed.⁷⁴ This methodology was attempted on the two racemic compounds **31** and **32** in their free base forms (Figure 3.4).

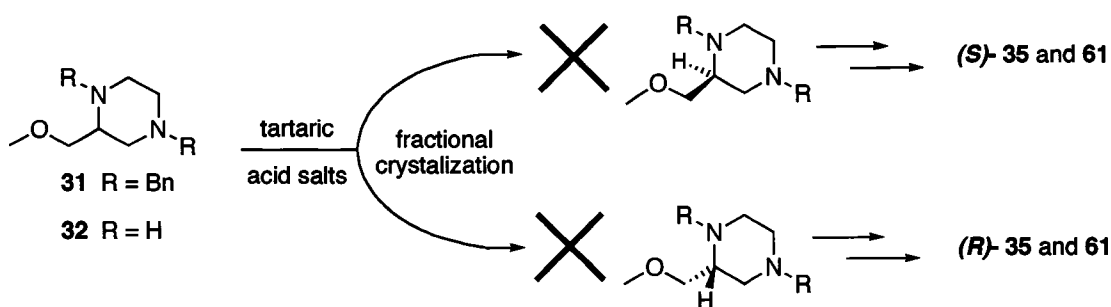


Figure 3.4: Failed resolution strategy attempted by Kusche to isolate stereochemically pure piperazine intermediates.

Compounds **31** and **32** can be easily synthesized in quantities (gram scale) amenable to the resolution technique (as per Figure 1.12, Walker, 2001). Multiple attempts to form crystals from tartaric and benzoyl tartaric acid using different solvents and solvent mixtures all resulted in the formation of oils. Additionally, semi-preparative chiral HPLC columns were used in an attempt to

isolate final compounds in quantities sufficient for bio-assay (1 – 2 mg). These attempts also failed to generate satisfactory results. Rather than belaboring the resolution methods, alternate chiral synthetic approaches were investigated.

Because of their widespread use in biologically active molecules, piperazine rings have received significant attention in medicinal chemistry literature. The modification of the nitrogen atoms is relatively straightforward, since general amine chemistry is typically employed. However, the functionalization of the ring carbon atoms is more synthetically challenging. The most common way to accomplish this is through synthesis from α -amino acids. Recently, routes that utilize direct alkylating methods have been developed.³⁵ There is also a considerable quantity of literature devoted to the isolation and synthesis of non-racemic piperazine compounds. These syntheses encompass a wide range of methods including enzymatic kinetic resolution,¹⁰⁴ traditional fractional crystallization¹⁰⁵ and a myriad of synthetic strategies.¹⁰⁶⁻¹¹⁰ Of the literature we reviewed, the work of Naylor¹¹¹ caught our attention because of the ease of synthesis of alcohol (**S**)-**94** (Figure 3.5).

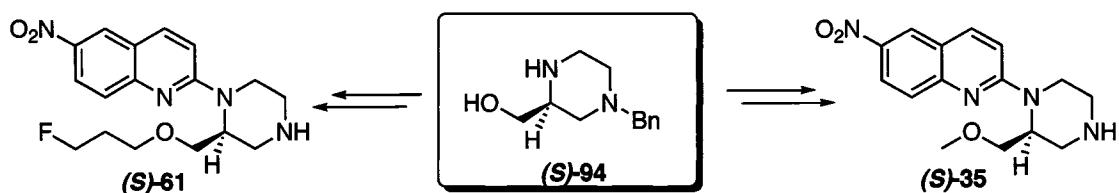


Figure 3.5: Key intermediate alcohol described by Naylor as a precursor for the enantiomers of MOM-NQP and MeProF-NQP.

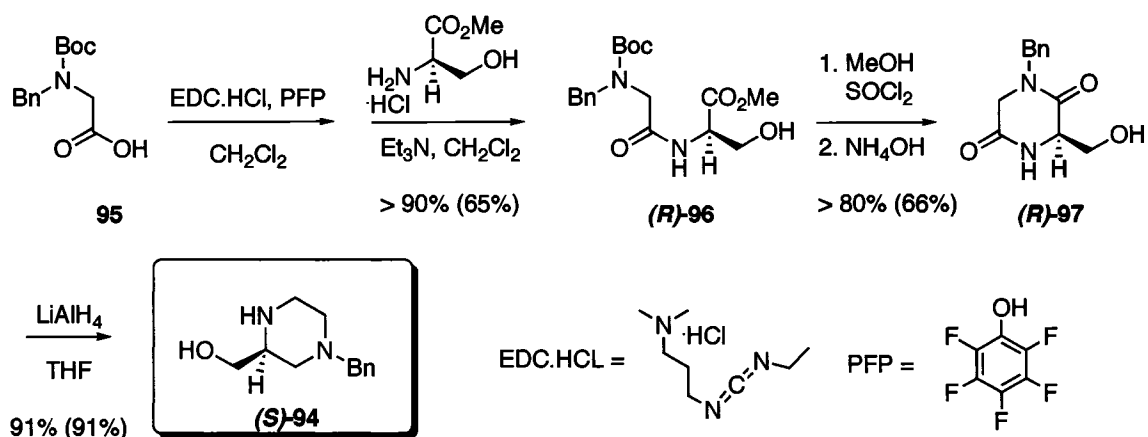
The features of this intermediate that appealed to us were, 1) the hydroxymethyl side chain that provided a direct handle for the synthesis of non

racemic MOM-NQP **35** and MeProF-NQP **61**; 2) the benzyl group was installed as a protecting group, in the correct position for us to accomplish our Gilman quinoline coupling reaction and 3) the chiral center seemed stable to most chemical transformations and did not easily racemize. Indeed, the authors elaborated (**S**)-**94** in five additional synthetic steps and the final product still showed an enantiomeric excess (ee) of >99% (HPLC). The transformations included a Swern oxidation that introduced an aldehyde on the side chain, and this afforded an acidic α -hydrogen on the chiral carbon. It was critical to use N-methylmorpholine as the base, in place of the usual Et₃N, which resulted in preservation of the stereochemical center. The convenience of this method, coupled with the apparent robustness of the chiral center, encouraged us to abandon our efforts to achieve resolution through the more tedious crystallization or chromatographic techniques and proceed with our asymmetric synthesis.

Note: for all of the schemes shown in this chapter, only one stereoisomer is indicated. However, bear in mind that these routes were usually run in parallel, employing both enantiomers. The results for the stereoisomer not shown were usually consistent with the results provided for the other. The range of yields reported below the synthetic steps are the range observed for both stereoisomers.

3.2 Synthesis of the Enantiomers of MOM-NQP

Since the method described by Naylor¹¹¹ suited our needs we adapted the method directly toward our synthetic goals (Scheme 3.1).

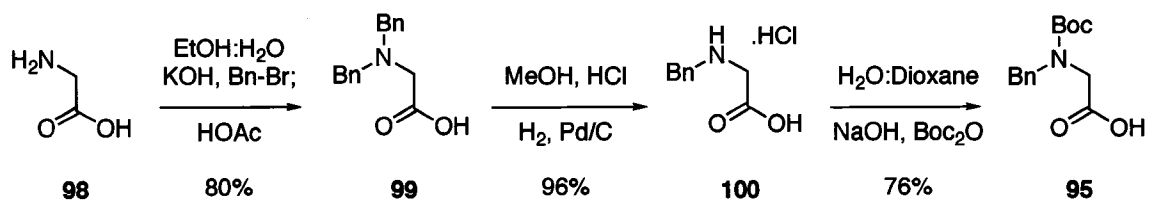


Scheme 3.1: Our synthesis of key amino alcohol (**S**)-**94** using D-serine. Naylor's reported yields are in parentheses.¹¹¹

The carboxyl group of protected, N-Boc-N-Bn glycine **95** was activated by the conversion to the pentafluorophenolic ester with 1-[3-(dimethylamino)propyl]-3-ethylcarbodiimide hydrochloride (EDC.HCl) and pentafluorophenol (PFP). The activated ester (structure not shown) was then coupled to D-serine methyl ester hydrochloride in CH₂Cl₂ (DCM) to provide dipeptide (**R**)-**96**. Naylor and co-workers reported only modest (~65%) yields for this transformation but in our hands the coupling provided excellent results with yields consistently in the mid nineties. We also found that the coupling reaction could be run in reagent grade DCM, without concern for maintaining dry conditions, with no change in chemical yield.

The piperazinedione (**R**)-**97** was generated in a two-step process. The Boc protecting group was removed in the first step using thionyl chloride in MeOH to form the secondary amine hydrochloride salt (not shown). The isolated intermediate was then dissolved in methanol and treated with ammonium hydroxide to generate the amine free-base that cyclized with the ester to form (**R**)-**97**. Naylor's workup involved the removal of all volatile components followed by column chromatography with the very polar mixture of DCM:MeOH:NH₄OH (75:10:2). We found this to be tedious and problematic since the crude material included NH₄Cl that was not soluble in the organic solvent and therefore made loading a column difficult. We found that a simple aqueous work-up (saturated NaHCO₃; extracting with 4:1 CHCl₃:isopropyl alcohol) following the evaporation (*in vacuo*) of the methanol provided (**R**)-**97** with the same purity and with increased yield. The reduction of diamide (**R**)-**97** proceeded smoothly with LiAlH₄ in THF to give the benzyl protected aminoalcohol (**S**)-**94** in excellent yield.

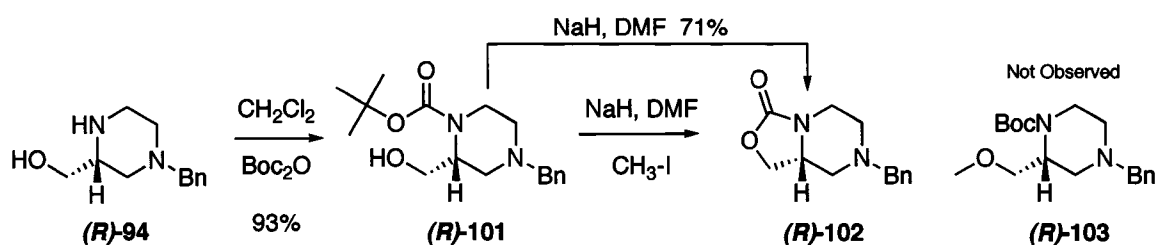
The di-protected glycine **95** was synthesized according to literature procedures that detailed the formation of monobenzylglycine hydrochloride **100**¹¹² and the final product **95**⁸³ (Scheme 3.2).



Scheme 3.2: Synthesis of N-Boc-N-Benzyl glycine.

Briefly, dibenzyl glycine **99** was generated through the base promoted alkylation of **98** with benzyl bromide. Catalytic hydrogenolysis with Pd/C in MeOH with 150 mol% of HCl provided an excellent yield of **100**, that was readily converted to product **95** with Boc₂O in water:dioxane. This sequence was easily accomplished, and **95** was typically produced in 15-18 g batches.

With benzyl protected alcohol intermediate (**S**)-**94**, it was necessary to convert the alcohol to a methyl ether so that the Gilman coupling to the quinoline could be accomplished. To eliminate reactivity of the amine, our initial strategy was to protect it with a Boc group and perform our usual alkylation with DMF, NaH and CH₃-I (Scheme 3.3).

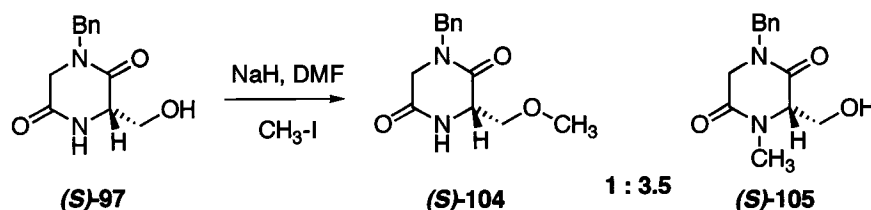


Scheme 3.3: Attempted O-methylation sequence using N-Boc as the protecting group.

The preliminary chemistry was performed with the (*R*)-enantiomer and the protection of the amine (*R*)-**94** went smoothly, with the Boc₂O in DCM producing (*R*)-**101** in excellent yield. However, when the alkylation was attempted to form ether (*R*)-**103**, the crude ¹H NMR did not show an –OCH₃ singlet, indicating the alkylation failed. The NMR also did not show a *t*-butyl singlet from the Boc protecting group, indicating that this group had reacted. Our assumption was the alkoxide reacted intramolecularly with the carbamate to displace the *t*-butoxy group and form the five-membered cyclic carbamate (*R*)-**102**. A control reaction,

in the absence of CH_3I , produced the same result and cyclized product (*R*)-**102** was isolated. Product identity was confirmed by NMR and GC/MS.

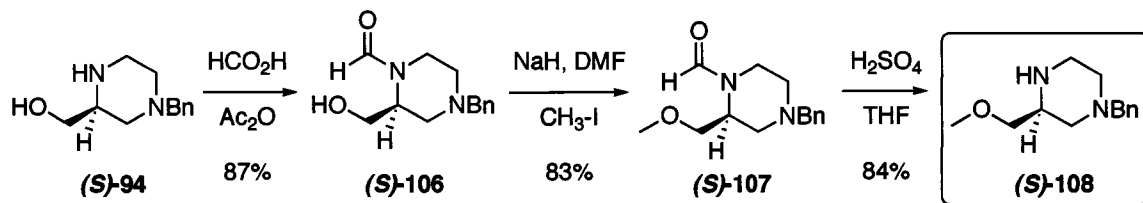
Another method needed to be identified to introduce the methyl group. We hoped initially that a selective O-alkylation (in the presence of an amide -NH) of diamide (*S*)-**97** would afford ether (*S*)-**104** that could then be reduced with LiAlH_4 to provide our desired piperazine (Scheme 3.4).



Scheme 3.4: Failed attempt to selectively introduce a methyl group to the alcohol.

Unfortunately, the pK_a differential between the amide -NH and the alcohol (both $\sim 16 - 17$) afforded a majority of the undesired N-alkylated product (*S*)-**105** in a ratio of 3.5:1 relative to the desired methyl ether (*S*)-**104**. This determination was made by integrating the methyl singlets in the crude ^1H NMR spectrum (- NCH_3 at 2.96 ppm; $-\text{OCH}_3$ at 3.30 ppm). Another attempt at selective O-alkylation involved the use of Ag_2O and CH_3I in acetonitrile according to the method of Andurkar.¹¹³ This method was extremely slow (4 day reaction time), did not produce satisfactory yields of (*S*)-**104** and required large amounts (> 1000 mol%) of CH_3I . With the poor results of these two attempts, we decided to abandon selective alkylation in favor of alternate protecting group strategies.

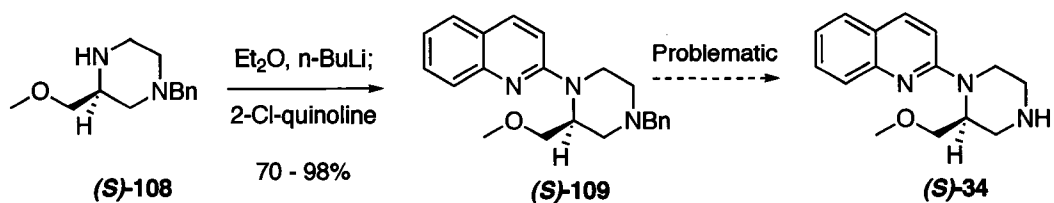
We decided to try another protection-alkylation sequence from intermediate **(S)**-**94**, employing N-formamide as the protecting group (Scheme 3.5).



Scheme 3.5: Successful alkylation strategy using N-formamide as a protecting group.

Since DMF (an N-formamide) as the reaction solvent does not interfere with O-alkylation, we figured the N-formyl protecting group would be a good alternative to N-Boc. Working on a 45 mg scale, the formamide group was introduced with acetic anhydride in formic acid according to Sheehan¹¹⁴ providing an excellent yield of N-formyl alcohol **(S)**-**106**. The product was subsequently alkylated under our standard conditions (DMF, NaH and CH₃-I) to afford methyl ether **(S)**-**107** in 83% yield. Deprotection of the formyl group with H₂SO₄ in THF at 60 °C afforded the sought after amine-ether **(S)**-**108** that was ready for Gilman coupling.

Given the success of this method on small scale we adapted it to our normal quantities (> 600 mg) of aminoalcohol **(S)**-**94** and found that the amine-ether **(S)**-**108** could be generated with comparable yields. At this point it seemed that the conversion to our targets, (*R*)- and (*S*)-MOM-NQP **35**, would be straightforward. The Gilman coupling was effective, giving good to excellent yields of the coupled benzyl protected quipazine **(S)**-**109** (Scheme 3.6).

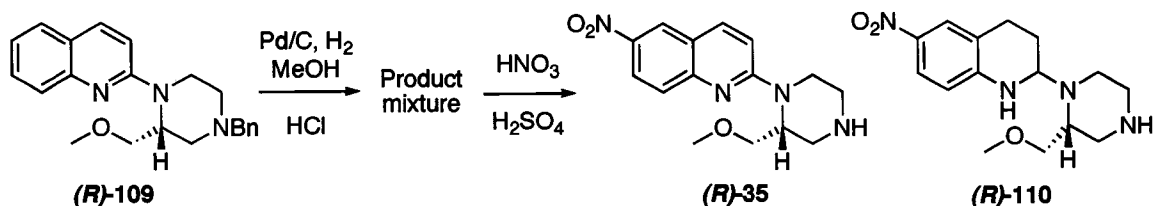


Scheme 3.6: Formation of N-Bn-MOM-quipazine with the Gilman coupling.

However, the removal of the benzyl group, initially thought to be a trivial step, proved to be a challenge. The initial de-benzylation attempt with **(S)-109** using 5% Pd/C (15% by weight) and H₂ in MeOH with 300 mol% HCl went very well. The conversion to product was clean, although very slow, requiring an overnight reaction time. During the course of the reaction, an additional equivalent of acid was added to protonate the quinoline ring, thinking that it may be poisoning the catalyst and slowing the reaction. Additional catalyst (25% by weight) was also added and the reaction allowed to proceed and additional 4 h. Following work-up, **(S)-34** was isolated in 96% yield with a minimal amount of impurities. The ¹H NMR was a match to a sample prepared according to our racemic strategy⁶⁷ validating our asymmetric synthetic methodology.

When this reaction was attempted on **(R)-109** however, a very different result was obtained. Under virtually identical conditions and after stirring overnight, two products were formed as observed by TLC and ¹H NMR. The product mixture was nitrated and the compounds protected with a Boc group to facilitate a more straightforward chromatographic separation. Following chromatography, the compounds were immediately deprotected. Interestingly, the proportion of side product (determined by ¹H NMR) was greatly reduced upon nitration, possibly as a result of its degradation in the strong acid. One of the

products was our target (*R*)-MOM-NQP (**(R)-35**). The other product was a compound showing only three aromatic proton signals in the ^1H NMR, indicating that quinoline ring reduction had occurred, possibly giving (**(R)-110**) (Scheme 3.7). Reductions of the quinoline ring are known under these conditions and reduction usually occurs on the nitrogen containing ring.¹¹⁵



Scheme 3.7: Debenzylation reaction giving side product formation from ring-reduction.

Concurrent with this study, the synthesis of (*R*)- and (*S*)- MeProF **61** (discussed later) was encountering the same benzyl group removal problems. In this series, Rainey-Ni was used as a catalyst and provided similar poor results. In this case, the removal *would not* go to completion (3 days, 40 psi of H_2) and side products were again forming as observed by TLC. Based on the lack of consistency for the debenzylation transformation, and the possibility that side products could be formed in significant quantities, catalytic hydrogenolysis of the benzyl groups was abandoned.

We next considered the use of 1-chloroethyl chloroformate (ACE-Cl, **111**) for the debenzylation transformation.¹¹⁶ This reagent is well known for its ability to dealkylate tertiary amines to provide good yields of secondary amine products. When cyclic amines are reacted with this reagent, there also occurs a preference towards the dealkylation of the noncyclic alkyl group. The use of this reagent for

the removal of benzyl groups from cyclic tertiary amines (piperazines, piperadines) is well documented.^{117, 118}

The mechanism of the dealkylation is shown in Figure 3.6 for the debenzilation of N-benzylmorpholine **112**. The amine is heated with **111** in refluxing dichloroethane (DCE) to afford the dealkylated chloroethyl carbamate intermediate **113** and benzyl chloride **114**. To complete the transformation all volatiles are removed (*in vacuo*) and the residue is treated with methanol and heated at 50 – 60 °C. The methanol reacts with the chloroethyl side chain to give intermediate **115** that decomposes to dimethylacetal **116** and N-morpholine carboxylic acid **117** that further decomposes to CO₂ and the product morpholine **118**; the later picks up the HCl generated in the reaction.

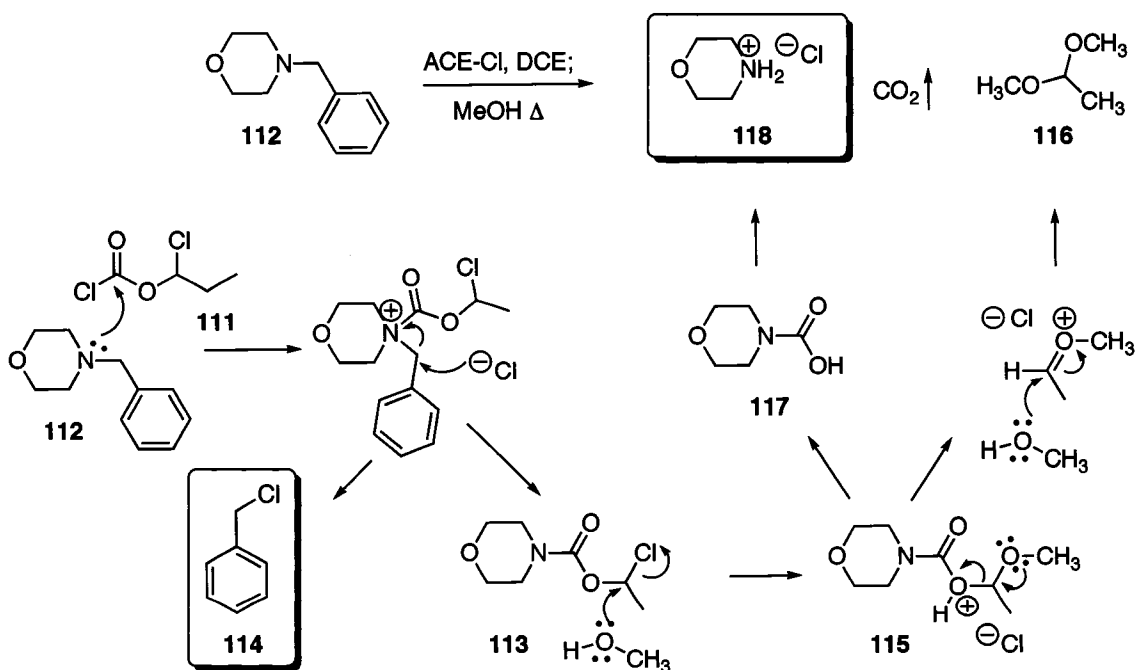
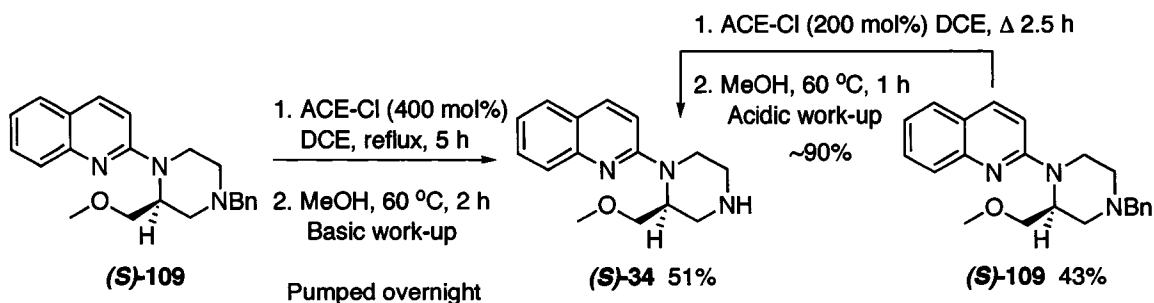


Figure 3.6: The mechanism of ACE-Cl dealkylation.

The first attempts at effecting this transformation provided confusing results. The reported conditions (~100 mol% ACE-Cl in DCE, reflux 1 h; then MeOH hydrolysis at 50 – 60 °C, 1 h) seemed to provide a complete conversion of the benzyl amine to the secondary amine product based on TLC analysis (product $R_f = \sim 0.15$ vs. starting material $R_f = 0.70$ MeOH:DCM 1:9); where the analysis showed no starting material and a large product spot. However, when the crude reaction mixture was analyzed the next day by ^1H NMR it appeared there were three products present and the benzyl group still appeared to be partially intact.

After considering this result, a follow-up TLC analysis was performed and this distinctly showed the presence of the N-Benzyl starting material ($R_f = 0.70$; MeOH:DCM 1:9). We figured that this had just been missed on the previous analysis and thought initially that the reaction had not gone to completion. Consequently, our next attempts at dealkylation utilized increased amounts of ACE-Cl reagent (400 mol%) and increased reaction times (reflux 4-5 h; then MeOH hydrolysis). Following this sequence, the material was chromatographed immediately and product yields in the 75 – 80 % range were afforded. Given these improved yields with the more rigorous conditions, we attempted a larger scale reaction for our coupled tertiary amine (**S**)-109. The conditions of this reaction were exactly as described immediately above. However, the crude material was not chromatographed immediately following the work-up and was kept under high vacuum overnight. The crude weight the next morning was very high (150%) and a TLC showed that a significant quantity of starting material

remained. Following chromatography, we obtained product **(S)**-**34** and starting material **(S)**-**109** in yields of 51% and 43% respectively (Scheme 3.8).

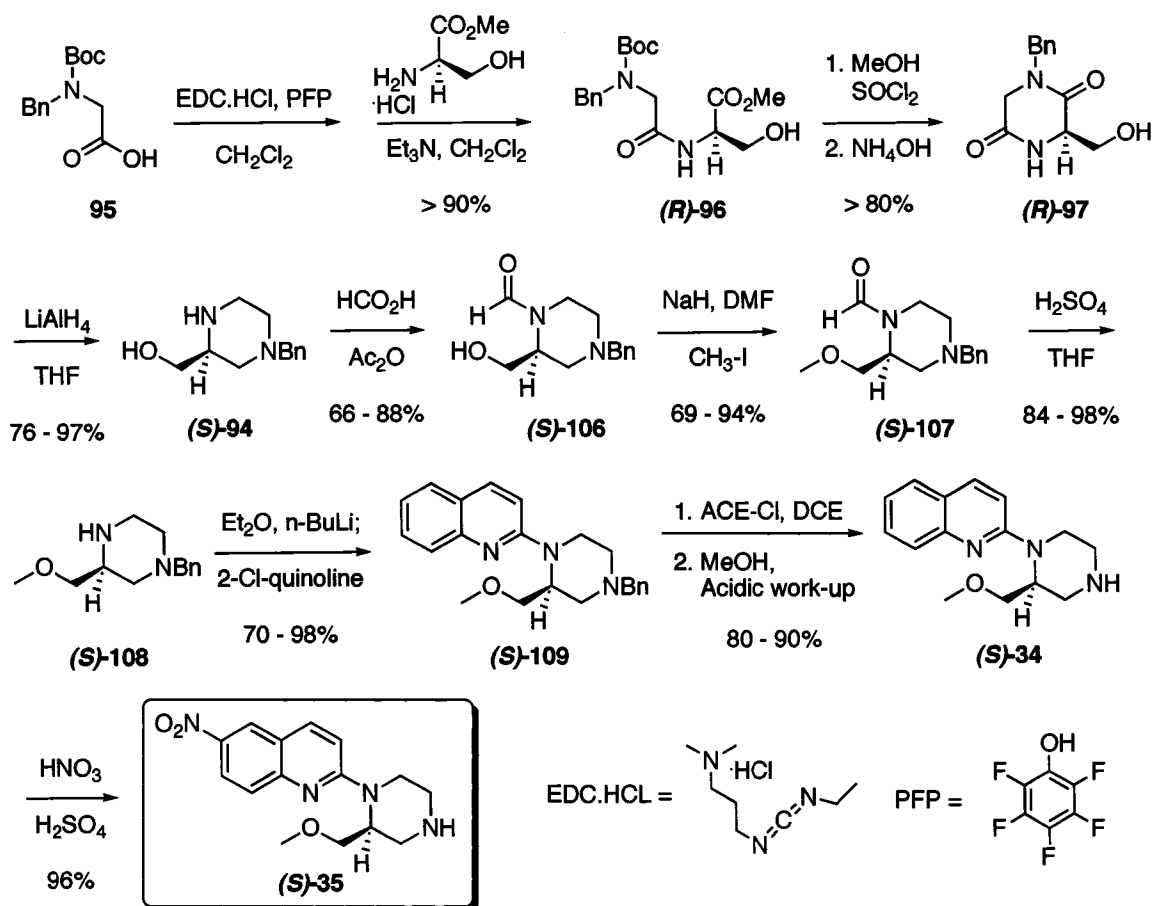


Scheme 3.8: Refinement of the ACE-Cl mediated debenzylation reaction.

Since the yields of products from immediate chromatography (75 – 80%) varied greatly from the materials that pumped overnight (~50%) we concluded that something was reacting within the crude material as it sat on the pump. It became obvious after considering the literature^{117, 118} and the reaction mechanism (discussed above) that we were simply alkylating our amine with the benzyl chloride **114** that was formed as a reaction side product (See mechanism, Figure 3.5). Our work-up conditions after the methanol hydrolysis, were to evaporate the reaction solvent then dilute the residue with saturated NaHCO₃ and DCM. The basic (pH ~9) aqueous layer was extracted with DCM to afford the crude product. Unfortunately, this also extracted **114** and any ACE-Cl reagent **111** that wasn't destroyed in the workup. When these reagents were concentrated and allowed to sit for 16 h overnight, the alkylation reaction took place.

The recovered benzyl amine **(S)**-109 was subjected again to the debenylation reaction conditions (Scheme 3.8). This time less rigorous conditions were used (ACE-Cl 200 mol%, reflux 2.5 h), and the work-up was changed. Following the hydrolysis step with methanol, the crude residue was dissolved in 1 N HCl and washed with a few portions of DCM. A check of these washes by TLC showed that a UV active non-polar material had been removed (probably benzyl chloride). The aqueous phase was then made basic and extracted with DCM to afford **(S)**-34 in ~90% yield. This material did not show reactivity once it had been concentrated and allowed to stand for extended periods of time. Furthermore, the purity of the isolated product was high enough so that column chromatography was not required. For the last transformation, the nitration of **(S)**-34 was achieved in > 90% yield in all cases to afford the final target **(S)**-35.

The complete synthesis for **(S)**-35 is shown above and the yields below each step represents the range obtained for both isomers (Scheme 3.9). The asymmetric syntheses of the enantiomers of MOM-NQP were accomplished in nine steps from inexpensive amino acid starting materials. Given the typical yields for each of these transformations, the final compounds are routinely be obtained in ~40% overall yield. Given optimal yields for each step, this overall yield could go as high as 60%.



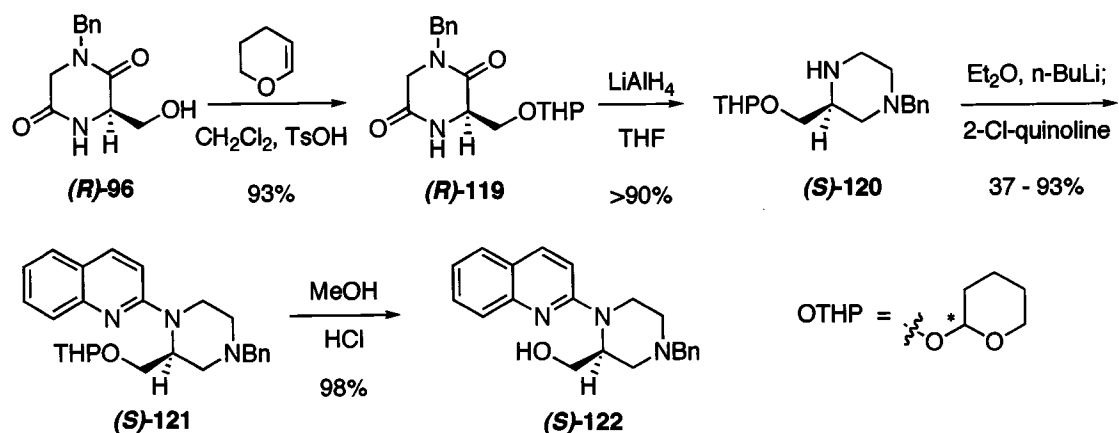
Scheme 3.9: The complete synthesis of (*S*)-MOM-NQP; the (*R*)- stereoisomer was similarly prepared.

3.3 Synthesis of the Enantiomers of MeProF-NQP

The synthesis of (*R*)- and (*S*)- MeProF-NQP **61** utilized the same asymmetric peptide **96** that was used in the synthesis of (*R*)- and (*S*)- MOM-NQP **35**. However, there were two criteria that we wanted to meet so that we could avoid synthetic complications. Firstly, we wanted to avoid performing the synthesis of (*R*)- and (*S*)- **61** from **35** as was done for (*rac*)-**61**, so the BBr_3 demethylation step could be avoided (see Chapter 2, Scheme 2.6). Secondly, we understood that we could not have a fluorinated side chain present during the

Gilman coupling step since the halogen lacked stability under the alkyllithium coupling conditions (as per Chapter 2, Figure 2.1). Consequently, we desired to discover a protecting group for the alcohol of diamide **97** that could withstand the transformations (diamide reduction and Gilman⁶⁹ coupling) to the coupled quipazine and then be easily removed. This strategy would allow us the convenience of obtaining the alcohol side chain without the need for the inconsistent BBr₃ demethylation reaction. Furthermore, it would allow us to use the same side chain extension chemistry that we had developed for (*rac*)-MeProF **61** (as per Scheme 2.6).

Because of its stability to basic reaction conditions and the ease with which it is introduced and removed⁷⁹, our first choice of a new alcohol protecting group was the tetrahydropyranyl ether (-OTHP). Given the general lack of nucleophilicity of amides we felt that a selective protection of the alcohol (*R*)-**96** could be accomplished in the presence of the secondary amide. Our choice of the THP protecting group happened to be a correct one, as demonstrated by the facile synthesis of the benzyl protected quipazine alcohol (*S*)-**122** shown below (Scheme 3.10). The introduction of the THP group was accomplished according to the method of Bernady¹¹⁹ and utilized excess dihydropyran (460 mol%) in DCM with *p*-toluenesulfonic acid as the catalyst (3 – 5 mol%). The reaction was complete after 30 min, and following chromatography, an excellent yield of (*R*)-**119** was obtained as a ~6:4 mixture of diastereomers (C-2 of the THP ring). The reduction of (*R*)-**119** went easily with LiAlH₄ in refluxing THF to give protected piperazine (*S*)-**120** in excellent yields.



Scheme 3.10: Facile production of benzyl protected quipazine alcohol (**S**)-**122** using the OTHP group for alcohol protection.

Compound (**S**)-**120** underwent Gilman⁶⁹ quinoline coupling to provide (**S**)-**121**, however, the yields were inconsistent. The best yield (93%) was obtained with a piperazine that had not been column purified following the LiAlH_4 reduction. As such, this is explained simply as a lingering anomaly. The removal of the THP group was consistent, giving excellent yields of (**S**)-**122**. Conversion to alcohol (**S**)-**122** was accomplished very cleanly, in high yield by stirring in MeOH with 220 mol% of HCl overnight.

Given the ease of synthesis of alcohol (**S**)-**122**, it is worthwhile to discuss the option of abandoning the previously described synthesis of (*R*)- and (*S*)-MOM-NQP (Scheme 3.9) in favor of adopting the new THP protected methodology (Figure 3.7). Simply alkylating (**S**)-**122** with DMF, NaH and $\text{CH}_3\text{-I}$ would provide MOM-NQP intermediate (**S**)-**109** in an equal number of steps (seven) from the amino acid starting materials. For future studies, if large quantities of the enantiomers of MOM and MeProF are required, it may be

desirable to generate bulk quantities of (*R*)- and (*S*)- **122** so two synthetic routes will not be required to acquire all of the targets.

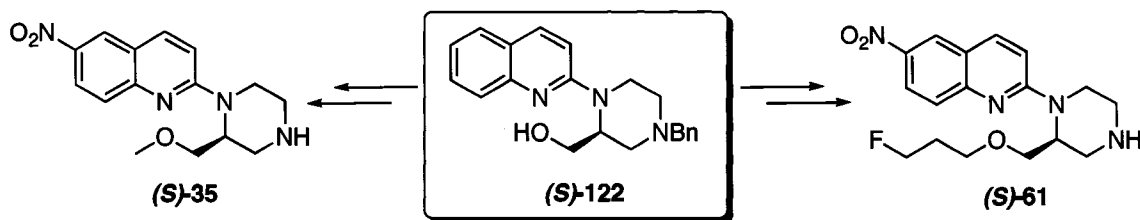
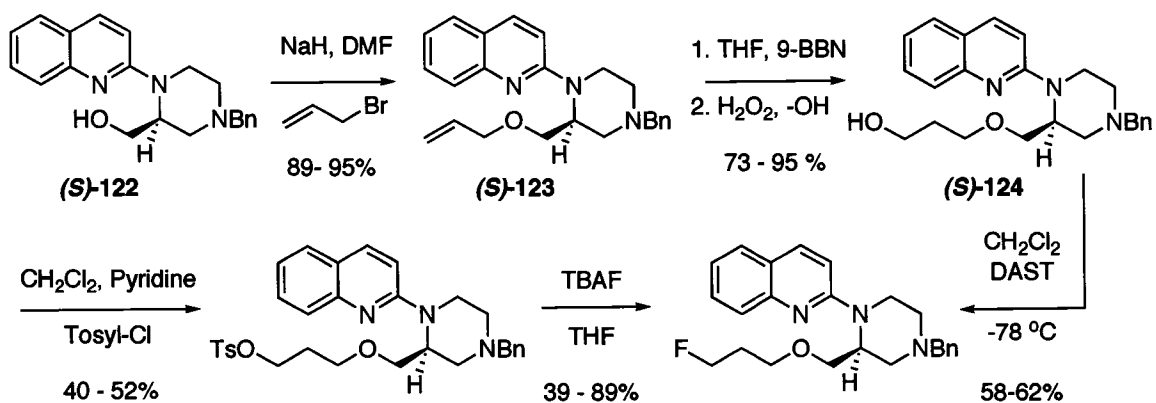


Figure 3.7: Intermediate benzyl alcohol (*S*)-**122** to generate both asymmetric targets.

The conversion of the alcohol side chain of (*S*)-**122** to the fluorinated propyl side chain followed the same basic methodology (as per Scheme 2.6) that was utilized for the conversion of *N*-Boc alcohol **58** to (*rac*)-MeProF **61** (Scheme 3.11).



Scheme 3.11: Synthesis of the fluoropropyl side chain from the key alcohol intermediate (*S*)-**122** using two distinct fluorination strategies.

The reaction conditions were identical in all cases, with the exception of the alkylation step ((*S*)-**122** → (*S*)-**123**) where care was taken to use ≤ 5 mol% excess of allyl bromide to avoid quaternization of the tertiary amine. This change

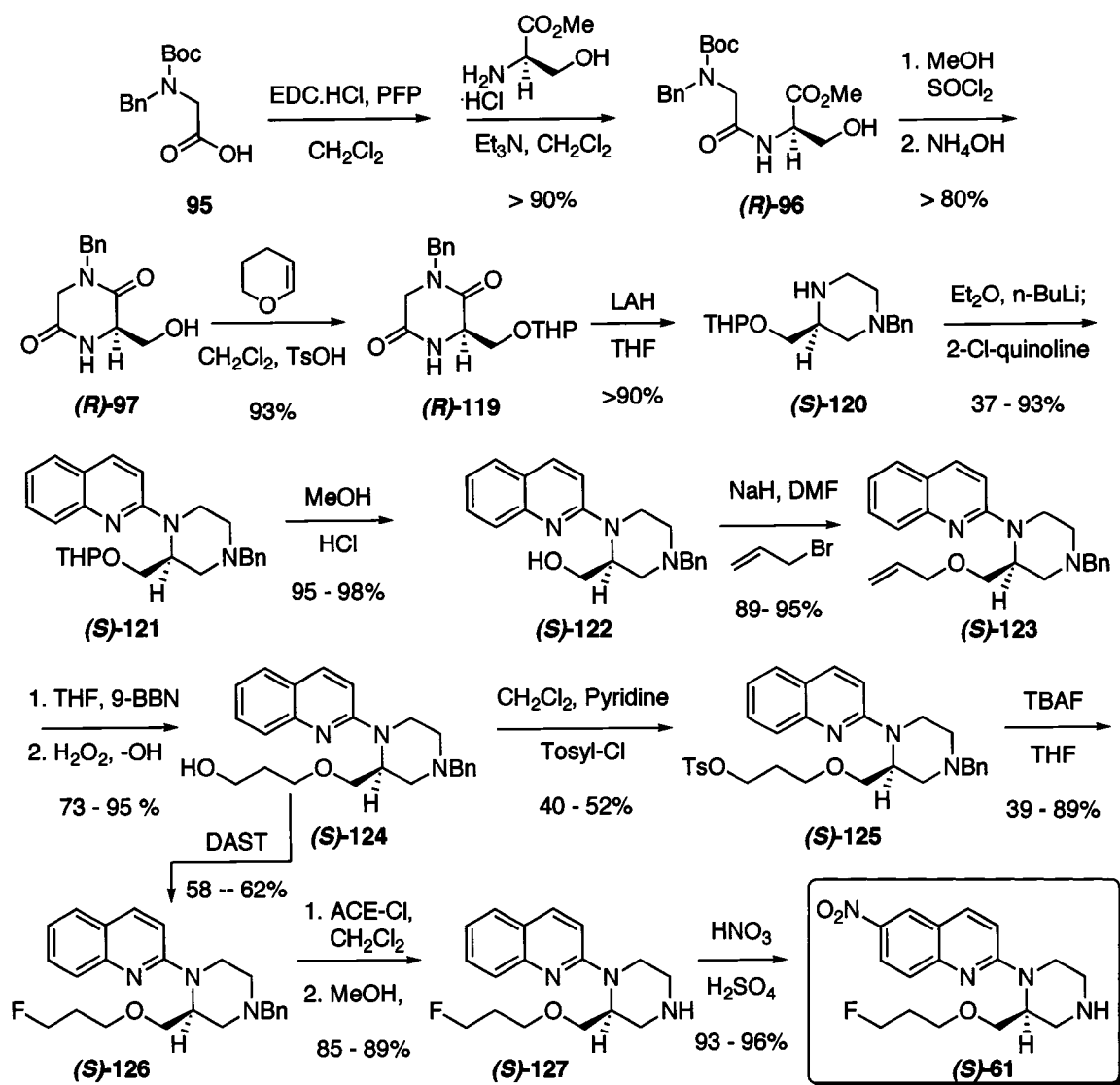
in concentration did not effect the conversion to ether **(S)-123** and excellent yields of product were obtained. The hydroboration-oxidation sequence went smoothly producing alcohol **(S)-124** in high yield. Interestingly, the conversion of **(S)-124** to tosylate **(S)-125** could only be achieved in modest yields of 40-52% (yields with the Boc protecting group were consistently > 70%). This range of tosylate yields was maintained with 100, 200, and 400 mol% of tosyl chloride. This conversion was not investigated in detail. However it is suggested that future attempts utilize dimethylaminopyridine (DMAP) as a catalyst with only 100 – 150 mol% of tosyl chloride. The formation of very polar material was observed with reactions involving 400 mol% of tosyl chloride and it may result from amine quaternization. Fluorination of **(S)-125** using 150 mol% of TBAF in THF initially gave very poor results with yields of **(S)-126** being < 50%. Later attempts, using 1500 mol% of TBAF, afforded yields > 80% and **(S)-126** was easily separated from the remaining TBAF with column chromatography. The combined yield for the tosylation-fluorination sequence was, at best, 47 %.

An alternate fluorination method was investigated to enhance the chemical yield of the fluorinated product **(S)-126**. Diethyl aminosulfurtrifluoride (DAST) is well known for its ability to convert alcohols to alkyl fluorides.¹²⁰ The DAST reagent was effectively used in DCM at -78 °C to convert alcohol **(S)-124** directly to the fluoride **(S)-126** in yields of ~60%. Although not a large improvement from the two-step process, this alternative synthetic transformation does provide a modest increase in yield and shorten synthetic time. Benzyl tosylate **(S)-125**, is not an appropriate radiochemical precursor since two lengthy chemical

transformations would be required following the fluorination to generate the target tracer. Consequently, it is not necessary to generate this intermediate, and the DAST route can be routinely used.

The final conversion of the benzyl protected fluoride **(S)-126** to MeProF product **(S)-61** follows the same ACE-Cl and nitration sequence that was used for *(R)*- and *(S)*- MOM-NQP. The ACE-Cl promoted debenzylation reactions provided consistent good results since the crude material was always chromatographed immediately following the work-up so that subsequent alkylation was avoided. The acidic work up has not yet been utilized in this series, however, it is recommended that it be the standard method for obtaining the crude products from ACE-Cl reactions. The usual nitration of **(S)-127** to provide target material **(S)-61** completed the synthesis.

The complete synthetic scheme for the formation of *(R)*- and *(S)*- MeProF **61** is shown below and is completed in 11 – 12 steps from the amino acid starting materials with the best overall yield being 32% (Scheme 3.12).

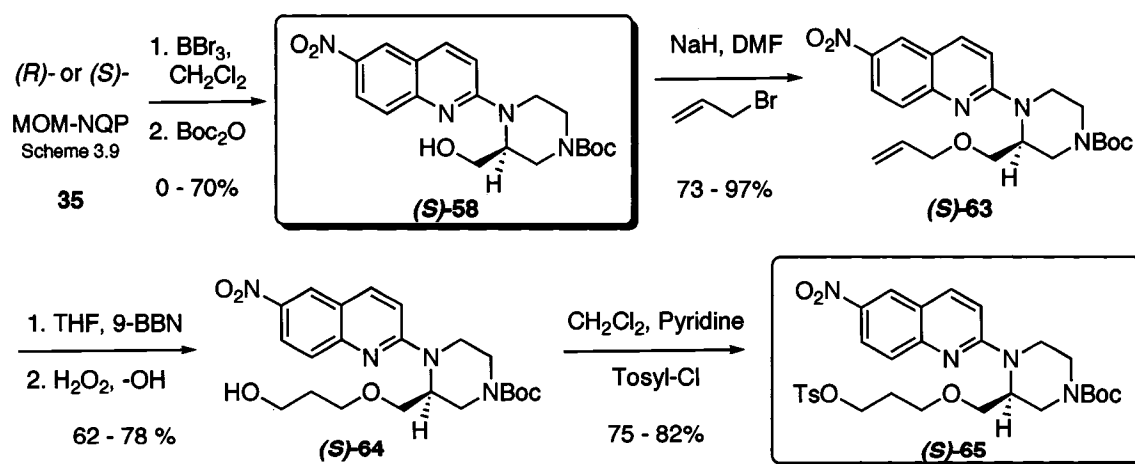


Scheme 3.12: The complete synthesis of (S)-MeProF-NQP; the (R)- stereoisomer was similarly prepared.

3.4 The Synthesis of Enantiomeric Radiolabelling Precursors

The precursors for radiochemical synthesis studies were synthesized initially in an identical manner to the racemic targets (Scheme 3.13). The enantiomers of **35** were treated with boron tribromide to remove the methyl group and the Boc group was introduced to generate the key N-Boc protected alcohol **(S)-58**. This radiochemical precursor for (*R*)- and (*S*)- [^{11}C]**35** has not yet been utilized in any radiosyntheses based on the presumed poor *in vivo* properties (e.g. long equilibration time), discussed earlier in Chapter 2 (Sandell, 2002), that would not afford a useful carbon-11 imaging agent.

The MeProF tosylate precursor **(S)-65** was again synthesized from Boc intermediate **(S)-58** in an identical manner to the racemic variant. These approaches are summarized again below and the radiochemical precursors are boxed (Scheme 3.13).



Scheme 3.13: Synthesis of enantiomeric radiolabelling precursors (boxed). Only the (*S*)-intermediates are shown.

Since this pathway involves the inconsistent BBr_3 demethylation reaction, an alternate synthesis was desired, particularly one that began from the key asymmetric intermediate, N-benzyl alcohol (**(S)**-122). It has been shown already how this compound can afford both cold asymmetric agents (**35** and **61**), and an efficient conversion of (**S**)-122 to Boc alcohol (**(S)**-58 would provide a GRAND UNIFICATION of the asymmetric pathway by affording all targets, from a common intermediate (Figure 3.8).

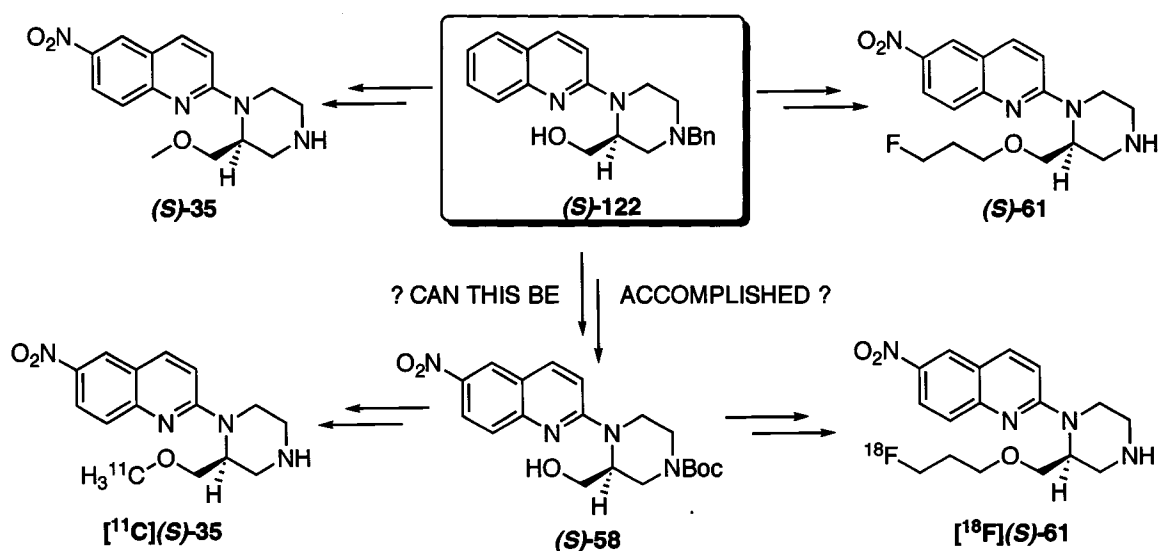
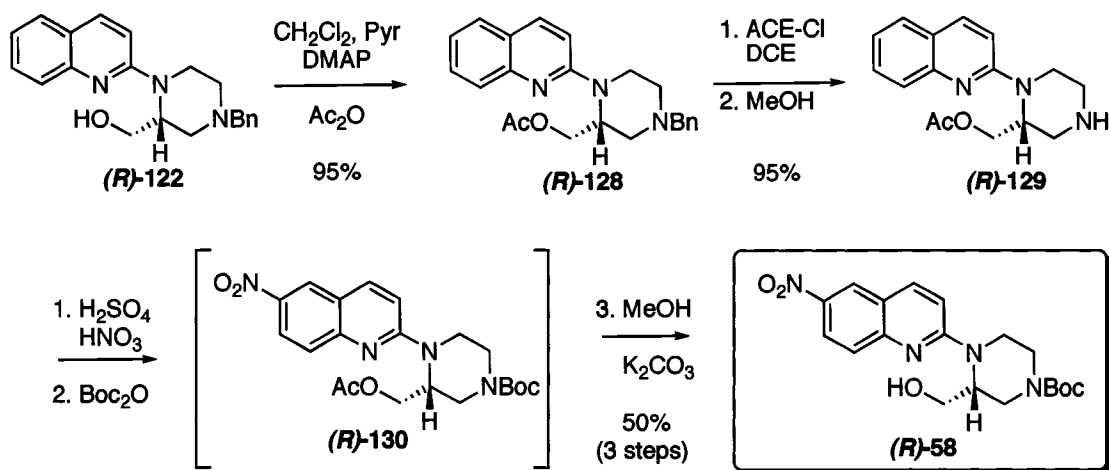


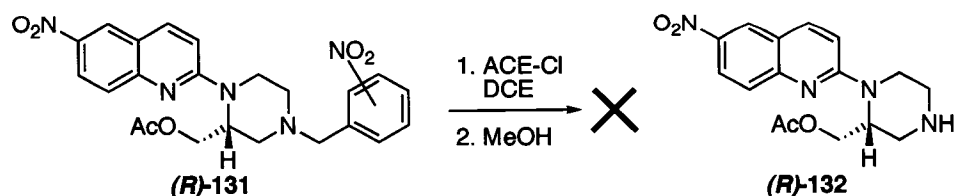
Figure 3.8: Intermediate N-benzyl alcohol (**(S)**-122) as a plausible precursor for all asymmetric targets.

To achieve this transformation a relatively simple synthetic strategy has been developed using only the (*R*)-stereoisomer, (*R*)-122 (Scheme 3.14). A key feature of this synthesis was the need for an acid stable protecting group for the alcohol so the nitration could be accomplished.



Scheme 3.14: Synthesis of Boc alcohol radiochemical precursor (*R*)-58 from the key intermediate N-benzyl alcohol (*R*)-122.

When the alcohol is subjected to cold H_2SO_4 and HNO_3 a reaction occurs (perhaps an oxidation) to form a water soluble product that does not extract into organic solvents under basic (pH 9) conditions. This result suggests that a carboxylate anion may be present. The acetate group was chosen as the alcohol protecting group since it shows a general stability to rather acidic conditions.⁷⁹ The introduction of the acetate protecting group was accomplished using typical conditions (Ac_2O , Pyr, cat. DMAP in DCM) to afford acetate (*R*)-128 in 95% yield. In one experiment, this material was nitrated with 300 mol% HNO_3 to afford dinitro product (*R*)-131 that surprisingly would not debenzylate under our usual ACE-Cl reaction conditions (Scheme 3.15).



Scheme 3.15: Attempted debenzylation of the nitrobenzyl intermediate.

The alternate approach performed the debenzoylation first to afford **(R)-129** in a yield of 95% (Scheme 3.14). In the work-up, care was taken to ensure that the aqueous layer did not become too basic and cause acetate hydrolysis by using only saturated NaHCO₃ to bring the mixture to basic pH. The secondary amine acetate **(R)-129** was then nitrated under our standard conditions and protected with Boc₂O in the work-up to afford the crude intermediate N-Boc acetate **(R)-130**. Following the evaporation of the extraction solvent, selective hydrolysis of the acetate was accomplished using K₂CO₃ in methanol at room temperature to afford the key radiolabelling precursor intermediate **(R)-58** in an overall yield of 45% from N-Benzyl alcohol **(R)-122**.

This synthetic route has demonstrated that the conversion of **(R)-122** to key Boc intermediate **(R)-58** is a reality, and can be accomplished with moderate yields. The low yield of the final nitration step likely occurred because of conditions that caused acetate deprotection and subsequent reactivity of the alcohol to form the water-soluble product mentioned above. Less acidic nitration conditions may be employed that will minimize this side-reactivity and subsequent reduction in chemical yield.¹²¹ This synthesis of **(R)-58** demonstrates the ability of N-Benzyl alcohol **(R)-122** to act as a key intermediate for the generation of all asymmetric targets detailed in this chapter.

The pairs of enantiomers that were generated from this work all demonstrated equal and opposite optical rotations in polarimetry experiments. The differences in the optical rotations for a pair of enantiomers was typically less than 5%. More quantitative determinations of optical purity (enantiomeric

excess, ee) need to be established, and experiments to provide these determinations are being planned. We hope to utilize gas chromatography with a chiral stationary phase to quantify the enantiomeric excess of our final compounds. Should these chromatographic separations fail to adequately resolve the enantiomers, the %ee determinations will be made using the NMR method of Mosher.¹²²

Mosher's method reacts an enantiomerically pure acid chloride (*R*)-**133** with an optically active molecule (for example (*S*)-**61**) to form a compound with 2 or more stereocenters **134** (Figure 3.9). The trifluoromethyl group (circled) will be diastereotopic as a result of the (*S*)- and (*R*)- configurations at the other chiral center. An analysis of product **134** with ¹⁹F NMR allows for the determination of enantiomeric excess by the integration of trifluoromethyl signals.

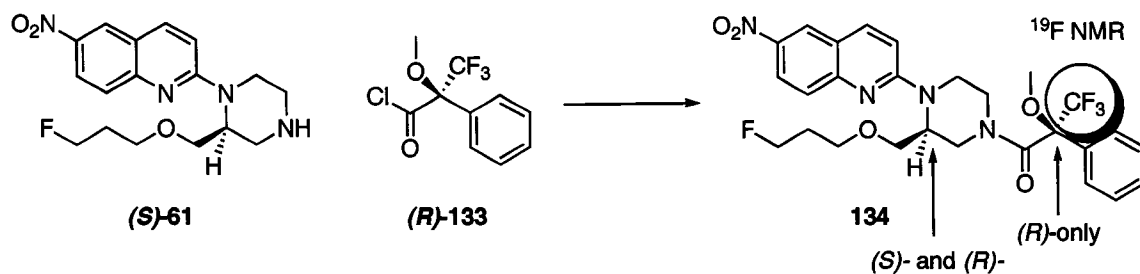


Figure 3.9: Reaction of (*S*)-MeProF with Mosher's reagent. The trifluoromethyl group can be analyzed by ¹⁹F NMR to quantify enantiomeric excess.

CHAPTER 4

OTHER ASYMMETRIC-LIKE SYNTHESSES

4.1 Introduction for the 2'-Aryl-6-Nitroquipazines

Given the success of the asymmetric synthesis for generating the enantiomers of **35** and **61**, we thought that this technology might be useful for generating other 2'-substituted-6-nitroquipazine analogs using different amino acids.

Of particular interest was the generation of 2'-aryl-6-nitroquipazine analogs containing phenyl and benzyl substituents (**135** and **136**, Figure 4.1). These ligands will someday serve as test agents for the hypothesis that 6-NQP analogs containing dual aromatic ring motifs (quinoline ring and phenyl or benzyl substituent) *may* allosterically modulate ligand transport and binding at the substrate (5-HT) binding site of SERT because of their prospective steroid like qualities.



Figure 4.1: Our 2'-aryl target ligands: 2'-phenyl- and 2'-benzyl-6-nitroquipazine.

This hypothesis was developed from a collection of evidence from several researchers, that indicates certain steroids and steroid-like molecules, as well as commercial SSRI's, *can* allosterically influence the binding characteristics and

transport properties of ligands at the substrate (endogenous 5-HT) binding site of SERT. A common structural motif to these ligands (steroids excluded) is the presence of two aromatic ring functional groups. We hypothesize that this ligand structural feature may promote select influences on SERT function.

Plenge demonstrated that the dissociation rates of [³H]imipramine **4** and [³H]paroxetine **9** from SERT could be modulated in a dose-dependent manner by the addition of micromolar concentrations of non-radiolabelled paroxetine **9** or citalopram **28** (Figure 4.2 for structures).

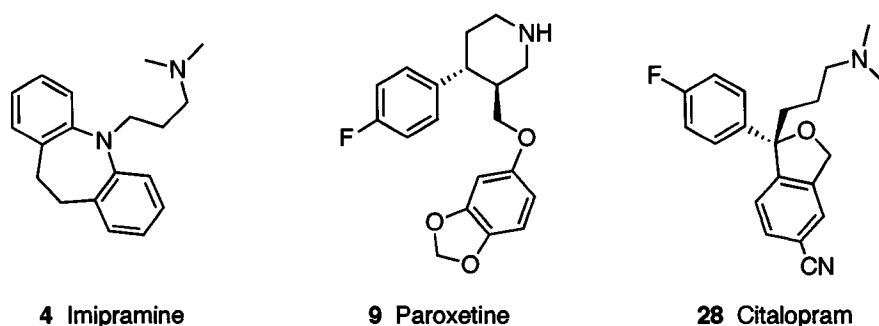


Figure 4.2: Compound structures from the study of Plenge, 1985, 1991.^{123,124}

The addition of **28** caused a decrease in the rate of dissociation from SERT for both radioligands (increased affinity). Compound **9** caused an increase in the dissociation rate for [³H]**4** (decreased affinity) and a decrease in dissociation for [³H]**9** (increased affinity). Since these experiments were run under non-competitive conditions ([³H]**4** was diluted ~50 fold at the time of **9** or **28** addition), the modulatory effect had to arise from a ligand-protein interaction at a different or allosteric binding site on SERT.^{123, 124} Recent affinity modulation (Af-M) studies on SERT mutants have provided additional evidence that the allosteric site is independent from the reuptake inhibitor binding site.¹⁴

Interestingly, the SSRI sertraline **7** has shown Af-M properties at the norepinephrine transporter (NET) by decreasing the dissociation rate of the NET selective ligand, [³H]nisoxetine **137**. The results suggest that the allosteric binding site may be a common feature of the biogenic amine transporters (Figure 4.3).¹²⁵

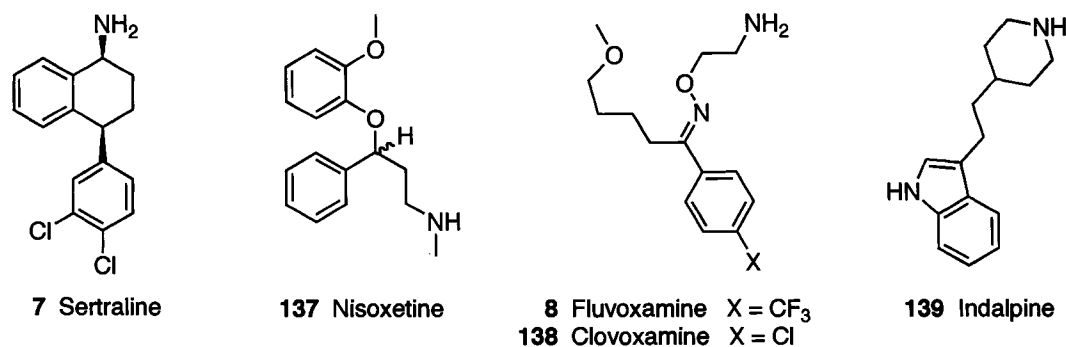


Figure 4.3: Compound structures from the study of Plenge, 1997.¹²⁵

What was most intriguing from the work of Plenge, were the results of an experiment that evaluated the Af-M properties of around 10 SSRI's under the same assay conditions.¹²⁵ The experiments demonstrated that SSRI's possessing two aromatic rings in their structure show enhanced ability to allosterically modulate ligand affinity at the substrate binding site of SERT. The study showed that the SSRI's Fluvoxamine **8**, Clovoxamine **138** and Indalpine **139** (Figure 4.3), *that do not have two aromatic rings*, were the least potent Af-M ligands. This subtle structural observation is key for the development of our hypothesis, that may also involve Af-M ligand conformational flexibility. In that, ligands that have decreased structural rigidity seem to demonstrate diminished Af-M activity.

Chang demonstrated a similar Af-M phenomenon at SERT when examining transport velocities of [³H]5-HT **1** and the binding characteristics of the cocaine analog [³H]CFT **140**. The observations were made using the steroids β -estradiol **141** and estradiol **142** and the steroid analog tamoxifen **143** (Figure 4.4).¹²⁶

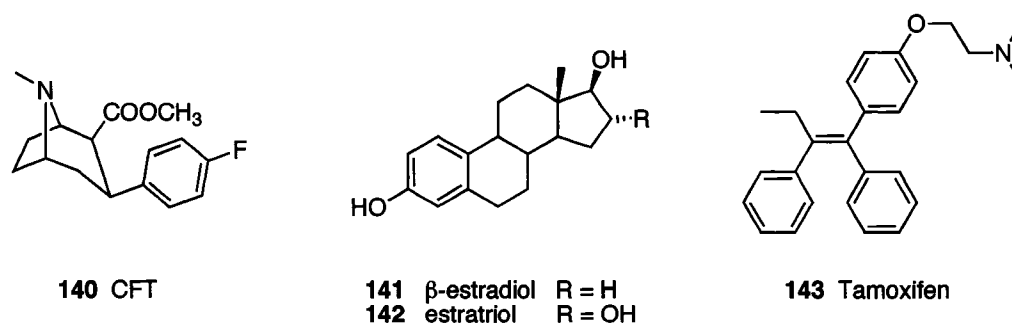


Figure 4.4: Compound structures from the study of Chang, 1999.¹²⁶

Similar to Plenge, Chang observed a dose-dependent decrease in [³H]**1** uptake, and also observed a decrease in [³H]**140** dissociation from the SERT substrate site, in the presence of micromolar concentrations of **141**. Drugs **142** and **143** also displayed the ability to inhibit [³H]**1** uptake, but with decreased potency. The similarities of the results to the work of Plenge are notable and they *may suggest a relationship between steroid qualities, dual aromatic ring structural motifs, ligand flexibility and affinity modulation properties.*

Our laboratory has identified two flavonoids, **144** and **145**, that demonstrate Af-M properties towards the dissociation rate of [³H]paroxetine **9** from the reuptake site on SERT.¹²⁷ These flavonoid compounds also possess dual aromatic ring motifs and are conformationally limited (Figure 4.5).

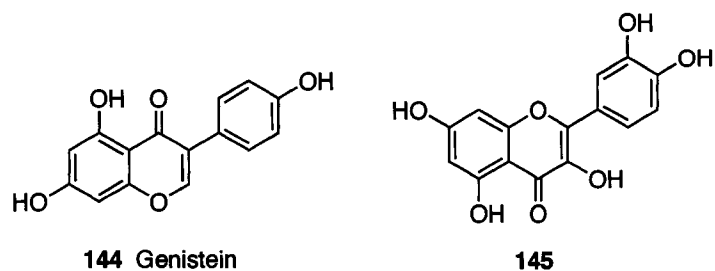


Figure 4.5: Compound structures from the study of Weller, 2002.¹²⁷

Furthermore, flavonoids have been shown to possess steroidal qualities¹²⁸ and our experiments provide additional evidence that rigid, steroid-like molecules demonstrate affinity modulation properties at SERT.

Other evidence that may further link steroids and SSRI's possessing two aromatic functional groups comes from the work of Griffin (Figure 4.6).¹²⁹

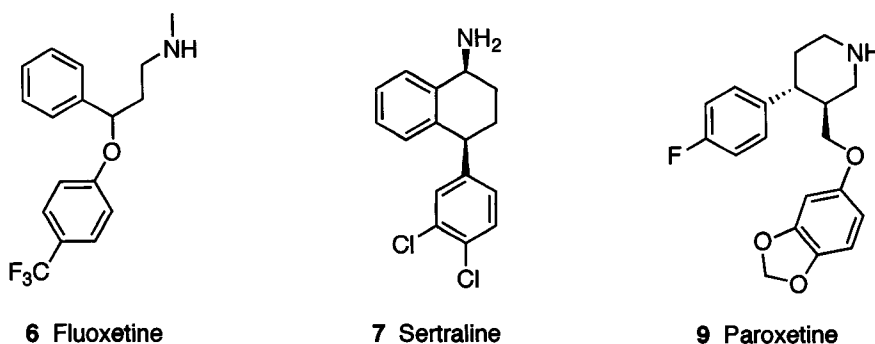


Figure 4.6: Compound structures from the study of Griffin, 1999.¹²⁹

Griffin demonstrated that the SSRI's fluoxetine **6**, sertraline **7** and paroxetine **9** (all with two aromatic rings) interact with neurosteroid enzymes within the CNS, and affect the oxidative and reductive pathways of their respective steroid enzymatic substrates. The results present additional evidence that SSRI's having two aromatic rings may possess some "steroid-like" qualities that afford these overlapped properties with steroids and steroid analogs.

Yet another possible correlation exists with the sexual dysfunction (SD) that results from SSRI therapy.¹³⁰ Many patients (occurrence may be as high as 80%) experience SD as a result of SSRI administration and this effect is thought to be highly dose-dependent.¹³¹ Although the exact mechanisms of SSRI induced SD remain less clear, correlations of SD to low levels of estradiol **141** in females have been observed.¹³² Studies have demonstrated that in some instances switching to a different SSRI medication can ameliorate these side effects. Interestingly, two medications that have shown decreased incidence of SD side effects both possess only a single aromatic ring; Bupropion **146**¹³³ and Fluvoxamine **8** (Figure 4.7).¹³⁴

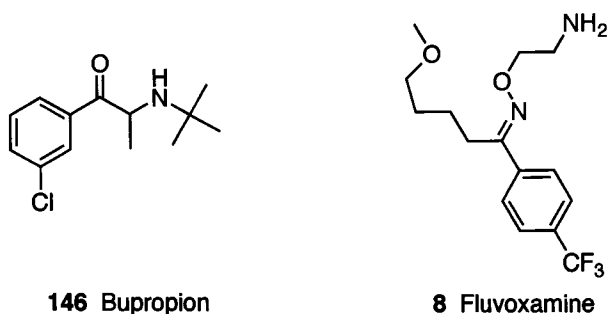


Figure 4.7: Two pharmaceutical agents with reduced incidence of sexual dysfunction side effects.

The reductions in SD for **146** have been observed in double blind studies where direct comparisons to SSRI's with two aromatic functional groups were made, and a statistically significant difference was noted.¹³⁵ Provided that SSRI's have been shown to interact with steroid enzymes,¹²⁹ and that changes in endogenous hormone levels can lead to sexual dysfunction,¹³² it is reasonable to hypothesize that SSRI's induce SD side effects through interactions with various sites associated with the neuroendocrine system. By switching to medications

that have only one aromatic functional group (rather than two, like **6**, **7**, **9**, and **28**), one could eliminate the interactions with steroid receptors since the single aromatic moiety compounds structurally less like steroids. Hence, we suggest that SSRI's that have two aromatic ring moieties provide the binding affinity modulation *and* promote sexual dysfunction qualities as a result of their steroid mimic qualities.

Given the potential use of our 6-NQP analogs in SSRI therapies, we focused to minimize these potential sexual side effects by designing ligands devoid of the two aromatic functional group structural motif. Towards the generation of novel PET imaging agents and to provide a handle for radionuclide introduction, our ligand design strategy has utilized an alkyl side chain replacement for one of the aromatic rings (similar to fluvoxamine **8**). Preliminary biochemical studies in our lab, following the techniques of Plenge,¹²⁵ have shown that MOM-NQP **35** does not display affinity modulation properties at SERT.¹²⁷ To an extent, this supports our initial hypothesis that ligands devoid of two aromatic moieties are with minimal Af-M qualities. To further test the dual aromatic functional group – steroid mimic hypothesis, we sought to purposely alter our 6-NQP analogs by introducing the dual aromatic ring structural motif through the synthesis of quipazine analogs Phen-NQP **135** and Ben-NQP **136** (Figure 4.8).

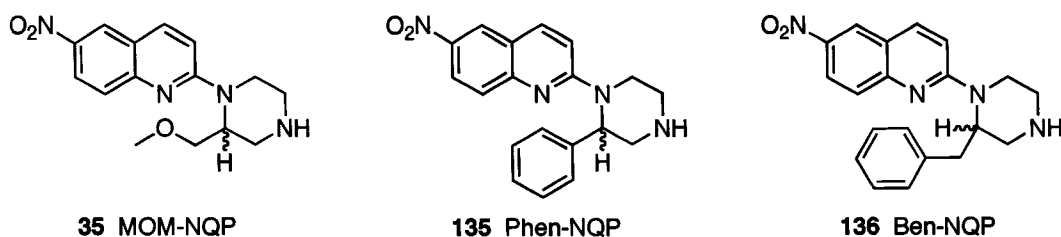


Figure 4.8: Refined lead agent MOM-NQP, and new dual aromatic ring ligands Phen-NQP and Ben-NQP.

With ligands **135** and **136**, we would now be able to test our hypothesis that 6-NQP analogs containing dual aromatic functional groups may allosterically modulate ligand transport and binding at SERT because of their steroid qualities. Doing so, would allow us to compare, *within the same chemical family*, changes in the affinity modulation properties as a result of the introduction of a second aromatic group. The ligands could be further tested at steroid receptors to truly evaluate their steroid qualities. With this goal in mind we began our syntheses of the 2'-aryl-6-nitroquipazines **135** and **136**.

4.2 Synthesis of 2'-Aryl-6-nitroquipazines

The first attempts at generating a 2'-aryl agent focused on the synthesis of a 2-phenyl substituted piperazine. There are several literature accounts of piperazine syntheses related to our target and many of them begin from ethyl bromophenyl acetate **147** or a similar alpha bromo ester.^{136, 137} Roderick utilized **147** in a reaction with ethylene diamine to generate 2-phenyl piperazineone **148** and we hoped to utilize a similar procedure, with N,N-dibenzylethylene diamine

(DBEDA) as the nucleophile, in an analogous manner to Rondu's method for the generation of piperazine ester **150** (Figure 4.9).⁶⁸

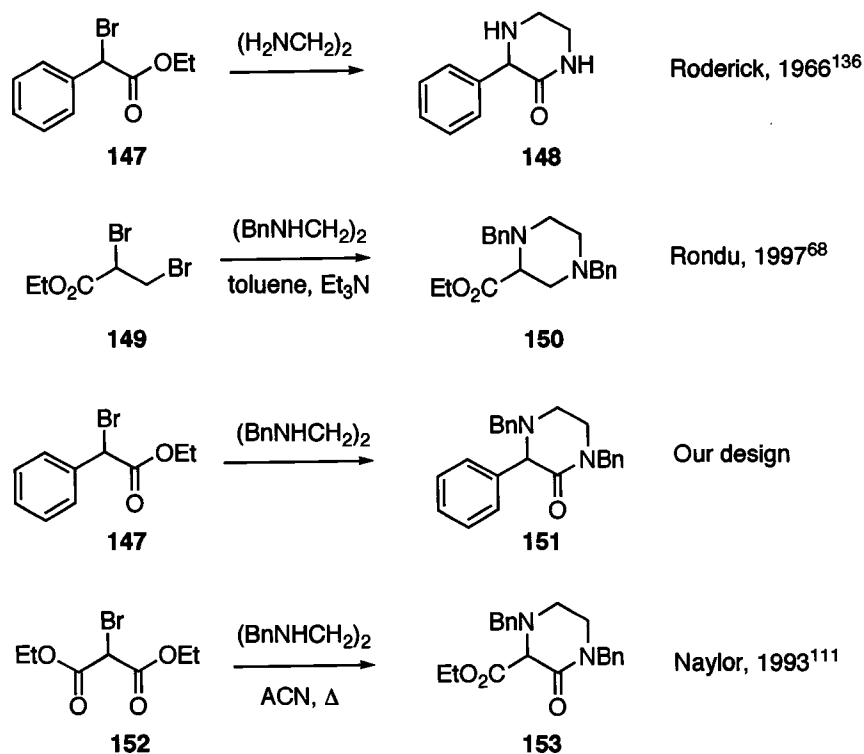
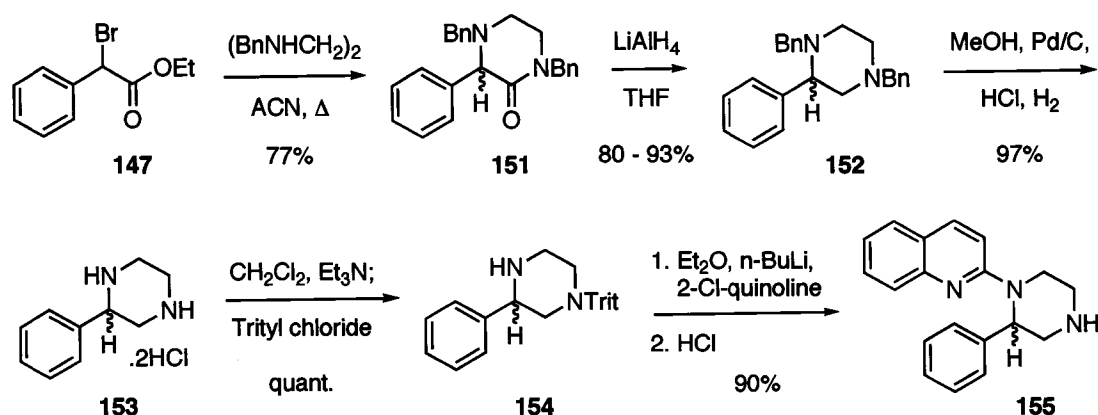


Figure 4.9: Various strategies for piperazine synthesis and our design for obtaining a phenyl piperazine.

Our first attempts to generate **151** from bromo ester **147**¹³⁸ and DBEDA utilized conditions analogous to those of Rondu, with ~1:1 ratio of **147** and DBEDA with 110 mol% Et_3N in toluene at 80 °C. A TLC (EtOAc:Hexanes, 2:3) showed a non-polar ($R_f = 0.63$) ninhydrin active and UV active spot that appeared to be the desired target. However, following chromatography, a ^1H NMR spectrum clearly showed that this material was not desired product **151**. However, while sitting for two days, the chromatography column had leaked and an oil had been deposited on the counter top. This material was analyzed by

TLC (EtOAc:Hexanes, 2:3) and was considerably more polar ($R_f = 0.29$), showed minimal UV activity and was only very slightly active to ninhydrin staining (faint pink). This material however, was very clearly product **151** by ^1H NMR. The column fractions were analyzed again and a 58% yield of **151** was obtained. We were pleased with this result but given the side products that were generated via this route, we felt that alternate synthetic conditions could be found to increase the product yield.

Naylor had cyclized diethyl bromomalonate **152** with 200 mol% DBEDA in refluxing acetonitrile and obtained good yields of piperazinone **153** (Figure 4.9).¹¹¹ Attempting this strategy with bromo ester **147** resulted in a good conversion to product **151** with a yield of 77%. Satisfied with this result we proceeded further with our synthesis (Scheme 4.1).

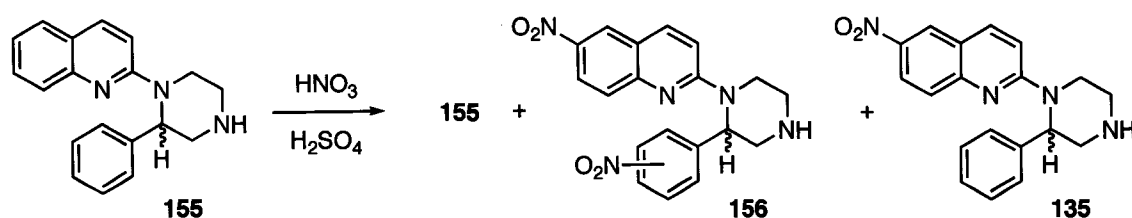


Scheme 4.1: Initial synthesis of 2'-phenylquipiazine.

The cyclized material **151** was reduced to piperazine **152** with LiAlH_4 in THF and removal of the benzyl groups by catalytic hydrogenolysis provided **153** in excellent yields. The less hindered amine was protected with a trityl group and

protected piperazine **154** was coupled to 2-chloroquinoline. Following deprotection, 2'-phenylquipazine **155** was obtained in 90% yield.

Unfortunately, we naively thought that a regioselective nitration of the quinoline ring might be possible since it was activated by the piperazine nitrogen. However, this was not the case. Using 400 mol% of HNO₃, a mixture of dinitrated products was formed. Reducing the HNO₃ to 100 mol% provided a mixture of unnitrated starting material **155**, dinitrated mixture **156** and what appeared to be desired product **135** (Scheme 4.2).

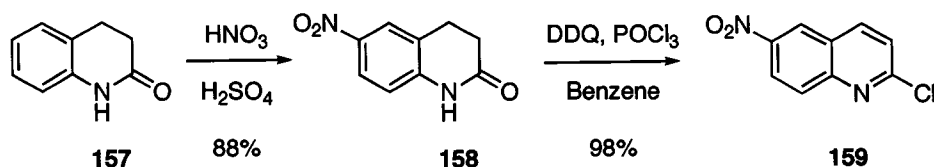


Scheme 4.2: Nitration attempt with 100 mol% of nitric acid forming a complex product mixture.

Attempts to isolate **135** through various protection-purification-deprotection cycles with N-Boc and N-formyl protecting groups all failed to generate a pure sample of **135** so an alternate synthetic route was pursued.

The obvious solution was to avoid the nitration step altogether, by coupling protected piperazine **154** to an already nitrated quinoline ring. A literature search demonstrated that the strategy could be accomplished, in that researchers working with quipazines had already established the utility of 2-chloro-6-nitroquinoline **159** for these purposes (as per Figure 4.10).¹³⁹ The

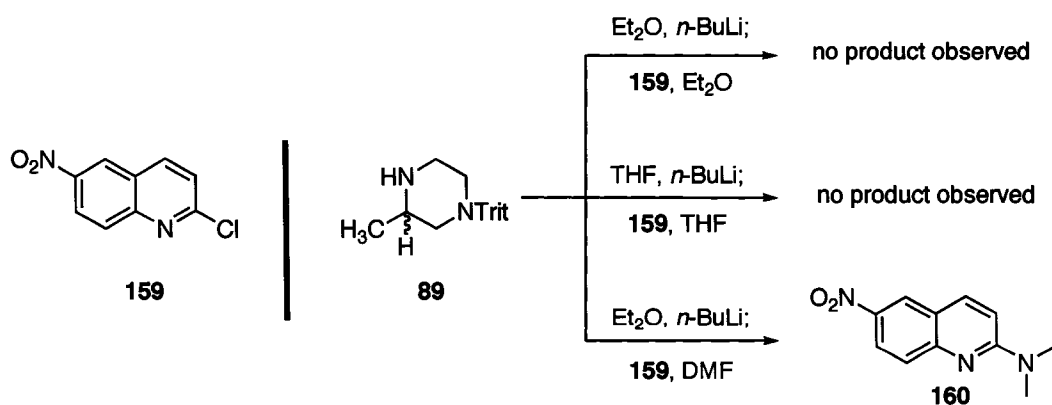
nitroquinoline can be synthesized easily from commercially available hydrocarbostyryl **157** in two steps (Scheme 4.3).



Scheme 4.3: Synthesis of 2-chloro-6-nitroquinoline.

Nitration of **157** provided a mixture of 6- and 8-nitrostyryls. The 6-nitro regioisomer **158** could easily be isolated through recrystallization from EtOAc or rinsing the crude solids with cold EtOAc. Chloro nitroquinoline **159** was generated through a one-pot, chlorination-oxidation reaction of amide **158** with 2,3-dichloro-5,6-dicyano-1,4-benzoquinone (DDQ) and POCl_3 .

With nitrated quinoline **159** in hand, Gilman coupling reactions (similar to those described previously) with trityl protected methylpiperazine **89** were attempted and these all proved unsuccessful (Scheme 4.4).

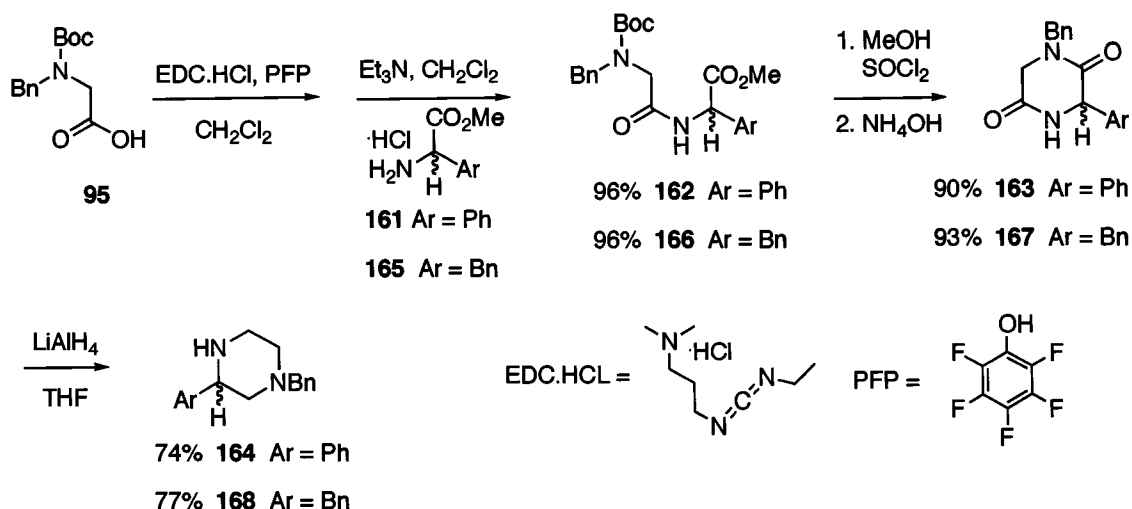


Scheme 4.4: Gilman coupling attempts with 2-chloro-6-nitroquinoline.

Quinoline **159** was exceptionally insoluble in ether, relative to the 2-chloroquinoline, and the usual Gilman conditions did not lead to product formation. The more polar etheral solvent, THF was utilized and this resulted in similar poor results. Using DMF as the solvent for **159**, provided a small amount of a product-like (yellow colored) material by TLC. However, after isolation, the material was shown to be 2-dimethylamino-6-nitroquinoline **160**, that was formed upon displacement of the dimethylamide ion from the DMF solvent.

Although discouraged by these results, we were encouraged by literature accounts detailing piperazine couplings to **159**, and related quinolines, using excess amine in DMF at elevated temperatures (as shown in Figure 4.10).^{54, 72, 73,}
¹³⁹ We proceeded to study the thermal coupling reaction with benzyl and phenyl piperazines, using three different nitrogen protecting groups; N-trityl, N-formyl and N-benzyl. The protected piperazines were coupled to **159** under a variety of conditions (solvent, temperature, concentrations, ratios) and the discussion of these coupling attempts follows below. First, we'll discuss the application of the asymmetric synthesis to acquire our aryl piperazines and then the synthetic transformations necessary for the introduction of our protecting groups

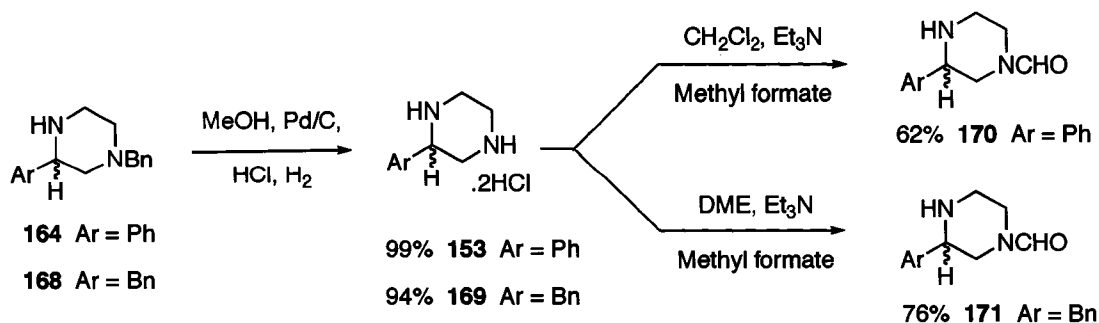
The peptide coupling was performed according to the method of Naylor,¹¹¹ using phenylglycine or phenylalanine methyl ester hydrochlorides **161** and **165**, respectively. The starting materials were synthesized from the commercially available amino acids using SOCl₂ in MeOH.¹⁴⁰ Both couplings went smoothly, providing excellent yields of dipeptides **162** and **166** that were routinely cyclized to the piperazindiones **163** and **167** (Scheme 4.5).



Scheme 4.5: Synthesis of the N-benzyl aryl piperazines using the 'assymetric' methodology described in Chapter 3.

The reduction of the diamides with LiAlH_4 in THF provided our N-benzyl protected aryl piperazines **164** and **168** in good yields. The synthesis of these piperazines, again, demonstrated the ease to which the non-racemic compounds *could* be generated from the commercially available D or L amino acid starting materials.

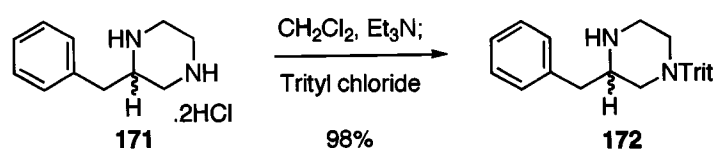
The N-formyl protected piperazines **170** and **171** were selectively formed from dihydrochlorides **153** and **169** using methyl formate in DCM or DME with Et_3N as a base (Scheme 4.6).¹⁴¹



Scheme 4.6: Synthesis of N-formyl protected aryl piperazines.

Since these reactions were run under heterogenous conditions, it was important at the outset that the hydrochlorides be fine powders to ensure adequate mixing. The piperazine hydrochlorides **153** and **169** were easily formed from **164** and **168** using standard hydrogenolysis conditions. The phenyl dihydrochloride **153** was also generated from dibenzyl piperazine **152** under the same catalytic conditions, according to Scheme 4.1 above.

The synthesis of the trityl protected phenylpiperazine **154** was described above (Scheme 4.1). The benzyl analog **172** was synthesized in an identical manner from **171** in excellent yield (Scheme 4.7).



Scheme 4.7: Synthesis of N-benzyl protected benzyl piperazine.

Our thermal coupling studies were adapted from those of Lee¹³⁹ who utilized 500 mol% of N-formyl piperazine **173** with **159** in DMF to generate 6-nitroquipazine **22** in 95% yield following deprotection (Figure 4.10).

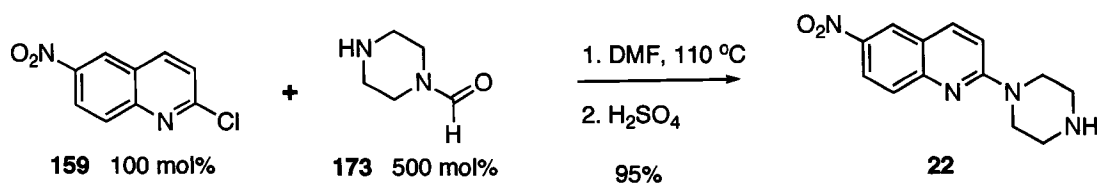


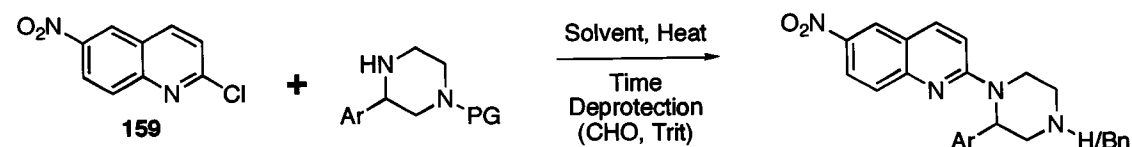
Figure 4.10: Lee's reported thermal coupling to form 6-nitroquipazine.

However, we decided to use a maximum of 200 mol% of amine since our piperazine fragments were synthetically valuable to us, in contrast to the

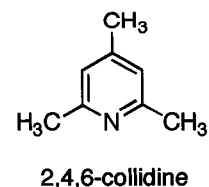
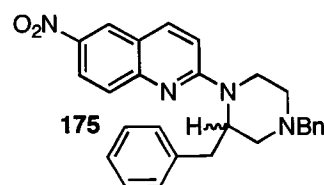
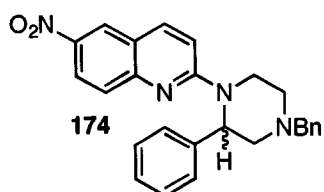
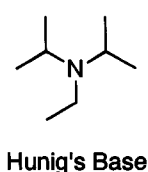
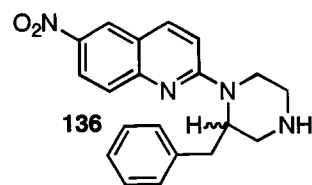
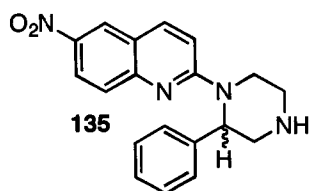
inexpensive and commercially available **173**. Our thermal synthesis trials (Table 4.1) began with the N-trityl protected phenyl and benzyl piperazines (**154** and **172**, respectively, Entry 1 and 2). These fragments were reacted with **159** in DMF at 110 °C and we were pleased that the coupling reaction occurred as observed by the formation of a non-polar spot by TLC ($R_f = >0.55$, EtOAc:Hexanes, 2:3) that had the distinctive yellow nitroquipazine color. The new spots were distinct from the 2-dimethyl-aminoquinoline **160** ($R_f = 0.29$, EtOAc:Hexanes, 2:3) observed with the Gilman coupling attempts in DMF. Thus, we were confident that the desired transformation was occurring. However, when the products were isolated and the trityl groups removed, very poor yields of the products (**135** and **136**) were obtained (< 20%) in both cases.

Interestingly, there was also a very polar ($R_f = 0.0$, EtOAc:Hexanes, 2:3; $R_f = \sim 0.4$, MeOH:CH₂Cl₂, 1:9) material observed by TLC that had the same distinctive yellow color as the product. We suspected that the material was coupled product that had deprotected under the conditions of the coupling reaction and we investigated this further for the phenyl case (Entry 1). After flushing the material from a column we attempted to isolate it from the rest of the polar side products by treating the mixture with excess Boc₂O in DCM.

Table 4.1: Summary of the thermal coupling experiments. For the amine substrate, **Ar** denotes the side chain aromatic functionality and **PG** denotes the nitrogen protecting group used for that entry. Mol% indicates amount of amine substrate relative to quinoline **159** (100 mol%). For trityl and formyl protecting groups, standard acidic deprotection conditions were used as described earlier in Chapters 2 and 3.

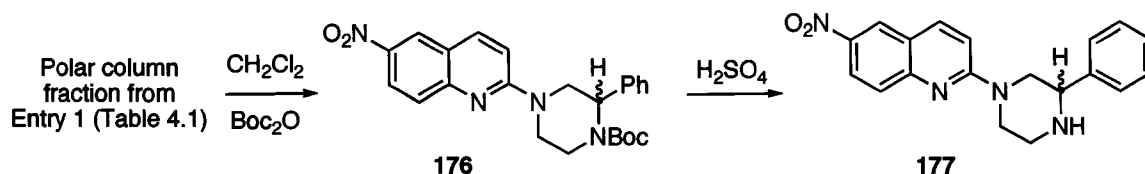


Entry	#	Amine		Conditions				Outcome	
		Ar	PG	Mol%	Solvent	Temp	Time(h)	Product	Yield
1	154	Ph	trityl	200	DMF	110 °C	20	135	15%
2	172	Bn	trityl	200	DMF	110 °C	6	136	18%
3	170	Ph	formyl	200	DMF	130 °C	20	135	54%
4	171	Bn	formyl	200	DMF	120 °C	44	136	46%
5	168	Bn	Bn	200	DMF	155 °C	24	175	37% ^a
6	168	Bn	Bn	200	Cl-Ben	155 °C	44	175	43%
7	164	Ph	Bn	200	Cl-Ben	130 °C	40	174	29% ^a
8	171	Bn	formyl	200	Cl-Ben	135 °C	39	136	<25% ^b
9	168	Bn	Bn	200	DMSO	120 °C	20	175	74%
10	171	Bn	formyl	200	DMSO	120 °C	44	136	45%
11	164	Ph	Bn	200	DMSO	120 °C	24	174	76%
12	164	Ph	Bn	200	DMSO	80 °C	44	174	63%
13	168	Bn	Bn	100	DMSO	120 °C	20	175	46%
			w/ Hunig's Base	200					
14	164	Ph	Bn	100	DMSO	120 °C	29	174	59%
			w/ 2,4,6-collidine	200	(.35 M)				
15	164	Ph	Bn	100	DMSO	115 °C	40	174	53%
			w/ 2,4,6-collidine	200	(.91 M)				



a) yield off the column in question, other material present; b) estimated, not isolated

The yellow spot showed a distinct change in polarity ($R_f = 0.29$, EtOAc:Hexanes, 2:3) suggesting that the Boc protecting group had been introduced. After isolating the product **176** by column chromatography and removing the protecting group we found that we had isolated the 3'-phenyl isomer **177** of our desired product **135** (Scheme 4.8).



Scheme 4.8: Isolation of 3'-phenyl-6-nitroquipazine.

The yield of **177** (29%) was nearly double the yield of the target **135** (15%). The results clearly suggested that N-trityl was not a good protecting group for this transformation. It also suggested that the 3'-isomer **177** is readily formed. An observation that is not surprising, since the phenyl substituent provides steric hindrance towards the formation of the 2'-isomer.

Following these initial encouraging results, our attention turned to the use of the formamide and benzyl protected piperazine coupling fragments. The reactions involving the N-formyl protected phenyl and benzyl piperazines (**170** and **171** respectively, Entries 3 and 4) gave improved yields (54% and 46%, respectively) of their respective products and this is attributed to the increased stability of the N-formyl protecting group. A side product observed in these transformations was 2-dimethylamino-6-nitroquinoline **160**. Clearly, the DMF solvent is again contributing to the formation of **160**, by a displacement of the

dimethylamine group under the coupling reaction conditions. Compound **160** was also a side product from a Gilman coupling attempt using DMF as per Scheme 4.4. It should also be noted that doubling the reaction time (Entry 4 vs. 3) did not improve the overall yield of the reaction. In all attempts involving DMF as a solvent, the reactions never went to completion, as **159** was still clearly visible by TLC.

Our next experiments utilized N-benzyl protected benzyl piperazine **168** with DMF and chlorobenzene (Cl-Ben) as reaction solvents (Entries 5 and 6). Again, using DMF, we observed the same formation of **160** as a result of solvent participation in the reaction. The N-benzyl product **175** was formed with decreased yield and the purity of **175** isolated from column purification was low because a range of unidentifiable side products coeluted with the product. The use of chlorobenzene as the reaction solvent inhibited the reaction, as observed (TLC) by the slow disappearance of quinoline **159**. However, the formation of side product **160** was eliminated and the product **175** isolated from the column was of much higher purity than that from the DMF reaction. Interestingly, when the benzyl protected phenyl piperazine **164** was reacted under similar conditions in chlorobenzene (Entry 7), poor conversion to the product **174** was observed and the product isolated from the column was contaminated with unidentifiable side products. The use of N-formyl benzyl piperazine **171** in chlorobenzene was remarkably slow (Entry 8). After 39 h very little product formation was observed by TLC and no attempt to isolate the product was made.

Of the experiments that had been completed (Entries 1 – 8), the best coupling results were demonstrated with N-formyl piperazines and DMF as the reaction solvent. However, these conditions were hampered by the unwanted formation of **160** as a result of solvent participation in the reaction. Additionally, with the poor results observed in chlorobenzene, we were compelled to believe that the polarity of DMF played an important role in assisting the transformation; very likely through the stabilization of charged intermediates and/or transition states. Consequently, we decided to try DMSO as a reaction solvent and entries 9 – 15 summarize these transformations.

For the first time, we observed the consumption of our quinoline starting material **159** by TLC. The initial trial (Entry 9) produced an excellent 74% yield of **175** from our benzyl protected benzyl piperazine **168** at a relatively low temperature (120 °C) in 20 h. Although DMSO is often difficult to remove following a reaction, the crude coupled product can easily be isolated by flooding the reaction contents with water and extracting the aqueous mixture twice with ether. The combined extracts are then washed with five portions of water and two portions of brine to provide the crude material that is virtually free from DMSO and can be chromatographed immediately. The Entry 9 transformation was also much cleaner than the all reactions performed in DMF. The reduced formation of unidentifiable side products resulted in simpler chromatographic separation and increased product purity.

Another intriguing observation was the general lack of reactivity of the N-formyl protected benzyl piperazine **171** to the DMSO conditions. The reaction

was exceptionally slow and after 2 days only a 45% conversion to product was observed (Entry 10). This decreased reactivity could be explained by a reduction in the nucleophilicity of the amine lone pair of electrons as a result of the electron withdrawing influence of the formamide protecting group. The inductive effect resulting from the formal positive charge in resonance structures **179** and **180** is thought to lessen the availability of the lone-pair electrons for nucleophilic attack (Figure 4.11).

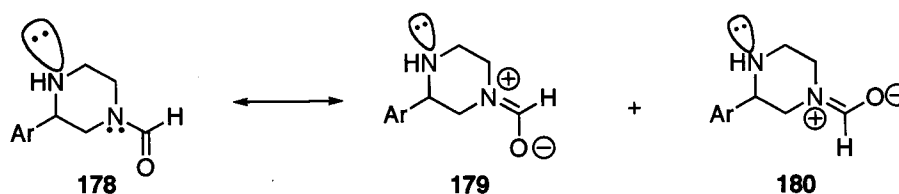


Figure 4.11: Reduction in amine nucleophilicity as a result of inductive effects from the formyl protecting group.

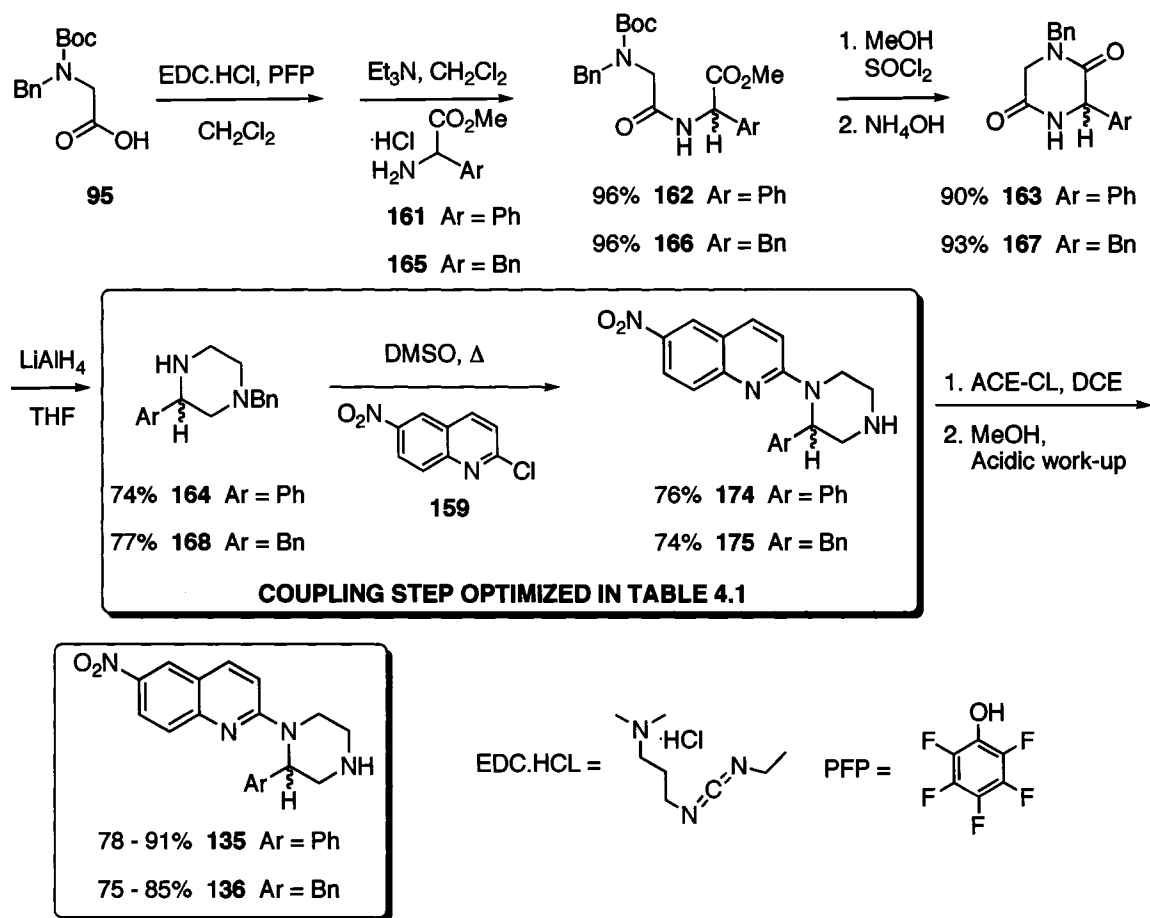
Given the poor DMSO coupling result with the N-formyl piperazine **171** we returned our attention to N-benzyl protected phenyl piperazine **164**. When **164** was coupled to **158** in DMSO, coupling results were obtained that were similar to those for **168** (Entry 11). A clean reaction and a good conversion to product afforded **174** in yield of 76%. This reaction was repeated at a lower temperature (80 °C, Entry 12) and although slower (reaction time of 44 h, **159** was not consumed), a good yield of **174** was still obtained. We felt that we had finally established reaction conditions that provided consistent, satisfactory results with both piperazine substrates. What was even more pleasing was the ability to achieve yields > 70% with only 200 mol% of our piperazine fragments.

Pragmatically, we were still throwing away half of our amine starting material in every coupling reaction, and the yields based on our piperazine starting materials were only ~38%. In an attempt to reduce our amine starting material utilization, we experimented with some non-nucleophilic amine bases as additives to act as a sponge for the HCl that is generated in the coupling reaction (Entries 13-15). The amine bases we chose were Hunig's base (diisopropylethyl amine) and 2,4,6-collidine (Table 4.1). The bases were utilized as 200 mmol% additives in a 1:1 mixture of **159** and benzyl protected piperazine (**164** or **168**). When Hunig's base was utilized with piperazine **168** (Entry 13), the overall conversion was low and it was evident by TLC that additional side products were forming. Still, the yield of product relative to the piperazine (46%) showed a ~10% increase over the prior DMSO conditions that utilized 200 mol% of amine (e.g. Entry 12 vs. Entry 13). Collidine was used twice with two different amounts of solvent and provided a marked improvement over the Hunig's base conditions, giving a much cleaner conversion and yields that approached 60%. The yields relative to the piperazine were now ~20% greater than those observed with 200% mol% of piperazine and no additive base (e.g. Entry 12 vs. Entry 14). Increasing the concentration of the reactants by reducing the amount of solvent didn't seem to have much of an effect on the overall transformation (Entry 15).

We had now established a simple and relatively efficient method of generating our 2'-aryl-6-nitroquipazine agents with the thermal coupling methodology. Furthermore, the reactions are simple to perform: place the starting materials in an 8 mL vial, add stirbar and solvent, seal under argon and

place in an oil bath at a temperature of 120 °C. The reaction workup and chromatography are straightforward giving products with high purity. Additionally, the best results were obtained with the N-benzyl protected piperazines (**164** and **168**) that could easily be generated using the 'asymmetric' methodology adapted from Naylor (Scheme 4.5). We had earlier established good benzyl deprotection conditions using ACE-Cl, so the final products (**135** and **136**) can be obtained in good overall yields.

The complete syntheses of our 2'-aryl-6-nitroquipazine analogs are detailed in Scheme 4.9 and are accomplished in five steps with > 40% yields from the amino acid starting materials **161** and **165**. The nitroquinoline coupling fragment **159**, is easily synthesized from a commercially available starting material **157** in 86% yield.



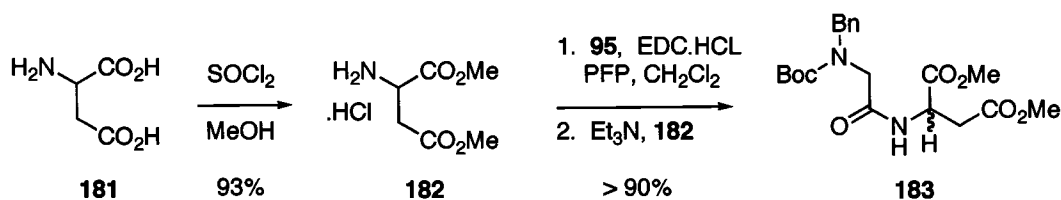
Scheme 4.9: Complete, optimized synthesis of the 2'-aryl-6-nitroquipazine targets. The thermal coupling step was optimized as detailed in Table 4.1.

4.3 The Alternate Assymmetric-Like synthesis of 2'-EtOMe-NQP

Given the potential need for the enantiomers of the ethyl side chain analog **78**, it was undertaken to see if Naylor's synthesis¹¹¹ could be applied to these targets. The obvious choice for an amino acid building block was aspartic acid since the R group contained a 2-carbon ester that could be reduced to the alcohol and afford the methoxyethyl ether.

The racemic acid **181** was utilized since proof of concept was all that was desired and the aspartate dimethyl ester hydrochloride **182** was generated with

excess SOCl_2 in refluxing methanol.¹⁴⁰ Diester **182** underwent the Naylor peptide coupling under the reported conditions to provide dipeptide **183** in excellent yields (Scheme 4.10).



Scheme 4.10: Synthesis of the racemic aspartyl dipeptide.

When considering the cyclization step though, we realized that we may encounter a problem. Our dipeptide **183** presented two opportunities for ring-closing amide formation 1) with the amino-acid ester and 2) with the side chain ester (Figure 4.12) to provide six and seven membered ring products **184** and **185**, respectively. Given the relative stabilities of the ring sizes, we were concerned about the formation of isomeric product mixtures. Indeed, these ring closures, being 6-exo-trig and 7-exo-trig, are both 'favored' according to Baldwin⁹² so a mixture of cyclized products was expected.

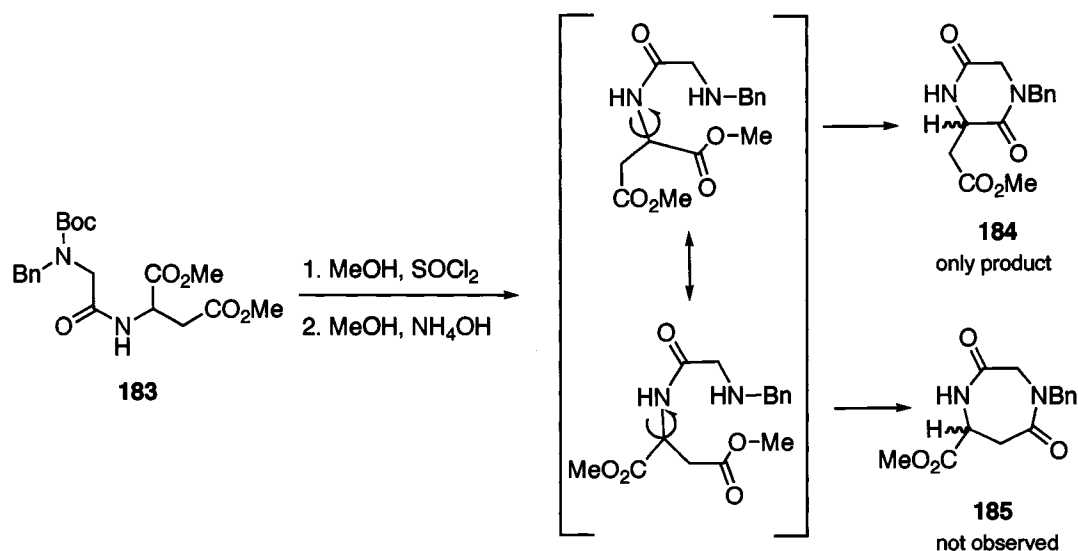
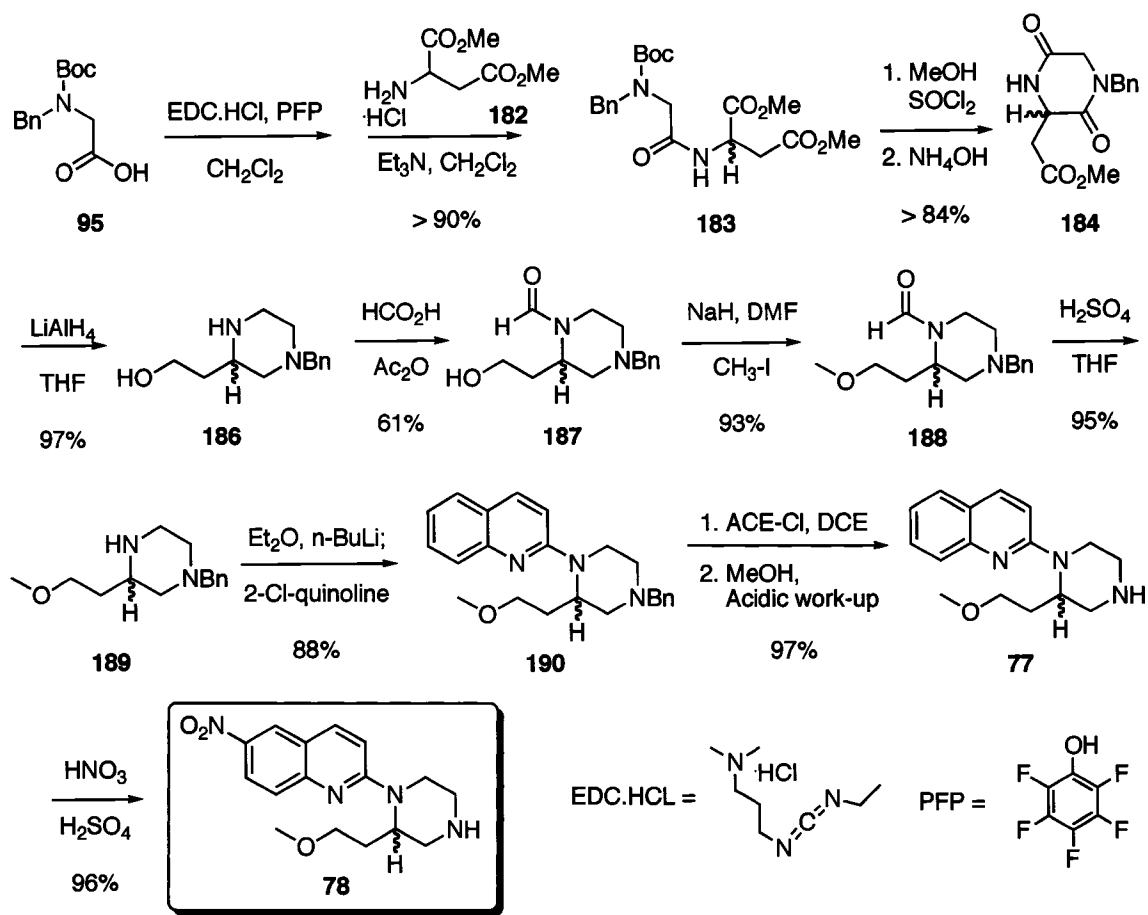


Figure 4.12: The peptide cyclization step showing the opportunities for two isomeric products.

Interestingly, when the crude reaction product was analyzed by ¹H and ¹³C NMR it was clearly shown to contain a single, major isomeric product. More careful inspection of the ¹H NMR spectra indicated the presence of another product, but this made up < 2% of the total material. The major product was later proven to be the desired 6-membered piperazine dione **184**, once the synthesis had been carried through to product **78**. The selectivity for this single product is curious since both ring sizes are known to be relatively stable.

With the fortunate formation of a single major cyclized product, we proceeded with our synthesis (Scheme 4.11) and reduction of dione **184** with LiAlH₄ in THF provided the crude piperazine alcohol **186** in 97% yield. Since this alcohol is a homolog of the alcohol **94** from the asymmetric MOM-NQP synthesis (Scheme 3.9, Chapter 3) we used the same synthetic strategy to generate target quipazine **78**.



Scheme 4.11: Complete synthesis of 2'-methoxyethyl-6-nitroquipazine using dimethyl aspartate amenable for asymmetric preparations.

The crude alcohol **186** was converted to N-formyl alcohol **187** that was alkylated with $\text{CH}_3\text{-I}$ to provide **188**. After removal of the formyl group, **189** was coupled to 2-chloroquinoline to provide benzyl-protected quipazine **190**. The removal of the benzyl group with ACE-Cl, followed by the acidic work-up, provided unnitrated quipazine **77** in an excellent 97% yield. The ^1H NMR spectra of **77** was identical to the material generated via the previously described route (Chapter 2, Scheme 2.9) confirming that 6-membered ring dione **184** had been generated upon cyclization of peptide **183**. The nitration of **77** provided target EtOMe-NQP **78**. The alternate synthesis of **78** established proof of concept for

the future asymmetric synthesis of **78**, provided that racemization does not occur at some point. The racemic EtOMe-NQP **78** generated via this route was synthesized in nine steps with a 40% overall yield from the amino acid starting materials.

CHAPTER 5

BIOLOGICAL DATA

5.1 Serotonin Transporter Binding Affinity of Target Ligands

The initial evaluation of our new ligands is performed through a standard radioligand displacement binding assay. The method utilizes the procedure of Habert¹⁴² as described by Mathis¹⁴³ and it is summarized below. The assay is used to determine the binding affinity (K_i) of the ligands at SERT. Lower K_i values (more dilute concentrations) represent higher affinity ligands.

Tissue Preparation – The cerebral cortex from commercially available (Pel-Freez Biologicals, Inc.) frozen male rat brains is suspended in twenty volumes of 50 mM Tris-HCl buffer (pH 7.4 at ambient temperature) and homogenized. The brain mixture is centrifuged and the supernatant decanted. The tissue pellet was suspended in the same volume of Tris-HCl buffer and heated at 37 °C for 10 min before centrifuging and decanting the supernatant. The final tissue suspension is generated by adding 50 mM Tris-HCl buffer (~ 1 mL for every milligram of wet tissue) containing 5 mM KCl and 120 mM NaCl to the pellet and mixing. The brain prep suspension is used immediately in the assay.

Radioligand Displacement Binding Assay – To the tissue preparation suspension (0.8 mL) is added a solution of [³H]Paroxetine ([³H]Px) in Tris-HCl buffer (0.1 mL, 2 – 3 nM, final concentration of 0.2 – 0.3 nM) followed by decreasing

concentrations of challenge ligand (0.1 mL, 10^{-5} – 10^{-10} M; final concentrations of 10^{-6} – 10^{-11} M) to give a total assay volume of 1.0 mL. Three assay solutions were prepared for each concentration of challenge ligand. Total binding (defined below) was determined by adding 0.1 mL of [3 H]Px solution and 0.1 mL of Tris-HCl buffer (no challenge ligand) to 0.8 mL of tissue solution. Non-specific binding was determined by adding a solution of 6-Nitroquipazine **22** in Tris-HCl buffer (0.1 mL, 10 μ M, final concentration 1 μ M) to 0.1 mL of [3 H]Px solution 0.8 mL of tissue solution. The mixtures were incubated at 25 °C for 3 hours then diluted with 5 mL of cold (4 °C) Tris-HCl buffer. These solutions were rapidly filtered through Schleicher and Schuell #32 glass fiber filters (presoaked with 0.5% polyethylenamine solution) using a Brandel cell harvester (protein is collected on the filter, unbound [3 H]Px is washed away). The filters were washed twice with 5 mL of cold Tris-HCl buffer, transferred to scintillation vials and scintillation fluid was added. The radioactivity remaining on the filters ([3 H]Px still bound to protein) was determined using a Packard 1500 Tri-Carb liquid scintillation counter.

Data Analysis – The total specific binding of [3 H]Px to SERT is defined as the difference between total binding and nonspecific binding. Total binding is the total amount of [3 H]Px that was bound to protein, including specific and nonspecific interactions. Nonspecific binding is determined using a high concentration (1 μ M) of the non-radioactive, selective SERT ligand 6-NQP **22**. Since the high concentration (4000 fold or greater) of **22** results in nearly all of the available SERT being bound by **22**, the radioactivity present after filtration

represents the [³H]Px that was bound to other macromolecules in the assay matrix.

The [³H]Px binding observed for test agent samples is reported as a percentage of the total specific binding. When this data is plotted, a binding curve like that shown in Figure 5.1 will result.

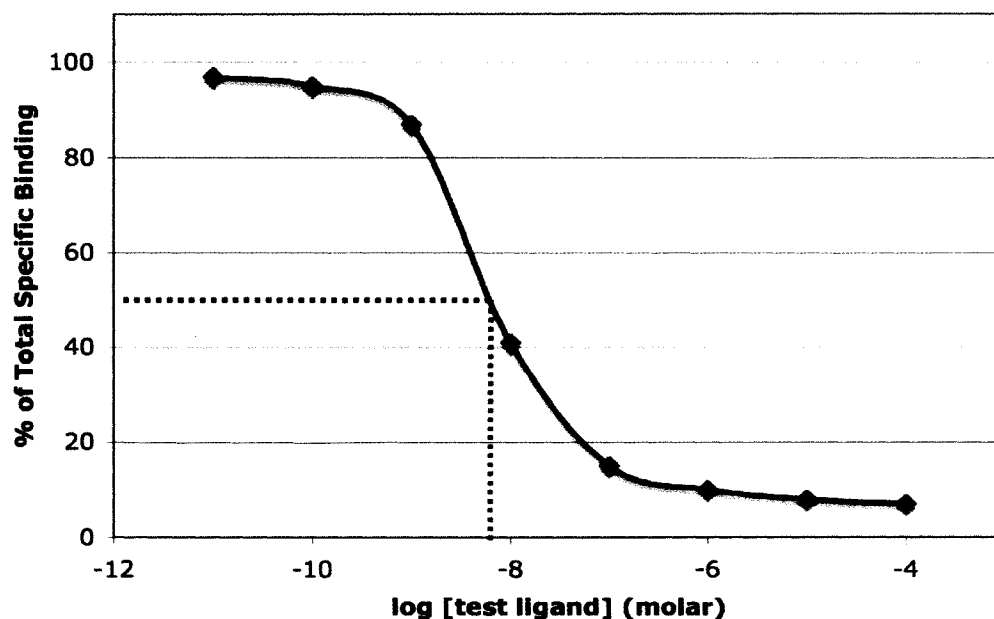
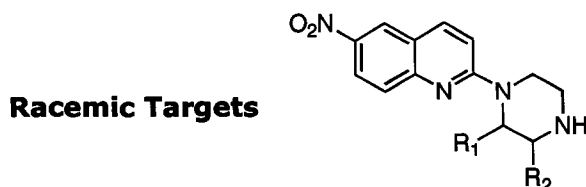


Figure 5.1: Sample binding curve from a radioligand displacement binding assay. No error bars are indicated. The dotted lines demonstrate an estimation of the IC₅₀ value.

For our experiments, each data point is an average of three determinations from the same assay. Since the figure above is an example, no error bars are indicated. Using GraphPad Prism software IC₅₀, (inhibitor concentration that blocks 50% of [³H]Px binding) values were determined. On the above graph this value can be estimated as a concentration slightly less than 10⁻⁸ M. The inhibition binding constant (K_i) is determined from the IC₅₀ values using the following equation: $K_i = IC_{50}/(1 + [L]/K_D)$.¹⁴⁴ Where [L] = concentration

of [³H]Px used in the assay (0.2 – 0.3 nM) and K_D = 0.15 nM (known constant¹⁴²). Final K_i values are reported as an average of at least three different assay determinations on different days. A standard ligand, 6-NQP **22** (known K_i = 0.16 nM), was analyzed in each assay to evaluate assay performance.

Table 5.1: Comprehensive SERT binding affinity data for all racemic compounds from our lab that have been tested. The entries above the dotted line were also shown in Table 1.3.



Cmpd.	R₁	R₂	K_i (pM)	Ref.
22	H	H	163 ± 53	64
24	CH ₃	H	81 ± 61	64
25	H	CH ₃	4560 ± 2400	64
35	CH ₂ OCH ₃	H	2.48 ± 0.28	70
55	CH ₂ OH	H	12.7 ± 3.0	a
61	CH ₂ OCH ₂ CH ₂ CH ₂ F	H	3.96 ± 0.88	a
48	CH ₂ CH ₂ CH ₂ OCH ₃	H	2.12 ± 1.13	74
50	CH ₂ CH ₂ CH ₂ F	H	2.48 ± 0.19	74
191	CH ₂ CH ₂ CH ₃	H	41.5 ± 19.9	74
192	CH ₂ CH ₂ CH ₂ CH ₂ CH ₂ F	H	79.6 ± 21.2	74

^aPresent study

A comprehensive summary of our SERT binding data for racemic targets is presented in Table 5.1 (Data above the dashed line was also shown in Table 1.3). From our initial SAR studies, discussed in Chapter 1, we demonstrated a 56 fold decrease in SERT binding affinity with the 3'-methyl positional isomer **25** relative to the 2'-isomer **24**. As a result, we maintained the alkyl substituents at the 2'-position for all of our quipazine targets. This ligand design strategy has proven successful, as all new racemic targets (**55** and **61**, present study; **48**, **50**,

191, 192, Kusche, 2006) have demonstrated sub-nanomolar binding affinity at SERT that remains improved relative to parent ligand **6-NQP 22**.

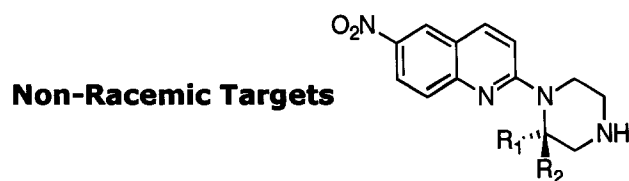
An interesting trend from the SAR data suggests an oxygen heteroatom in the side chain provides an enhancement SERT binding affinity. This trend can be observed by comparing side chains of similar length (excluding hydrogens). For example, MOM-NQP **35** and Prop-NQP **191** both have three atoms in the side chain (MOM, C-O-C; Prop, C-C-C) and **35** demonstrates a 17-fold increase in binding affinity relative to **191**. A similar trend is observed with MeProF-NQP **61** (C-O-C-C-C) and PentF-NQP **192** (C-C-C-C-C) where **61** demonstrates a 20-fold increase in binding affinity relative to **192**. It is plausible that the oxygen atom enhances SERT binding affinity by acting as a hydrogen bond acceptor in the Ar2 binding domain at SERT or as an electronegative contact for positively charged amino acid residues or ions (salt-bridge interactions). Interestingly, the alcohol side chain ligand **55** shows a slight decrease in SERT binding affinity relative to the methyl ether side chain analogs (**35** and **48**). This decrease in affinity may result from the OH group being a hydrogen bond donor, rather than an acceptor (like the methyl ethers). Additionally, moving the oxygen atom further from the piperazine ring does not seem to alter the enhanced binding affinity observed with oxygenated side chains, as evidenced by the low binding affinity of propyl analog **48**.

A fluorine atom might also provide a similar contact, as evidenced by a comparison of ProF-NQP **50** and Prop-NQP **191**, where a fluorine-for-hydrogen replacement is made at the end of the side chain. The fluorinated variant **50**,

displays a 17-fold increase in potency over **191**, a difference identical to that observed between **35** and **191**.

The non-racemic 6-NQP analogs that have been evaluated by our group are shown in Table 5.2.

Table 5.2: SERT binding data for the non-racemic ligands.



Cmpd.	R₁	R₂	K_i (pM)	Ref.
(R)24	H	CH ₃	91 ± 16	103
(S)24	CH ₃	H	68 ± 21	103
(S)35	H	CH ₂ OCH ₃	1*	a
(R)35	CH ₂ OCH ₃	H	47*	a

^aPresent study; *Preliminary value

The enantiomers of 2'-methyl-NQP **24** did not demonstrate significant differences in SERT binding affinity, as evidenced by the overlap of their error bars. It is plausible the methyl side chain may be too short for a significant change in biological activity to be observed, as a result of stereoselective interactions at SERT. The enantiomers of the longer side chain MOM-NQP **35**, have demonstrated more pronounced differences in their binding affinities, but reliable values have yet to be confirmed. The preliminary results indicate that an approximate 47-fold difference in affinity exists between the isomers, with the (S)-isomer **(S)-35** being the more potent form. The increased binding affinity observed for **(S)-35**, relative to the racemate may result from a more optimal

contact of the methoxymethyl side chain with the Ar2 binding region (see pharmacophore model Chapter 1, Figure 1.11). Likewise, the converse argument can be made for the decreased affinity of (*R*)-**35**. Efforts to establish more accurate K_i values for these targets are presently underway and we hope to confirm these values through determinations at an independent laboratory.

To date, the only compound from our work that has been tested for SERT selectivity is [^3H]Prop-NQP **191**.⁷⁴ Since [^3H]**191** was not significantly displaced by the NET and DAT selective ligands, Nisoxetine and GBR12935 respectively, the interaction of [^3H]**191** with NET and DAT is presumed to be minimal.¹⁴⁵ Although the selectivity of [^3H]**191** suggests that collectively our family of 2'-substituted quipazines may demonstrate significant SERT selectivity, these results can not serve as a definitive measure of SERT selectivity for all new target ligands.

The target compounds from this study that remain to be tested for their binding affinity (K_i) at SERT are shown in Figure 1.2.

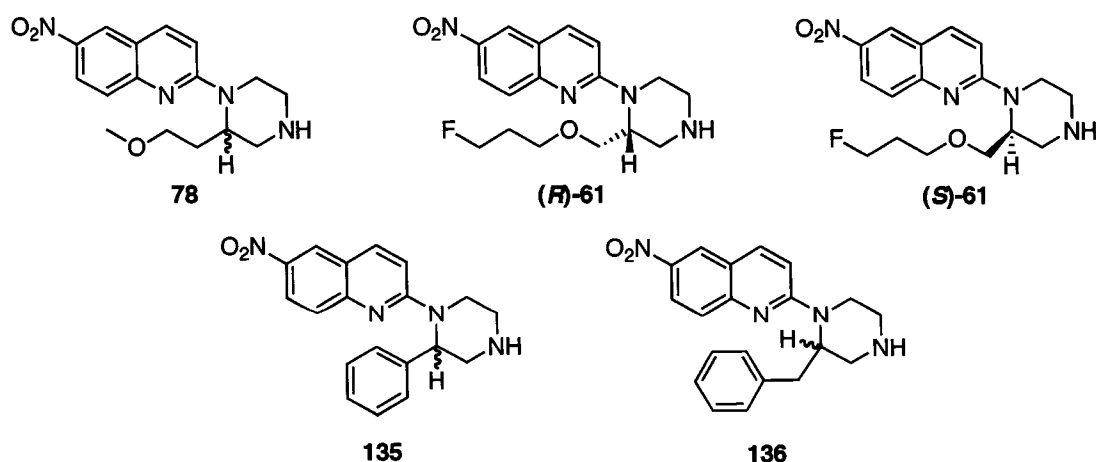


Figure 5.2: New ligands from this study that remain to be tested for activity at SERT. The 2'-aryl agents also need to be evaluated for affinity modulation properties.

More rigorous biochemical studies with the 2'-aryl-6-nitroquipazine ligands **135** and **136** will serve to evaluate their affinity modulation properties at SERT as per the discussions in Chapter 4. The methods utilized for these studies will mirror those of Plenge¹²⁴ that have been adapted for experiments in our laboratory.¹²⁷

5.2 Preliminary *in vivo* Evaluation of Racemic PET Agent [¹⁸F]MeProF-NQP

The new SERT PET radioligand [¹⁸F]MeProF [¹⁸F]**61** has undergone preliminary *in vivo* evaluation in rats to determine whole body organ tracer distribution. Within the brain, these studies were expanded to include the quantification of radioligand presence in discrete brain regions. This study also involved a preliminary evaluation of the *in vivo* metabolism of [¹⁸F]**61** in blood plasma and brain. Our primary investigator, Dr. John Gerdes, performed these studies in collaboration with Dr's Jim O'Neil, Scott Taylor and Jamie Eberling at the Lawrence Berkeley National Laboratory (LBNL). The scientists and facilities at this institution provide the necessary knowledge and resources for this study, including instrumentation dedicated to radiochemical experiments, a radiochemical synthesis lab and an on-site cyclotron for the preparation of the fluorine-18 tracer.

For all data collected in these studies, the following general procedure was used for the administration of tracer [¹⁸F]**61** and sacrifice of the animals: Radiotracer [¹⁸F]**61** was synthesized according to the synthetic protocols detailed

in Chapter 2, Section 2.7. Male Sprague-Dawley rats were anesthetized and received a 35 – 50 μCi tail vein injection of radioligand [^{18}F]61 in a saline matrix. Following a set period of time (15, 30, 60, 120 or 240 min), the animal was sacrificed with a large dose of anesthetic followed by exsanguination. The subsequent data collection protocols are summarized below.

Blood Metabolism – Radioligand metabolism in blood was determined at 15 and 60 minutes post injection. Blood was collected from the sacrificed animal and centrifuged. The supernatant blood plasma was decanted, extracted with MeOH and the mixture centrifuged to separate the layers. The methanolic extracts were first analyzed by UV/radioactive TLC and for both the 15 and 60 minute extracts the major radioactive product had an R_f that matched an unlabelled, standard sample of 61. The methanolic extract was further analyzed by reversed phase HPLC (UV and radioactivity detection) using a coinjection of unlabelled standard 61. The major (> 95%) radioactive fraction had a retention time identical to that of unlabelled 61. These results were consistent at 15 and 60 minutes and suggest that tracer [^{18}F]61 is relatively inert to metabolic degradation in the blood or the metabolites are not detected by this method.

Brain Metabolism – Radioligand metabolism in the brain was determined at 60 and 240 minutes post injection. Following sacrifice, the brain was carefully removed, placed in buffer and homogenized. The brain homogenate was extracted with methanol and the mixture centrifuged to separate the layers. The

analysis of the brain extracts was identical to those from the blood, and again the major (> 95%) radioactive fractions for both time points (60 and 240 minutes) was parent radioligand [^{18}F]61.

Whole Body Tracer Distribution – Organ tracer distribution measurements were collected at 15, 30, 60, 120 and 240 minutes. Following sacrifice, the organs were carefully excised and the tissues analyzed for radioactivity (counted). The data for each time point represent an average of three replicate measurements from separate animals and the results are decay corrected. The whole body tracer distribution data is presented in Figure 5.3.

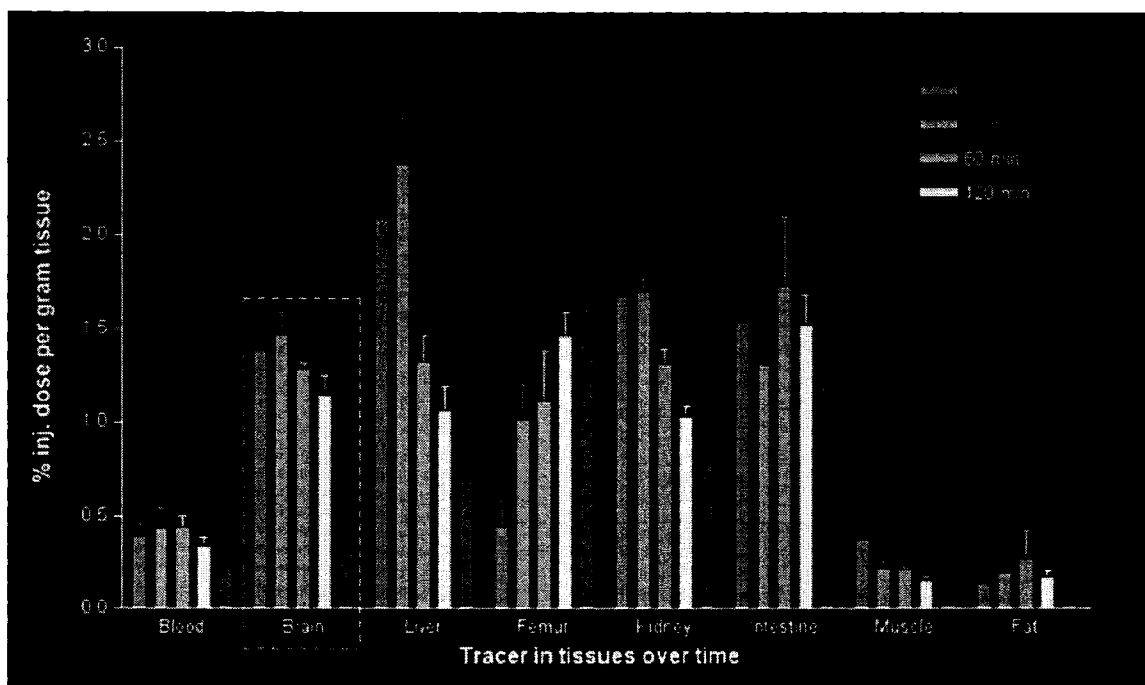


Figure 5.3: Whole body rat tracer distribution data with [^{18}F]MeProF. Data is reported as an average of three measurements. The brain study (boxed) was expanded to include brain sub-regions (Figure 5.4)

The distribution data demonstrate adequate brain penetration of the radioligand. The penetration was rapid (maximal radioactivity after 15 min) and tracer washout was observed over the experiment time course (gradual decline in radioactivity from 30 – 240 minutes). The gradual increase in radioactivity observed in bone (femur) suggests that ionic fluorine-18 is being generated as a result of some metabolic defluorination.

The tracer distribution study was extended to sub-regions of the brain to evaluate regional brain uptake as function of relative SERT distributions. Following animal sacrifice, the brains were carefully removed and the discrete brain regions were meticulously dissected and the radioactivity counted. The data for each time point represent an average of three replicate measurements and the results are decay corrected. The regional brain tracer distribution data is presented in Figure 5.4.

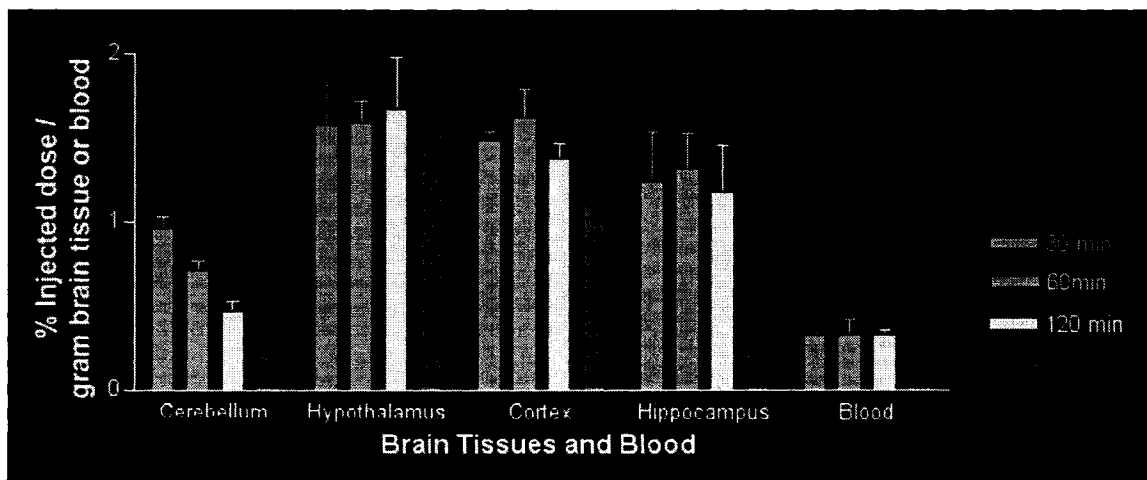


Figure 5.4: Rat tracer distribution data for discrete brain regions. Data is reported as an average of three measurements.

The greatest radiotracer uptake was observed in the SERT rich hypothalamus, and the moderate density cortex, and hippocampus. Radioligand uptake in the cerebellum, known to have low SERT densities, was reduced relative to the other regions and washout of the tracer was observed over the experiment time course. The radioactivity in the cerebellum after 240 minutes was almost equivalent to the amount in blood suggesting that minimal nonspecific binding is observed. At 240 minutes, the target (hypothalamus, cortex, hippocampus) to non-target (cerebellum) ratios of radiotracer accumulation were greater-than or equal to two. The preliminary results demonstrate that [^{18}F]61 may provide quantitative determination of SERT densities within moderate and low density target regions. Furthermore, the metabolic analyses suggest that [^{18}F]61 does not succumb to measureable metabolic degradation, with the exception of some *in vivo* defluorination as evidence by the accumulation of radioactivity in bone.

Additional studies to evaluate the performance of [^{18}F]61 in rats and non-human primates are underway at LBNL. Currently, a rat micro-PET study is being planned to compare racemic [^{18}F]61 with both (*R*)- and (*S*)- forms of the tracer. Following this study, a non-racemic [^{18}F]61 PET agent may be identified that possesses superior rodent *in vivo* qualities over its enantiomer and the racemate. Non-human primate studies in macaque monkeys with racemic [^{18}F]61 have also begun. These studies will be invaluable for determining if [^{18}F]61 possesses the necessary *in vivo* characteristics to advance it as PET agent for human imaging studies. The quantification of target to non-target binding ratios in primates is a critical determinant for ligand advancement.

Additional primate study components will involve a more rigorous treatment of metabolite formation including the identification of metabolic products with tandem liquid chromatography-mass spectroscopy.

At the close of these studies, we hope to have identified a non-racemic [¹⁸F]61 lead agent that we will advance for imaging human SERT. Follow up studies will compare our lead agent to the current standard SERT PET agents [¹¹C]DASB 13 and [¹¹C]AFM 14. Following these studies, the efficacy of our tracer to target the SERT shall be established.

CHAPTER 6

CONCLUSIONS AND FUTURE WORK

This study has successfully identified [^{18}F](*rac*)-MeProF-NQP [^{18}F]**61** as a new candidate SERT PET imaging agent (Figure 6.1).

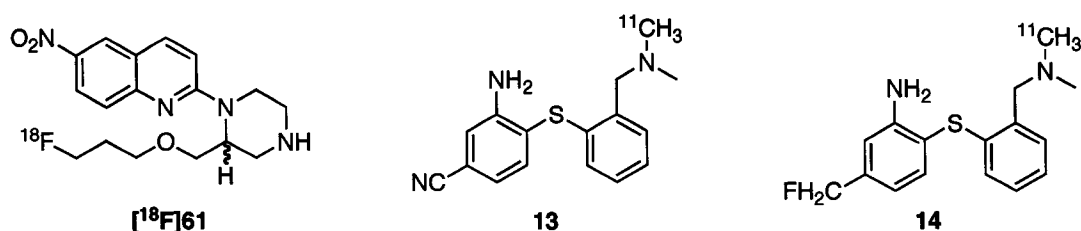


Figure 6.1: New SERT PET agent [^{18}F](*rac*)-MeProF-NQP and current standard ligands DASB **13** and [^{11}C]AFM **14**.

The *in vivo* properties, demonstrated thus far in rat, provide compelling evidence that [^{18}F]**61** may emerge as new standard SERT agent. What remains to be seen, is will [^{18}F]**61** meet the necessary *in vivo* performance requirements in non-human primates? Will [^{18}F]**61** or one of the non-racemic variants, provide the signal to noise ratios necessary for the reliable quantification of medium and low density SERT regions? Importantly, will [^{18}F]**61** outperform the current standard SERT PET agents DASB **13** and [^{11}C]AFM **14** in comparison studies? The answers to these questions are currently being sought in collaboration with researchers at LBNL.

This dissertation has also demonstrated relatively simple route(s) to non-racemic 6-nitroquipazine analogs using an efficient asymmetric synthesis methodology adapted from the method of Naylor.¹¹¹ For the syntheses of (*R*)-

and (S)- MOM-NQP **35** and MeProF-NQP **61**, a key intermediate **122** was identified that would provide all of the target compounds in the series (Figure 6.2).

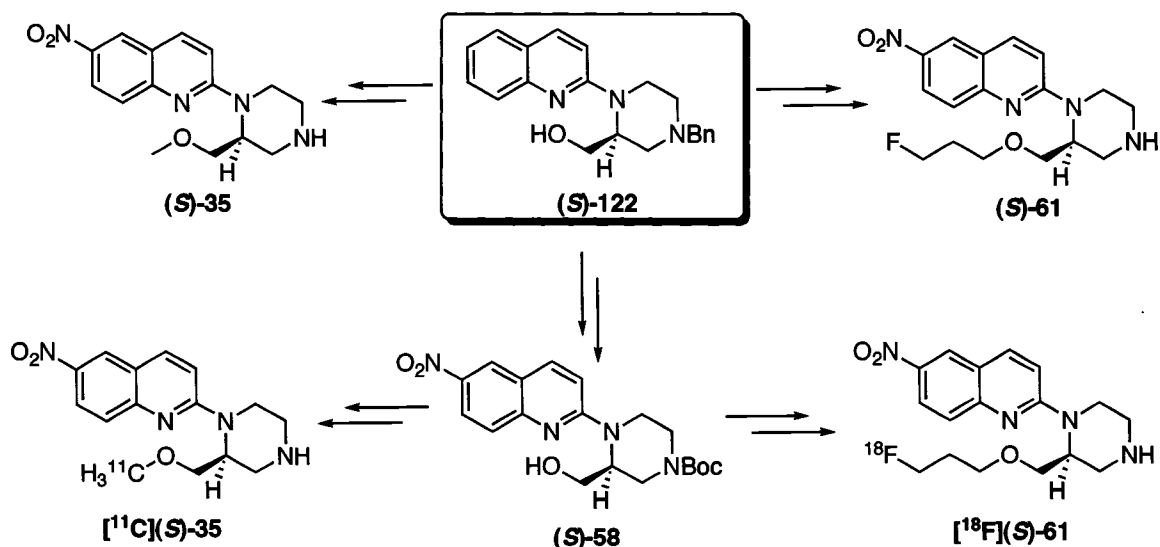


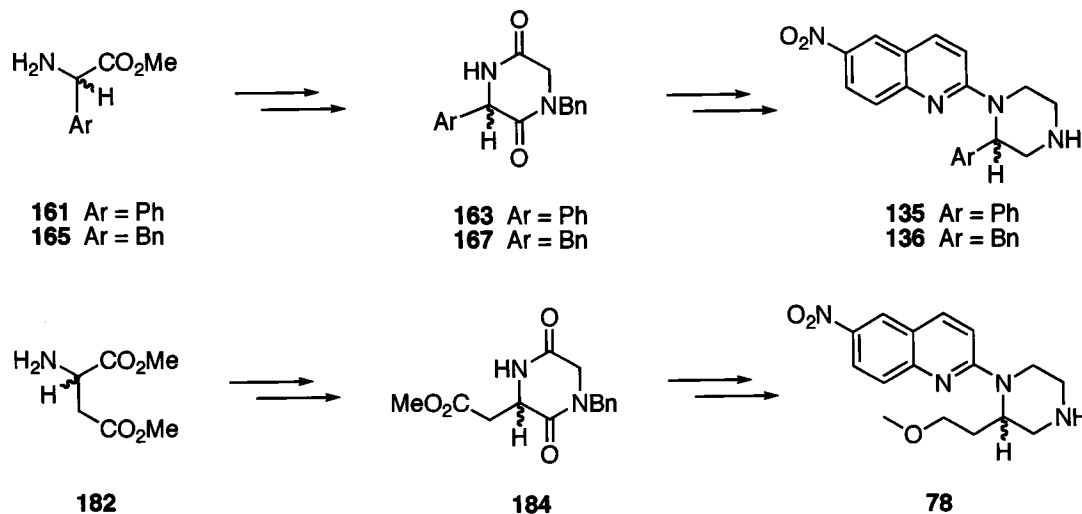
Figure 6.2: Intermediate N-benzyl alcohol (S)-122 as a precursor for all asymmetric targets.

Intermediate (S)-122 provides the unradiolabelled targets ((S)-35 and (S)-61) and the key radiolabelling precursor intermediate (S)-58 that affords both target radioligands [¹¹C](S)-35 and [¹⁸F](S)-61.

We have also demonstrated that the method of Naylor can readily be adapted to other amino acids starting materials. Chapter Four of the present study was dedicated to a discussion of these efforts as they related to the synthesis of our 2'-aryl-6-nitroquipazine analogs **135** and **136** and an alternate synthesis of EtOMe-NQP **78** (Figure 6.3a). Brian Kusche has adapted Naylor's method to perform asymmetric syntheses of 6-NQP analogs with three, four and

five carbon side chains (**48**, **195** and **196**), beginning with both isomers of glutamic acid **193** (Figure 6.3b).⁷⁴

a) Present study



b) Kusche, 2006

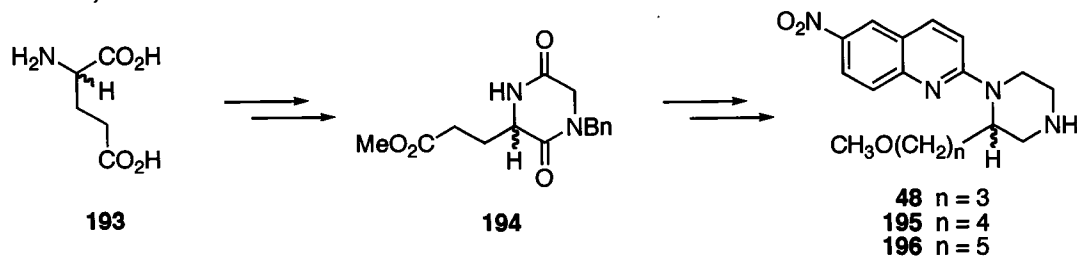


Figure 6.3: Summary new SERT agents synthesized using the methodology of Naylor, with different amino acid starting materials. Although not indicated, the compounds from Kusche⁷⁴ were synthesized in non-racemic form.

We have now successfully utilized five different amino acid starting materials for the synthesis of novel 6-NQP analogs. The potential to discover additional SERT ligands using this methodology is obvious and the utilization of unnatural or synthetic α -amino acids provide endless opportunity for diversification at the 2'-position of quipazine. The incorporation of heteroatoms other than oxygen, particularly sulfur and nitrogen, would provide additional SAR

data for the Ar2 binding region of SERT and also a handle for the introduction of radionuclides.

What is most lacking from this work is a complete set of biological data. Unfortunately, technical issues have limited the amount of SERT binding data that has been collected. The determinations of the K_i values for all of the ligands developed here are in progress. However, new compounds that have been rigorously tested have demonstrated very high affinity for SERT with K_i values in the low picomolar range (Figure 6.4).

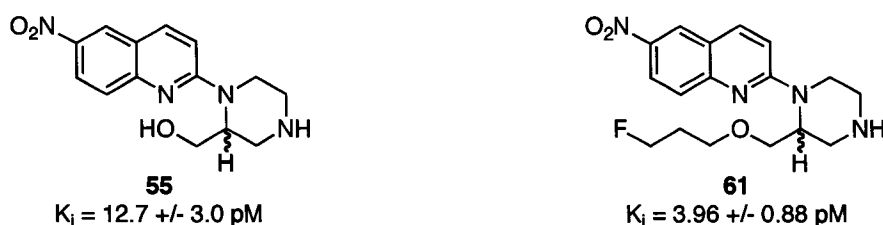


Figure 6.4: New SERT ligands from this study and their determined SERT binding affinity.

The selectivity of new compounds for SERT relative to the other biogenic amine transporters, NET and DAT, still needs to be evaluated. Despite the promising preliminary *in vivo* PET data accumulated for [^{18}F](*rac*)-MeProF-NQP, it is still possible that a lack of selectivity for SERT may limit its use as an effective SERT tracer.

CHAPTER 7

EXPERIMENTAL

7.1 General Methods

All reagents and solvents were purchased from commercial suppliers (Aldrich, Acros, Alfa Aesar, Fisher Scientific, VWR, Lancaster) and used without further purification unless otherwise stated. Anhydrous dichloromethane (CH_2Cl_2 , DCM) was distilled from calcium hydride (CaH_2) or purchased from a chemical supplier. Anhydrous tetrahydrofuran (THF) and diethyl ether (ether, Et_2O) were distilled from Na/benzophenone or purchased from a chemical supplier. Anhydrous N,N-dimethylformamide (DMF), 1,2-dichloroethane (DCE), 1,2-dimethoxyethane (DME), carbon tetrachloride (CCl_4), dimethylsulfoxide (DMSO), pyridine, triethylamine (TEA, Et_3N), benzene and chlorobenzene (Cl-Ben) were purchased from commercial suppliers. Dihydropyran (DHP) was distilled prior to use. Recrystallization of p-toluenesulfonyl chloride (tosyl chloride, Ts-Cl) was according to the method of Armarego.¹⁴⁶ Solutions of *n*-butyllithium were titrated prior to use.¹⁴⁷ Methyltriphenylphosphonium iodide was synthesized according to the method of McCortney.¹⁴⁸

All non-aqueous reactions were carried out in oven-dried glassware and magnetically stirred unless otherwise stated. Reactions requiring anhydrous conditions were run under an atmosphere of argon. Brine, refers to a saturated aqueous solution of non-iodized salt, available at a grocery store. Water refers to

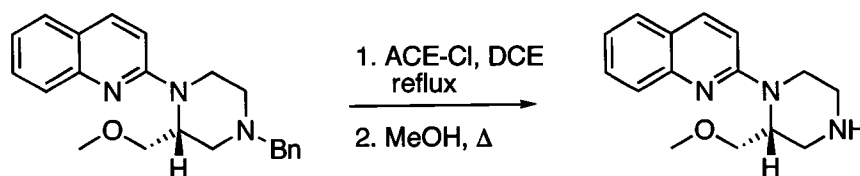
deionized water. All aqueous solutions were prepared using deionized water. For all reactions, the dried (K_2CO_3 , $MgSO_4$ or Na_2SO_4 as indicated) organic phases were filtered (fluted filter paper or cotton plug) prior to evaporation. All solvent evaporations and/or extract concentrations were performed with a Buchii rotary evaporator under reduced pressure. Thin-layer chromatography was performed with EM Science, Silica gel 60 F₂₅₄ aluminum-backed plates. Visualization of TLC plates was facilitated with UV light (254 and 365 nm) and/or ninhydrin-staining (11 mM in EtOH). Column chromatography was performed with EM Science, Silica gel 60 (230-400 mesh ASTM). Chromatography solvent mixtures are reported as volume:volume ratios.

Nuclear magnetic resonance (NMR) spectra were obtained on a Varian Unity Plus 400 spectrometer. Proton NMR (1H NMR) spectra were recorded at 400 MHz and the chemical shifts are reported in parts per million (ppm, δ) relative to residual protonated solvent signal ($CDCl_3$, 7.26 ppm; D_2O , 4.63 ppm; $DMSO-d_6$, 2.49 ppm). Carbon NMR (^{13}C NMR) spectra were recorded at 100 MHz and the chemical shifts are reported in parts per million (ppm, δ) relative to solvent signal ($CDCl_3$, 77 ppm; $DMSO-d_6$, 39.5 ppm) or with 1,4-dioxane as an internal standard (for D_2O ; 67.4 ppm). Proton NMR spectra are reported as follows: chemical shift (multiplicity, coupling constant(s) in Hertz, number of protons). Optical rotations were obtained on a Perkin-Elmer 241 Polarimeter at ambient, room temperature using a 10 cm (1 dm) cell. The concentration of the solutions analyzed is reported as; $c = (\text{grams of solute})/(\text{solution volume in mL})$. Optical rotations were calculated using the relationship $[\alpha]_D^{25} = \alpha/L \cdot c$; where α is

the instrument reading, L is the length of the sample cell (1 dm) and c is the concentration of solute (described immediately above). Gas chromatography/mass spectroscopy (GC/MS) data was collected on an Agilent Technologies electron impact (EI) 5973Network mass selective detector connected to an Agilent Technologies 6890N Gas Chromatography system equipped with an Agilent HP-5MS crosslinked 5% PH ME Siloxane column (30m x 0.25 mm; 0.25 micron). High-resolution mass spectra (HRMS) were obtained with a Micromass LCT electrospray ionization (ESI) spectrometer connected to a Waters 2790 Separations Module. A chromatography column was not used in these analyses. Biotage purifications were run on a Biotage Horizon Flash Collector connected to a Biotage Horizon Pump and Horizon Detector.

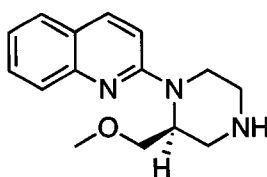
7.2 Experimentals

The synthetic procedures detailed in this section are organized by compound number in ascending order.

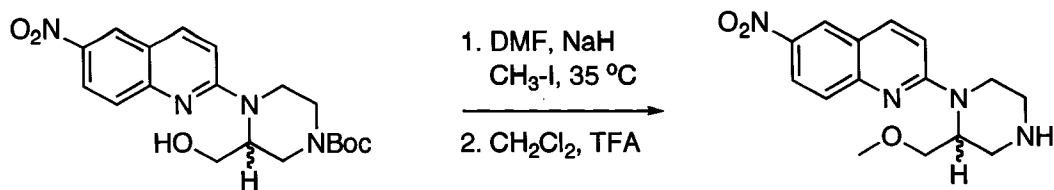


(R)-(+)-2-[2-(Methoxymethyl)piperazin-1-yl]quinoline (R)-34. To a 0 °C solution of methyl ether (R)-109 (0.119 g, 0.34 mmol) in dry dichloroethane (8 mL) under argon was added 1-chloroethyl chloroformate (0.093 g, 0.65 mmol). After stirring at 0 °C for 10 min the flask was heated at reflux for 2.5 h. The

solution was cooled slightly and the volatile components were evaporated. The residue was dissolved in methanol (10 mL), heated at 60 - 70 °C for 1 h, and then the solvent was evaporated. The residue was dissolved in 15 mL 1 M HCl and washed with CH₂Cl₂ (4 x 15 mL). The aqueous phase was made basic with 4 M NaOH, diluted with saturated NaHCO₃ (20 mL) and extracted with CH₂Cl₂ (4 x 10 mL). The combined extracts were dried (K₂CO₃) and concentrated to give **(R)-34** as a pale colored oil (0.081 g, 92%). TLC *R_f* 0.1 (MeOH:CH₂Cl₂, 1:9). ¹H NMR (400 MHz, CDCl₃): δ 1.93 (bs, NH, 1H), 2.87 (m, 1H), 2.98 (dd, *J* = 4.0 Hz and 12.5 Hz, 1H), 3.11-3.20 (m, 2H), 3.29-3.37 (m, 4H, overlapped singlet at 3.36, OCH₃), 3.48 (dd, *J* = 4.8 and 9.2 Hz, 1H), 3.86 (m, 1H), 4.36 (bd, 1H), 4.57 (bm, 1H), 6.97 (d, *J* = 9.2 Hz, 1H), 7.21 (m, 1H), 7.52 (m, 1H), 7.59 (m, 1H), 7.68 (d, *J* = 8.8 Hz, 1H), 7.88 (d, *J* = 9.2 Hz, 1H); ¹³C NMR (100 MHz, CDCl₃): δ 41.4, 46.0, 46.2, 50.7, 59.0, 69.7, 109.1, 122.1, 126.5, 127.1, 129.4, 137.3, 147.8, 156.9; (*R*) - [α]_D²⁵ +103.4 (c 0.0086, CHCl₃); HRMS (ESI-TOF) *m/z* (*M* + *H*)⁺ calcd. for C₁₅H₂₀N₃O 258.1606 found 258.1610.

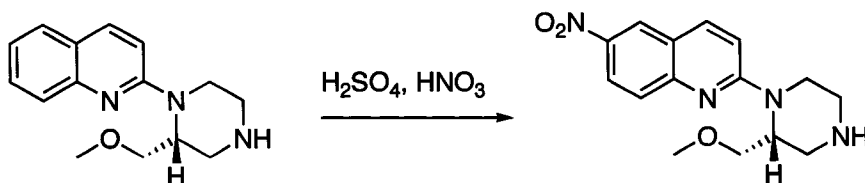


(S)-(-)-2-[2-(Methoxymethyl)piperazin-1-yl]quinoline (S)-34. The title compound was similarly prepared and provided identical spectroscopic data. (*S*) - [α]_D²⁵ -102.2 (c 0.0101, CHCl₃).

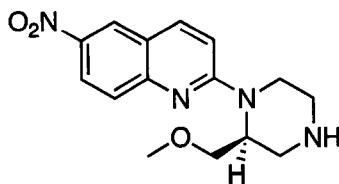


2-[2-(Methoxymethyl)piperazin-1-yl]-6-nitroquinoline 35. To a solution of N-Boc alcohol **58** (0.0077 g, 0.02 mmol) in dry DMF (1 mL) under argon was added sodium hydride (0.012 g, 0.5 mmol) producing a dark red mixture. Iodomethane (8 μ L, 0.13 mmol) was added and the reaction flask placed in an oil bath at 35 $^{\circ}$ C. An immediate color change to orange occurred and a TLC confirmed that the starting material had been consumed. The excess hydride was destroyed with a few drops of methanol and the reaction contents were partitioned between water and ether (10 mL each). The organic phase was separated and the aqueous phase extracted with two additional portions of ether (15 mL). The combined extracts were dried (K_2CO_3) and concentrated to give the crude product. The residue was dissolved in CH_2Cl_2 and trifluoroacetic acid (5 mL each). After stirring 1.5 h the solution was made basic with 1:5 K_2CO_3 :water solution. The aqueous phase was extracted with two 20 mL portions of CH_2Cl_2 . The extracts were dried (K_2CO_3) and concentrated to afford **35** as a yellow film (0.007 g, 120%). TLC R_f 0.14 (MeOH: CH_2Cl_2 , 1:9). The product's 1H NMR spectrum was consistent to the known spectra.⁶⁷ 1H NMR (400 MHz, $CDCl_3$): δ 1.77 (bs, 1H), 2.87 (td, J = 3.3, 11.7 Hz, 1H), 2.98 (dd, J = 4.4, 12.5 Hz, 1H), 3.15 – 3.28 (m, 2H), 3.32 (m, 1H), 3.37 (s, 3H), 3.60 (dd, J = 5.5, 9.2, 1H), 3.85 (dd, J = 7.7, 9.2 Hz, 1H), 4.50 (bm, 1H), 4.66 (bm, 1H), 7.08 (d, J = 9.2 Hz, 1H), 7.65 (d, J = 9.2 Hz, 1H), 7.96 (d, J = 9.2 Hz, 1H), 8.29 (dd, J = 2.6, 9.2 Hz, 1H), 8.54 (d, J = 2.6

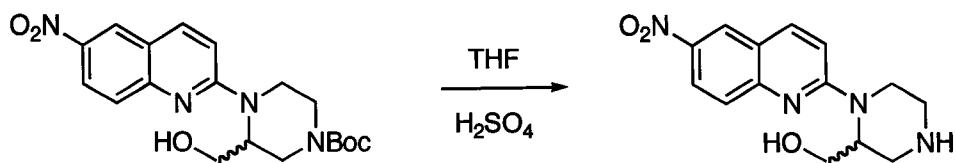
Hz, 1H); ^{13}C NMR (100 MHz, CDCl_3): δ 45.9, 46.3, 50.9, 59.1, 70.2, 110.9, 121.0, 123.5, 124.2, 127.0, 138.5, 141.7, 151.4, 158.5; HRMS (ESI-TOF) m/z ($\text{M} + \text{H}$) $^+$ calcd. for $\text{C}_{15}\text{H}_{19}\text{N}_4\text{O}_3$ 303.1457 found 303.1448.



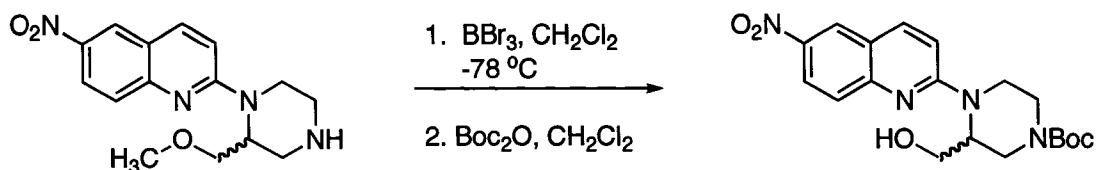
(R)-(+)-2-[2-(Methoxymethyl)piperazin-1-yl]-6-nitroquinoline (R)-35. To a 0 °C solution of **(R)-34** (0.038 g, 0.15 mmol) in conc. H_2SO_4 (2 mL) was added HNO_3 (15.4 M, 0.038 mL, 0.59 mmol). The reaction was stirred 17 min then quenched by pipetting onto ice. The solution was basified with 4 M NaOH then diluted with saturated NaHCO_3 (10 mL). The bright yellow aqueous mixture was extracted with CH_2Cl_2 (3 x 10 mL) and the combined extracts dried (K_2CO_3) and concentrated to provide **(R)-35** as a bright yellow-orange oily solid (0.040 g, 91%). TLC R_f 0.14 (MeOH: CH_2Cl_2 , 1:9). The spectroscopic data for **(R)-35** was identical to that for the racemic material. (R) - $[\alpha]_D^{25} +138.8$ (c 0.0016, CHCl_3).



(S)-(-)-2-[2-(Methoxymethyl)piperazin-1-yl]-6-nitroquinoline (S)-35. The title compound was similarly prepared and provided identical spectroscopic data. (S) - $[\alpha]_D^{25} -137.8$ (c 0.0023, CHCl_3).



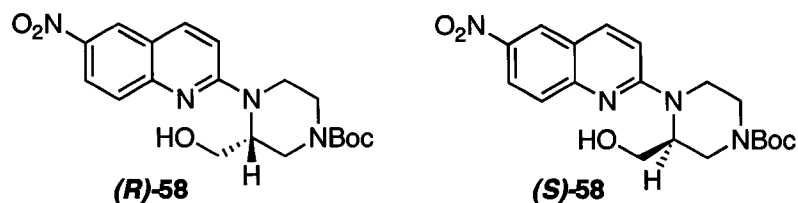
2-[2-(Hydroxymethyl)piperazin-1-yl]-6-nitroquinoline 55. To **58** (0.035 g, 0.090 mmol) dissolved in THF (2 mL) was added H₂SO₄ (4 M, 5 mL) and the solution stirred at ambient temperature until a TLC showed consumption of starting material (~2 h). The solution was pipetted into cold 4 M NaOH (8 mL) then diluted with saturated NaHCO₃ (10 mL). The aqueous mixture was extracted with CH₂Cl₂ (4 x 8 mL) and the combined extracts were dried (K₂CO₃) and concentrated to provide **55** as an oily bright yellow solid (0.019 g, 73%). TLC *R_f* 0.04 (MeOH:CH₂Cl₂, 1:9). ¹H NMR (400 MHz, CDCl₃): δ 2.70 – 3.10 (bs, 2H) overlapped with 2.92 (td, *J* = 3.3, 11.7 Hz, 1H), 3.07 (dd, *J* = 4.0, 11.7 Hz, 1H), 3.21 (bd, *J* = 11 Hz, 1H), 3.36 (bd, *J* = 12.1 Hz, 1H), 3.56 (td, *J* = 3.3, 12.5 Hz, 1H), 4.02 (dd, *J* = 4.4, 11 Hz, 1H), 4.15 (dd, *J* = 5.5, 11 Hz, 1H), 4.26 (bd, *J* = 12.5 Hz, 1H), 4.83 (bs, 1H), 7.08 (d, *J* = 9.5 Hz, 1H), 7.61 (d, *J* = 9.5, 1H), 7.96 (d, *J* = 9.5 Hz, 1H), 8.28 (dd, *J* = 2.6, 9.5 Hz, 1H), 8.52 (d, *J* = 2.6 Hz, 1H); ¹³C NMR (100 MHz, CDCl₃): δ 42.7, 46.0, 48.2, 52.0, 64.7, 111.2, 121.1, 123.7, 124.2, 127.0, 138.7 141.9, 151.1, 159.1; HRMS (ESI-TOF) *m/z* (M + H)⁺ calcd. for C₁₄H₁₇N₄O₃ 289.1301 found 289.1304.



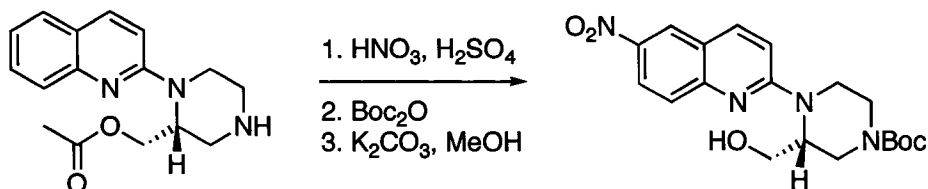
2-[4-(*tert*-Butoxycarbonyl)-2-(hydroxymethyl)piperazin-1-yl]-6-nitroquinoline

58. To a $-78\text{ }^{\circ}\text{C}$ stirring solution of MOM-NQP **35** (0.143 g, 0.474 mmol) in dry CH_2Cl_2 (75 mL) under argon was added (dropwise) borontribromide solution (1 M in CH_2Cl_2 , 2.37 mL, 2.37 mmol). The addition turned the mixture black initially and then faded to a turbid orange. The reaction was maintained at $-78\text{ }^{\circ}\text{C}$ for 3 h then warmed to ambient temperature and stirred 18 h. The reaction was quenched with saturated NaHCO_3 (20 mL), transferred to a separatory funnel and shaken vigorously. The organic phase was separated and the aqueous layer extracted with CH_2Cl_2 (30 mL) and CHCl_3 :isopropyl alcohol, 4:1 (3 x 30 mL). The combined organic phases were dried (K_2CO_3), and concentrated to give a crude residue. The crude residue was dissolved in about 20 mL of CH_2Cl_2 and to this was added a solution of di-*tert*-butyldicarbonate (0.124 g, 0.569 mmol) in CH_2Cl_2 (5 mL). The solution was stirred for 5 min, concentrated and the residue purified by column chromatography (silica gel, EtOAc:Hexanes, 3:2) to afford **58** as a bright yellow foam (0.129 g, 70%). TLC R_f 0.11 (EtOAc:Hexanes, 2:3). ^1H NMR (400 MHz, CDCl_3): δ 1.47 (s, 9H), 3.09 – 3.62 (bm, 4H), 3.66 – 3.96 (bm, 2H), 3.98 – 4.43 (bm, 3H), 4.82 (bm, 1H), 7.07 (d, $J = 9.2$ Hz, 1H), 7.61 (d, $J = 9.2$ Hz, 1H), 7.97 (d, $J = 9.2$ Hz, 1H), 8.25 (dd, $J = 2.6, 9.2$ Hz, 1H), 8.47 (d, $J = 2.6$ Hz, 1H); ^{13}C NMR (100 MHz, CDCl_3): δ 28.2, 40.2 (broad), 42.5 (broad), 43.9 (broad), 53.9, 59.8 (broad), 61.2 (broad), 80.5, 111.0 (broad),

121.1, 123.5, 124.0, 126.7, 138.7, 141.8, 150.6, 155.5 (broad), 158.8 (broad);
HRMS (ESI-TOF) m/z ($M + H$)⁺ calcd. for C₁₉H₂₅N₄O₅ 389.1825 found 389.1810.

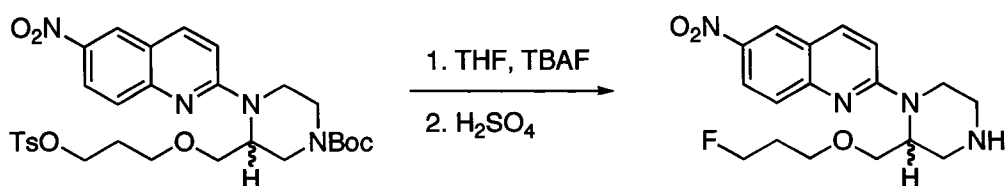


(R)-(+)- and (S)-(-)-2-[4-(tert-Butoxycarbonyl)-2-(hydroxymethyl)piperazin-1-yl]-6-nitroquinoline (R)-58 and (S)-58. The title compounds were similarly prepared and provided identical spectroscopic data. **(R)-58** - $[\alpha]_D^{25} +93.3$ (c 0.012, CHCl₃); **(S)-58** - $[\alpha]_D^{25} -91.4$ (c 0.013, CHCl₃).



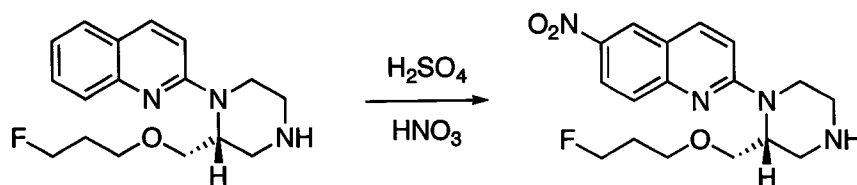
(R)-2-[4-(tert-butoxycarbonyl)-2-(Hydroxymethyl)piperazin-1-yl]-6-nitroquinoline (R)-58. To a 0 °C solution of acetate **(R)-129** (0.108 g, 0.378 mmol) in conc. H₂SO₄ (7 mL) was added (dropwise) HNO₃ (15.4 M, 0.1 mL, 1.54 mmol). After stirring 15 min at 0 °C the reaction mixture was carefully pipetted into 200 mL of cold saturated NaHCO₃ in a separatory funnel containing ice. The bright yellow aqueous mixture was extracted with CH₂Cl₂ (3 x 40 mL) and the combined extracts were dried (K₂CO₃) and treated with di-*tert*-butyldicarbonate (0.20 g, 0.917 mmol). When a TLC showed that amine protection was complete, the solvent was decanted from the drying agent and evaporated. The residue was dissolved in methanol (10 mL) treated with K₂CO₃ and stirred at ambient

temperature for ~ 1 h. A TLC showed consumption of starting material and the methanol was evaporated and the residue partitioned between 20 mL each of saturated NaHCO₃ and CH₂Cl₂. The organic phase was separated and the aqueous phase extracted with CH₂Cl₂ (2 x 10 mL). The combined extracts were dried (K₂CO₃) and concentrated to provide the crude material that was purified by column chromatography (silica gel, EtOAc:Hexanes, 2:3 – 3:2) to provide (*R*)-**58** as a yellow foam (0.074 g, 50%). This product was spectroscopically identical to the **58** generated via the alternate BBr₃ deprotection route.



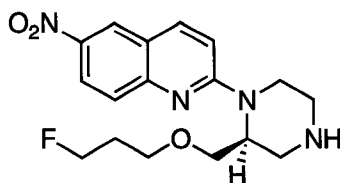
2-[2-((3-Fluoropropoxy)methyl)piperazine-1-yl]-6-nitroquinoline 61. To a solution of tosylate **65** (0.0238 g, 0.040 mmol) in dry THF (400 μ L) was added a solution of TBAF in THF (1 M, 0.06 mL, 0.06 mmol). The reaction was sealed under argon and heated at 55 – 60 °C for 3 h. After cooling, the THF was evaporated and the residue was purified by column chromatography (silica gel, EtOAc:Hexanes, 1:3) to afford the N-Boc protected intermediate as a yellow film (0.0137 g, 77%). TLC R_f 0.27 (EtOAc:Hexanes, 2:3). To the intermediate N-Boc fluoride (0.0217 g, 0.048 mmol) in a flask at 0 °C was added cold (-10 °C) conc. H₂SO₄ (3 mL). Immediate bubbling was observed as the N-Boc group deprotected and the flask was swirled to clear the sides of material. After 5 min the contents were pipetted onto ice, made basic with 4 M NaOH and further diluted with saturated NaHCO₃. The yellow aqueous mixture was extracted with

CH₂Cl₂ (3 x 10 mL) and the combined extracts dried (K₂CO₃) and concentrated to give the crude material that was purified by column chromatography (silica gel, MeOH:CH₂Cl₂, 1:39 – 1:19) to afford **61** as a yellow film (0.013 g, 80%). TLC *R_f* 0.16 (MeOH:CH₂Cl₂, 1:9). ¹H NMR (400 MHz, CDCl₃): δ 1.80 – 2.00 (m, 3H, overlapped bs of NH and dp, *J*_{F-H} = 26.0 Hz, FCH₂CH₂-, *J*_{H-H} = 6.2 Hz), 2.87 (m, 1H), 2.99 (m, 1H), 3.12 – 3.36 (m, 3H), 3.58 (t, *J* = 6.2 Hz, 2H), 3.68 (dd, *J* = 5.5, 9.5 Hz, 1H), 3.88 (dd, *J* = 7.3, 9.5 Hz, 1H), 4.44 (dt, *J*_{F-H} = 47.2, FCH₂-, *J*_{H-H} = 5.9 Hz, 2H, overlapped with a bs at 4.50, 1H), 4.66 (bs, 1H), 7.08 (d, *J* = 9.2 Hz, 1H), 7.63 (d, *J* = 9.2, 1H), 7.95 (d, *J* = 9.2, 1H), 8.28 (dd, *J* = 2.6, 9.2 Hz, 1H), 8.52 (d, *J* = 2.6, 1H); ¹³C NMR (100 mHz, CDCl₃): δ 30.7 (*J*_{C-F} = 19.8 Hz, FCH₂CH₂-), 41.3, 45.9, 46.4, 50.0, 67.0 (*J*_{C-F} = 6.1 Hz, FCH₂CH₂CH₂-), 68.5, 81.0 (*J*_{C-F} = 164.8 Hz, FCH₂-), 111.1, 121.1, 123.6, 124.2, 127.1, 138.4, 141.8, 151.4, 158.7; HRMS (ESI-TOF) *m/z* (M + H)⁺ calcd. for C₁₇H₂₂N₄O₃F 349.1676 found 349.1674.

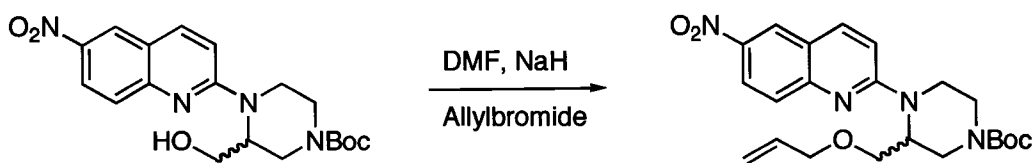


(R)-(+)-2-[2-((3-Fluoropropoxy)methyl)piperazine-1-yl]-6-nitroquinoline (R)-61**.** To a 0 °C solution of **(R)-127** (0.065 g, 0.214 mmol) in conc. H₂SO₄ (6 mL) was added HNO₃ (15.4 M, 0.028 mL, 0.431 mmol). The reaction was stirred for 17 min then quenched by pipetting onto ice. The solution was made basic with 4 M NaOH then diluted with saturated NaHCO₃ (20 mL). The bright yellow aqueous mixture was extracted with CH₂Cl₂ (3 x 20 mL) and the combined

extracts dried (K_2CO_3) and concentrated to provide the crude product that was purified by column chromatography (silica gel, four column lengths EtOAc:Hexanes, 4:1, then MeOH:CH₂Cl₂, 1:39 – 1:9) to provide (*R*)-**61** as a bright yellow-orange oil (0.070 g, 93%). TLC R_f 0.16 (MeOH:CH₂Cl₂, 1:9). This product was spectroscopically identical to the **61** formed via the alternate N-Boc protected route. (*R*) - $[\alpha]_D^{25} +111.6$ (c 0.0021, CHCl₃).



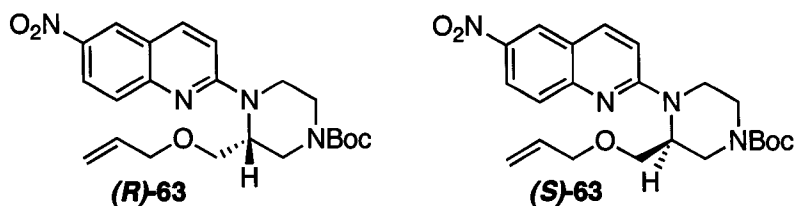
(S)-(-)-2-[2-((3-Fluoropropoxy)methyl)piperazine-1-yl]-6-nitroquinoline (S)-61. The title compound was similarly prepared and provided identical spectroscopic data. (*S*) - $[\alpha]_D^{25} -113.2$ (c 0.0011, CHCl₃).



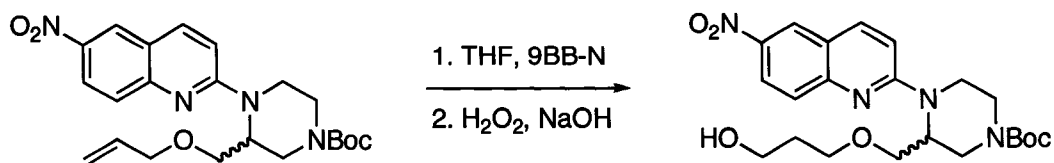
2-[4-(*tert*-Butoxycarbonyl)-2-(allyloxymethyl)piperazine-1-yl]-6-

nitroquinoline 63. To a 0 °C solution of Boc alcohol **58** (0.194 g, 0.50 mmol) in dry DMF (8 mL) under argon was added NaH (95%, 0.046 g, 1.92 mmol) in one portion. Allyl bromide (0.302 g, 2.5 mmol) was added (dropwise) to the deep red mixture and the reaction warmed to ambient temperature. After stirring 1.5 h a TLC showed consumption of starting material and the reaction mixture was carefully added to a separatory funnel containing ether (30 mL) and 16 mL each of water and saturated NaHCO₃. The aqueous phase was separated and the

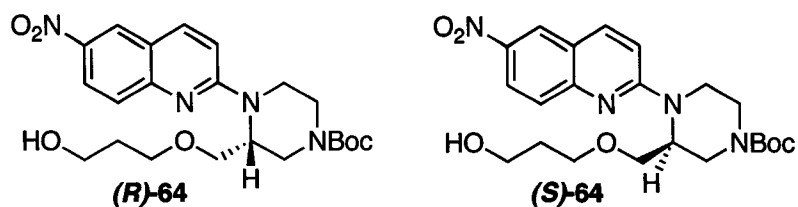
organic phase was washed with brine (2 x 20 mL), dried (K₂CO₃) and concentrated to provide the crude material that was purified by column chromatography (silica gel, EtOAc:Hexanes, 2:3) to afford **63** as a bright yellow foam (0.192 g, 90%). TLC *R_f* 0.33 (EtOAc:Hexanes, 2:3). ¹H NMR (400 MHz, CDCl₃): δ 1.49 (s, 9H), 2.96 – 3.37 (bm, 3H, includes dd at 3.17), 3.49 – 3.68 (m, 2H, includes t at 3.61), 3.93 – 4.78 (bm, 6H, includes bs at 4.00 and bd at 4.30), 5.04 – 5.31 (bm, 2H), 5.82 (bm, 1H), 7.08 (d, *J* = 9.2 Hz, 1H), 7.63 (d, *J* = 9.2 Hz, 1H), 7.95 (d, *J* = 9.2 Hz, 1H), 8.25 (dd, *J* = 2.6, 9.2 Hz, 1H), 8.49 (d, *J* = 2.6 Hz, 1H); ¹³C NMR (100 MHz, CDCl₃): δ 28.3, 40.0 (broad), 42.6 (broad), 43.7 (broad), 51.6 (broad), 66.6 (broad), 72.2, 80.1, 111.0, 117.0, 121.1, 123.5, 124.1, 127.2, 134.3, 138.6, 141.9, 151.1, 154.9, 158.4; HRMS (ESI-TOF) *m/z* (M + H)⁺ calcd. for C₂₂H₂₉N₄O₅ 429.2138 found 429.2119.



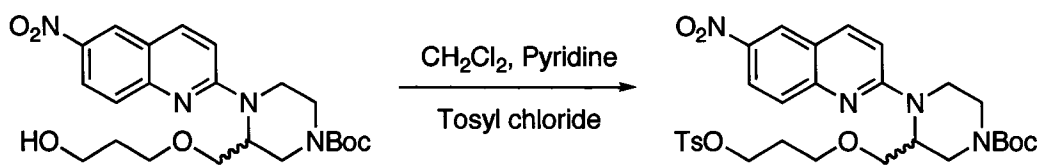
(*R*)-(+)- and (*S*)-(–)-2-[4-(*tert*-Butoxycarbonyl)-2-(allyloxymethyl)piperazine-1-yl]-6-nitroquinoline (*R*)-63** and (*S*)-**63**.** The title compounds were similarly prepared and provided identical spectroscopic data. (***R***-**63** - [α]_D²⁵ +89.4 (c 0.0086, CHCl₃); (***S***-**63** - [α]_D²⁵ –83.0 (c 0.010, CHCl₃).



2-[4-(*tert*-Butoxycarbonyl)-2-((3-hydroxypropoxy)methyl)piperazine-1-yl]-6-nitroquinoline 64. To the allyl ether **63** (0.075 g, 0.175 mmol) in dry THF (600 μ L) under argon was added a solution of 9-BBN in THF (0.5 M, 950 μ L, 0.475 mmol). The reaction was heated to 55 $^{\circ}$ C and maintained for 1 h. After cooling to 0 $^{\circ}$ C 0.6 mL of 1 M NaOH was added (dropwise) followed by 0.6 mL of 30% H_2O_2 . The mixture was stirred for 5 min and a TLC confirmed consumption of starting material. The mixture was poured into 20 mL of saturated NaHCO_3 and the aqueous phase extracted with CH_2Cl_2 (3 x 10 mL). The combined extracts were dried (K_2CO_3) and concentrated to give the crude material that was purified by column chromatography (silica gel, EtOAc:Hexanes, 3:2) to afford **64** as a bright yellow foam (0.057 g, 73%). TLC R_f 0.11 (EtOAc:Hexanes, 2:3). ^1H NMR (400 MHz, CDCl_3): δ 1.49 (s, 9H), 1.73 (bm, 2H), 2.98 – 3.37 (bm, 3H), 3.41 – 3.89 (bm, 7H), 4.02 – 4.53 (bm, 3H), 4.71 (bm, 1H), 7.06 (d, $J = 9.2$ Hz, 1H), 7.64 (d, $J = 9.2$ Hz, 1H), 7.96 (d, $J = 9.2$ Hz, 1H), 8.25 (dd, $J = 2.6, 9.2$ Hz, 1H), 8.49 (d, $J = 2.6$ Hz, 1H); ^{13}C NMR (100 MHz, CDCl_3): δ 28.3, 32.1, 40.1, 42.5, 43.8, 51.7, 59.1, 61.2, 66.8, 67.6, 68.5, 70.3, 80.5, 110.8, 121.2, 123.6, 124.2, 127.2, 138.8, 142.0, 151.0, 154.9, 158.3; HRMS (ESI-TOF) m/z ($\text{M} + \text{H}$) $^+$ calcd. for $\text{C}_{22}\text{H}_{31}\text{N}_4\text{O}_6$ 447.2244 found 447.2226.

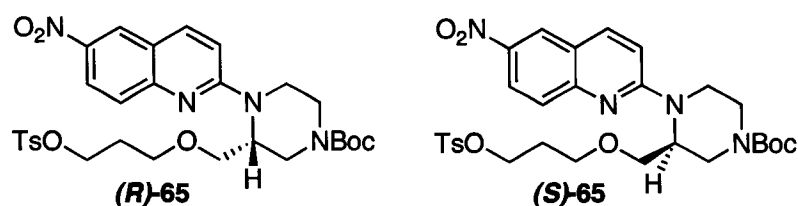


(R)-(+)- and (S)-(-)-2-[4-(*tert*-Butoxycarbonyl)-2-((3-hydroxypropoxy)methyl)piperazine-1-yl]-6-nitroquinoline (*R*)-64 and (*S*)-64. The title compounds were similarly prepared and provided identical spectroscopic data. (*R*)-64 - $[\alpha]_D^{25} +38.9$ (c 0.0055, CHCl₃); (*S*)-64 - $[\alpha]_D^{25} -37.5$ (c 0.0067, CHCl₃).

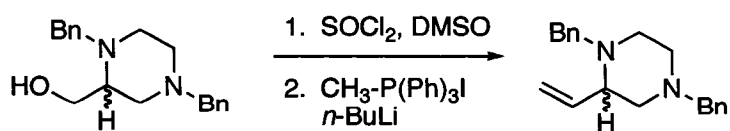


2-[4-(*tert*-Butoxycarbonyl)-2-((3-(4-methylbenzenesulfonate)propoxy)methyl)piperazine-1-yl]-6-nitroquinoline 65. To a 0 °C solution of alcohol **64** (0.095 g, 0.213 mmol) in dry CH₂Cl₂ (1.2 mL) and pyridine (100 μL) was added *p*-toluenesulfonyl chloride (0.170 g, 0.895 mmol) in one portion. The reaction was sealed under argon and maintained in an ice bath until the bath warmed to ambient temperature. After 24 h the reaction contents were partitioned between saturated NaHCO₃ (20 mL) and CH₂Cl₂ (10 mL). The organic phase was separated and the aqueous phase was extracted with CH₂Cl₂ (2 x 10 mL). The combined extracts were dried (K₂CO₃) and concentrated to give the crude material that was purified by column chromatography (silica gel, EtOAc:Hexanes, 1:3 – 2:3) to afford **65** as a bright yellow foam (0.103 g, 80%). TLC *R*_f 0.22 (EtOAc:Hexanes, 2:3). ¹H NMR (400 MHz, CDCl₃): δ 1.48 (s, 9H), 1.79 (bm, 2H),

2.42 (s, 3H), 2.94 – 3.30 (bm, 3H), 3.44 – 3.60 (bm, d shaped, 4H), 4.02 (bm, 2H), 4.10 - 4.24 (m, 2H, includes d at 4.20), 4.50 (bm, 1H), 4.65 (bm, 1H), 7.07 (d, $J = 9.2$ Hz, 1H), 7.30 (d, $J = 8.1$ Hz, 2H), 7.63 (d, $J = 9.2$ Hz, 1H), 7.72 (d, $J = 8.1$ Hz, 2H), 7.95 (d, $J = 9.2$ Hz, 1H), 8.26 (dd, $J = 2.6, 9.2$ Hz, 1H), 8.50 (d, $J = 2.6$ Hz, 1H); ^{13}C NMR (100 MHz, CDCl_3): δ 21.6, 28.3, 29.2, 39.8 (broad), 42.6 (broad), 43.7 (broad), 51.4 (very broad), 66.7, 67.3, 68.0 (very broad), 80.2, 111.2, 121.2, 123.5, 124.2, 127.2, 127.7, 129.8, 133.0, 138.5, 141.9, 144.7, 151.1, 154.8, 158.5; HRMS (ESI-TOF) m/z ($M + H$)⁺ calcd. for $\text{C}_{29}\text{H}_{36}\text{N}_4\text{O}_8\text{S}$ 601.2332 found 601.2336.



(R)-(+)- and (S)-(-)-2-[4-(*tert*-Butoxycarbonyl)-2-((3-(4-methylbenzenesulfonate)propoxy)methyl)piperazine-1-yl]-6-nitroquinoline (R)-65 and (S)-65. The title compounds were similarly prepared and provided identical spectroscopic data. **(R)-65** - $[\alpha]_D^{25} +42.3$ (c 0.00063, CHCl_3); **(S)-65** - $[\alpha]_D^{25} -42.1$ (c 0.00057, CHCl_3).

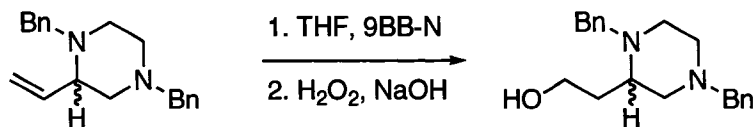


1,4-Dibenzyl-2-ethenylpiperazine 72. To a -78 °C solution of oxalyl chloride (2 M in CH_2Cl_2 , 14 mL, 28 mmol) in dry CH_2Cl_2 (60 mL) under argon was added (dropwise) a solution of DMSO (4 mL, 56 mmol) in CH_2Cl_2 (10 mL). After stirring

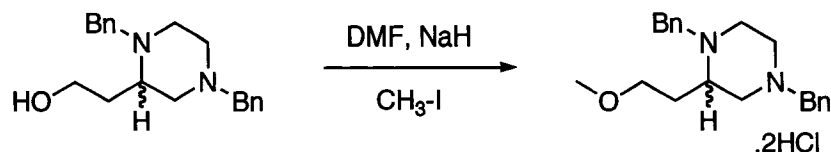
20 min at -78 °C, a solution of alcohol **30** (7.45 g, 25 mmol) in CH₂Cl₂ (18 mL) was added (dropwise), followed by triethylamine (17.6 mL, 127 mmol) after another 20 min. After stirring for 10 min at -78 °C, the mixture was warmed to ambient temperature over 2 h. The mixture was diluted with water (75 mL) and the organic phase separated. The aqueous phase was extracted with CH₂Cl₂ (2 x 50 mL) and the combined extracts washed with saturated NaHCO₃ (100 mL), dried (K₂CO₃) and concentrated to provide the crude aldehyde that was pumped under high vacuum for 10 min and then used immediately in the next step.

To a 0 °C suspension of methyltriphenylphosphonium iodide (10.0 g, 24.8 mmol) in dry THF (70 mL) was added a solution of *n*-BuLi in hexane (2.4 M, 10.0 mL, 24 mmol) producing a red-orange solution. Following 1 h, a solution of aldehyde (3.60 g, 12.3 mmol) in dry THF (15 mL) was added (dropwise) and the reaction warmed slowly to ambient temperature overnight. The reaction was quenched by the addition of saturated NaHCO₃ solution (150 mL), and the THF evaporated. The aqueous mixture was extracted with CH₂Cl₂ (3 x 50 mL) and the combined extracts dried (K₂CO₃) and concentrated to give the crude material that was purified by column chromatography (silica gel, EtOAc:Hexanes, 1:3) to provide **72** as an oil (2.73 g, 76%). TLC *R*_f 0.42 (EtOAc:Hexanes, 2:3). ¹H NMR (400 MHz, CDCl₃): δ 2.10 – 2.25 (m, 3H), 2.66 – 2.77 (m, 3H), 2.96 (td, *J* = 2.9, 9.2 Hz, 1H), 3.10 (d, part of AB pattern, *J* = 13.6, 1H), 3.51 (m, AB pattern, *J* = 13.2 Hz, 2H), 4.08 (d, part of AB pattern, *J* = 13.6 Hz, 1H), 5.21 (dd, *J* = 1.8, 10.3 Hz, 1H), 5.30 (dd, *J* = 1.8, 17.6 Hz, 1H), 5.86 (m, 1H), 7.22 – 7.40 (m, 10H); ¹³C

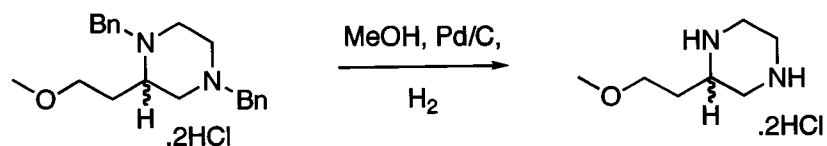
NMR (100 MHz, CDCl₃): δ 50.9, 53.0, 59.0, 59.1, 62.9, 65.0, 117.9, 126.7, 127.0, 128.1, 128.2, 129.07, 129.14, 137.9, 138.6.



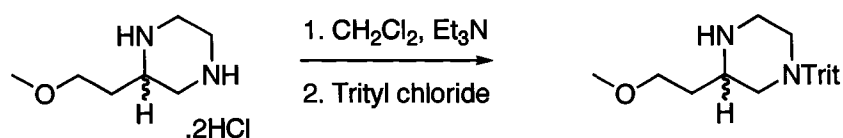
1,4-Dibenzyl-2-(2-hydroxyethyl)piperazine 73. To a solution of alkene **72** (2.62 g, 8.97 mmol) in dry THF (50 mL) under argon was added (dropwise) a solution of 9-BBN in THF (0.5 M, 27 mL, 13.5 mmol). After stirring 5 min the reaction was heated at 50 °C for 1 h then cooled to 0 °C in an ice bath. To the reaction was added (dropwise) 1 M NaOH (23 mL), followed by 30% H₂O₂ (23 mL). Following the additions, the reaction was warmed to ambient temperature and a TLC confirmed consumption of starting material. The THF was evaporated and the aqueous mixture extracted with CH₂Cl₂ (3 x 50 mL). The combined extracts were dried (K₂CO₃) and concentrated to provide the crude material that was purified by column chromatography (silica gel, EtOAc:Hexanes, 2:3 – 3:2, to remove non-polar material then EtOAc:CHCl₃, 4:1) to provide **73** as an oil (2.39 g, 86%). TLC *R_f* 0.34 (MeOH:CH₂Cl₂, 1:9). ¹H NMR (400 MHz, CDCl₃): δ 1.81 – 1.91 (bm, 1H), 1.99 – 2.09 (bm, 1H), 2.26 – 2.36 (m, 2H), 2.42 (dd, *J* = 6.8, 11.3 Hz, 1H), 2.51 (m, 1H), 2.64 (dd, *J* = 2.9, 11.3 Hz, 1H), 2.83 (m, 1H), 2.92 (m, 1H), 3.39 (bd, *J* = 12.6 Hz, 1H), 3.49 (m, AB pattern, *J* = 12.9 Hz, 2H), 3.74 (m, 1H), 3.87 (m, 1H), 4.17 (bd, *J* = 12.9 Hz, 1H), 4.87 (bs, 0.6H, -OH), 7.23 – 7.29 (m, 2H), 7.29 – 7.34 (m, 8H); ¹³C NMR (100 MHz, CDCl₃): δ 30.9, 49.3 (broad), 51.4, 55.7, 57.7, 58.0, 60.7, 63.0, 127.0 (2 overlapped peaks), 128.1, 128.2, 128.88, 128.93, 137.7, 138.1.



1,4-Dibenzyl-2-(2-methoxyethyl)piperazine 74. To a 0 °C solution of alcohol **73** (2.40 g, 7.7 mmol) in dry DMF (25 mL) was added NaH (95%, 0.461 g, 19.2 mmol) in one portion. After stirring 5 min, iodomethane (0.50 mL, 8.03 mmol) was added (dropwise) and the reaction warmed to ambient temperature. After stirring for 1 h, the excess NaH was destroyed by the careful addition of water and the solution was diluted with 50 mL each of water and saturated NaHCO₃ solution. The aqueous mixture was extracted with ether (3 x 40 mL) and the combined extracts dried (K₂CO₃) and concentrated to give the crude material that was purified by column chromatography (silica gel, EtOAc:Hexanes, 2:3) to afford **75** (free base form) as an almost colorless oil (1.74 g, 70%). TLC *R_f* 0.52 (MeOH:CH₂Cl₂, 1:9). The oil was dissolved in ether and treated with HCl gas to produce a white precipitate that was collected by filtration, washed with ether, and dried *in vacuo* to give **74** as a white solid (2.0 g, 94% from free base). The material was characterized as the free base. ¹H NMR (400 MHz, CDCl₃): δ 1.92 (bm, 2H), 2.25 (bm, 3H), 2.48 – 2.75 (bm, 4H), 3.22 – 3.32 (m, 4H, includes 3H s at 3.28), 3.35 – 3.46 (m, 3H), 3.54 (bd, *J* = 13.2 Hz, 1H), 3.98 (m, 1H), 7.20 – 7.38 (m, 10H); ¹³C NMR (100 MHz, CDCl₃): δ 29.2, 50.3, 52.8, 57.3, 57.5, 57.8, 63.0, 70.1, 126.7, 126.9, 128.1 (two overlapped peaks), 128.9, 129.0, 138.2, 139.1.

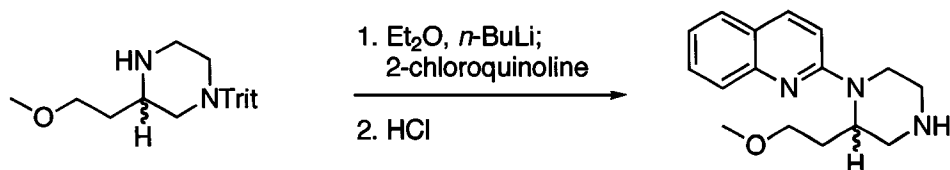


2-(2-Methoxyethyl)piperazine dihydrochloride 75. To a solution of **74** (2.00 g, 5.0 mmol) in methanol (100 mL) was added Pd/C (5%, 0.30 g). The flask was sealed with a rubber septa and hydrogen gas was bubbled through the solution via balloon. The reaction was monitored by TLC until the starting material was gone then the mixture was filtered (Celite) and the filtrate concentrated to provide **75** as a white solid (1.05 g, 97%). ^1H NMR (400 MHz, D_2O): δ 1.75 – 1.90 (m, 2H), 3.06 (dd, $J = 12.5, 14.3$ Hz, 1H), 3.15 (s, 3H), 3.17 – 3.29 (m, 2H), 3.43 (t, $J = 5.8$ Hz, 2H), 3.50 – 3.62 (m, 4H); ^{13}C NMR (100 MHz, D_2O , 1,4-dioxane int. std.): δ 30.3, 40.7, 41.4, 45.1, 52.7, 59.1, 68.9.



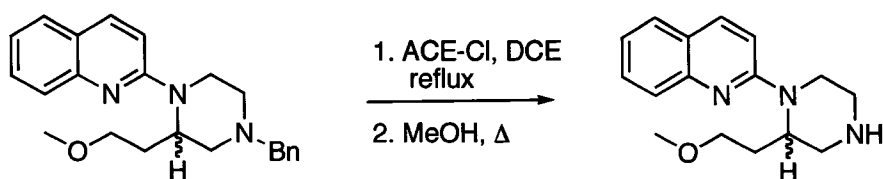
3-(2-Methoxyethyl)-1-triphenylmethylpiperazine 76. To a stirring suspension of piperazine **75** (1.05 g, 4.83 mmol) in dry CH_2Cl_2 under argon (30 mL) was added anhydrous triethylamine (2.7 mL, 19.4 mmol). The resultant clear solution was cooled to 0 °C and a solution of trityl chloride (1.4 g, 5.02 mmol) in dry CH_2Cl_2 (9 mL) was added (dropwise). The reaction was stirred 10 min at 0 °C then warmed to ambient temperature and stirred for 4 h. The solution was washed with saturated NaHCO_3 solution (30 mL) and brine (2 x 20 mL), dried (K_2CO_3) and the solvent evaporated to provide **76** as a white solid (1.89 g, quantitative). ^1H NMR (400 MHz, CDCl_3): δ 1.21 (bs, 1H), 1.63 (bm, 2H), 2.86 –

3.22 (bm, 7H), 3.31 (s, 3H), 3.41 (m, 2H), 7.10 – 7.58 (m, 15H); ^{13}C NMR (100 MHz, CDCl_3): δ 34.1, 46.3, 48.8, 53.6, 54.6, 58.6, 70.0, 77.1, 125.9, 127.4, 129.3, 142.6.

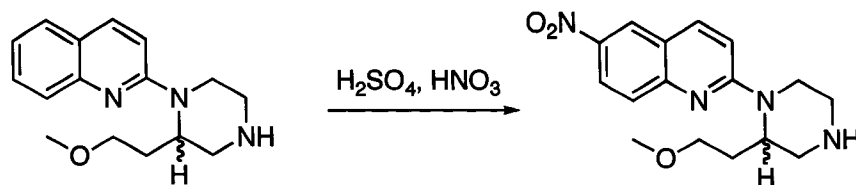


2-[2-(2-Methoxyethyl)piperazin-1-yl]quinoline 77. To a 0 °C solution of trityl piperazine **76** (0.530 g, 1.37 mmol) in dry ether (15 mL) under argon was added (dropwise) *n*-butyllithium (2.45 M in hexane, 1.37 mmol) producing a slightly colored turbid solution. After stirring for 20 min, a solution of 2-chloroquinoline (0.150 g, 0.91 mmol) in ether (4 mL) was added (dropwise) and the solution allowed to stir for 20 min at 0 °C then at ambient temperature for 14 h. The reaction was diluted with ether (10 mL), washed with saturated NaHCO_3 (2 x 25 mL) and brine (1 x 25 mL), dried (K_2CO_3) and concentrated to give the crude material that was purified by column chromatography (silica gel, EtOAc:Hexanes, 1:3) to provide the coupled product (TLC R_f 0.54; EtOAc:Hexanes, 2:3) that was not spectroscopically characterized and immediately deprotected. The intermediate product was dissolved in acetone (3 mL) and 3 M HCl (6 mL) and the flask swirled. The mixture was further diluted with 1 M HCl (15 mL) and after 5 min was transferred to a separatory funnel and washed with CH_2Cl_2 (4 x 15 mL). The aqueous mixture was made basic with 4 N NaOH, diluted with saturated NaHCO_3 solution (20 mL) and extracted with CH_2Cl_2 (4 x 20 mL). The combined extracts were dried and concentrated to afford **77** as a pale colored oil

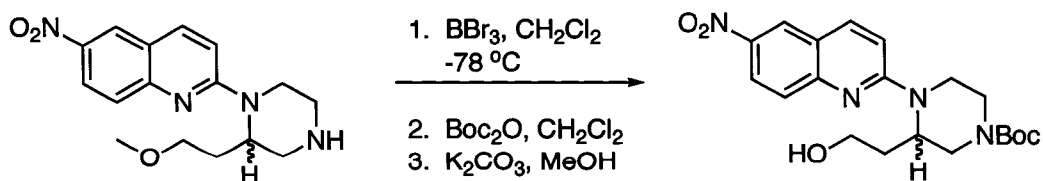
(0.227 g, 92%). TLC R_f 0.12 (MeOH:CH₂Cl₂, 1:9). ¹H NMR (400 MHz, CDCl₃): δ 1.76 (bs, NH, 1H), 2.01 (m, 1H), 2.11 (m, 1H), 2.86 (m, 1H), 3.03 – 3.16 (m, 4H), 3.24 (s, 3H), 3.33 (m, 1H), 3.44 (m, 1H), 4.51 (bm, 1H), 4.62 (bm, d shaped, 1H), 7.03 (d, J = 9.5 Hz, 1H), 7.19 (m, 1H), 7.51 (m, 1H), 7.57 (bd, J = 8.1 Hz, 1H), 7.66 (bd, J = 8.4 Hz, 1H), 7.86 (d, J = 9.5 Hz, 1H); ¹³C NMR (100 MHz, CDCl₃): δ 28.3, 39.7, 46.3, 48.9, 49.3, 58.5, 69.5, 109.5, 121.9, 122.8, 126.3, 127.1, 129.3, 137.2, 147.9, 157.1.



2-[2-(2-Methoxyethyl)piperazin-1-yl]quinoline 77. To a 0 °C solution of methyl ether **190** (0.370 g, 1.02 mmol) in dry dichloroethane (15 mL) under argon was added 1-chloroethyl chloroformate (0.293 g, 2.05 mmol). After stirring 10 min, the flask was heated at reflux for 3 h then cooled and the solvent evaporated. The residue was dissolved in methanol (10 mL) and heated at 60 - 65 °C. After 1.25 h the methanol was evaporated and the residue was dissolved in 20 mL 1 M HCl and washed with CH₂Cl₂ (4 x 15 mL). The aqueous phase was made basic with 4 M NaOH, diluted with saturated NaHCO₃ (20 mL) and extracted with CH₂Cl₂ (4 x 20 mL). The combined extracts were dried (K₂CO₃) and concentrated to give **77** as a pale colored oil (0.270 g, 97%). This product was identical to that synthesized via the N-Trit protected piperazine.



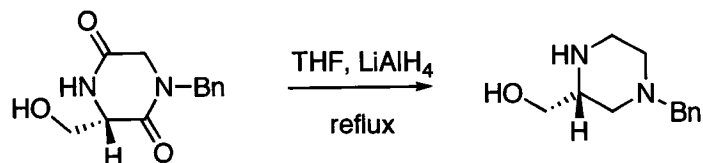
2-[2-(2-Methoxyethyl)piperazin-1-yl]-6-nitroquinoline 78. To a 0 °C solution of **77** (0.196 g, 0.72 mmol) in conc. H₂SO₄ (8 mL) was added HNO₃ (15.4 M, 0.094 mL, 1.45 mmol). The reaction was stirred for 15 min and was then quenched by pouring onto ice. The solution was basified with 4 M NaOH and diluted with saturated NaHCO₃ (30 mL). The bright yellow aqueous mixture was extracted with CH₂Cl₂ (3 x 30 mL) and the combined extracts dried (K₂CO₃) and concentrated to provide **78** as a yellow-orange oily solid (0.220 g, 96%). TLC *R_f* 0.17 (MeOH:CH₂Cl₂, 1:9). ¹H NMR (400 MHz, CDCl₃): δ 1.75 (bs, 1H, NH), 2.05 (m, 1H), 2.16 (m, 1H), 2.85 (m, 1H), 2.97 – 3.19 (m, 4H), 3.24 (s, 3H), 3.30 (m, 1H), 3.45 (m, 1H), 4.57 (bm, 1H), 4.78 (bm, 1H), 7.15 (d, *J* = 9.5 Hz, 1H), 7.61 (d, *J* = 9.5 Hz, 1H), 7.93 (d, *J* = 9.5 Hz, 1H), 8.27 (dd, *J* = 2.6, 9.5 Hz, 1H), 8.51 (d, *J* = 2.6 Hz, 1H); ¹³C NMR (100 MHz, CDCl₃): δ 28.8, 39.7, 46.2, 48.9, 49.5, 58.4, 69.1, 111.2, 120.8, 123.4, 124.1, 126.7, 138.3, 141.5, 151.5, 158.5; HRMS (ESI-TOF) *m/z* (M + H)⁺ calcd. for C₁₆H₂₁N₄O₃ 317.1614 found 317.1609.



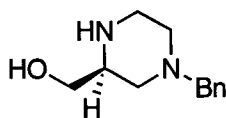
2-[4-(tert-Butoxycarbonyl)-2-(2-Hydroxyethyl)piperazin-1-yl]-6-nitroquinoline 79. To a -78 °C stirring solution of **78** (0.200 g, 0.634 mmol) in dry CH₂Cl₂ (100 mL) under argon was added (dropwise) boron tribromide

solution (1 M in CH₂Cl₂, 3.17 mL, 3.17 mmol). The reaction was maintained at -78 °C until the bath warmed to ambient temperature over 15 h. The reaction was quenched with saturated NaHCO₃ (50 mL), transferred to a separatory funnel and shaken vigorously. The organic phase was separated and the aqueous layer extracted with CH₂Cl₂ (40 mL) and CHCl₃:isopropyl alcohol, 4:1 (2 x 40 mL). The combined organic phases were dried (K₂CO₃), concentrated and the residue dissolved in about 20 mL of CH₂Cl₂. To the yellow solution was added a solution of di-*tert*-butyldicarbonate (0.276 g, 0.127 mmol) in CH₂Cl₂ (5 mL). The solution was stirred for 20 min, concentrated and the residue purified by column chromatography (silica gel, EtOAc:Hexanes, 2:3 – 3:2) to afford the di-Boc **80** and mono-Boc **79** protected products that were combined and the solvent evaporated. The residue was dissolved in MeOH (8 mL) treated with excess K₂CO₃ and heated at 60 °C until only the mono-Boc product **79** was present by TLC. The methanol was evaporated and the residue partitioned between CH₂Cl₂ and saturated NaHCO₃ (20 mL each). The organic phase was separated and the aqueous phase extracted with CH₂Cl₂ (2 x 10 mL). The combined extracts were dried (K₂CO₃) and concentrated to give the crude material that was purified by column chromatography (silica gel, EtOAc:Hexanes, 2:3 – 3:2) to afford **79** as a yellow foam (0.119 g, 47 %). TLC *R_f* 0.17 (EtOAc:Hexanes, 3:2). ¹H NMR (400 MHz, CDCl₃): δ 1.47 (s, 9H), 1.81 – 2.10 (bm, 2H, 2 humps), 2.97 – 2.48 (bm, 4H), 3.66 (bm, 1H), 3.92 – 4.28 (bm, 3H), 4.92 and 5.04 (bm, 1.6H), 7.08 (d, *J* = 9.2 Hz, 1H), 7.55 (d, *J* = 9.2 Hz, 1H), 7.95 (d, *J* = 9.2 Hz, 1H), 8.23 (dd, *J* = 2.6, 9.2 Hz, 1H), 8.44 (d, *J* = 2.6 Hz, 1H); ¹³C NMR (100 MHz, CDCl₃): δ 28.3, 32.3,

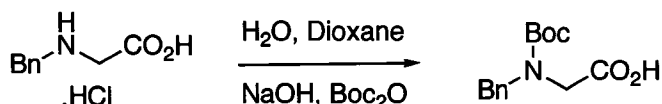
40.3, 42.6, 46.2, 47.6, 48.6, 58.0, 80.3, 110.9, 121.0, 124.05, 124.08, 126.1, 139.3, 142.0, 150.5, 154.8, 158.3.



(R)-(-)-4-Benzyl-2-(hydroxymethyl)piperazine (R)-94. To a 0 °C suspension of dione (**S**)-**97** (0.905 g, 3.86 mmol) in dry THF (90 mL) under argon was added LiAlH₄ (0.600 g, 15.8 mmol) in small portions. After the effervescence subsided the flask was heated at reflux for 5 h. The solution was cooled, stirred an additional hour then the excess LiAlH₄ was quenched by the careful, sequential addition of 0.6 mL water, 1.2 mL 4 N NaOH and 0.6 mL water. The solids that formed were filtered (Celite) and the filtrate concentrated to give (**R**)-**94** as a pale colored oil (0.737 g, 92%). This crude material was used without further purification in subsequent reactions. A 0.170 g portion was purified (Biotage 12M KP-NH column, MeOH:CHCl₃, 1:199) for spectroscopic purposes giving 0.148 g of (**R**)-**94** as a pale colored oil. TLC *R_f* 0.04 (MeOH:CH₂Cl₂, 1:9). ¹H NMR (400 MHz, CDCl₃): δ 1.93 (m, 1H, triplet shape), 2.13 (dd, *J* = 2.9, 11.0 Hz, 1H), 2.54 (bs, 2H), 2.71 (m, 2H, doublet shape), 2.87 – 2.98 (m, 2H), 3.03 (dt, 2.9, 12.1 Hz, 1H), 3.45 – 3.54 (m, 3H), 3.59 (dd, *J* = 4.0, 11.0 Hz, 1H), 7.23 – 7.35 (m, 5H); ¹³C NMR (100 MHz, CDCl₃): δ 44.9, 53.4, 55.6, 56.1, 63.3, 63.7, 127, 128.1, 129.1, 137.6; (*R*) - [α]_D²⁵ -16.0 (c 0.015, CHCl₃).

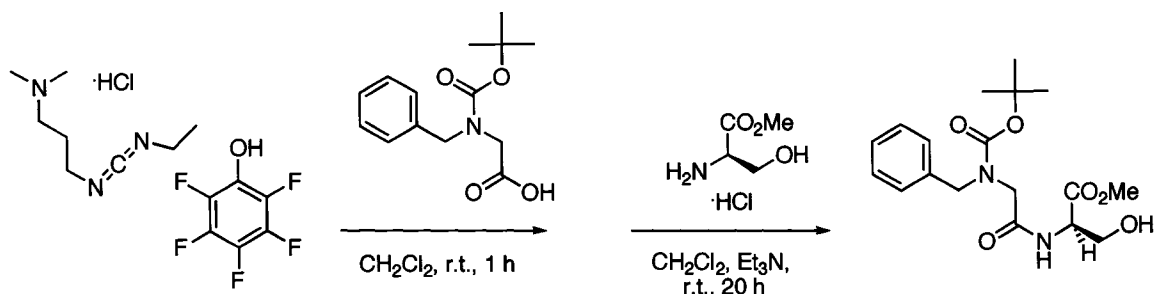


(S)-(+)-4-Benzyl-2-(hydroxymethyl)piperazine (S)-94. The title compound was similarly prepared and provided identical spectroscopic data. (S) - $[\alpha]_D^{25} +16.3$ (c 0.018, CHCl₃).



N-tert-Butoxycarbonyl-N-benzylglycine 95. The synthesis of **95** is adopted from the method of Le Bail.⁸³ To a solution of benzyl glycine **100** (15.5 g, 76.8 mmol) in water and dioxane (190 mL each) was added NaOH (12.3 g, 307 mmol) followed by di-*tert*-butyldicarbonate (18.4 g, 84.5 mmol) in portions. The reaction was stirred at ambient temperature for 19 h then the contents were reduced to half volume by evaporation *in vacuo*. To the reduced solution was added 140 mL of CH₂Cl₂ and the mixture stirred so the biphasic mixture was well mixed. The mixture was cooled in an ice bath and 1 M HCl was added (dropwise) until a pH of 3 – 4 was reached (~ 240 mL). The mixture was transferred to a separatory funnel and the organic phase separated. The aqueous phase was extracted with CH₂Cl₂ (3 x 50 mL) and the combined extracts were dried (MgSO₄, do not use K₂CO₃) and concentrated to provide **95** as a pale solid (15.6 g, 76%). TLC *R_f* 0.24 (MeOH:CH₂Cl₂, 1:9). ¹H NMR (400 MHz, CDCl₃): (approximate 1:1 mixture of amide rotamers) δ 1.48 (s, 9H), 3.83 (s, 1H), 3.97 (s, 1H), 4.51 (s, 1H), 4.55 (s, 1H), 7.21 – 7.37 (m, 5H), 10.90 (bs, 0.7H, -CO₂H); ¹³C NMR (100 MHz, CDCl₃):

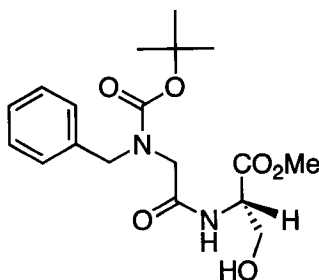
(approximate 1:1 mixture of amide rotamers) δ 28.2, 28.3, 47.5, 50.8, 51.6, 80.9, 81.2, 127.5, 127.6, 128.1, 128.6, 137.0, 137.1, 175.2, 175.8.



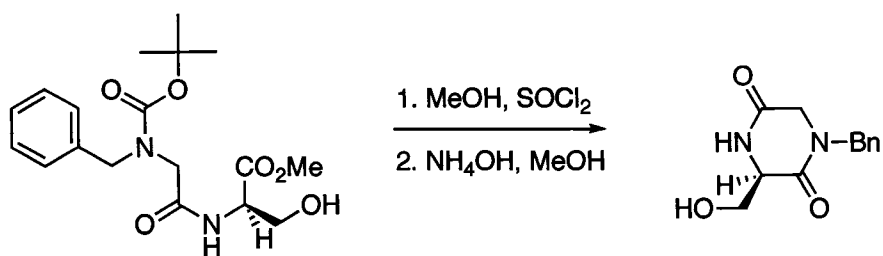
GENERAL PEPTIDE COUPLING PROCEDURE described for:

N-tert-Butoxycarbonyl-N-benzylglycyl-D-serine Methyl Ester (*R*)-96. The synthesis of (*R*)-96 is adapted from the method of Naylor.¹¹¹ To a stirring suspension of EDC.HCl (1.15 g, 6 mmol) in reagent grade CH₂Cl₂ (20 mL) was added a solution of pentafluorophenol (1.5g, 8.1 mmol) in CH₂Cl₂ (10 mL) followed by a solution of N-Boc-N-Benzyl glycine **95** (1.32 g, 5.0 mmol) in CH₂Cl₂ (20 mL). The solution was stirred at ambient temperature for 1 h then triethylamine (2.5 mL, 18 mmol) was added with additional CH₂Cl₂ (10 mL). The amino acid methyl ester hydrochloride (serine methyl ester HCl for this example, 0.93 g, 6 mmol) was then added in small portions. The final solution was stirred for 20 h at ambient temperature and was then washed with aqueous sodium carbonate (1 M, 100 mL), aqueous citric acid (1 M, 100 mL) and water (50 mL). The organic phase was dried (K₂CO₃) and concentrated to afford the crude product that was purified by column chromatography (silica gel, EtOAc:Hexanes, 2:3 – 3:2) to afford (*R*)-96 as a clear viscous oil (1.72 g, 94% yield). *R_f* = 0.52

(MeOH:CH₂Cl₂, 1:9). The spectroscopic data of (*R*)-**96** was consistent with the literature.¹¹¹

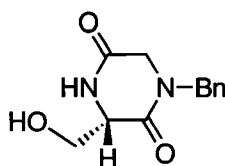


N-tert-Butoxycarbonyl-N-benzylglycyl-L-serine Methyl Ester (*S*)-96**.** The title compound was similarly prepared, and provided identical spectroscopic data.

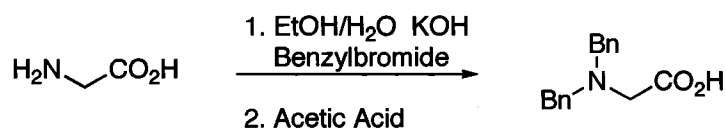


(*R*)-1-Benzyl-3-(hydroxymethyl)piperazine-2,5-dione (*R*)-97**.** The synthesis of (*R*)-**97** is adapted from the method of Naylor.¹¹¹ To a stirring 0 °C solution of dipeptide (*R*)-**96** (1.76 g, 4.81 mmol) in methanol (10 mL) was slowly added excess thionyl chloride (~ 1.7 mL) to avoid sputtering. Following the addition, the solution was warmed to ambient temperature and allowed to stir for 2.5 h. The solvent was evaporated and the residue triturated with ~20 mL diethyl ether to produce a white solid that was collected by filtration. The solid was dissolved in methanol (20 mL) and treated with ammonium hydroxide (20 mL) at ambient temperature. The solution was stirred for 16 h then the solvent was evaporated. The residue was partitioned between saturated NaHCO₃ (20 mL) and

CHCl₃:isopropyl alcohol, 4:1 (50 mL). The organic phase was separated and the aqueous phase extracted with CHCl₃:isopropyl alcohol, 4:1 (4 x 30 mL). The combined organic phases were dried (K₂CO₃) and concentrated to afford (*R*)-**97** as a white solid (1.01 g, 90%). *R*_f = 0.19 (MeOH:CH₂Cl₂, 1:9). This material was of sufficient purity for subsequent reactions and had spectroscopic data consistent with the literature.¹¹¹

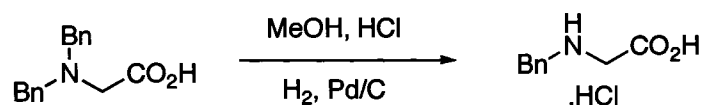


(S)-1-Benzyl-3-(hydroxymethyl)piperazine-2,5-dione (S)-97. The title compound was similarly prepared and provided identical spectroscopic data.

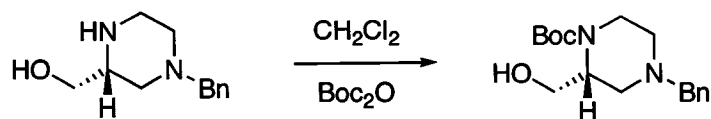


N,N-Dibenzylglycine 99. The synthesis of **99** is adopted from the method of Velluz.¹¹² To a 45 °C solution of glycine (10 g, 133 mmol) and KOH (25 g, 445 mmol) in ethanol and water (75 mL each) was added (dropwise) benzyl bromide (48.9 g, 286 mmol) from an addition funnel. Following the addition, the reaction was heated at reflux for 2 h then cooled and stirred at ambient temp for 16 h. The solvent was evaporated to a volume of 125 mL, transferred to a 400 mL beaker and heated to boiling with stirring. To the boiling solution was carefully added 10 mL of glacial acetic acid, producing a large mass of white precipitate. The solids were collected by filtration, washed with 200 – 300 mL of cold water

and then dried under vacuum give **99** as a white solid (27.2 g, 80%). ^1H NMR (400 MHz, $\text{DMSO-}d_6$): δ 3.16 (s, 2H), 3.74 (s, 4H), 7.21 – 7.38 (m, 10H), 12.4 (bs, 0.4H); ^{13}C NMR (100 MHz, $\text{DMSO-}d_6$): δ 52.9, 56.7, 127.0, 128.2, 128.5, 138.9, 172.2.



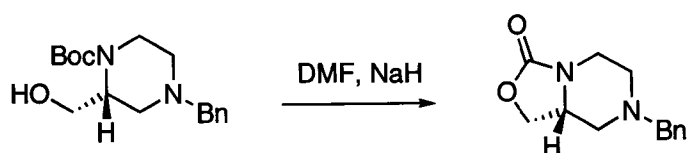
N-Benzylglycine Hydrochloride 100. The synthesis of **100** is adopted from the method of Velluz.¹¹² To glycine **99** (10.26 g, 40.2 mmol) suspended in methanol (140 mL) was added HCl (12 M, 5 mL, 60 mmol) and Pd/C (5%, 1.5 g). This mixture was hydrogenated using a Parr apparatus until no more hydrogen was consumed, repressurizing (max. 50 psi) the flask if necessary. The mixture was filtered (Celite), and the filtrate concentrated to provide **100** as a white solid (7.8 g, 96%). ^1H NMR (400 MHz, $\text{DMSO-}d_6$): δ 3.79 (s, 2H), 4.15 (s, 2H), 7.40 (m, 3H), 7.57 (m, 2H), 9.87 (bs, 2H), 13.8 (bs, 0.5H); ^{13}C NMR (100 MHz, $\text{DMSO-}d_6$): δ 46.2, 49.6, 128.6, 128.9, 130.2, 131.6, 167.6.



(R)-4-Benzyl-1-(tert-butoxycarbonyl)-2-(hydroxymethyl)piperazine (R)-101.

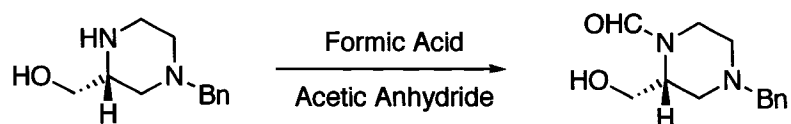
To a stirring solution of alcohol **(R)-94** (0.138 g, 0.669 mmol) in reagent grade CH_2Cl_2 (10 mL) was added a solution of di-*tert*-butyldicarbonate (0.175 g, 0.803 mmol) in CH_2Cl_2 (4 mL). The reaction was stirred 20 h at ambient temperature then the solvent was evaporated leaving an oily residue that was purified by

column chromatography (silica gel, EtOAc:Hexanes, 2:3) to provide (*R*)-**101** as a colorless oil (0.190 g, 93%). TLC R_f 0.35 (EtOAc:Hexanes, 3:2). ^1H NMR (400 MHz, CDCl_3): δ 1.44 (s, 9H), 2.07 (td, $J = 4.0, 11.7$, 1H), 2.27 (dd, $J = 4.0, 11.4$, 1H), 2.80 (bd, 1H), 2.96 (m, 1H, bd shape), 3.30 – 3.55 (m, 3H, overlap of a broad multiplet at 3.36 and singlet shape at 3.47), 3.87 (m, 2.5H, possible OH overlap), 4.05 (bs, 1H), 7.23 – 7.35 (m, 5H); ^{13}C NMR (100 MHz, CDCl_3): δ 28.3, 41.3 (broad), 51.3 (broad), 52.4, 54.8, 62.9, 66.2, 79.8, 127.3, 128.4, 128.8, 137.0, 155.1 (broad).



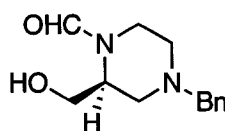
(*R*)-7-Benzyl-tetrahydro-1*H*-oxazolo[3,4-*a*]pyrazin-3(5*H*)-one (*R*)-102. To a 0 °C solution of Boc alcohol (*R*)-**101** (0.046 g, 0.15 mmol) in dry DMF was added sodium hydride (0.011 g, 0.45 mmol). After stirring 5 min, the reaction was stirred at ambient temperature for 4 h then the excess hydride was carefully quenched with water and the mixture partitioned between water (8 mL) and ether (10 mL). The organic phase was separated and the aqueous phase was extracted with two additional portions of ether (15 mL). The combined organic phases were dried (K_2CO_3) and concentrated to provide the crude product that was purified by column chromatography (silica gel, EtOAc:Hexanes, 1:3 – 4:1) to provide (*R*)-**102** as a colorless oil (0.025 g, 71%). TLC R_f 0.14 (EtOAc:Hexanes, 3:2). ^1H NMR (400 MHz, CDCl_3): δ 1.93 (m, triplet shape, 1H), 2.10 (td, $J = 3.7, 11.7$ Hz, 1H), 2.78 – 2.91 (m, 2H), 3.11 (td, $J = 3.7, 12.5$ Hz, 1H), 3.55 (m, AB

pattern, $J = 13.2$ Hz, 2H), 3.78 (m, dd shaped, 1H), 3.83 – 3.91 (m, 2H), 4.35 (m, 1H), 7.27 – 7.36 (m, 5H); ^{13}C NMR (100 MHz, CDCl_3): δ 41.0, 51.8, 53.1, 56.7, 62.8, 65.4, 127.4, 128.4, 129.0, 137.2, 156.9; GC/MS (EI) m/z (M) $^+$ 91 (base), 187, 232 (parent).



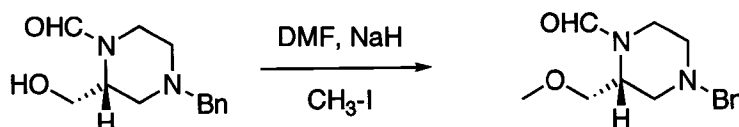
(R)-(+)-4-Benzyl-2-(hydroxymethyl)piperazine-1-carbaldehyde (R)-106. To a 0 °C solution of alcohol **(R)-94** (0.567 g, 2.75 mmol) in formic acid (88%, 8 mL) was added (dropwise) acetic anhydride (2.33 mL, 24.7 mmol). The reaction was stirred for 30 min at 0 °C then warmed to ambient temperature. Following 1 h a TLC showed consumption of starting material and the reaction was diluted with ice, placed back in an ice bath and made basic with 4 N NaOH (~50 mL). The aqueous mixture was further diluted with saturated NaHCO_3 (30 mL) and extracted with CH_2Cl_2 (4 x 20 mL). The combined extracts were dried (K_2CO_3) and concentrated to give an orange-brown oil that was purified by column chromatography (silica gel, $\text{MeOH}:\text{CHCl}_3$, 1:199 – 1:49) to afford **(R)-106** as an almost colorless oil (0.521g, 67%). TLC R_f 0.34 ($\text{MeOH}:\text{CH}_2\text{Cl}_2$, 1:9). ^1H NMR (400 MHz, CDCl_3): (approximate 1:1 mixture of amide rotamers) δ 2.05 (td, $J = 3.7, 11.7$ Hz, 0.5H), 2.13 (td, $J = 3.7, 11.7$ Hz, 0.5H), 2.28 (dd, $J = 4.0, 11.7$ Hz, 1H), 2.87 (m, 1H), 2.90 – 3.02 (m, 1H, looks like dd), 3.12 (td, $J = 4.0, 12.8$ Hz, 0.5H), 3.41 – 3.59 (m, 3.5H), 3.64 – 3.75 (m, 1H), 3.85 (m, 0.5H, looks like dd), 3.97 (dd, $J = 5.5, 11.4$ Hz, 0.5H), 4.08 (dd, $J = 7.3, 11.4$ Hz, 0.5H), 4.20 (bd, 0.5H), 4.38 (m, 0.5H), 7.25 – 7.36 (m, 5H), 8.06 (s, 0.5H), 8.08 (s, 0.5H); ^{13}C

NMR (100 MHz, CDCl₃): δ 37.3, 43.9, 49.1, 52.1, 52.9, 54.36, 54.44, 55.5, 62.7, 62.8, 63.6, 65.2, 127.5, 127.6, 128.4, 128.5, 128.8, 128.9, 136.8, 137.2, 161.8, 161.9; (*R*) - [α]_D²⁵ +56.1 (c 0.050, CHCl₃); HRMS (ESI-TOF) *m/z* (M + H)⁺ calcd. for C₁₃H₁₉N₂O₂ 235.1447 found 235.1446.



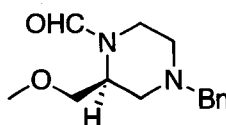
(S)-(-)-4-Benzyl-2-(hydroxymethyl)piperazine-1-carbaldehyde (S)-106. The title compound was similarly prepared and provided identical spectroscopic data.

(*S*) - [α]_D²⁵ -53.8 (c 0.052, CHCl₃).

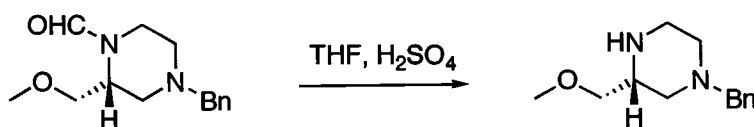


(R)-(+)-4-Benzyl-2-(methoxymethyl)piperazine-1-carbaldehyde (R)-107. To a 0 °C solution of alcohol (*R*)-**106** (0.502 g, 2.14 mmol) in dry DMF (20 mL) was added NaH (95%, 0.154 g, 6.43 mmol) in one portion. After stirring 5 min, iodomethane (0.319g, 2.25 mmol) was added (dropwise) and the mixture stirred for 20 min at 0°C then at ambient temp for 1.5 h. The excess NaH was destroyed by the careful addition of water and the solution was diluted with 40 mL each of water and saturated NaHCO₃. The aqueous mixture was extracted with ether (2 x 40 mL) and ethyl acetate (2 x 40 mL). The combined extracts were washed with brine (50 mL), dried (K₂CO₃) and concentrated to give a brown oil that was purified by column chromatography (silica gel, MeOH:CHCl₃, 1:199 – 1:49) to afford (*R*)-**107** as an almost colorless oil (0.360 g, 69%). TLC *R_f* 0.49

(MeOH:CH₂Cl₂, 1:9). ¹H NMR (400 MHz, CDCl₃): (approximate 3:7 mixture of amide rotamers) δ 2.00 – 2.12 (m, 1.3H), 2.18 (dd, *J* = 3.7, 11.7 Hz, 0.7H), 2.80 – 2.92 (m, 2H), 2.93 – 3.02 (m, 1H), 3.29 – 3.38 (m, 3H, two singlets overlapped), 3.41 – 3.76 (m, 5H, many intermixed peaks), 4.16 (bd, 0.7H), 4.60 (m, 0.3H), 7.25 – 7.35 (m, 5H, overlapped with CDCl₃), 8.04 (s, 0.7H), 8.07 (s, 0.3H); ¹³C NMR (100 MHz, CDCl₃): δ 36.7, 42.7, 47.0, 52.3, 53.2, 53.7, 54.1, 58.8, 59.0, 62.5, 62.6, 69.5, 70.6, 127.2, 128.3, 128.7, 137.7, 161.3, 161.9; (*R*) - [α]_D²⁵ +39.8 (c 0.036, CHCl₃); HRMS (ESI-TOF) *m/z* (*M* + *H*)⁺ calcd. for C₁₄H₂₁N₂O₂ 249.1603 found 249.1598.

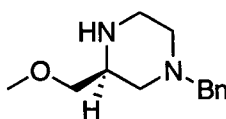


(S)-(-)-4-Benzyl-2-(methoxymethyl)piperazine-1-carbaldehyde (S)-107. The title compound was similarly prepared and provided identical spectroscopic data. (*S*) - [α]_D²⁵ -37.6 (c 0.036, CHCl₃).

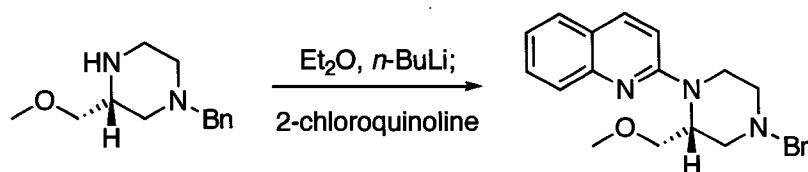


(R)-(-)-1-Benzyl-3-(methoxymethyl)piperazine (R)-108. A solution of the protected methylether (*R*)-107 (0.320 g, 1.29 mmol) in THF (3 mL) and 4 M H₂SO₄ (9 mL) was heated at 55 °C for 5 h. After cooling, the reaction contents were poured into 20 mL of cold (-10 °C) 4 M NaOH and diluted with 20 mL of saturated NaHCO₃. The mixture was extracted with CH₂Cl₂ (4 x 15 mL) and the combined extracts dried (K₂CO₃) and concentrated to provide (*R*)-108 as a pale

oily solid (0.274 g, 96%). This product was of adequate purity for the subsequent transformations. TLC R_f 0.14 (MeOH:CH₂Cl₂, 1:9). ¹H NMR (400 MHz, CDCl₃): δ 1.85 (t, J = 10.3 Hz, 1H), 2.11 (td, J = 3.3, 11.0 Hz, 1H), 2.35 (bs, 1H, NH), 2.74 (m, 2H, triplet shape), 2.90 (m, 1H, td shape), 2.96 – 3.06 (m, 2H), 3.25 – 3.36 (m, 5H, OCH₃ singlet present at 3.33), 3.50 (m, AB pattern, J = 13.2 Hz, 2H), 7.22 – 7.33 (m, 5H, overlapped with CDCl₃); ¹³C NMR (100 MHz, CDCl₃): δ 45.2, 53.8, 54.4, 55.9, 59.0, 63.4, 75.1, 126.9, 128.1, 129.1, 138.0; (*R*) - $[\alpha]_D^{25}$ -17.4 (c 0.027, CHCl₃); HRMS (ESI-TOF) m/z ($M + H$)⁺ calcd. for C₁₃H₂₁N₂O 221.1654 found 221.1654.

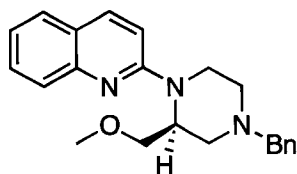


(S)-(+)-1-Benzyl-3-(methoxymethyl)piperazine (S)-108. The title compound was similarly prepared and provided identical spectroscopic data. (*S*) - $[\alpha]_D^{25}$ +14.4 (c 0.030, CHCl₃).

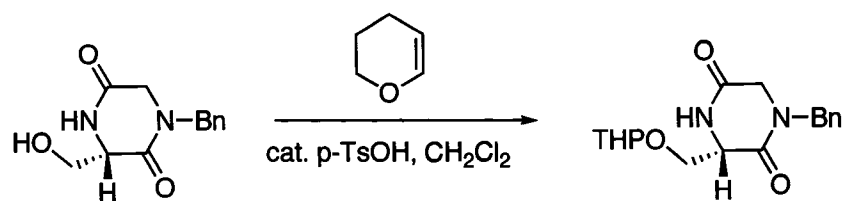


(R)-(+)-2-[4-Benzyl-2-(methoxymethyl)piperazin-1-yl]quinoline (R)-109. To a 0 °C solution of piperazine (*R*)-108 (0.273 g, 1.24 mmol) in dry ether (16 mL) under argon was added (dropwise) a solution of *n*-butyllithium in hexane (2.45 M, 1.24 mmol) producing a clear yellow solution. After stirring 20 min a solution of 2-chloroquinoline (0.134 g, 0.821 mmol) in ether (3 mL) was added (dropwise) and the solution allowed to stir for 10 min at 0 °C then at ambient temperature for

16 h. The reaction contents were diluted with ether (15 mL), washed with saturated NaHCO₃ (2 x 20 mL) and brine (20 mL), dried (K₂CO₃) and concentrated to give the crude material that was purified by column chromatography (silica gel, EtOAc:Hexanes, 1:3) to provide (*R*)-109 as a thick, light yellow oil (0.275 g, 96%). TLC *R_f* 0.42 (EtOAc:Hexanes, 2:3). ¹H NMR (400 MHz, CDCl₃): δ 2.17 – 2.27 (m, 2H), 2.95 (bd, *J* = 10.3 Hz, 1H), 3.11 (bd, *J* = 11.7 Hz, 1H), 3.21 (m, 1H), 3.33 (s, 3H), 3.49 – 3.63 (m, 3H), 3.87 (m, 1H), 4.45 (bd, 1H), 4.57 (bs, 1H), 6.98 (d, *J* = 9.2 Hz, 1H), 7.21 (m, 1H), 7.27 (m, 1H, overlapped with CDCl₃), 7.31 – 7.39 (m, 4H), 7.52 (m, 1H), 7.59 (d, *J* = 8.1 Hz, 1H), 7.68 (d, *J* = 8.4 Hz, 1H), 7.87 (d, *J* = 9.2 Hz); ¹³C NMR (100 MHz, CDCl₃): δ 40.8, 51.6, 53.1, 59.0, 62.7, 69.8, 109.4, 122.1, 122.9, 126.5, 127.0, 127.1, 128.2, 128.8, 129.4, 137.3, 138.3, 147.9, 156.8; (*R*) - [*α*]_D²⁵ +53.2 (c 0.028, CHCl₃).



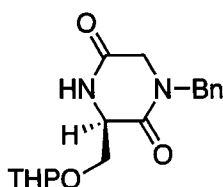
(S)-(-)-2-[4-Benzyl-2-(methoxymethyl)piperazin-1-yl]quinoline (S)-109. The title compound was similarly prepared and provided identical spectroscopic data. (*S*) - [*α*]_D²⁵ -52.8 (c 0.027, CHCl₃).



(S)-1-Benzyl-3-((tetrahydro-2H-pyran-2-yloxy)methyl)piperazine-2,5-dione

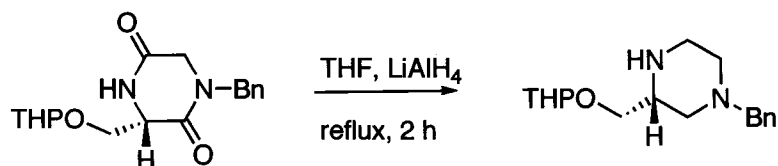
(S)-119. To a 0 °C suspension of piperazinedione (**S**)-**97** (0.913 g, 3.90 mmol) in HPLC grade CH₂Cl₂ (40 mL) under argon was added dihydropyran (1.64 g, 19.5 mmol) followed by *p*-toluenesulfonic acid monohydrate (0.025 g, 0.13 mmol). The flask was swirled to remove solids stuck to the sides and the sides were rinsed with CH₂Cl₂ as needed. After ~30 minutes, all solids had dissolved and the reaction was shown complete by a TLC that showed a new, more non-polar spot. The reaction was poured into an aqueous mixture of 30 mL each of saturated NaHCO₃, brine and water. The organic phase was separated and the aqueous phase extracted with CH₂Cl₂ (3 x 15 mL). The combined extracts were dried (K₂CO₃) and concentrated giving ~ 2 g of crude material. The crude material was dissolved in ~20 mL CH₂Cl₂ and 4 g of silica gel was added. The mixture was concentrated and the solid was loaded onto a silica gel column and chromatographed with MeOH:CH₂Cl₂, 1:39, as eluent. When the product began to elute the solvent was switched to MeOH:CH₂Cl₂, 1:19, to provide (**S**)-**119** as a white solid (1.153 g, 93%) and a 6:4 diastereomeric mixture. TLC *R*_f 0.32 (MeOH:CH₂Cl₂, 1:9). ¹H NMR (400 MHz, CDCl₃): (approximately 6:4 mixture of diastereomers) δ 1.40 – 1.70 (m, 6H), 3.50 (m, 1H), 3.69 – 3.77 (m, 2H), 3.79 – 3.85 (m, 1H), 3.92 (s, 0.6H), 3.96 (s, 0.4H), 4.05 (dd, *J* = 2.9, 9.9 Hz, 0.4H), 4.12 (dd, *J* = 5.5, 10.3 Hz, 0.6H), 4.23 (m, 1H), 4.33 (d, *J* = 14.7 Hz, 0.4H), 4.38 (d, *J*

= 14.7 Hz, 0.6H), 4.62 (m, 1H), 4.83 (d, $J = 14.7$ Hz, 0.6H), 4.90 (d, $J = 14.7$ Hz, 0.4H), 6.41 (bs, 0.4H, NH), 6.52 (bs, 0.6H, NH), 7.24 – 7.36 (m, 5H); ^{13}C NMR (100 MHz, CDCl_3): δ 18.9, 19.0, 25.1, 30.1, 30.2, 49.2, 49.3, 49.7, 49.8, 55.9, 62.0, 62.1, 69.5, 69.8, 98.9, 99.1, 128.1, 128.2, 128.5, 128.8, 128.9, 135.0, 164.4, 164.6, 166.0, 166.3.



(*R*)-1-Benzyl-3-((tetrahydro-2*H*-pyran-2-yloxy)methyl)piperazine-2,5-dione

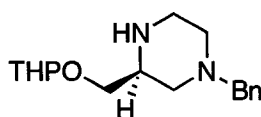
(*R*)-119. The title compound was similarly prepared and provided identical spectroscopic data.



(*R*)-1-Benzyl-3-[(tetrahydro-2*H*-pyran-2-yloxy)methyl]piperazine (*R*)-120.

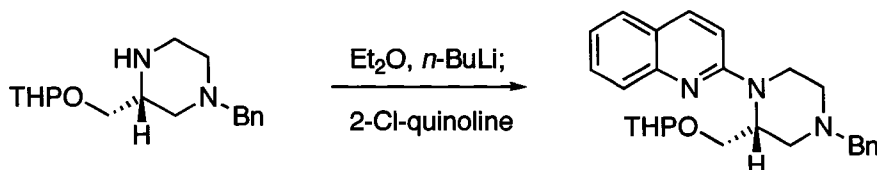
To a 0 °C suspension of THP ether (*S*)-119 (1.153 g, 3.62 mmol) in dry THF (60 mL) under argon was added LiAlH_4 (0.566 g, 14.89 mmol) in small portions, producing a gentle effervescence. The mixture was maintained on ice until the bubbling stopped, then heated at reflux for 2 h. The solution was cooled, stirred 1 h then the excess LiAlH_4 was quenched by the careful, sequential addition of 0.6 mL water, 1.2 mL 4 M NaOH solution and 0.6 mL water. The solids that formed were filtered (Celite) and the filtrate concentrated to give (*R*)-120 as a pale colored oil (1.076 g, quantitative). TLC R_f 0.14 (MeOH: CH_2Cl_2 , 1:9). ^1H NMR

(400 MHz, CDCl₃): δ 1.44 – 1.62 (m, 4H), 1.64 – 1.74 (m, 1H), 1.74 – 1.94 (m, 2H), 2.08 – 2.17 (m, 1H), 2.35 (bs, 1H, NH), 2.71 – 2.79 (m, 2H), 2.87 – 2.95 (m, 1H), 2.95 – 3.08 (m, 2H), 3.26 (m, 0.5H), 3.36 (dd, $J = 4.0, 9.9$ Hz, 0.5H), 3.45 – 3.52 (m, 3H, large singlet like peak overlapped), 3.61 – 3.73 (m, 1H), 3.78 – 3.86 (m, 1H), 4.56 (m, 1H); ¹³C NMR (100 MHz, CDCl₃): δ 19.4, 19.5, 25.3, 30.5, 45.1, 53.4, 53.5, 54.5, 54.7, 55.7, 62.2, 62.4, 63.3, 69.5, 69.9, 98.8, 99.5, 127.0, 128.2, 129.1, 137.9.



(S)-1-Benzyl-3-[(tetrahydro-2H-pyran-2-yloxy)methyl]piperazine (S)-120.

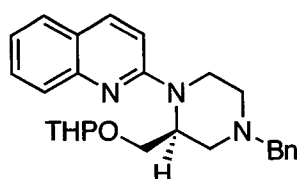
The title compound was similarly prepared and provided identical spectroscopic data.



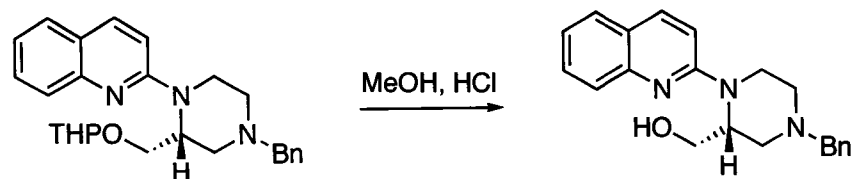
(R)-2-[4-Benzyl-2-[(tetrahydro-2H-pyran-2-yloxy)methyl]piperazin-1-

yl]quinoline (R)-121. To a 0 °C solution of THP piperazine (**R**)-120 (0.533 g, 1.84 mmol) in dry ether (25 mL) under argon was added (dropwise) *n*-butyllithium (2.33 M in hexane, 1.84 mmol) producing a brown-yellow turbid solution that stirred 20 min. A solution of 2-chloroquinoline (0.200 g, 1.22 mmol) in ether (5 mL) was slowly added (dropwise) and the solution was then allowed to stir for 20 min at 0 °C then at ambient temperature for 16 h. The reaction contents were

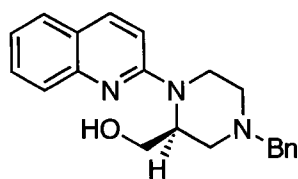
diluted with ether (15 mL), washed with saturated NaHCO₃ (2 x 20 mL) and brine (2 x 10 mL), dried (K₂CO₃) and concentrated to give the crude material that was purified by column chromatography (silica gel, EtOAc:Hexanes, 1:3) to provide **(R)-121** as a light yellow oil (0.471 g, 93%). TLC *R_f* 0.41 (EtOAc:Hexanes, 2:3). ¹H NMR (400 MHz, CDCl₃): (approximately 6:4 mixture of diastereomers) δ 1.30 – 1.86 (m, 6H), 2.18 – 2.34 (m, 2H), 2.99 (m, 1H), 3.13 (m, 0.6H, doublet shape), 3.19 – 3.34 (m, 1.4H), 3.42 – 3.59 (m, 2.3H), 3.60 – 3.71 (m, 1H), 3.74 – 3.84 (m, 1H), 3.90 (m, 1.3H, leaning doublet shape), 4.19 (m, 0.3H, triplet shaped), 4.48 – 4.68 (m, 3H, broad overlaps), 7.04 (d, *J* = 9.2 Hz, 1H), 7.23 (m, 1H), 7.30 (m, 1H), 7.34 – 7.44 (m, 4H), 7.55 (m, 1H), 7.60 (m, 1H, doublet shape), 7.73 (m, 1H, doublet shape), 7.87 (m, 1H, two unsymmetrical doublets offset); ¹³C NMR (100 MHz, CDCl₃): δ 18.9, 19.1, 25.2, 25.3, 30.3, 40.4, 40.5, 51.8, 52.0, 52.6, 53.1, 53.4, 61.6, 61.9, 62.7, 62.9, 64.2, 64.6, 98.2, 99.2, 109.4, 109.7, 121.9, 122.8, 126.4, 126.9, 127.0, 128.1, 128.8, 128.9, 129.2, 136.8, 137.0, 138.2, 138.3, 147.8, 156.9.



(S)-2-[4-Benzyl-2-[(tetrahydro-2H-pyran-2-yloxy)methyl]piperazin-1-yl]quinoline (S)-121. The title compound was similarly prepared and provided identical spectroscopic data.

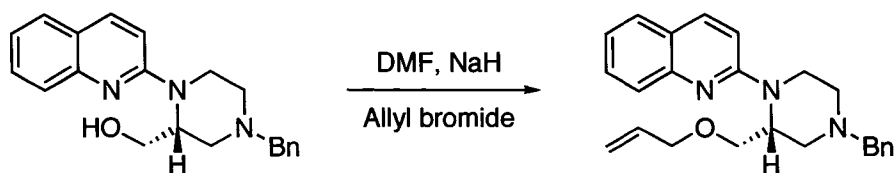


(R)-(+)-2-[4-Benzyl-2-(hydroxymethyl)piperazin-1-yl]quinoline (R)-122. To a solution of starting material **(R)-121** (0.302 g, 0.723 mmol) in reagent grade methanol (15 mL) was added conc. HCl (1.3 mL, 1.6 mmol). The solution was stirred overnight (21 h) and was then diluted carefully with saturated NaHCO₃ (20 mL). The methanol was evaporated and the aqueous mixture extracted with CH₂Cl₂ (3 x 8 mL). The combined extracts were dried (K₂CO₃) and concentrated to give **(R)-122** as an amber solid (0.250 g, quantitative). This material was pure enough for subsequent transformations. TLC *R_f* 0.12 (EtOAc:Hexanes, 2:3). ¹H NMR (400 MHz, CDCl₃): δ 2.26 (td, *J* = 3.7, 11.4 Hz, 1H), 2.41 (dd, *J* = 4.0, 11.4 Hz, 1H), 2.97 (m, 1H), 3.09 (m, 1H), 3.45 – 3.65 (m, 3H), 3.99 (dd, *J* = 3.3, 11 Hz, 1H), 4.10 (bd, 1H), 4.17 (dd, *J* = 5.9, 11 Hz, 1H, overlapped with previous bd at 4.10), 4.80 (bm, 1H), 4.97 (bs, 0.2H, -OH), 6.96 (d, *J* = 9.2 Hz, 1H), 7.24 (m, 1H, overlapped with CDCl₃), 7.31 (m, 1H), 7.33 – 7.40 (m, 4H), 7.54 (m, 1H), 7.60 (bd, *J* = 8.1 Hz, 1H), 7.69 (bd, *J* = 8.4 Hz, 1H), 7.87 (d, *J* = 9.2 Hz, 1H); ¹³C NMR (100 MHz, CDCl₃): δ 42.4, 52.5, 53.0, 55.4, 62.9, 65.2, 109.9, 122.4, 122.9, 126.1, 127.1, 127.3, 128.4, 128.8, 129.5, 137.4, 137.5, 147.2, 157.4; (*R*) - [α]_D²⁵ +226.1 (c 0.025, CHCl₃).



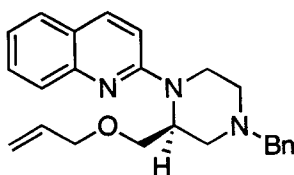
(S)-(-)-2-[4-Benzyl-2-(hydroxymethyl)piperazin-1-yl]quinoline (S)-122. The title compound was similarly prepared and provided identical spectroscopic data.

(S) - $[\alpha]_D^{25} -226.3$ (c 0.016, CHCl_3).

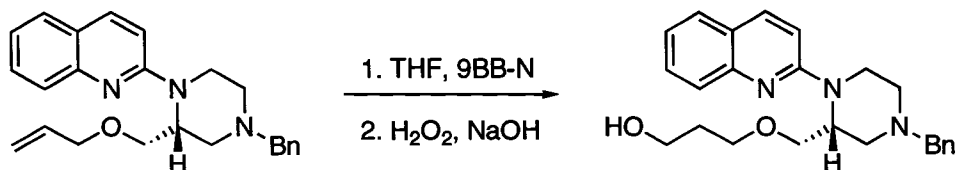


(R)-(+)-2-[4-Benzyl-2-(allyloxymethyl)piperazin-1-yl]quinoline (R)-123. To a 0 °C solution of the alcohol (**R**)-122 (0.241 g, 0.723 mmol) in dry DMF (11 mL) under argon was added sodium hydride (95%, 0.052 g, 2.17 mmol). The turbid solution was stirred 15 min then allyl bromide (0.092 g, 0.759 mmol) was added (dropwise). The reaction was stirred 10 min at 0 °C then warmed to ambient temperature and stirred for 18 h. The excess hydride was destroyed by the careful addition of 8 mL of saturated NaHCO_3 solution and the mixture diluted further with 8 mL of water. This aqueous mixture was extracted with ether (4 x 15 mL) and the combined extracts were washed with brine (2 x 10 mL), dried (K_2CO_3) and concentrated to give the crude product that was purified by column chromatography (silica gel, EtOAc:Hexanes, 1:9 – 1:3) to provide (**R**)-123 an an amber oil (0.214 g, 79%). TLC R_f 0.46 (EtOAc:Hexanes, 2:3). ^1H NMR (400 MHz, CDCl_3): δ 2.20 – 2.29 (m, 2H), 2.98 (m, 1H, doublet shape), 3.17 – 3.27 (m,

2 H), 3.51 – 3.66 (m, 3H), 3.94 – 4.05 (m, 3H), 4.48 (bd, $J = 12.8$ Hz, 1H), 4.61 (bs, 1H), 5.13 (dq, $J = 1.5, 10.4$ Hz, 1H), 5.20 (dq, $J = 1.5, 17.2$ Hz, 1H), 5.83 (m, 1H), 7.01 (d, $J = 9.2$ Hz, 1H), 7.23 (m, 1H), 7.30 (m, 1H), 7.34 – 7.42 (m, 4H), 7.55 (m, 1H), 7.61 (dd, $J = 1.1, 8.1$ Hz, 1H), 7.73 (d, $J = 8.4$ Hz, 1H), 7.87 (d, $J = 9.2$ Hz, 1H); ^{13}C NMR (100 MHz, CDCl_3): δ 40.8, 51.8, 53.0, 53.1, 62.8, 67.2, 72.0, 109.4, 116.7, 122.1, 122.9, 126.5, 127.0, 127.1, 128.2, 128.8, 129.3, 134.7, 137.3, 138.3, 147.9, 156.8; (*R*) - $[\alpha]_D^{25} +51.3$ (c 0.017, CHCl_3).



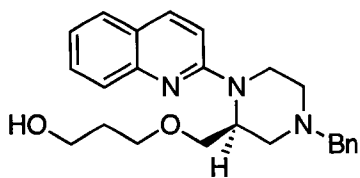
(S)-(-)-2-[4-Benzyl-2-(allyloxymethyl)piperazin-1-yl]quinoline (S)-123. The title compound was similarly prepared and provided identical spectroscopic data. (*S*) - $[\alpha]_D^{25} -51.4$ (c 0.015, CHCl_3).



(R)-(+)-2-[4-Benzyl-2-[(3-hydroxypropoxy)methyl]piperazin-1-yl]quinoline

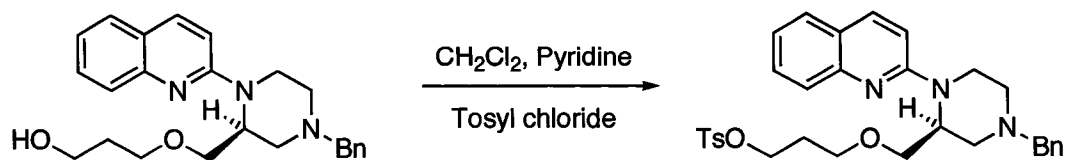
(R)-124. To a 0 °C solution of the allyl ether (*R*)-123 (0.214 g, 0.57 mmol) in dry THF (6 mL) under argon was added 9-BBN (0.5 M in THF, 1.55 mmol). Following the addition, the reaction was heated to 60 °C and maintained for 1 h. The contents were cooled to 0 °C and 3.5 mL of 1 M NaOH was added (dropwise) followed by an equal volume of 30% H_2O_2 . After stirring ~10 min the THF was evaporated and the residue partitioned between CH_2Cl_2 and saturated

NaHCO₃ (25 mL each). The organic phase was separated and the aqueous phase extracted with CH₂Cl₂ (3 x 15 mL). The combined organic extracts were dried (K₂CO₃) and concentrated to give the crude material that was purified by column chromatography (silica gel, EtOAc:Hexanes, 1:9 – 3:2) to afford (*R*)-**124** as an amber oil (0.163g, 73%). TLC *R_f* 0.1 (EtOAc:Hexanes, 2:3). ¹H NMR (400 MHz, CDCl₃): δ 1.67 (p, *J* = 5.9 Hz, 2H), 2.17 – 2.27 (m, 2H), 2.40 (bs, 1H), 2.97 (bd, *J* = 11.0 Hz, 1H), 3.07 (bd, *J* = 11.4 Hz, 1H), 3.25 (td, *J* = 2.9, 12.5 Hz, 1H), 3.44 – 3.69 (m, 7H), 3.87 (m, 1H, triplet shape), 4.39 (bd, *J* = 12.8 Hz, 1H), 4.64 (bs, 1H), 6.97 (d, *J* = 9.2 Hz, 1H), 7.21 (m, 1H), 7.26 – 7.32 (m, 1H), 7.32 – 7.40 (m, 4H), 7.53 (m, 1H), 7.59 (m, 1H), 7.69 (d, *J* = 8.4 Hz, 1H), 7.87 (d, *J* = 9.2 Hz, 1H); ¹³C NMR (100 MHz, CDCl₃): δ 32.0, 40.8, 51.5, 53.1, 53.2, 61.3, 62.8, 68.5, 70.1, 109.4, 122.1, 122.9, 126.4, 127.06, 127.12, 128.2, 128.9, 129.4, 137.3, 138.2, 147.8, 156.8; (*R*) - [α]_D²⁵ +46.3 (c 0.016, CHCl₃).



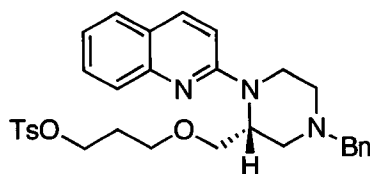
(S)-(-)-2-[4-Benzyl-2-[(3-hydroxypropoxy)methyl]piperazin-1-yl]quinoline

(S)-124. The title compound was similarly prepared and provided identical spectroscopic data. (*S*) - [α]_D²⁵ -47.2 (c 0.013, CHCl₃).



(S)-(-)-2-[4-Benzyl-2-[(3-(4-methylbenzenesulfonate)propoxy)methyl]

piperazin-1-yl]quinoline (S)-125. To a 0 °C solution of alcohol (S)-124 (0.196 g, 0.50 mmol) in dry CH₂Cl₂ (4 mL) and pyridine (400 μL) was added *p*-toluenesulfonyl chloride (0.114 g, 0.60 mmol) in one portion. The flask was sealed under argon and maintained in the ice bath until the ice bath warmed to ambient temperature. Following 26 h, the reaction contents were partitioned between saturated NaHCO₃ (20 mL) and CH₂Cl₂ (10 mL). The organic phase was separated and the aqueous phase was extracted with CH₂Cl₂ (3 x 10 mL). The combined organic extracts were dried (K₂CO₃) and concentrated to give the crude material that was purified by column chromatography (silica gel, EtOAc:Hexanes, 1:9 – 1:3) to afford (S)-125 as a pale colored oil (0.127 g, 47%). TLC *R*_f 0.27 (EtOAc:Hexanes, 2:3). ¹H NMR (400 MHz, CDCl₃): δ 1.73 (p, *J* = 6.2 Hz, 2H), 2.16 – 2.25 (m, 2H), 2.4 (s, 3H), 2.94 (bd, *J* = 11.0 Hz, 1H), 3.02 (bd, *J* = 11.4 Hz, 1H), 3.18 (m, 1H), 3.38 – 3.62 (m, 5H), 3.78 (t, *J* = 8.8 Hz, 1H), 3.97 (t, *J* = 6.2 Hz, 2H), 4.42 (bd, 1H), 4.52 (bs, 1H), 6.95 (d, *J* = 9.5 Hz, 1H), 7.19 – 7.24 (m, 1H), 7.25 – 7.30 (m, 3H, tosylate doublet dominates shape), 7.30 – 7.38 (m, 4H), 7.52 (m, 1H), 7.59 (m, 1H), 7.67 (bd, *J* = 8.1 Hz, 1H), 7.73 (d, *J* = 8.1 Hz, 2H), 7.85 (d, *J* = 9.2 Hz, 1H); ¹³C NMR (100 MHz, CDCl₃): δ 21.5, 29.2, 40.6, 51.5, 53.0, 53.1, 62.7, 66.4, 67.6, 67.9, 109.4, 122.1, 122.8, 126.4, 127.0, 127.1, 127.8, 128.2, 128.8, 129.3, 129.7, 133.0, 137.2, 138.3, 144.5, 147.8, 156.8; (S)-[α]_D²⁵ –25.0 (c 0.0075, CHCl₃).



(R)-(+)-2-[4-Benzyl-2-[(3-(4-methylbenzenesulfonate)propoxy)methyl]

piperazin-1-yl]quinoline (R)-125. The title compound was similarly prepared

and provided identical spectroscopic data. (*R*) - $[\alpha]_D^{25}$ This compounds optical rotation was never evaluated.



(S)-(-)-2-[4-Benzyl-2-[(3-fluoropropoxy)methyl]piperazin-1-yl]quinoline (S)-

126. To a solution of tosylate (**S**)-125 (0.128 g, 0.234 mmol) in dry THF (2.5 mL)

was added a solution of TBAF in THF (1 M, 0.35 mL, 0.352 mmol). The flask

was sealed under argon and heated at 55 – 60 °C for 3.5 h. After cooling, the

solvent was evaporated and the residue purified by column chromatography

(silica gel, EtOAc:Hexanes, 1:9 – 1:3) to afford (**S**)-126 as a pale colored oil

(0.071 g, 78%). TLC R_f 0.45 (EtOAc:Hexanes, 2:3). ^1H NMR (400 MHz, CDCl_3):

δ 1.80 (dp, $J_{\text{F-H}} = 25.6$ Hz, $\text{FCH}_2\text{CH}_2^-$, $J_{\text{H-H}} = 6.2$ Hz, 2H), 2.20 – 2.28 (m, 2H),

2.98 (m, 1H), 3.11 (m, 1H), 3.23 (td, $J = 3.7, 12.8$ Hz, 1H), 3.46 – 3.66 (m, 5H),

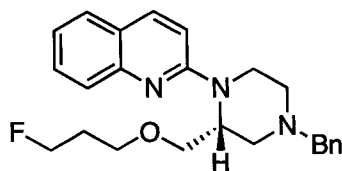
3.89 (t, $J = 8.8$ Hz, 1H), 4.35 (dt, $J_{\text{F-H}} = 46.9$, FCH_2^- , $J_{\text{H-H}} = 5.9$ Hz, 2H), 4.45 (bd,

1H, overlapped with signal at 4.35), 4.59 (bm, 1H), 6.99 (d, $J = 9.2$ Hz, 1H), 7.22

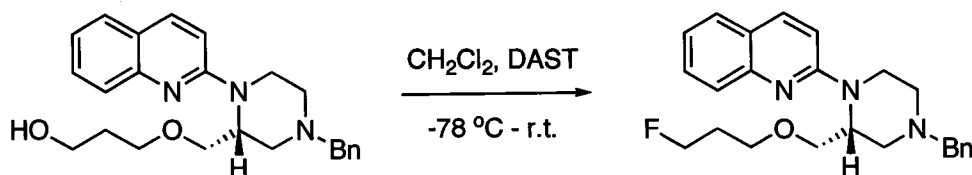
(m, 1H), 7.26 – 7.32 (m, 1H), 7.32 – 7.41 (m, 4H), 7.53 (m, 1H), 7.60 (m, 1H),

7.70 (d, $J = 8.4$ Hz, 1H), 7.87 (d, $J = 9.2$ Hz, 1H); ^{13}C NMR (100 MHz, CDCl_3): δ

30.7 (d, $J_{C-F} = 19.8$ Hz, FCH_2CH_2-), 40.7, 51.6, 52.9, 53.3, 62.8, 66.7 (d, $J_{C-F} = 4.6$ Hz, $FCH_2CH_2CH_2-$), 67.8, 81.1 (d, $J_{C-F} = 163.3$ Hz, FCH_2-), 109.4, 122.1, 122.9, 126.5, 127.0, 127.1, 128.2, 128.8, 129.4, 137.2, 138.3, 147.8, 156.8; (S) - $[\alpha]_D^{25} -39.9$ (c 0.0048, $CHCl_3$).

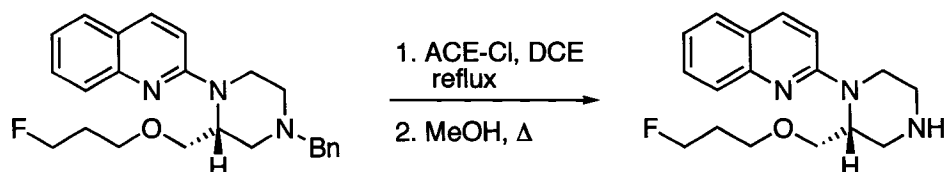


(R)-(+)-2-[4-Benzyl-2-[(3-fluoropropoxy)methyl]piperazin-1-yl]quinoline (R)-126. The title compound was similarly prepared and provided identical spectroscopic data. (R) - $[\alpha]_D^{25} +40.2$ (c 0.0098, $CHCl_3$).



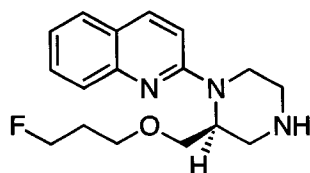
(R)-(+)-2-[4-Benzyl-2-[(3-fluoropropoxy)methyl]piperazin-1-yl]quinoline (R)-126. ALTERNATE ROUTE To a -78 °C solution of alcohol (R)-124 (0.111 g, 0.283 mmol) in dry CH_2Cl_2 (9 mL) under argon was added DAST (0.061 g, 0.38 mmol). The insulated bath was allowed to warm to ambient temperature over 24 h then the reaction was diluted with CH_2Cl_2 (10 mL) and saturated $NaHCO_3$ solution (20 mL). The organic phase was separated and the aqueous phase extracted with CH_2Cl_2 (2 x 10 mL). The combined organic extracts were dried (K_2CO_3), and concentrated to give the crude product that was purified by column chromatography (silica gel, EtOAc:Hexanes, 1:3) to provide (R)-126 as a pale oil

(0.069 g, 62%). TLC R_f 0.45 (EtOAc:Hexanes, 2:3). Spectroscopic data for (*R*)-**126** with DAST was identical to that reported for (*S*)-**126** generated via TBAF fluorination.



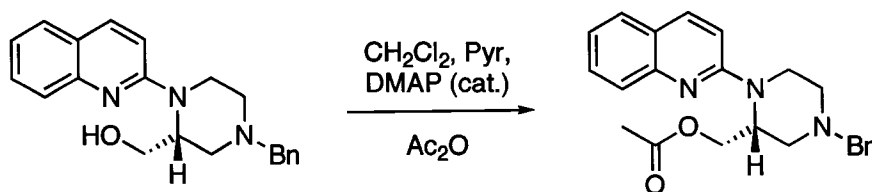
(*R*)-(+)-2-[2-[(3-fluoropropoxy)methyl]piperazin-1-yl]quinoline (*R*)-127. To a 0 °C solution of fluoride (*R*)-**126** (0.098 g, 0.249 mmol) in dry dichloroethane (5 mL) under argon was added 1-chloroethyl chloroformate (0.142 g, 0.994 mmol). After stirring 5 min, the reaction was heated at reflux for 7 h, cooled, then stirred at ambient temperature for 10 h. The volatile components were evaporated and the residue was dissolved in methanol (10 mL) and heated at 60 °C for 1.5 h. The solvent was evaporated to dryness and the residue partitioned between CH_2Cl_2 and saturated NaHCO_3 (10 mL each). The organic phase was separated and the aqueous phase was extracted with three additional portions of CH_2Cl_2 . The combined organic extracts were dried (K_2CO_3) and concentrated to give the crude product that was immediately purified by column chromatography (silica gel, EtOAc:Hexanes, 4:1, then MeOH: CH_2Cl_2 , 1:39 – 1:9) to provide (*R*)-**127** as a pale colored oil (0.065 g, 87%). TLC R_f 0.13 (MeOH: CH_2Cl_2 , 1:9). ^1H NMR (400 MHz, CDCl_3): δ 1.89 (dp, $J_{\text{F-H}} = 25.6$ Hz, FCH_2CH_2 -, $J_{\text{H-H}} = 6.2$ Hz, 2H), 2.20 (bs, 1H, NH), 2.88 (m, 1H), 3.00 (m, 1H), 3.12 – 3.21 (m, 2H), 3.32 (bd, $J = 12.1$ Hz, 1H), 3.55 – 3.61 (m, 3H), 3.90 (m, 1H), 4.36 (bd, 1H), 4.47 (dt, $J_{\text{F-H}} = 47.2$, FCH_2 , $J_{\text{H-H}} = 5.9$ Hz, 2H), 4.59 (bm, 1H), 6.97 (d, $J = 9.5$ Hz, 1H), 7.21 (m, 1H), 7.52 (m,

1H), 7.59 (d, $J = 8.1$ Hz, 1H), 7.68 (d, $J = 8.4$ Hz, 1H), 7.88 (d, $J = 9.2$ Hz, 1H); ^{13}C NMR (100 MHz, CDCl_3): δ 30.7 (d, $J_{\text{C-F}} = 19.8$ Hz, $\text{FCH}_2\text{CH}_2^-$), 41.3, 46.0, 46.2, 50.7, 66.9 (d, $J_{\text{C-F}} = 6.1$ Hz, $\text{FCH}_2\text{CH}_2\text{CH}_2^-$), 68.0, 81.2 (d, $J_{\text{C-F}} = 163.2$ Hz, FCH_2^-), 109.2, 122.2, 122.9, 126.5, 127.1, 129.4, 137.3, 147.8, 156.9; (*R*) - $[\alpha]_D^{25} +56.2$ (c 0.0065, CHCl_3).



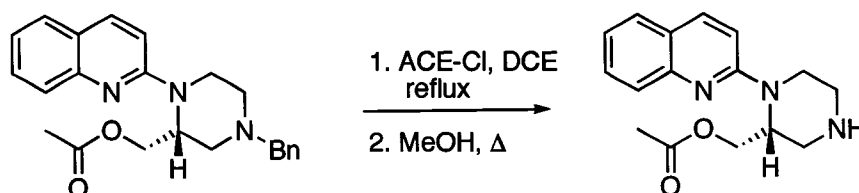
(S)-(-)-2-[2-[(3-fluoropropoxy)methyl]piperazin-1-yl]quinoline (S)-127. The title compound was similarly prepared and provided identical spectroscopic data.

(*S*) - $[\alpha]_D^{25} -56.7$ (c 0.0031, CHCl_3).



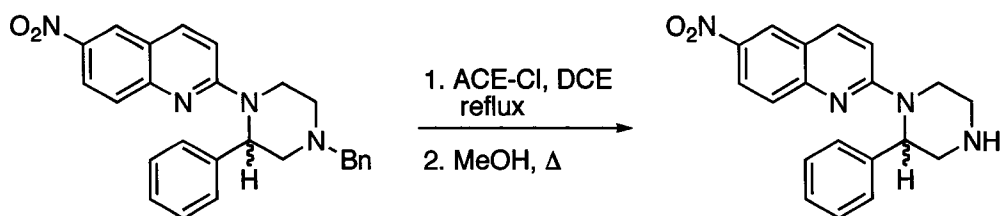
(R)-2-[2-(acetoxymethyl)-4-benzylpiperazin-1-yl]quinoline (R)-128. To a 0 °C solution of alcohol (*R*)-122 (0.212 g, 0.64 mmol) in dry CH_2Cl_2 (14 mL) under argon was added pyridine (0.1 mL, 1.27 mmol), acetic anhydride (0.072 mL, 0.76 mmol) and 4-dimethylaminopyridine (DMAP, 0.004 g, 0.03 mmol). After stirring at 0 °C for 4 h, the reaction was shown complete by TLC, with the formation of a new, non-polar spot. The reaction contents were diluted with 10 mL of CH_2Cl_2 and washed with saturated NaHCO_3 (2 x 20 mL). The organic phase was dried (K_2CO_3) and concentrated to provide the crude material that was purified by

column chromatography (silica gel, EtOAc:Hexanes, 1:3) to provide (*R*)-**128** as an oil that slowly formed a pale solid upon standing (0.226 g, 95%). TLC R_f 0.42 (EtOAc:Hexanes, 2:3). ^1H NMR (400 MHz, CDCl_3): δ 1.76 (s, 3H), 2.21 – 2.30 (m, 2H), 2.96 – 3.03 (m, 2H), 3.35 (td, $J = 3.3, 12.5$ Hz, 1H), 3.45 (d, $J = 13.2$ Hz, 1H), 3.65 (d, $J = 13.2$ Hz, 1H), 4.37 – 4.51 (m, 3H), 4.85 (bm, 1H), 6.99 (d, $J = 9.2$ Hz, 1H), 7.23 (m, 1H), 7.29 (m, 1H), 7.32 – 7.41 (m, 3H), 7.54 (m, 1H), 7.60 (bd, $J = 8.1$ Hz, 1H), 7.70 (bd, $J = 8.4$ Hz, 1H), 7.89 (bd, $J = 9.2$ Hz, 1H); ^{13}C NMR (100 MHz, CDCl_3): δ 20.7, 40.4, 50.3, 52.8, 53.2, 61.4, 62.7, 109.2, 122.2, 122.9, 126.6, 127.1, 128.2, 128.8, 129.4, 137.3, 138.2, 147.7, 156.8, 171.0.



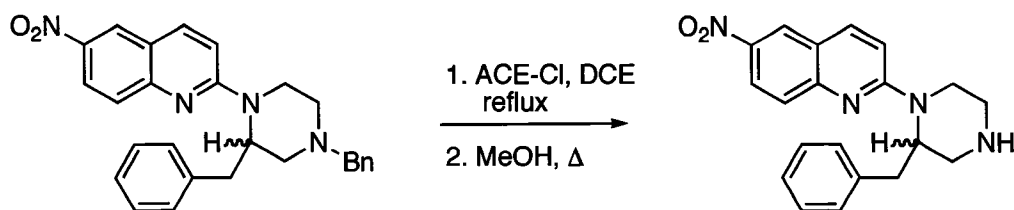
(*R*)-2-[2-(acetoxymethyl)piperazine-1-yl]quinoline (*R*)-129**.** To a 0 °C solution of acetate (*R*)-**128** (0.150 g, 0.4 mmol) in dry dichloroethane (6 mL) under argon was added 1-chloroethyl chloroformate (0.114 g, 0.8 mmol). After stirring 10 min, the flask was heated at reflux for 2 h then cooled and the solvent evaporated. The residue was dissolved in methanol (6 mL) and heated at 60 - 65 °C for 1.25 h then the methanol was evaporated. The residue was dissolved in 20 mL 1 M HCl and washed with CH_2Cl_2 (3 x 10 mL). The aqueous phase was carefully made basic with saturated NaHCO_3 and extracted with CH_2Cl_2 (4 x 10 mL). The combined extracts were dried (Na_2SO_4) and concentrated to give (*R*)-**129** as a pale colored oil that formed a solid upon standing (0.108 g, 95%). TLC R_f 0.22 (MeOH: CH_2Cl_2 , 1:9). ^1H NMR (400 MHz, CDCl_3): δ 1.80 (bs, 1H), 1.86 (s, 3H),

2.84 (td, $J = 2.9, 11.7$ Hz, 1H), 2.99 (dd, $J = 3.3, 12.5$ Hz, 1H), 3.09 – 3.23 (m, 3H), 4.30 – 4.40 (m, 2H), 4.46 (dd, $J = 8.1, 11.0$ Hz, 1H), 4.77 (bm, 1H), 6.96 (d, $J = 9.2$ Hz, 1H), 7.20 (m, 1H), 7.51 (m, 1H), 7.58 (bd, $J = 7.7$ Hz, 1H), 7.68 (bd, $J = 8.4$ Hz, 1H), 7.87 (d, $J = 9.2$ Hz, 1H); ^{13}C NMR (100 MHz, CDCl_3): δ 20.7, 40.8, 45.9, 46.0, 49.7, 60.5, 109.0, 122.2, 122.8, 126.5, 127.0, 129.4, 137.3, 147.6, 156.9, 170.9.



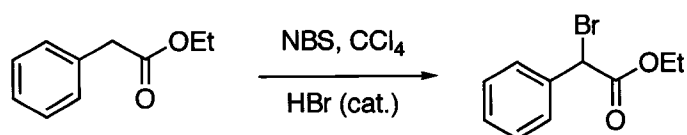
2-[2-Phenylpiperazin-1-yl]-6-nitroquinoline 135. To a solution of quipazine **174** (0.097 g, 0.23 mmol) in dry dichloroethane (4 mL) under argon was added 1-chloroethyl chloroformate (0.066 g, 0.46 mmol). After stirring for 5 min the reaction was heated at reflux for 2 h, then stirred at ambient temp for 16 h. The solvent was evaporated and the residue dissolved in methanol (8 mL) and heated at 65 °C for 2 h. The methanol was evaporated and the residue was dissolved in 1 M HCl (20 mL) and washed with CH_2Cl_2 (4 x 15 mL). The aqueous phase was made basic with 4 M NaOH, diluted with saturated NaHCO_3 (20 mL) and extracted with CH_2Cl_2 (4 x 20 mL). The combined organic extracts were dried (K_2CO_3) and concentrated to give **135** as a yellow foam (0.070 g, 91%). TLC R_f 0.31 (MeOH: CH_2Cl_2 , 1:9). ^1H NMR (400 MHz, CDCl_3): δ 1.89 (bs, NH, 1H), 3.02 (td, $J = 3.7, 12.1$ Hz, 1H), 3.18 (bm, doublet shape, $J = 12.1$ Hz, 1H), 3.32 – 3.42 (m, 2H), 3.71 (bd, $J = 13.2$ Hz, 1H), 4.68 (bd, $J = 13.2$ Hz, 1H), 5.69

(bs, 1H), 6.98 (d, $J = 9.5$ Hz, 1H), 7.24 – 7.29 (m, 1H, overlapped with CDCl_3), 7.29 – 7.38 (m, 4H), 7.65 (d, $J = 9.5$ Hz, 1H), 7.93 (d, $J = 9.2$ Hz, 1H), 8.29 (dd, $J = 2.6, 9.5$ Hz, 1H), 8.52 (d, $J = 2.6$ Hz, 1H); ^{13}C NMR (400 MHz, CDCl_3): δ 41.3, 45.7, 49.5, 54.8, 110.7, 121.1, 123.6, 124.2, 127.0, 127.1, 127.2, 128.9, 138.8, 138.9, 141.8, 151.5, 158.8; HRMS (ESI-TOF) m/z ($M + H$)⁺ calcd. for $\text{C}_{19}\text{H}_{19}\text{N}_4\text{O}_2$ 355.1508 found 355.1507.

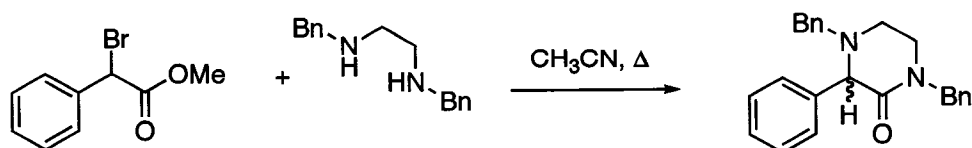


2-[2-Benzylpiperazin-1-yl]-6-nitroquinoline 136. To a solution of quipazine **175** (0.083 g, 0.19 mmol) in dry dichloroethane (4 mL) under argon was added 1-chloroethyl chloroformate (0.054 g, 0.38 mmol). The reaction was heated at reflux for 2 h then stirred at ambient temperature for 16 h. The solvent was evaporated and the residue dissolved in methanol (8 mL) and heated at 65 °C for 2 h. The mixture was concentrated and the residue was dissolved in 20 mL 1 M HCl and washed with CH_2Cl_2 (4 x 8 mL). The aqueous phase was made basic with 4 M NaOH, diluted with saturated NaHCO_3 (10 mL) and extracted with CH_2Cl_2 (3 x 8 mL). The combined extracts were dried (K_2CO_3) and concentrated to give **136** as a yellow-orange foam (0.056 g, 85%). R_f 0.24 (MeOH: CH_2Cl_2 , 1:9). ^1H NMR (400 MHz, CDCl_3): δ 2.05 (bs, NH, 1H), 2.83 – 2.98 (m, 3H), 3.05 (m, broad doublet shape, 1H), 3.21 – 3.29 (m, 2H), 3.38 (td, $J = 2.9, 12.8$ Hz, 1H), 4.45 (bs, 1H), 4.78 (bs, 1H), 6.96 (d, $J = 9.2$ Hz, 1H), 7.19 (m, 1H), 7.27 – 7.35 (m, 4H), 7.69 (d, $J = 9.5$ Hz, 1H), 7.90 (d, $J = 9.2$ Hz, 1H), 8.31 (d, $J = 2.6,$

9.5 Hz, 1H), 8.52 (d, $J = 2.6$ Hz, 1H); ^{13}C NMR (100 MHz, CDCl_3): δ 34.4, 40.9, 46.2, 46.8, 54.0, 110.8, 121.0, 123.6, 124.2, 126.4, 127.1, 128.5, 129.4, 138.4, 138.9, 141.8, 151.5, 158.4; HRMS (ESI-TOF) m/z ($M + H$) $^+$ calcd. for $\text{C}_{20}\text{H}_{21}\text{N}_4\text{O}_2$ 349.1665 found 349.1678.

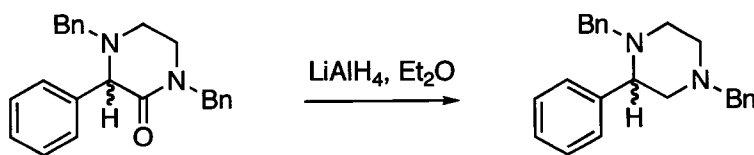


Ethyl Bromophenylacetate 147. The synthesis of **147** is adapted from the method of Epstein.¹³⁸ To a solution of ethyl phenylacetate (1.03 g, 6.28 mmol) in CCl_4 (16 mL) was added NBS (1.15 g, 6.47 mmol) and two drops of HBr (48%). The mixture was heated to reflux and maintained until the solids floated on top of the solvent. This mixture was cooled and filtered through a pad of Fluorosil (Magnesium silicate) the pad was rinsed with CH_2Cl_2 and the filtrate concentrated to give the crude product that was purified by column chromatography (silica gel, EtOAc:Hexanes, 1:3) to afford **147** as a clear, loose oil (1.50 g, 98%). TLC R_f 0.60 (EtOAc:Hexanes, 2:3). ^1H NMR (400 MHz, CDCl_3): δ 1.28 (t, 3H), 4.24 (m, AB pattern O- CH_2 - CH_3 , 2H), 5.35 (s, 1H), 7.34 – 7.40 (m, 3H), 7.53 – 7.58 (m, 2H); ^{13}C NMR (100 MHz, CDCl_3): δ 13.9, 46.8, 62.5, 128.6, 128.8, 129.2, 135.8, 168.2.



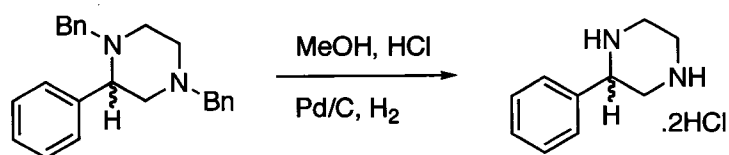
1,4-Dibenzyl-3-phenylpiperazine-2-one 151. To a stirred solution of N,N-dibenzyl ethylenediamine (10.2 g, 42.5 mmol) in acetonitrile (55 mL) under argon

was added a solution of bromo ester **147** (5.17 g, 21.3 mmol). This solution was heated at reflux for 6 h then stirred for 38 h at ambient temperature. The solvent was evaporated and the residue partitioned between 1 M NaOH (60 mL) and ether (50 mL). The organic phase was separated and the aqueous phase extracted with ether (2 x 40 mL). The combined organic phases were washed with brine (2 x 30 mL), dried (Na₂SO₄) and the solvent evaporated to give 12.5 g of crude material that was purified by column chromatography (silica gel, EtOAc:Hexanes, 1:9 – 1:3) to afford **151** as a very thick oil (5.85 g, 77%). TLC *R_f* 0.29 (EtOAc:Hexanes, 2:3). ¹H NMR (400 MHz, CDCl₃): δ 2.47 (td, *J* = 3.7, 12.1 Hz, 1H), 2.97 (dt, *J* = 3.3, 12.1 Hz, 1H), 3.09 – 3.18 (m, 2H), 3.47 (td, *J* = 3.7, 11.0, 1H), 3.75 (d, *J* = 13.2 Hz, 1H), 4.14 (s, 1H), 4.59 (m, AB pattern, *J* = 14.3 Hz, 2H), 7.22 – 7.42 (m, 15H); ¹³C NMR (400 MHz, CDCl₃): δ 45.8, 46.6, 50.2, 58.8, 71.2, 127.2, 127.5, 127.8, 128.2 (two overlapped peaks), 128.4, 128.6, 128.7, 129.0, 136.8, 137.7, 139.4, 168.3.

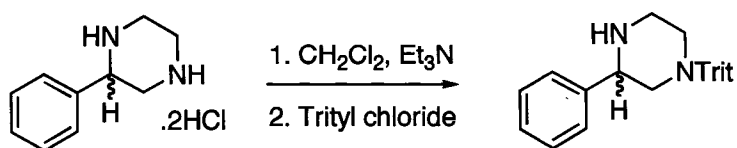


1,4-Dibenzyl-2-phenylpiperazine 152. To a solution of amide **151** (1.19 g, 3.34 mmol) in dry THF (20 mL) was added LiAlH₄ (0.597 g, 15.7 mmol) in one portion. The mixture was heated at reflux for 5 h. After cooling, the excess LiAlH₄ was quenched by the careful, sequential addition of 0.25 mL water, 0.5 mL 4 N NaOH and 0.25 mL water. The mixture was stirred 15 min and the solids that formed were filtered (Celite) and the filtrate concentrated to give the crude material that

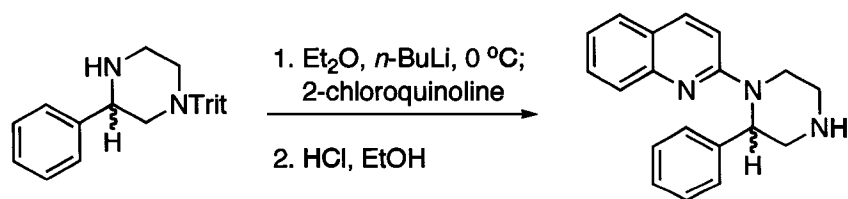
was purified by column chromatography (silica gel, EtOAc:Hexanes, 2:3) to provide **152** as a white solid 0.922 g, 81%). TLC R_f 0.52 (EtOAc:Hexanes, 2:3). ^1H NMR (400 MHz, CDCl_3): δ 2.14 – 2.21 (m, 1H), 2.22 – 2.32 (m, 2H), 2.78 (m, 1H), 2.83 – 2.91 (m, 3H), 3.43 (dd, $J = 2.6, 10.3$ Hz, 1H), 3.50 (m, singlet shape, 2H), 3.79 (d, $J = 13.2$ Hz, 1H), 7.17 – 7.52 (m, 15H); ^{13}C NMR (100 MHz, CDCl_3): δ 51.7, 53.2, 58.9, 62.0, 62.9, 67.3, 126.7, 127.0, 127.4, 128.0, 128.2, 128.4, 128.7, 129.2, 137.8, 139.0, 142.2.



2-Phenylpiperazine dihydrochloride 153. To a suspension of dibenzyl piperazine **152** (0.500 g, 1.46 mmol) in methanol (25 mL) was added HCl (12 M, 0.24 mL, 2.92 mmol) and 5% Pd/C (0.075 g). The flask was sealed with a septa and H_2 was bubbled through the solution via balloon. The reaction was monitored by TLC until **152** was consumed, refilling H_2 if necessary. The reaction mixture was filtered (Celite) and the filtrate concentrated to provide **153** as a white solid (0.345 g, quantitative). ^1H NMR (400 MHz, D_2O): δ 3.37 (m, 1H), 3.49 (m, 1H), 3.57 (m, 1H), 3.63 – 3.76 (m, 3H), 4.59 (m, 1H, overlapped with HOD), 7.31 – 7.40 (m, 5H); ^{13}C NMR (100 MHz, $\text{DMSO}-d_6$): δ 39.0, 41.0, 44.5, 55.4, 128.1, 129.0, 129.8, 133.1.



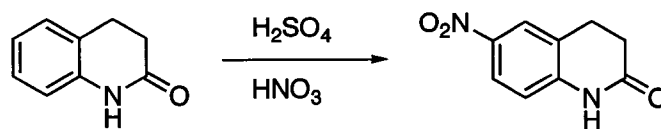
3-Phenyl-1-triphenylmethylpiperazine 154. To a stirring suspension of piperazine **153** (0.433 g, 1.84 mmol) in dry CH_2Cl_2 (20 mL) under argon was added anhydrous triethylamine (1.0 mL, 7.4 mmol). The resultant clear solution was cooled to 0 °C and a solution of trityl chloride (0.514 g, 1.84 mmol) in dry CH_2Cl_2 (5 mL) was added (dropwise). The reaction was stirred an additional 10 min at 0 °C then warmed to ambient temperature and stirred for 1.5 h. The solution was washed with saturated NaHCO_3 (30 mL) and the aqueous solution extracted with CH_2Cl_2 (2 x 15 mL). The combined organic extracts were dried (K_2CO_3) and concentrated to provide **154** as a white solid (0.760 g, quantitative). TLC R_f 0.50 (MeOH: CH_2Cl_2 , 1:9). ^1H NMR (400 MHz, CDCl_3): δ 1.23 (bs, 1H), 1.53 (m, t shape, 1H), 1.67 (m, t shape, 1H), 3.06 – 3.14 (m, 2H), 3.20 (m, 1H), 3.35 (m, 1H), 4.20 (m, 1H), 7.15 – 7.65 (m, 20H); ^{13}C NMR (100 MHz, CDCl_3): δ 46.7, 48.2, 56.0, 61.2, 77.1, 126.0, 126.9, 127.3, 127.5, 127.9, 128.3, 129.3 (broad), 142.6.



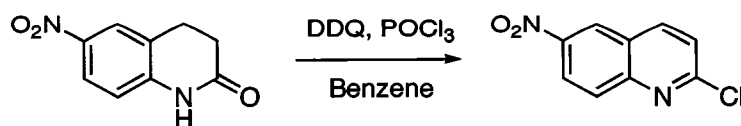
2-(2-Phenylpiperazin-1-yl)quinoline 155. To a 0 °C solution of N-trityl piperazine **154** (0.605 g, 1.49 mmol) in dry ether (20 mL) under argon was added (dropwise) a solution of *n*-butyllithium in hexanes (2.33 M, 0.64 mL, 1.49 mmol).

The orange turbid solution was stirred for 20 min. then a solution of 2-chloroquinoline (0.163 g, 1.0 mmol) in dry ether (4 mL) was added dropwise forming a green-blue solution. The reaction was maintained at 0 °C for an additional 50 min then stirred at ambient temperature for 19 h. The solution was diluted with ether (10 mL) and washed with saturated NaHCO₃ (2 x 20 mL) and brine (2 x 15 mL), dried (K₂CO₃) and concentrated to provide the crude material that was purified by column chromatography (silica gel, EtOAc:Hexanes, 1:3) to afford a yellow foam intermediate (0.555 g, 104%) TLC *R_f* 0.58 (EtOAc:Hexanes 2:3) that was not spectroscopically characterized and immediately deprotected. To a suspension of the crude intermediate (0.555g, 1.04 mmol) in 95% ethanol (20 mL) was added 6 M HCl (4 mL). The flask was swirled until the sides were cleared of solids and a homogenous solution resulted. Stirring continued at ambient temperature for 10 min then the reaction contents were diluted with ~20 mL of CH₂Cl₂. The mixture was made basic with 4 M NaOH and diluted with 20 mL saturated NaHCO₃. The organic phase was separated and the aqueous phase extracted with CH₂Cl₂ (3 x 15 mL). The combined organic extracts were dried (K₂CO₃) and concentrated to provide the crude product that was purified by column chromatography (silica gel, eluting first with EtOAc:CHCl₃, 4:1, to remove non-polar impurities, then MeOH:CH₂Cl₂, 1:9) to provide **155** as a pale colored oil (0.260 g, 86 %). TLC *R_f* 0.24 (MeOH:CH₂Cl₂, 1:9). ¹H NMR (400 MHz, CDCl₃): δ 1.79 (bs, NH, 1H), 3.02 (td, *J* = 3.7, 12.1 Hz, 1H), 3.15 (m, 1H), 3.32 – 3.41 (m, 2H), 3.65 (m, 1H), 4.63 (m, 1H), 5.56 (m, singlet shape, 1H), 6.87 (d, *J* = 9.2 Hz, 1H), 7.17 – 7.25 (m, 2H), 7.29 – 7.34 (m, 4H), 7.53 (m, 1H), 7.58 (m, doublet

shape, 1H), 7.69 (d, $J = 9.2$ Hz, 1H), 7.84 (d, $J = 9.2$ Hz, 1H); ^{13}C NMR (100 MHz, CDCl_3): δ 41.4, 45.9, 50.0, 54.7, 109.1, 122.1, 122.9, 126.5, 126.7, 127.1, 127.2, 128.7, 129.5, 137.6, 139.7, 147.9, 157.3.

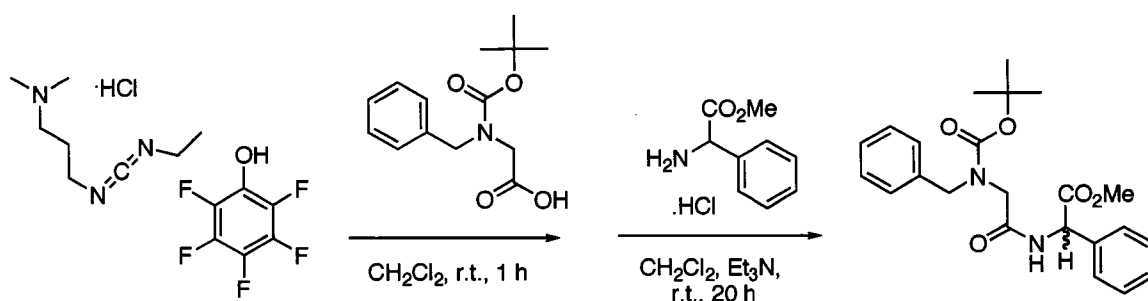


3,4-Dihydro-6-nitroquinolin-2(1H)-one 158. To a -5 °C solution of hydrocarbostyryl **157** (1.089 g, 7.4 mmol) in conc. H_2SO_4 (20 mL) was slowly added water (5 mL). After the solution cooled back to -5 °C, nitric acid (15.4 M, 0.49 mL, 7.5 mmol) was added, three drops at a time, in three minute increments to minimize heating. Ten minutes following the addition, the reaction contents were transferred to a beaker and 60 mL of cold water was slowly added with stirring, forming a white precipitate. The precipitate mixture was cooled on ice for 15 min, and the solids were collected by filtration and washed sparingly with a few portions of cold EtOAc. The solids were dried under high vacuum providing **158** as a pale colored solid (1.258 g, 88%). ^1H NMR (400 MHz, CDCl_3): δ 2.73 (m, 2H, triplet shape), 3.10 (m, 2H, triplet shape), 6.93 (m, 1H, doublet shape), 8.08 – 8.13 (m, 2H), 9.28 (bs, NH, 1H); ^{13}C NMR (100 MHz, CDCl_3): δ 25.0, 29.9, 115.5, 123.85, 123.93, 124.1, 142.8, 143.2, 171.7.



2-Chloro-6-nitroquinoline 159. To a suspension of **158** (1.06 g, 5.5 mmol) in benzene (20 mL) under argon was added DDQ (1.25 g, 5.5 mmol) followed by

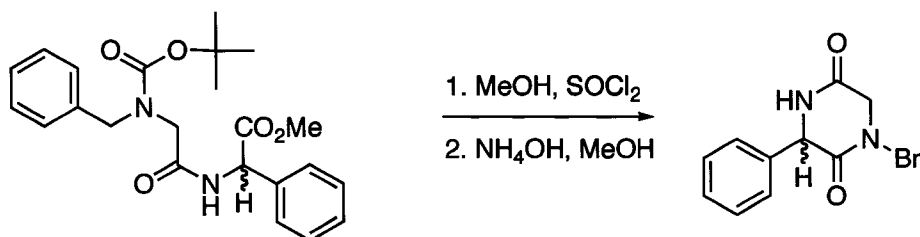
POCl₃ (2.55 mL, 4.20 g, 27.4 mmol) in a dropwise manner. The bright yellow-orange mixture was heated at reflux for 3 h. After cooling, 20 mL of cold water was added and the mixture was brought to neutral pH with 4 M NaOH. The solids were collected by filtration and washed with cold water and ~20 mL of cold ether. The filtrate was extracted with EtOAc (3 x 60 mL) and the combined extracts were dried (K₂CO₃) and concentrated to give a solid. Both batches of solids were combined and dissolved with heating in ~30 mL of THF. Silica gel (6 g) was added and the solvent evaporated to adsorb the crude product onto the silica gel. The material was loaded onto a chromatography column, and purified (silica gel, EtOAc:Hexane, 1:9) to provide **159** as a tan solid (1.13 g, 98 %). TLC *R_f* 0.45 (EtOAc:Hexanes, 2:3). ¹H NMR (400 MHz, DMSO-*d*₆): δ 7.84 (d, *J* = 8.8 Hz, 1H), 8.16 (d, *J* = 9.2 Hz, 1H), 8.52 (dd, *J* = 2.6, 9.2 Hz, 1H), 8.79 (d, *J* = 8.8 Hz, 1H), 9.14 (d, *J* = 2.6 Hz, 1H); ¹³C NMR (100 MHz, DMSO-*d*₆): δ 124.1, 124.4, 125.1, 125.9, 129.7, 141.9, 145.3, 149.2, 153.6.



N-tert-Butoxycarbonyl-N-benzylglycyl-DL-phenylglycine Methyl Ester 162.

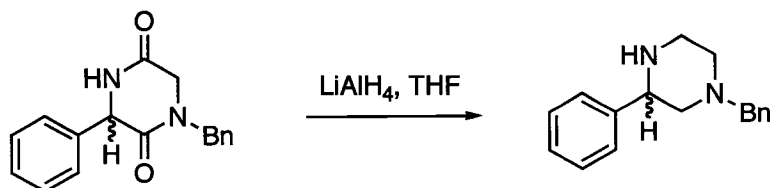
The general peptide coupling procedure was used as described above for **96**. Column chromatography of the crude product (silica gel, EtOAc:Hexanes, 1:3, to remove non-polar material, then EtOAc:Hexanes, 2:3, to elute the product)

provided **162** as a clear, viscous oil (1.87 g, 93%, solvent heavy). TLC R_f 0.33 (EtOAc:Hexanes, 2:3). ^1H NMR (400 MHz, CDCl_3): δ 1.47 (bs, 9H), 3.71 (s, 3H), 3.76 – 3.94 (bm, 2H), 4.42 (d, $J = 15$ Hz, 1H), 4.52 – 4.68 (bm, 1H), 5.50 (d, $J = 7.3$ Hz, 1H), 6.78 (bs, NH, 0.4H), 7.18 – 7.42 (m, 10H); ^{13}C NMR (100 MHz, CDCl_3): δ 28.2, 50.7, 51.7 (broad), 52.7, 56.1, 81.2, 127.1, 127.6, 128.2, 128.5, 128.7, 128.8, 136.2, 137.1, 155.4 (broad), 168.7 (broad), 170.8.

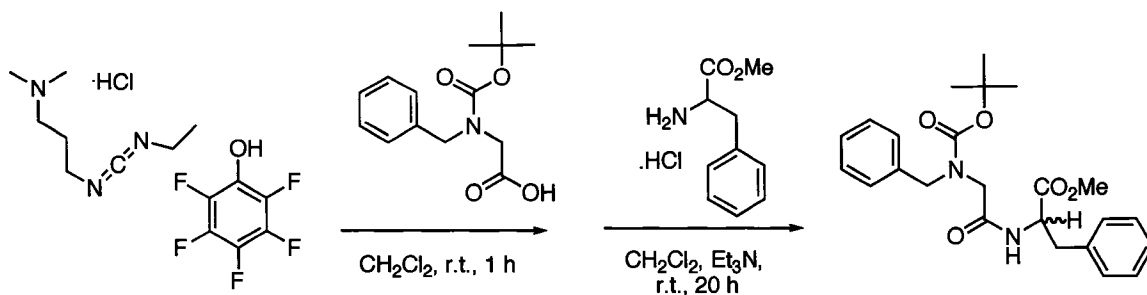


1-Benzyl-3-phenylpiperazine-2,5-dione 163. To a 0 °C solution of dipeptide **162** (1.873 g, 4.54 mmol) in methanol (25 mL) was slowly added excess thionyl chloride (1.5 mL) to avoid sputtering. Following the addition, the solution stirred at ambient temperature for 21 h. The solvent was evaporated and the residue was triturated with ~30 mL of ether to produce a solid that was collected by filtration. The solid was dissolved in methanol (~30 mL) and treated with ammonium hydroxide (29%, 10 mL) at ambient temperature. The solution was stirred for 20 h then concentrated (the flask sat sealed, in the hood for 2 months). The residue was partitioned between saturated NaHCO_3 (20 mL) and CHCl_3 :isopropyl alcohol, 4:1 (50 mL). The organic phase was separated and the aqueous phase extracted with CHCl_3 :isopropyl alcohol, 4:1 (4 x 50 mL). The combined organic phases were dried (K_2CO_3) and concentrated to afford **163** as a white solid (1.098 g, 86%) with adequate purity for subsequent transformations.

TLC R_f 0.54 (MeOH:CH₂Cl₂, 1:9). ¹H NMR (400 MHz, CDCl₃): δ 3.87 (m, quartet shape, AB pattern, J = 17.9 Hz, 2H), 4.55 (m, AB pattern, J = 14.3 Hz, 2H), 5.17 (bd, 1H), 6.89 (bs, NH, 1H), 7.14 – 7.18 (m, 2H), 7.26 – 7.41 (m, 8H); ¹³C NMR (100 MHz, CDCl₃): δ 48.7, 49.8, 59.5, 126.4, 128.1, 128.2, 128.8, 128.9, 129.1, 135.0, 137.0, 164.6, 166.0.



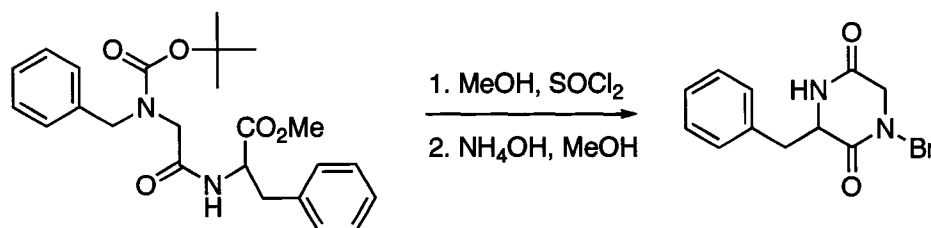
1-Benzyl-3-Phenylpiperazine 164. To a suspension of diamide **163** (1.16 g, 4.15 mmol) in dry THF (75 mL) was added LiAlH₄ (0.630 g, 16.6 mmol) in one portion, producing a gentle effervescence. The mixture was maintained on ice until the bubbling stopped, then the flask was heated at reflux for 5 h. The mixture was cooled and stirred an additional hour, then the excess LiAlH₄ was quenched by the careful, sequential addition of 0.6 mL water, 1.2 mL 4 M NaOH solution and 0.6 mL water. After stirring 10 min, the solids were filtered (Celite) and the filtrate concentrated. The crude material was purified by column chromatography (silica gel, MeOH:CHCl₃, 1:49) to provide **164** as a pale colored oily solid (0.780 g, 74 %). TLC R_f 0.24 (MeOH:CH₂Cl₂, 1:9). ¹H NMR (400 MHz, CDCl₃): δ 2.08 (m, triplet shape, 1H), 2.20 (dd, J = 4.4, 11 Hz, 1H, overlapped with bs, NH, 1H), 2.84 (m, doublet shaped, 1H), 2.91 (m, doublet shape, 1H), 3.02 – 3.12 (m, 2H), 3.55 (s, 2H), 3.89 (dd, J = 2.9, 10.3 Hz, 1H) 7.22 – 7.40 (m, 10H); ¹³C NMR (100 MHz, CDCl₃): δ 46.2, 53.1, 60.3, 61.1, 63.3, 127.0, 127.4, 128.2, 128.3, 129.2, 137.8, 142.4



N-tert-Butoxycarbonyl-N-benzylglycyl-DL-phenylalanine Methyl Ester 166.

The general peptide coupling procedure was used as described above for **96**.

Column chromatography of the crude product (silica gel, EtOAc:Hexanes, 1:3, to remove non-polar material, then EtOAc:Hexanes, 3:2, to elute the product) provided **166** as a clear, viscous oil (2.17 g, 102%, solvent heavy). TLC R_f 0.33 (EtOAc:Hexanes, 2:3). ^1H NMR (400 MHz, CDCl_3): δ 1.45 (s, 9H), 2.99 – 3.16 (bm, 2H), 3.72 (s, 3H), 3.79 (bd, $J = 16.1$ Hz, overlapped with bm, 2H), 4.30 – 4.50 (bm, 2H), 4.85 (m, 1H, quartet shaped), 6.27 (bs, 0.3H), 6.63 (bs, 0.3H), 7.05 – 7.11 (bm, 2H), 7.17 – 7.34 (m, 8H); ^{13}C NMR (100 MHz, CDCl_3): δ 28.2, 37.8, 50.2, 51.2 (v. broad), 52.3, 52.8 (broad), 81.1, 127.1, 127.6, 128.1 (broad), 128.6, 129.1, 135.6, 136.9, 155.3 (broad), 168.9 (broad), 171.5.



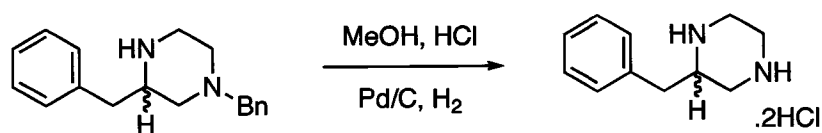
1,3-Dibenzylpiperazine-2,5-dione 167. To a 0 °C solution of dipeptide **166** (2.18 g, 5.11 mmol) in methanol (30 mL) was slowly added excess thionyl chloride (1.9 mL) to avoid sputtering. Following the addition, the solution stirred at ambient temperature for 2.5 h. The solvent was evaporated and the residue

was triturated with ~30 mL of ether, producing a white solid that was collected by filtration. The solid was dissolved in methanol (40 mL) and treated with ammonium hydroxide (29%, 10 mL) at ambient temperature. The solution was stirred for 18 h then concentrated. The solid residue was partitioned between saturated NaHCO₃ (40 mL), water (20 mL) and CHCl₃:isopropyl alcohol, 4:1 (40 mL). The organic phase was separated and the aqueous phase extracted with CHCl₃:isopropyl alcohol, 4:1 (3 x 40 mL). The combined organic phases were dried (K₂CO₃) and concentrated to afford **167** as a white solid (1.382 g, 92%) with adequate purity for subsequent transformations. TLC *R_f* 0.49 (MeOH:CH₂Cl₂, 1:9). ¹H NMR (400 MHz, CDCl₃): δ 2.99 (d, part of AB pattern, *J* = 17.6 Hz, 1H), 3.17 (m, AB pattern, 2H), 3.52 (d, part of AB pattern, *J* = 17.6 Hz, 1H), 4.35 (m, 1H), 4.48 (m, AB pattern, *J* = 14.7 Hz, 1H), 6.39 (bs, NH, 1H), 7.13 – 7.35 (m, 10H, overlapped with CDCl₃); ¹³C NMR (100 MHz, CDCl₃): δ 40.5, 48.2, 49.6, 56.4, 127.4, 128.1, 128.59, 128.63, 128.8, 130.0, 134.65, 134.68, 165.2, 166.3.

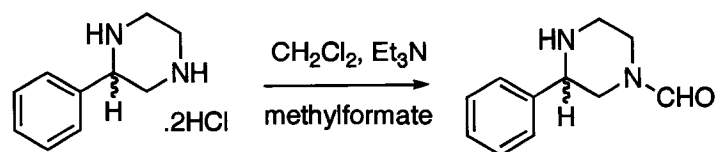


1,3-Dibenzylpiperazine 168. To a 0 °C suspension of dione **167** (1.38 g, 4.7 mmol) in dry THF (120 mL) was added LiAlH₄ (0.713 g, 18.8 mmol) in two portions, producing a gentle effervescence. The mixture was maintained on ice until the bubbling stopped, then the reaction was heated at reflux for 2.5 h. The solution was cooled and stirred for an additional 19 h then the excess LiAlH₄ was quenched by the careful, sequential addition of 0.7 mL water, 1.3 mL 4 M NaOH

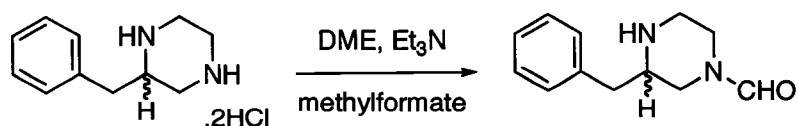
and 0.7 mL water. The solids that formed will filtered (Celite) and the filtrate concentrated to provide **168** as a pale colored solid (1.29 g, 103%, with THF) that slowly formed from an oil. TLC R_f 0.21 (MeOH:CH₂Cl₂, 1:9). ¹H NMR (400 MHz, CDCl₃): δ 1.93 (m, triplet shape, 1H), 2.11 (td, J = 2.9, 11.0 Hz, 1H, overlapped with bs, NH, 1H), 2.58 (dd, 8.8, 13.2 Hz, 1H), 2.70 – 2.77 (m, 2H), 2.79 – 2.87 (m, 2H), 2.92 (dt, J = 2.3, 11.7 Hz, 1H), 3.02 (m, 1H), 3.51 (dd, AB pattern, J = 12.8 Hz, 2H), 7.18 – 7.33 (m, 10H); ¹³C NMR (100 MHz, CDCl₃): δ 40.7, 45.6, 53.3, 56.2, 59.6, 63.3, 126.3, 127.0, 128.1, 128.4, 129.2, 137.9, 138.5.



2-Benzylpiperazine dihydrochloride 169. To a solution of piperazine **168** (1.25 g, 4.69 mmol) in methanol (20 mL) was added HCl (12 M, 0.78 mL, 9.38 mmol) and 5% Pd/C (0.188 g). The flask was sealed with a septum and H₂ was bubbled through the solution via balloon. The reaction was monitored by TLC until **168** was consumed, refilling H₂ if necessary. The mixture was filtered (Celite) and the filtrate concentrated to provide **169** as a white solid (1.10 g, 94%). ¹H NMR (400 MHz, D₂O): δ 2.90 (dd, AB pattern, J = 7.7, 14.3 Hz, 1H), 2.97 (dd, AB pattern, J = 7.0, 14.3 Hz, 1H), 3.13 (m, triplet shape, 1H), 3.22 (m, 2H), 3.52 – 3.59 (m, 3H), 3.72 (m, 1H), 7.15 – 7.32 (m, 5H); ¹³C NMR (100 MHz, D₂O, dioxane int. std 67.4 ppm): δ 36.8, 40.9, 41.4, 45.1, 54.6, 129.0, 130.3 (overlapped peaks), 133.9.

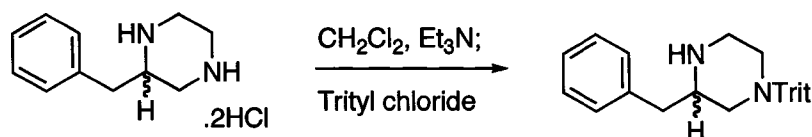


3-Phenylpiperazine-1-carbaldehyde 170. To a suspension of powdered piperazine **153** (0.206 g, 0.88 mmol) in CH_2Cl_2 (2 mL) was added triethylamine (0.26 mL, 1.85 mmol) followed by additional CH_2Cl_2 to facilitate stirring. The mixture was cooled to 0 °C and methylformate (0.06 mL, 0.96 mmol) was added. Stirring continued for 20 min at 0 °C then 24 h at ambient temperature. The mixture was diluted with saturated NaHCO_3 (6 mL) and extracted with CH_2Cl_2 (3 x 10 mL). The combined extracts were dried (K_2CO_3) and concentrated to provide the crude material that was purified by column chromatography (silica gel, $\text{MeOH}:\text{CH}_2\text{Cl}_2$, 1:39) to provide **170** as a oil (0.103 g, 62%). TLC R_f 0.35 ($\text{MeOH}:\text{CH}_2\text{Cl}_2$, 1:9). ^1H NMR (400 MHz, CDCl_3): (approximate 1:1 mixture of amide rotamers) δ 2.71 (dd, $J = 10.6, 12.8$ Hz, 0.5H), 2.83 – 2.93 (m, 1.5H), 3.11 – 3.22 (m, 1.5H), 3.34 (td, $J = 2.9, 11.7$ Hz, 0.5H), 3.55 (m, 1H), 3.70 (td, $J = 3.3, 10.6$ Hz, 1H), 4.40 (m, 1H), 7.27 – 7.44 (m, 5H), 8.07 (s, *CHO*, 0.5H), 8.10 (s, *CHO*, 0.5H); ^{13}C NMR (100 MHz, CDCl_3): δ 40.2, 45.5, 45.9, 46.8, 47.2, 53.1, 59.8, 61.4, 126.8, 126.9, 127.9, 128.1, 128.5, 128.6, 140.4, 140.7, 160.7, 160.8.



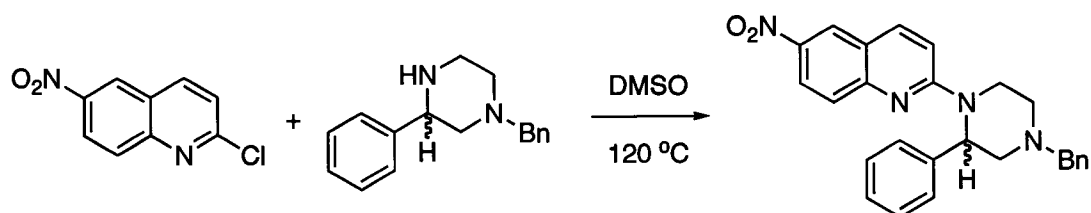
3-Benzylpiperazine-1-carbaldehyde 171. To a suspension of powdered piperazine **169** (0.304 g, 1.22 mmol) in dimethoxyethane (1.5 mL) was added triethylamine (0.35 mL, 2.56 mmol). The stirred mixture was cooled to 10 °C,

methylformate (0.11 mL, 1.83 mmol) was added and stirring was continued for 1 h at 10 °C then 24 h at ambient temperature. The mixture was diluted with saturated NaHCO₃ (6 mL) and extracted with CHCl₃:isopropyl alcohol, 4:1 (3 x 15 mL). The combined extracts were dried (K₂CO₃) and concentrated and the crude product was purified by column chromatography (silica gel, MeOH:CH₂Cl₂, 1:19 – 1:9) to provide **171** as an oil (0.189 g, 76%). TLC *R_f* 0.27 (MeOH:CH₂Cl₂, 1:9). ¹H NMR (400 MHz, CDCl₃): (approximate 1:1 mixture of amide rotamers) δ 2.0 (bs, NH, 1H), 2.54 – 2.72 (m, 2.5H), 2.75 – 2.89 (m, 2.5H), 2.96 (m, dd shape, 0.5H), 3.00 – 3.06 (m, 1H), 3.24 (td, *J* = 3.3, 11.7 Hz, 0.5H), 3.45 – 3.52 (m, 1H), 4.25 (m, doublet shape, 0.5H), 4.35 (m, doublet shape, 0.5H), 7.17 – 7.36 (m, 5H), 7.98 (s, 0.5H), 8.04 (s, 0.5H); ¹³C NMR (100 MHz, CDCl₃): δ 39.9, 40.0, 40.4, 45.0, 45.7, 46.1, 46.3, 51.3, 55.8, 57.1, 126.6, 126.7, 128.6, 128.7, 129.0, 129.1, 137.0, 137.3, 160.70, 160.75.



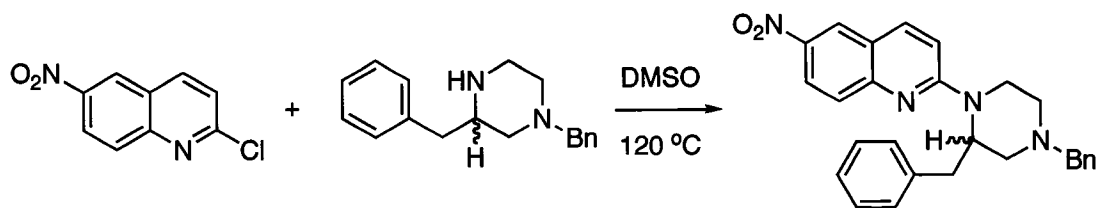
3-Benzyl-1-triphenylmethylpiperazine 172. To a stirred suspension of piperazine **169** (0.396 g, 1.59 mmol) in dry CH₂Cl₂ (20 mL) under argon was added anhydrous triethylamine (0.88 mL, 6.4 mmol). The resultant clear solution was cooled to 0 °C and a solution of trityl chloride (0.443 g, 1.59 mmol) in dry CH₂Cl₂ (7 mL) was added (dropwise). The reaction was stirred an additional 5 min at 0 °C then warmed to ambient temperature and stirred for 16 h. The solution was washed with saturated NaHCO₃ (40 mL) and brine (40 mL), and then dried (K₂CO₃) and concentrated to provide **172** as a white solid (0.650 g,

98%). TLC R_f 0.42 (MeOH:CH₂Cl₂, 1:9). ¹H NMR (400 MHz, CDCl₃): δ 1.35 (bs, 1H), 1.59 (bs, 2H), 2.42 (bs, 1H), 2.65 (dd, $J = 3.7, 13.2$ Hz, 1H), 2.85 – 3.16 (bm, 4H), 3.27 (m, 1H), 7.12 – 7.56 (m, 20H); ¹³C NMR (100 MHz, CDCl₃): δ 40.8, 46.4, 48.3, 54.4, 56.9 (all broad), 77.05, 125.9, 126.2, 127.4 (broad, 2 peaks), 128.4, 129.1, 129.3 (broad), 138.7.

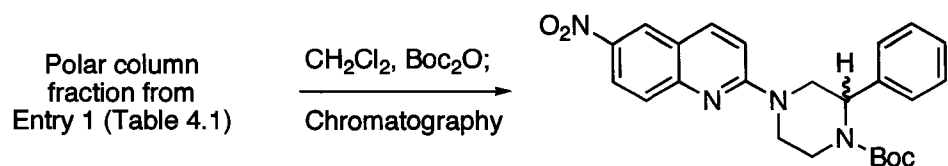


2-(4-Benzyl-2-phenylpiperazin-1-yl)-6-nitroquinoline 174. A suspension of quinoline **159** (0.0382 g, 0.183 mmol) and piperazine **164** (0.092 g, 0.365 mmol) in dry DMSO (0.5 mL) was sealed under argon in a vial and placed in a 120 °C oil bath for 24 h. The reaction mixture was pipetted into water (20 mL) and saturated NaHCO₃ (10 mL), then extracted with ether (2 x 20 mL). The combined ether extracts were washed with water (5 x 8 mL) and brine (20 mL), then dried (K₂CO₃) and concentrated. The crude material was purified by column chromatography (silica gel, EtOAc:Hexanes, 1:19 – 1:9) to provide **174** as an orange oil (0.060 g, 76%). TLC R_f 0.50 (EtOAc:Hexanes, 2:3). ¹H NMR (400 MHz, CDCl₃): δ 2.36 (td, $J = 2.9, 11.4$ Hz, 1H), 2.58 (dd, $J = 3.7, 11.7$ Hz, 1H), 3.02 (bd, $J = 10.3$ Hz, 1H), 3.66 (bd, $J = 12.8$ Hz, 1H), 3.41 – 3.54 (m, 3H), 4.54 (bd, $J = 12.8$ Hz, 1H), 5.86 (bs, 1H), 7.03 (d, $J = 9.2$ Hz, 1H), 7.22 – 7.43 (m, 10H), 7.65 (d, $J = 9.2$ Hz, 1H), 7.93 (d, $J = 9.2$ Hz, 1H), 8.29 (dd, $J = 2.6, 9.2$ Hz, 1H), 8.51 (d, $J = 2.6$ Hz, 1H); ¹³C NMR (100 MHz, CDCl₃): δ 40.9, 53.3, 54.1,

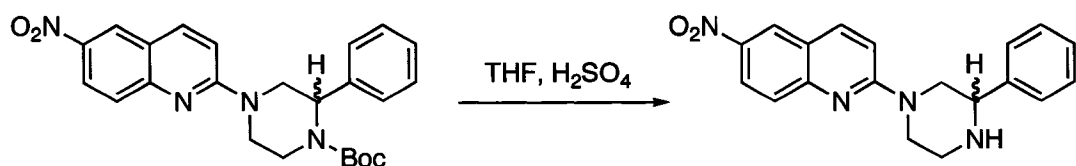
55.5, 62.8, 110.8, 121.0, 123.6, 124.3, 126.9, 127.0, 127.2, 127.5, 128.2, 128.3, 129.0, 137.6, 138.8, 139.7, 141.7, 151.5, 158.3.



2-(2,4-Dibenzylpiperazin-1-yl)-6-nitroquinoline 175. A suspension of quinoline **159** (0.035 g, 0.172 mmol) and piperazine **168** (0.090 g, 0.338 mmol) in dry DMSO (1.0 mL) was sealed under argon in a vial and placed in a 120 °C oil bath for 24 h. The reaction was pipetted into water (20 mL) and saturated NaHCO₃ (10 mL), and then extracted with ether (2 x 20 mL). The combined extracts were washed with water (5 x 5 mL) and brine (20 mL), then dried (K₂CO₃) and concentrated. The crude material was purified by column chromatography (silica gel, EtOAc:Hexanes, 1:9 – 2:3) to provide **175** as an orange oil (0.056 g, 74%). TLC *R_f* 0.39 (EtOAc:Hexanes, 2:3). ¹H NMR (400 MHz, CDCl₃): δ 2.08 (dd, *J* = 3.7, 11.7 Hz, 1H), 2.26 (td, *J* = 3.7, 11.7 Hz, 1H), 2.80 – 2.87 (m, 2H), 3.07 (m, bd shaped, 1H), 3.27 (dd, *J* = 9.9, 12.5 Hz, 1H), 3.40 – 3.50 (m, 2H, an AB doublet is overlapped here *J* = 12.8 Hz), 3.62 (d, part of AB pattern, *J* = 12.8 Hz, 1H), 4.45 (bs, 1H), 4.71 (bs, 1H), 6.98 (d, *J* = 9.2 Hz, 1H), 7.09 – 7.19 (m, 5H), 7.31 – 7.43 (m, 5H), 7.70 (d, *J* = 9.2 Hz, 1H), 7.92 (d, *J* = 9.2 Hz, 1H), 8.31 (dd, *J* = 2.6, 9.2 Hz, 1H), 8.53 (d, *J* = 2.6 Hz, 1H); ¹³C NMR (100 MHz, CDCl₃): δ 35.3, 40.7, 53.4, 54.5, 62.9, 110.8, 120.9, 123.6, 124.3, 126.2, 127.1, 127.3, 128.31, 128.34, 129.3, 129.4, 138.0, 138.4, 139.1, 141.7, 151.6, 158.1.

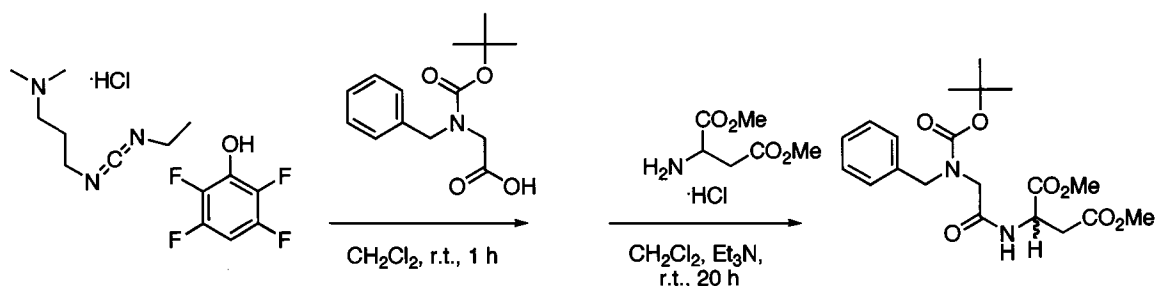


2-[4-(tert-Butoxycarbonyl)-3-phenylpiperazin-1-yl]-6-nitroquinoline 176. To the polar column fraction from Entry 1, Table 4.1 (0.111 g) dissolved in CH_2Cl_2 (5 mL) is added a solution of di-*tert*-butyldicarbonate (~0.11 g, 0.5 mmol) in CH_2Cl_2 (2 mL). The reaction was allowed to proceed for 5 h and TLC analysis showed the formation of a non-polar product (R_f 0.38, EtOAc:Hexanes, 2:3) consistent with Boc-protected quipazines. The solvent was evaporated and the residue purified by column chromatography (silica gel, EtOAc:Hexanes, 2:3) to provide **176** as a yellow foam (0.045 g). TLC R_f 0.38 (EtOAc:Hexanes, 2:3). ^1H NMR (400 MHz, CDCl_3): δ 1.40 (s, 9H), 3.43 – 3.53 (bm, 2H), 4.05 – 4.16 (bm, 2H), 4.21 – 4.28 (bm, 1H), 4.57 – 4.67 (bm, 1H), 5.32 (bs, 1H), 6.97 (d, $J = 9.2$ Hz, 1H), 7.21 – 7.26 (m, 1H), 7.28 – 7.37 (m, 4H), 7.72 (bs, 1H), 7.98 (d, $J = 9.2$ Hz, 1H), 8.32 (dd, $J = 2.6, 9.2$ Hz, 1H), 8.55 (d, $J = 2.6$ Hz, 1H).



2-(3-Phenylpiperazin-1-yl)-6-nitroquinoline 177. A solution of quipazine **176** (0.045 g, 0.10 mmol) in THF (0.5 mL) and 4 M H_2SO_4 (3 mL) was stirred at ambient temperature. The deprotection of the Boc group was found to be slow, so 3 drops of conc. H_2SO_4 was added. After 1 h, the reaction was complete (**176** gone by TLC) and the reaction was pipetted onto ice, made basic with 4 M NaOH and diluted with saturated NaHCO_3 (10 mL). The aqueous mixture was extracted

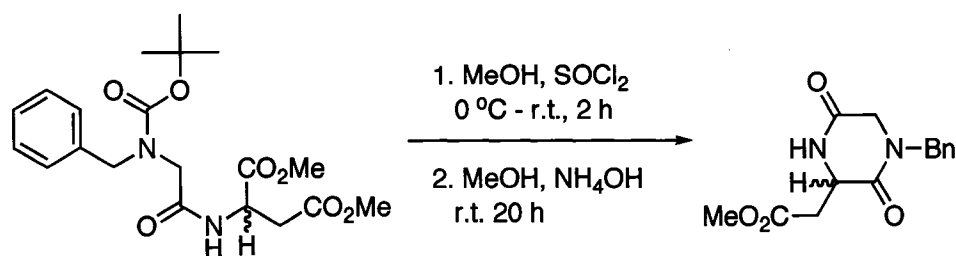
with CH_2Cl_2 (2 x 20 mL) and the combined extracts dried (K_2CO_3) and concentrated to provide **177** as a yellow-orange solid (0.032 g, 94%). TLC R_f 0.44 (MeOH: CH_2Cl_2 , 1:9). ^1H NMR (400 MHz, CDCl_3): δ 2.12 (bs, NH, 1H), 3.00 – 3.11 (m, 2H), 3.19 – 3.32 (m, 2H), 3.88 (dd, $J = 2.9, 10.6$ Hz, 1H), 4.63 (bd, $J = 12.8$ Hz, 2H), 7.08 (d, $J = 9.2$ Hz, 1H), 7.31 – 7.43 (m, 3H), 7.50 (m, doublet shape, 2H), 7.64 (d, $J = 9.2$ Hz, 1H), 7.96 (d, $J = 9.2$ Hz, 1H), 8.28 (dd, $J = 2.6, 9.2$ Hz, 1H), 8.52 (d, $J = 2.6$ Hz, 1H); ^{13}C NMR (100 MHz, CDCl_3): δ 44.9, 46.1, 52.1, 60.5, 110.9, 121.0, 123.6, 124.2, 127.1 (shouldered, 2 overlapping peaks), 128.1, 128.7, 138.7, 141.2, 141.9, 151.5, 158.4.



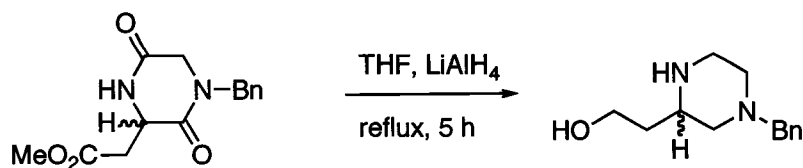
N-tert-Butoxycarbonyl-N-benzylglycyl-DL-aspartate Dimethyl Ester 183. The general peptide coupling procedure was used as described above for **96**.

Column chromatography of the crude product (silica gel, EtOAc:Hexanes, 1:3, to remove non-polar material, then EtOAc:Hexanes, 2:3, to elute product) provided **183** as a clear, viscous oil (1.96 g, 96%). TLC R_f 0.18 (EtOAc:Hexanes, 2:3). ^1H NMR (400 MHz, CDCl_3): δ 1.49 (s, 9H), 2.72 (bm, 1H), 2.99 (dd, $J = 3.6, 16.8$, 1H), 3.67 (s, 3H), 3.74 (s, 3H), 3.77 – 3.97 (bm, 2H), 4.42 (d, $J = 15.4$, 1H), 4.59 (bd, $J = 15.4$, 1H), 4.82 (bm, 1H), 6.82 (bs, 0.4H), 7.12 (bs, 0.3H), 7.20 – 7.34 (m, 5H); ^{13}C NMR (100 MHz, CDCl_3): δ 28.2, 35.9, 48.1, 50.3, 51.6 (broad), 51.9,

52.7, 81.1, 127.6, 128.2 (broad), 128.6, 137.1, 155.3 (broad), 169.1, 170.8 (broad), 171.2 (broad).

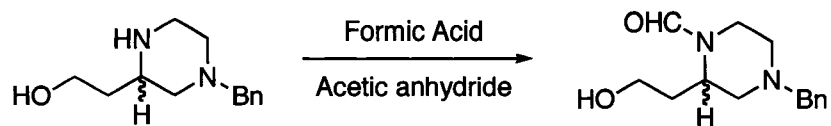


Methyl 2-(1-Benzyl-2,5-dioxopiperazin-3-yl)acetate 184. To a 0 °C solution of dipeptide **183** (1.9 g, 4.4 mmol) in methanol (25 mL) was added slowly excess thionyl chloride (2 mL) to avoid sputtering. Following the addition, the solution stirred at ambient temperature for 4.5 h. The solvent was evaporated and the oily residue was triturated with ether (20 mL). The ether was decanted and the process repeated. The still oily residue was dissolved in methanol (~45 mL) and treated with ammonium hydroxide (29%, 10 mL) at ambient temperature. The solution stirred for 16 h and the solvent was evaporated. The residue was partitioned between saturated NaHCO₃ (25 mL) and CHCl₃:isopropyl alcohol, 4:1 (20 mL). The organic phase was separated and the aqueous phase extracted with CHCl₃:isopropyl alcohol, 4:1 (3 x 20 mL). The combined organic phases were dried (K₂CO₃) and concentrated to afford **184** as a white solid (1.15 g, 97%) of adequate purity for subsequent steps. TLC *R_f* 0.38 (MeOH:CH₂Cl₂, 1:9). ¹H NMR (400 MHz, CDCl₃): δ 2.86 (dd, *J* = 8.1, 17.2 Hz, 1H), 3.06 (dd, *J* = 3.7, 17.2 Hz, 1H), 3.68 (s, 3H), 3.87 (m, 2H, qd shape), 4.40 (m, 1H), 4.59 (m, AB pattern, s shape), 7.05 (bs, 1H), 7.24 – 7.37 (m, 5H); ¹³C NMR (100 MHz, CDCl₃): δ 25.3, 38.0, 48.8, 49.8, 51.8, 52.2, 128.1, 128.4, 128.9, 134.8, 164.6, 165.2, 170.9.

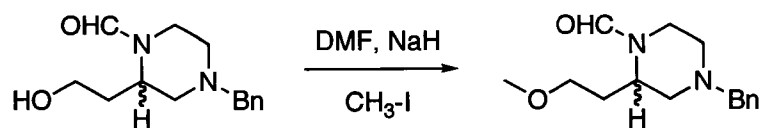


1-Benzyl-3-(2-hydroxyethyl)piperazine-2,5-dione 186. To a 0 °C suspension of amide **184** (1.15 g, 4.16 mmol) in dry THF (100 mL) under argon was added LiAlH₄ (0.949 g, 25 mmol) in 3 small portions. The mixture was heated at reflux for 5 h, then cooled. The excess LiAlH₄ was destroyed by the careful, sequential addition of 1 mL water, 2 mL 4 N NaOH and 1 mL water. After stirring 1h, the solids that formed were filtered (Celite) and the filtrate concentrated to give **186** as a pale colored oil (0.896 g, 98%). The crude material was used without purification in subsequent reactions.

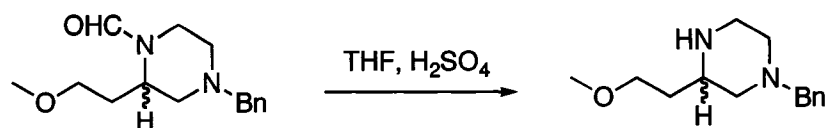
A pure sample of **186** was generated through the deprotection of N-formyl protected alcohol **187** (0.067g, 0.27 mmol) by dissolving **187** in THF (1 mL) and 4 M H₂SO₄ (3 mL) and heating at 55 °C for 3 h. The reaction was made basic with 4 M NaOH, diluted with saturated NaHCO₃ (10 mL) and extracted with CH₂Cl₂ (5 x 10 mL). The combined extracts were dried (K₂CO₃) and concentrated to provide pure **186** as an oily solid that solidified upon standing (0.052 g, 88%). TLC *R_f* 0.07 (MeOH:CH₂Cl₂, 1:9). ¹H NMR (400 MHz, CDCl₃): δ 1.55 (m, 2H), 1.80 (m, 1H), 1.99 (m, 1H), 2.70 – 3.06 (m, 6H, overlapped d at 2.73), 3.47 (s, 2H), 3.76 (m, 2H), 7.20 – 7.36 (m, 5H); ¹³C NMR (100 MHz, CDCl₃): δ 35.3, 45.3, 54.0, 55.4, 59.6, 61.7, 63.4, 127.0, 128.1, 129.1, 137.8.



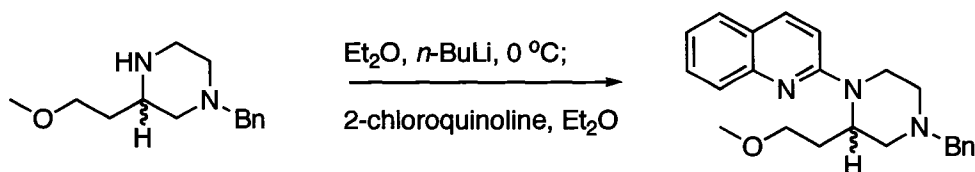
4-Benzyl-2-(2-hydroxyethyl)piperazine-1-carbaldehyde 187. To a 0 °C solution of amino alcohol **186** (0.853 g, 3.87 mmol) in formic acid (88%, 11 mL) was added (dropwise) acetic anhydride (3.25 g, 31.8 mmol). The reaction stirred at 0 °C for 30 min then at ambient temperature for an additional 45 min. Ice (~15 g) was added and the contents were transferred to a beaker and placed in an ice bath before the solution was brought to basic pH by the addition of 4 N NaOH. The contents were diluted with saturated NaHCO₃ (20 mL) and extracted with CH₂Cl₂ (5 x 20 mL). The combined extracts were dried (K₂CO₃) and concentrated to give the crude material that was purified by column chromatography (silica gel, MeOH:CHCl₃, 1:49) to afford **187** as an almost colorless oil (0.582g, 61%). TLC *R_f* 0.47 (MeOH:CH₂Cl₂, 1:9). ¹H NMR (400 MHz, CDCl₃): (approximate 7:3 mixture of amide rotamers) δ 1.66 – 1.85 (m, 1H), 1.95 – 2.12 (m, 1H), 2.14 – 2.34 (m, 2H), 2.72 – 2.97 (m, 2.7H), 3.08 (bm, 0.3H), 3.26 – 3.74 (m, 5.7H), 3.84 (m, 0.3H), 4.20 (m, 0.3H), 4.50 (m, 0.7H), 7.21 – 7.37 (m, 5H), 8.07 (m, 2 overlapped –CHO, 1H); ¹³C NMR (100 MHz, CDCl₃): δ 32.6, 33.6, 36.5, 42.6, 45.3, 51.0, 52.3, 52.9, 56.1, 56.7, 58.1, 58.2, 62.5, 62.6, 127.3, 128.3, 128.7, 128.8, 137.5, 161.6, 162.2.



4-Benzyl-2-(2-methoxyethyl)piperazine-1-carbaldehyde 188. To a 0 °C solution of alcohol **187** (0.500 g, 2.01 mmol) in dry DMF (8 mL) was added NaH (95%, 0.145 g, 6.04 mmol) in one portion. After stirring 5 min, iodomethane (0.300 g, 2.11 mmol) was added and the mixture stirred for 15 min at 0°C then at ambient temperature for 1.5 h. The excess NaH was destroyed by the careful addition of water and the mixture was diluted with 20 mL each of water and saturated NaHCO₃. The aqueous mixture was extracted with EtOAc (4 x 30 mL) and the combined extracts washed with brine (2 x 20 mL), dried (K₂CO₃) and concentrated to give the crude product that was purified by column chromatography (silica gel, MeOH:CHCl₃, 1:199 – 1:49) to afford **188** as a loose, almost colorless oil (0.493 g, 93%). TLC *R_f* 0.62 (MeOH:CH₂Cl₂, 1:9). ¹H NMR (400 MHz, CDCl₃): (approximate 7:3 mixture of amide rotamers) δ 1.81 (m, 0.7H), 1.91 (m, 0.3H), 1.97 – 2.11 (m, 1.3H), 2.14 – 2.34 (m, 1.7H), 2.74 (m, 1H), 2.79 – 2.95 (m, 1.7H), 3.17 – 3.36 (m, 5.7H), 3.39 – 3.57 (m, 2H), 3.75 (m, 0.7H), 4.20 (m, 0.7H), 4.50 (m, 0.3H), 7.22 – 7.38 (m, 5H), 8.03 (s, 1H); ¹³C NMR (100 MHz, CDCl₃): δ 29.8, 30.2, 36.2, 42.3, 46.0, 51.2, 52.7, 53.8, 55.7, 56.7, 58.5, 58.6, 62.7, 68.5, 69.9, 127.2, 128.3, 128.7, 138.0, 161.0, 161.4.



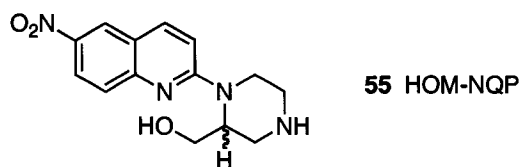
1-Benzyl-3-(2-methoxyethyl)piperazine 189. The N-formyl methylether **188** (0.493 g, 1.88 mmol) was dissolved in THF (3 mL) and 4 M H₂SO₄ (8 mL) and heated at 60 °C for 4 h. After cooling, the reaction was poured into 16 mL of cold (0 °C) 4 M NaOH and diluted with 10 mL of saturated NaHCO₃. The mixture was extracted with CH₂Cl₂ (4 x 20 mL) and the combined extracts were dried (K₂CO₃) and concentrated to provide **189** as a pale colored oil (0.420 g, 95%) with adequate purity for the subsequent transformations. TLC *R_f* 0.16 (MeOH:CH₂Cl₂, 1:9). ¹H NMR (400 MHz, CDCl₃): δ 1.54 – 1.63 (m, 3H), 1.75 (m, 1H), 2.02 (td, *J* = 3.7, 10.6 Hz, 1H), 2.69 – 2.79 (m, 2H), 2.83 – 2.95 (m, 3H), 3.29 (s, 3H), 3.44 (t, *J* = 6.6 Hz, 2H), 3.47 (m, AB pattern, *J* = 13.2 Hz, 2H), 7.20 – 7.33 (m, 5H); ¹³C NMR (100 MHz, CDCl₃): δ 34.2, 45.7, 53.3, 53.8, 58.6, 60.0, 63.3, 70.3, 126.9, 128.1, 129.0, 138.1.



2-[4-Benzyl-2-(2-methoxyethyl)piperazin-1-yl]quinoline 190. To a 0 °C solution of piperazine **189** (0.420 g, 1.79 mmol) in dry ether (20 mL) under argon was added (dropwise) a solution of *n*-butyllithium in hexane (2.45 M, 1.79 mmol) producing a clear amber solution. After stirring at 0 °C for 20 min, a solution of 2-chloroquinoline (0.195 g, 1.20 mmol) in ether (3.5 mL) was added (dropwise), producing a blood red solution. The reaction was stirred at 0 °C for 20 min then

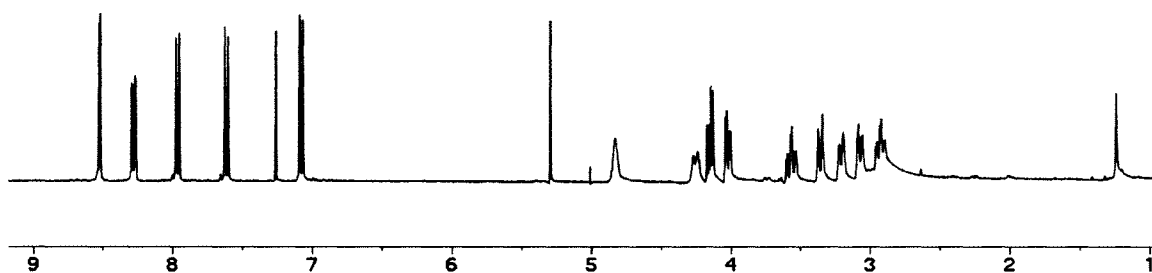
at ambient temperature for 3 h. The solution was diluted with ether (10 mL), washed with saturated NaHCO₃ (1 x 20 mL) and brine (1 x 20 mL), then dried (K₂CO₃) and concentrated. The crude product was purified by column chromatography (silica gel, EtOAc:Hexanes, 1:3) to provide **190** as a thick yellow oil (0.378 g, 88%). TLC *R_f* 0.37 (EtOAc:Hexanes, 2:3). ¹H NMR (400 MHz, CDCl₃): δ 2.12 (m, 1H), 2.17 – 2.32 (m, 3H), 2.89 (m, 1H), 2.99 (m, 1H), 3.23 (s, 3H, overlapped with), 3.22 – 3.41 (m, 3H), 3.46 (d, *J* = 13.2 Hz, 1H), 3.65 (d, *J* = 13.2 Hz, 1H), 4.59 (bm, 1H), 4.72 (bm, 1H), 7.06 (d, *J* = 9.2 Hz, 1H), 7.24 (m, 1H), 7.32 (m, 1H), 7.36 – 7.46 (m, 4H), 7.56 (m, 1H), 7.62 (m, 1H), 7.75 (d, *J* = 8.4 Hz, 1H), 7.88 (d, *J* = 9.2 Hz, 1H); ¹³C NMR (100 MHz, CDCl₃): δ 29.2, 39.3, 49.4, 53.5, 55.6, 58.2, 62.8, 69.5, 109.5, 121.8, 122.7, 126.3, 126.9 (two peaks), 128.1, 128.7, 129.2, 137.0, 138.4, 147.9, 156.8.

APPENDIX:
Select ^1H and ^{13}C NMR Spectra of Target Compounds.

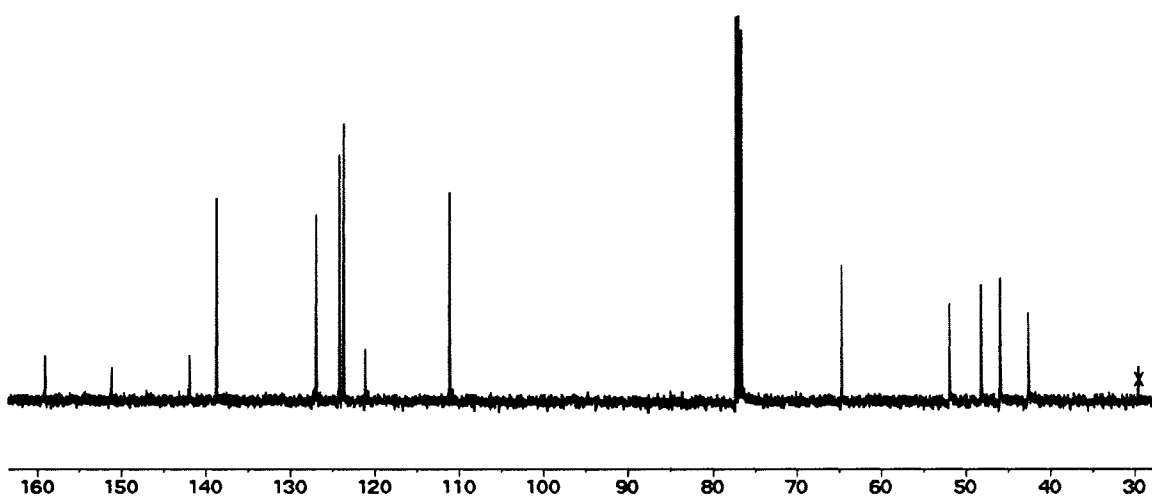


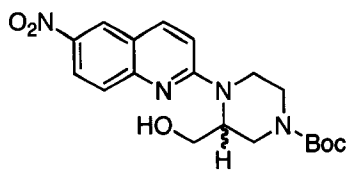
2-[2-(Hydroxymethyl)piperzin-1-yl]-6-nitroquinoline 55.

^1H NMR:



^{13}C NMR:



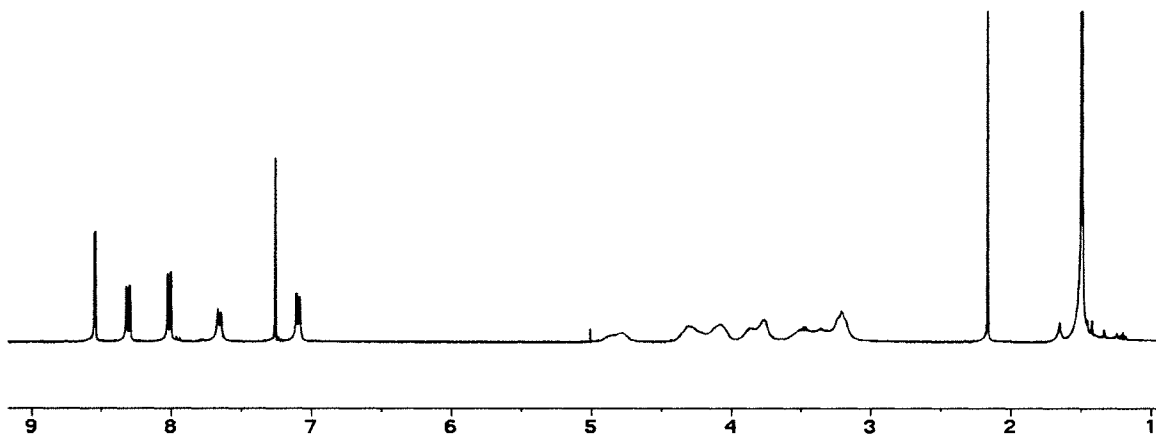


58 N-Boc-HOM-NQP

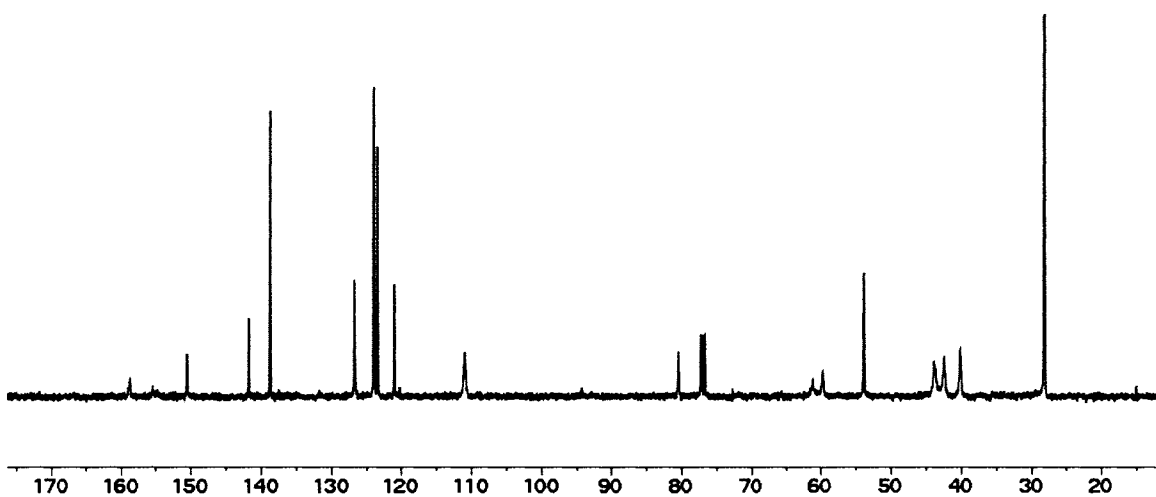
2-[4-(*tert*-Butoxycarbonyl)-2-(hydroxymethyl)piperazin-1-yl]-6-nitroquinoline

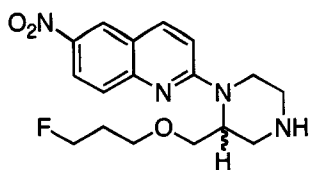
58.

^1H NMR:



^{13}C NMR:



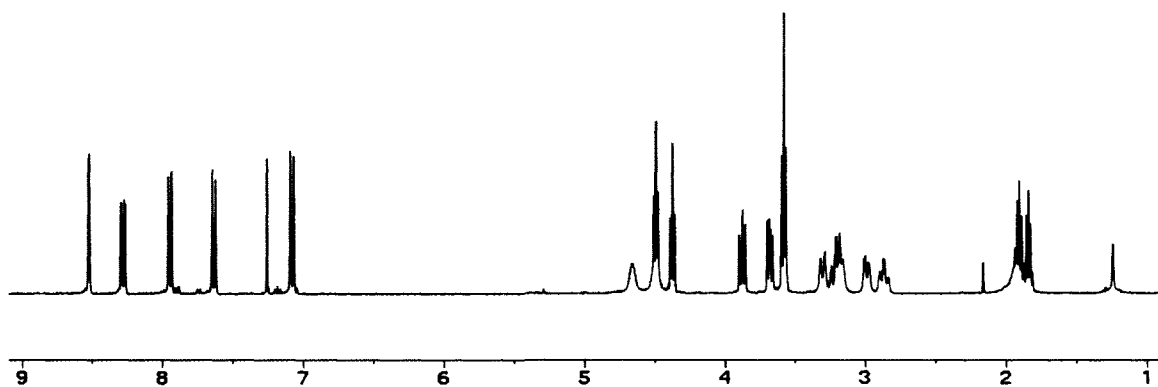


61 MeProF-NQP

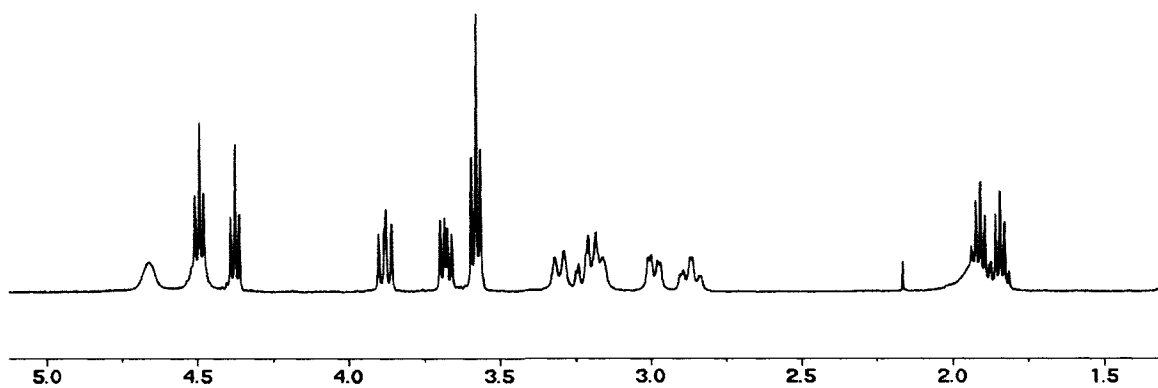
2-[2-((3-Fluoropropoxy)methyl)piperazine-1-yl]-6-nitroquinoline 61.

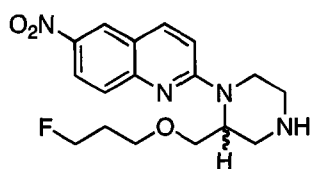
¹H NMR:

Full spectrum:



Zoomed spectrum:

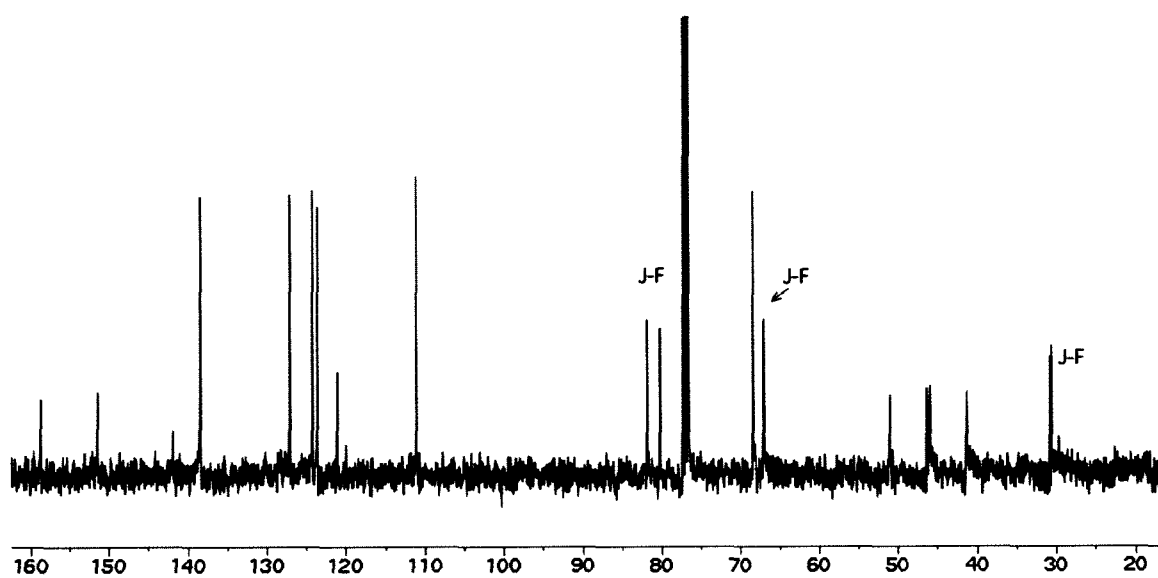




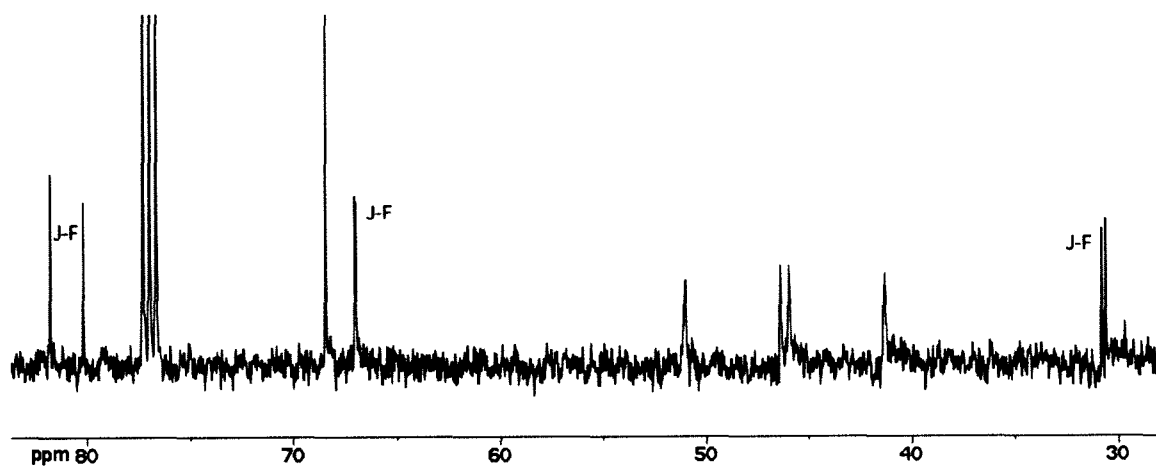
61 MeProF-NQP

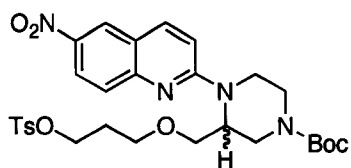
^{13}C NMR:

Full spectrum:



Zoomed spectrum:

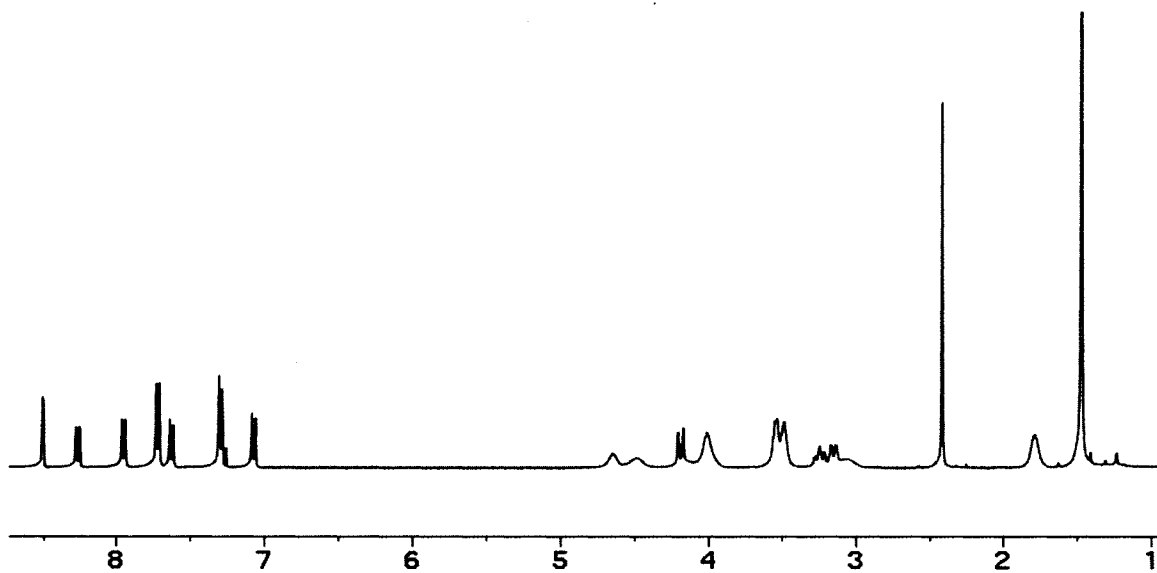




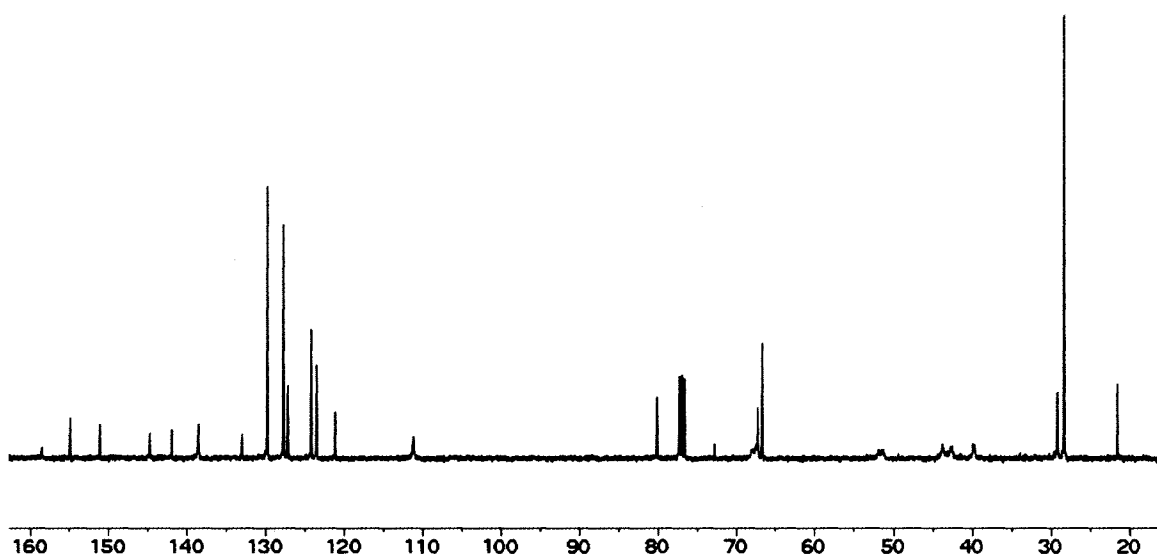
65 MeProF-Tosylate-NQP

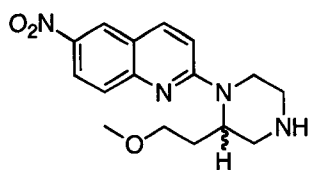
2-[4-(*tert*-Butoxycarbonyl)-2-((3-(4-methylbenzenesulfonate)propoxy)methyl)piperazine-1-yl]-6-nitroquinoline 65.

¹H NMR:



¹³C NMR:

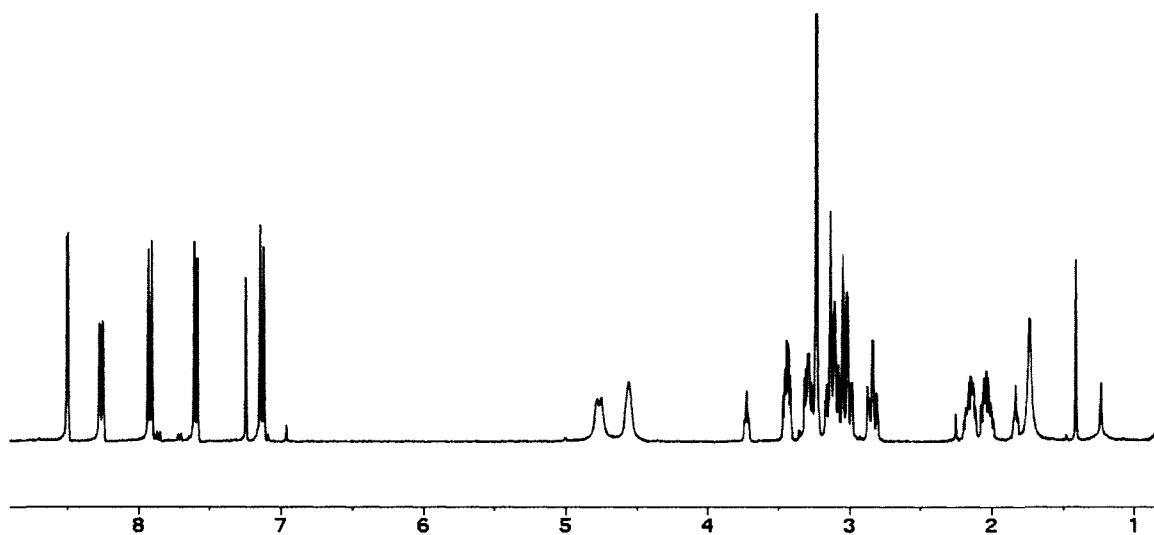




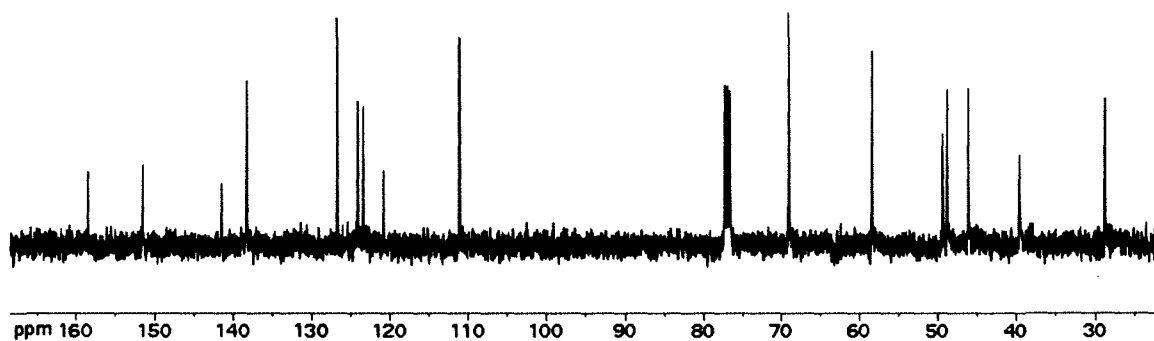
78 EtOMe-NQP

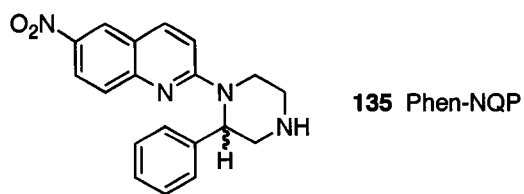
2-[2-(2-Methoxyethyl)piperazin-1-yl]-6-nitroquinoline 78.

¹H NMR:



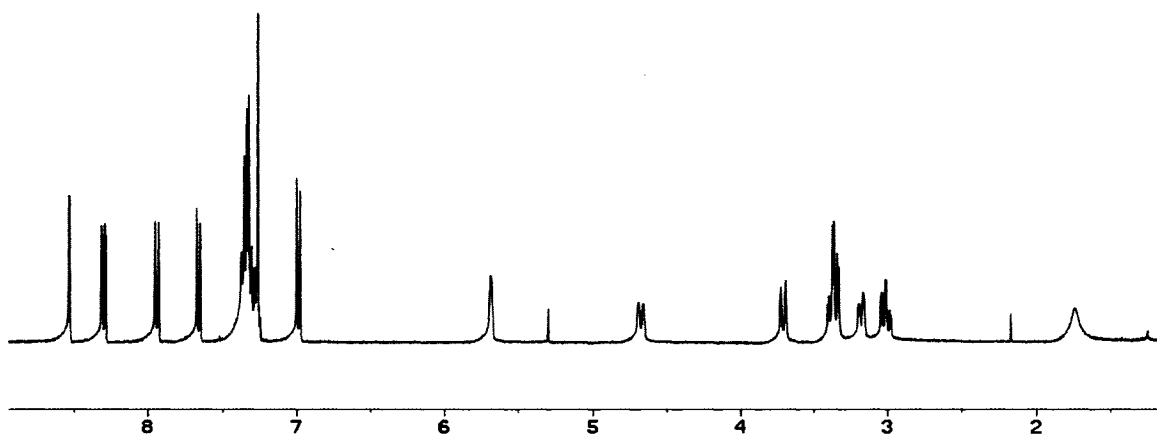
¹³C NMR:



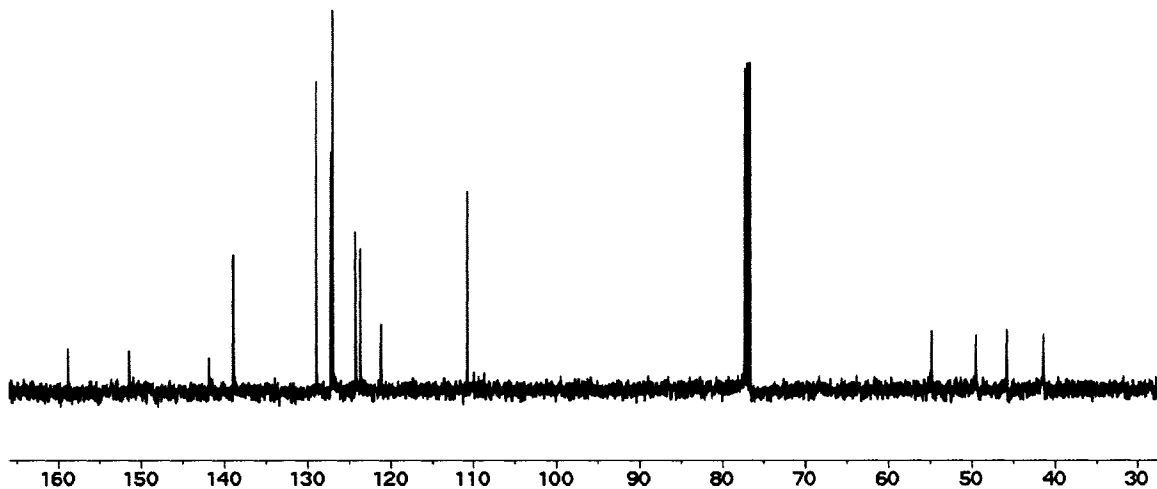


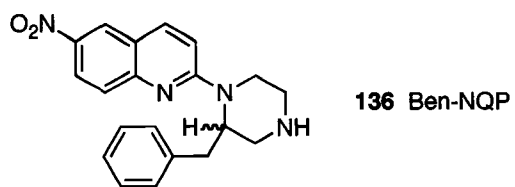
2-[2-Phenylpiperazin-1-yl]-6-nitroquinoline 135.

¹H NMR:



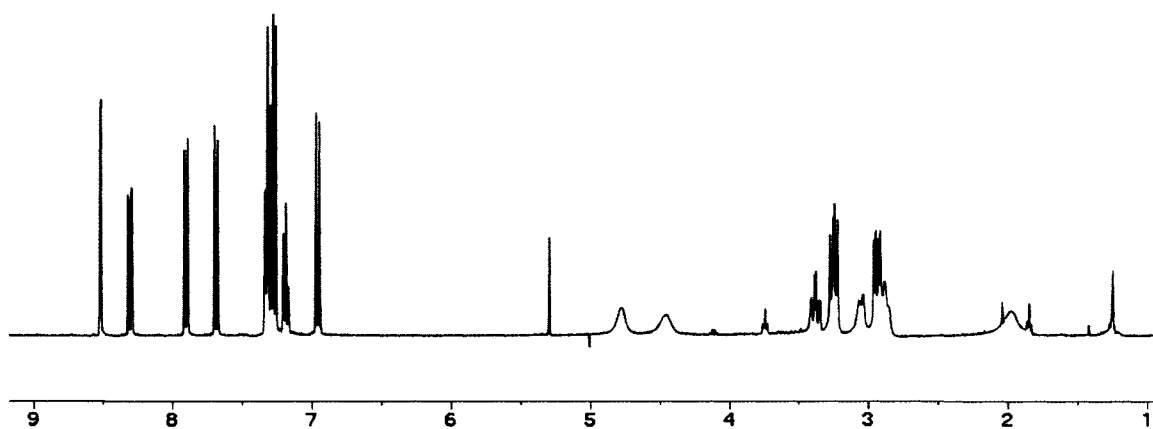
¹³C NMR:



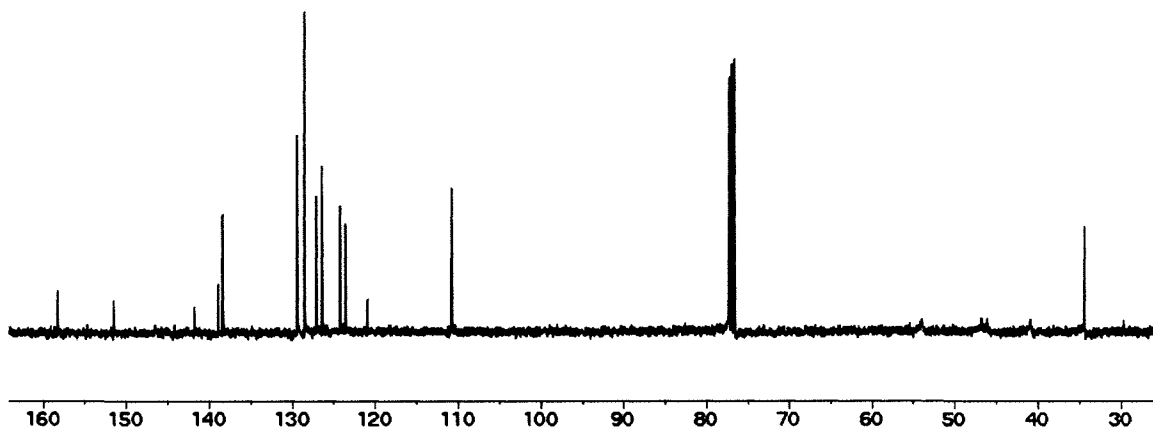


2-[2-Benzylpiperazin-1-yl]-6-nitroquinoline 136.

¹H NMR:



¹³C NMR:



LITERATURE CITED

1. Perrine, D. M., *The Chemistry of Mind-Altering Drugs*. 1st ed.; American Chemical Society: Washington D.C., 1996; p 480.
2. von Bohlen und Halbach, O.; Dermietzel, R., *Neurotransmitters and Neuromodulators: Handbook of Receptors and Biological Effects*. 1st ed.; Wiley-VCH Verlag GmbH: 2002; p 107-115.
3. Randall, D.; Burggren, W.; French, K., *Eckert Animal Physiology Mechanisms and Adaptations*. 4th ed.; W. H. Freeman and Company: New York, 1997; p 728.
4. Childers, W. E. J.; Robichaud, A. J., Recent Advances in Selective Serotonergic Agents. In *Annual Reports in Medicinal Chemistry*, Doherty, A. M., Ed. Elsevier: Amsterdam, 2005; Vol. 40, pp 17-33.
5. Glennon, R. A., Higher-end serotonin receptors: 5-HT(5), 5-HT(6), and 5-HT(7). *J Med Chem* **2003**, *46*, (14), 2795-812.
6. Pauwels, P. J., 5-HT Receptors and their Ligands, Tocris Review No. 25. In 2003.
7. Muller-Oerlinghausen, B.; Roggenbach, J.; Franke, L., Serotonergic platelet markers of suicidal behavior--do they really exist? *J Affect Disord* **2004**, *79*, (1-3), 13-24.
8. Tonini, M.; Vicini, R.; Cervio, E.; De Ponti, F.; De Giorgio, R.; Barbara, G.; Stanghellini, V.; Dellabianca, A.; Sternini, C., 5-HT7 receptors modulate peristalsis and accommodation in the guinea pig ileum. *Gastroenterology* **2005**, *129*, (5), 1557-66.
9. Chapman, M. E.; Wideman, R. F., Jr., Evaluation of the serotonin receptor blockers ketanserin and methiothepin on the pulmonary hypertensive responses of broilers to intravenously infused serotonin. *Poult Sci* **2006**, *85*, (4), 777-86.
10. Sommer, C., Serotonin in pain and analgesia: actions in the periphery. *Mol Neurobiol* **2004**, *30*, (2), 117-25.
11. Ravna, A. W.; Sylte, I.; Dahl, S. G., Molecular mechanism of citalopram and cocaine interactions with neurotransmitter transporters. *J Pharmacol Exp Ther* **2003**, *307*, (1), 34-41.
12. Ramamoorthy, S.; Bauman, A. L.; Moore, K. R.; Han, H.; Yang-Feng, T.; Chang, A. S.; Ganapathy, V.; Blakely, R. D., Antidepressant- and cocaine-sensitive human serotonin transporter: molecular cloning, expression, and chromosomal localization. *Proc Natl Acad Sci U S A* **1993**, *90*, (6), 2542-6.
13. Henry, L. K.; Field, J. R.; Adkins, E. M.; Parnas, M. L.; Vaughan, R. A.; Zou, M. F.; Newman, A. H.; Blakely, R. D., Tyr-95 and Ile-172 in transmembrane segments 1 and 3 of human serotonin transporters interact to establish high affinity recognition of antidepressants. *J Biol Chem* **2006**, *281*, (4), 2012-23.

14. Plenge, P.; Wiborg, O., High- and low-affinity binding of S-citalopram to the human serotonin transporter mutated at 20 putatively important amino acid positions. *Neurosci Lett* **2005**, 383, (3), 203-8.
15. Ravna, A. W.; Edvardsen, O., A putative three-dimensional arrangement of the human serotonin transporter transmembrane helices: a tool to aid experimental studies. *J Mol Graph Model* **2001**, 20, (2), 133-44.
16. Barker, E. L.; Blakely, R. D., Identification of a single amino acid, phenylalanine 586, that is responsible for high affinity interactions of tricyclic antidepressants with the human serotonin transporter. *Mol Pharmacol* **1996**, 50, (4), 957-65.
17. Chen, J. G.; Sachpatzidis, A.; Rudnick, G., The third transmembrane domain of the serotonin transporter contains residues associated with substrate and cocaine binding. *J Biol Chem* **1997**, 272, (45), 28321-7.
18. Sur, C.; Betz, H.; Schloss, P., A single serine residue controls the cation dependence of substrate transport by the rat serotonin transporter. *Proc Natl Acad Sci U S A* **1997**, 94, (14), 7639-44.
19. Huang, Y.; Lemieux, M. J.; Song, J.; Auer, M.; Wang, D. N., Structure and mechanism of the glycerol-3-phosphate transporter from *Escherichia coli*. *Science* **2003**, 301, (5633), 616-20.
20. Abramson, J.; Smirnova, I.; Kasho, V.; Verner, G.; Kaback, H. R.; Iwata, S., Structure and mechanism of the lactose permease of *Escherichia coli*. *Science* **2003**, 301, (5633), 610-5.
21. Ravna, A. W.; Sylte, I.; Kristiansen, K.; Dahl, S. G., Putative drug binding conformations of monoamine transporters. *Bioorg Med Chem* **2006**, 14, (3), 666-75.
22. Yamashita, A.; Singh, S. K.; Kawate, T.; Jin, Y.; Gouaux, E., Crystal structure of a bacterial homologue of Na⁺/Cl⁻-dependent neurotransmitter transporters. *Nature* **2005**, 437, (7056), 215-23.
23. Hesse, S.; Barthel, H.; Schwarz, J.; Sabri, O.; Muller, U., Advances in in vivo imaging of serotonergic neurons in neuropsychiatric disorders. *Neurosci Biobehav Rev* **2004**, 28, (6), 547-63.
24. Stockmeier, C. A., Involvement of serotonin in depression: evidence from postmortem and imaging studies of serotonin receptors and the serotonin transporter. *J Psychiatr Res* **2003**, 37, (5), 357-73.
25. Battaglia, G.; Zaczek, R.; De Souza, E. B., MDMA effects in the brain: pharmacological profile and evidence of neurotoxicity from neurochemical and autoradiographic studies. In *Ecstasy: the clinical, pharmacological and neurotoxicological effects of the drug MDMA*, Peroutka, S. J., Ed. Kluwer Academic Press: Boston, 1990; pp 171-199.

26. Rosel, P.; Menchon, J. M.; Oros, M.; Vallejo, J.; Cortadellas, T.; Arranz, B.; Alvarez, P.; Navarro, M. A., Regional distribution of specific high affinity binding sites for 3H-imipramine and 3H-paroxetine in human brain. *J Neural Transm* **1997**, *104*, (1), 89-96.
27. Plenge, P.; Mellerup, E. T.; Laursen, H., Regional distribution of the serotonin transport complex in human brain, identified with 3H-paroxetine, 3H-citalopram and 3H-imipramine. *Prog Neuropsychopharmacol Biol Psychiatry* **1990**, *14*, (1), 61-72.
28. Backstrom, I.; Bergstrom, M.; Marcusson, J., High affinity [3H]paroxetine binding to serotonin uptake sites in human brain tissue. *Brain Res* **1989**, *486*, (2), 261-8.
29. Cortes, R.; Soriano, E.; Pazos, A.; Probst, A.; Palacios, J. M., Autoradiography of antidepressant binding sites in the human brain: localization using [3H]imipramine and [3H]paroxetine. *Neuroscience* **1988**, *27*, (2), 473-96.
30. Dahlstrom, M.; Ahonen, A.; Ebeling, H.; Torniainen, P.; Heikkila, J.; Moilanen, I., Elevated hypothalamic/midbrain serotonin (monoamine) transporter availability in depressive drug-naive children and adolescents. *Mol Psychiatry* **2000**, *5*, (5), 514-22.
31. Malison, R. T.; Price, L. H.; Berman, R.; van Dyck, C. H.; Pelton, G. H.; Carpenter, L.; Sanacora, G.; Owens, M. J.; Nemeroff, C. B.; Rajeevan, N.; Baldwin, R. M.; Seibyl, J. P.; Innis, R. B.; Charney, D. S., Reduced brain serotonin transporter availability in major depression as measured by [123I]-2 beta-carbomethoxy-3 beta-(4-iodophenyl)tropane and single photon emission computed tomography. *Biol Psychiatry* **1998**, *44*, (11), 1090-8.
32. Frazer, A., Pharmacology of antidepressants. *J Clin Psychopharmacol* **1997**, *17* Suppl 1, 2S-18S.
33. Poe, T. E., Fluoxetine. A new antidepressant. *N C Med J* **1988**, *49*, (7), 391-2.
34. Schyler, D. J., PET Tracers and Radiochemistry. *Ann. Acad. Med. Singapore* **2004**, *33*, 146-154.
35. Berkheij, M.; van der Sluis, L.; Sewing, C.; den Boer, D. J.; Terpstra, J. W.; Hiemstra, H.; Bakker, W. I. I.; van den Hoogenband, A.; van Maarseveen, J. H., Synthesis of 2-substituted piperazines via direct alpha-lithiation. *Tet Lett* **2005**, *46*, 2369-2371.
36. Lundkvist, C.; Loc'h, C.; Halldin, C.; Bottlaender, M.; Ottaviani, M.; Coulon, C.; Fuseau, C.; Mathis, C.; Farde, L.; Maziere, B., Characterization of bromine-76-labelled 5-bromo-6-nitroquipazine for PET studies of the serotonin transporter. *Nucl Med Biol* **1999**, *26*, (5), 501-7.
37. Pirotte, B.; Goldman, S.; Dewitte, O.; Massager, N.; Wikler, D.; Lefranc, F.; Ben Taib, N. O.; Rorive, S.; David, P.; Brotchi, J.; Levivier, M., Integrated positron emission tomography and magnetic resonance imaging-guided resection of brain

- tumors: a report of 103 consecutive procedures. *J Neurosurg* **2006**, 104, (2), 238-53.
38. Mason, N. S.; Mathis, C. A., Positron Emission Tomography Agents for Central Nervous System Drug Development Applications. In *Annual Reports in Medicinal Chemistry*, Doherty, A. M., Ed. Elsevier: Amsterdam, 2005; Vol. 40, pp 49-68.
 39. Mathis, C. A.; Wang, Y.; Klunk, W. E., Imaging beta-amyloid plaques and neurofibrillary tangles in the aging human brain. *Curr Pharm Des* **2004**, 10, (13), 1469-92.
 40. Laruelle, M.; Slifstein, M.; Huang, Y., Relationships between radiotracer properties and image quality in molecular imaging of the brain with positron emission tomography. *Mol Imaging Biol* **2003**, 5, (6), 363-75.
 41. Wong, D. F.; Pomper, M. G., Predicting the success of a radiopharmaceutical for in vivo imaging of central nervous system neuroreceptor systems. *Mol Imaging Biol* **2003**, 5, (6), 350-62.
 42. Neumeyer, J. L.; Wang, S. Y.; Milius, R. A.; Baldwin, R. M.; Zea-Ponce, Y.; Hoffer, P. B.; Sybirska, E.; al-Tikriti, M.; Charney, D. S.; Malison, R. T.; et al., [123I]-2 beta-carbomethoxy-3 beta-(4-iodophenyl)tropane: high-affinity SPECT radiotracer of monoamine reuptake sites in brain. *J Med Chem* **1991**, 34, (10), 3144-6.
 43. Frankle, W. G.; Narendran, R.; Huang, Y.; Hwang, D. R.; Lombardo, I.; Cangiano, C.; Gil, R.; Laruelle, M.; Abi-Dargham, A., Serotonin transporter availability in patients with schizophrenia: a positron emission tomography imaging study with [11C]DASB. *Biol Psychiatry* **2005**, 57, (12), 1510-6.
 44. Szabo, Z.; Kao, P. F.; Scheffel, U.; Suehiro, M.; Mathews, W. B.; Ravert, H. T.; Musachio, J. L.; Marenco, S.; Kim, S. E.; Ricaurte, G. A.; et al., Positron emission tomography imaging of serotonin transporters in the human brain using [11C](+)McN5652. *Synapse* **1995**, 20, (1), 37-43.
 45. Reivich, M.; Amsterdam, J. D.; Brunswick, D. J.; Shiue, C. Y., PET brain imaging with [11C](+)McN5652 shows increased serotonin transporter availability in major depression. *J Affect Disord* **2004**, 82, (2), 321-7.
 46. McCann, U. D.; Szabo, Z.; Seckin, E.; Rosenblatt, P.; Mathews, W. B.; Ravert, H. T.; Dannals, R. F.; Ricaurte, G. A., Quantitative PET studies of the serotonin transporter in MDMA users and controls using [11C]McN5652 and [11C]DASB. *Neuropsychopharmacology* **2005**, 30, (9), 1741-50.
 47. Huang, Y.; Hwang, D. R.; Narendran, R.; Sudo, Y.; Chatterjee, R.; Bae, S. A.; Mawlawi, O.; Kegeles, L. S.; Wilson, A. A.; Kung, H. F.; Laruelle, M., Comparative evaluation in nonhuman primates of five PET radiotracers for imaging the serotonin transporters: [11C]McN 5652, [11C]ADAM, [11C]DASB, [11C]DAPA, and [11C]AFM. *J Cereb Blood Flow Metab* **2002**, 22, (11), 1377-98.

48. Brust, P.; Zessin, J.; Kuwabara, H.; Pawelke, B.; Kretzschmar, M.; Hinz, R.; Bergman, J.; Eskola, O.; Solin, O.; Steinbach, J.; Johannsen, B., Positron emission tomography imaging of the serotonin transporter in the pig brain using [11C](+)-McN5652 and S-([18F]fluoromethyl)-(+)-McN5652. *Synapse* **2003**, *47*, (2), 143-51.
49. Brust, P.; Hinz, R.; Kuwabara, H.; Hesse, S.; Zessin, J.; Pawelke, B.; Stephan, H.; Bergmann, R.; Steinbach, J.; Sabri, O., In vivo measurement of the serotonin transporter with (S)-([18F]fluoromethyl)-(+)-McN5652. *Neuropsychopharmacology* **2003**, *28*, (11), 2010-9.
50. Meyer, J. H.; Houle, S.; Sagrati, S.; Carella, A.; Hussey, D. F.; Ginovart, N.; Goulding, V.; Kennedy, J.; Wilson, A. A., Brain serotonin transporter binding potential measured with carbon 11-labeled DASB positron emission tomography: effects of major depressive episodes and severity of dysfunctional attitudes. *Arch Gen Psychiatry* **2004**, *61*, (12), 1271-9.
51. Huang, Y.; Hwang, D. R.; Bae, S. A.; Sudo, Y.; Guo, N.; Zhu, Z.; Narendran, R.; Laruelle, M., A new positron emission tomography imaging agent for the serotonin transporter: synthesis, pharmacological characterization, and kinetic analysis of [11C]2-[2-(dimethylaminomethyl)phenylthio]-5-fluoromethylphenylamine ([11C]AFM). *Nucl Med Biol* **2004**, *31*, (5), 543-56.
52. Huang, Y.; Bae, S. A.; Zhu, Z.; Guo, N.; Roth, B. L.; Laruelle, M., Fluorinated diaryl sulfides as serotonin transporter ligands: synthesis, structure-activity relationship study, and in vivo evaluation of fluorine-18-labeled compounds as PET imaging agents. *J Med Chem* **2005**, *48*, (7), 2559-70.
53. Frankle, W. G.; Huang, Y.; Hwang, D. R.; Talbot, P. S.; Slifstein, M.; Van Heertum, R.; Abi-Dargham, A.; Laruelle, M., Comparative evaluation of serotonin transporter radioligands 11C-DASB and 11C-McN 5652 in healthy humans. *J Nucl Med* **2004**, *45*, (4), 682-94.
54. Lee, B. S.; Chu, S.; Lee, K. C.; Lee, B. S.; Chi, D. Y.; Choe, Y. S.; Kim, S. E.; Song, Y. S.; Jin, C., Syntheses and binding affinities of 6-nitroquipazine analogues for serotonin transporter: Part 3. A potential 5-HT transporter imaging agent, 3-(3-[18F]fluoropropyl)-6-nitroquipazine. *Bioorg Med Chem* **2003**, *11*, (23), 4949-58.
55. Sandell, J.; Halldin, C.; Sovago, J.; Chou, Y. H.; Gulyas, B.; Yu, M.; Emond, P.; Nagren, K.; Guilloteau, D.; Farde, L., PET examination of [(11)C]5-methyl-6-nitroquipazine, a radioligand for visualization of the serotonin transporter. *Nucl Med Biol* **2002**, *29*, (6), 651-6.
56. Karramkam, M.; Dolle, F.; Valette, H.; Besret, L.; Bramouille, Y.; Hinnen, F.; Vaufray, F.; Franklin, C.; Bourg, S.; Coulon, C.; Ottaviani, M.; Delaforge, M.; Loc'h, C.; Bottlaender, M.; Crouzel, C., Synthesis of a fluorine-18-labelled derivative of 6-nitroquipazine, as a radioligand for the in vivo serotonin transporter imaging with PET. *Bioorg Med Chem* **2002**, *10*, (8), 2611-23.

57. Jagust, W. J.; Eberling, J. L.; Biegon, A.; Taylor, S. E.; VanBrocklin, H. F.; Jordan, S.; Hanrahan, S. M.; Roberts, J. A.; Brennan, K. M.; Mathis, C. A., Iodine-123-5-iodo-6-nitroquipazine: SPECT radiotracer to image the serotonin transporter. *J Nucl Med* **1996**, *37*, (7), 1207-14.
58. Jensen, S. B.; Bender, D.; Smith, D. F.; Scheel-Kruger, J.; Nielsen, E. O.; Olsen, G. M.; Peter, D.; Gjedde, A., Synthesis of (+/-) 3-(6-nitro-2-quinoliny)-[9-methyl-11C]-3,9-diazabicyclo-[4.2.1]-nonane ([11C-Methyl]NS 4194). *J Label Compd Radiopharm* **2002**, *45*, 181-189.
59. Jensen, S. B.; Smith, D. F.; Bender, D.; Jakobsen, S.; Peters, D.; Nielsen, E. O.; Olsen, G. M.; Scheel-Kruger, J.; Wilson, A.; Cumming, P., [11C]-NS 4194 versus [11C]-DASB for PET imaging of serotonin transporters in living porcine brain. *Synapse* **2003**, *49*, (3), 170-7.
60. Vaatstra, W. J.; Deiman-Van Aalst, W. M.; Eigeman, L., Du 24565, a quipazine derivative, a potent selective serotonin uptake inhibitor. *Eur J Pharmacol* **1981**, *70*, (2), 195-202.
61. Hashimoto, K.; Goromaru, T., Preparation of [3H]6-nitroquipazine, a potent and selective 5-hydroxytryptamine uptake inhibitor. *Radioisotopes* **1990**, *39*, (4), 168-9.
62. Hashimoto, K.; Goromaru, T., High-affinity binding of [3H]6-nitroquipazine to 5-hydroxytryptamine transporter in human platelets. *Eur J Pharmacol* **1990**, *187*, (3), 295-302.
63. Hashimoto, K.; Goromaru, T., High-affinity [3H]6-nitroquipazine binding sites in rat brain. *Eur J Pharmacol* **1990**, *180*, (2-3), 273-81.
64. Gerdes, J. M.; DeFina, S. C.; Wilson, P. A.; Taylor, S. E., Serotonin transporter inhibitors: synthesis and binding potency of 2'-methyl- and 3'-methyl-6-nitroquipazine. *Bioorg Med Chem Lett* **2000**, *10*, (23), 2643-6.
65. Wilson, P. A. A Simple Methodology for the Production of Three-Dimensional Models: Serotonin Transporter as an Example. PhD Dissertation. University of Montana, Missoula, MT, 2004.
66. Bolstad, E. S. D. Comparative Analysis of Serotonin and Norepinephrine Reuptake Inhibitor Pharmacophore Constructs for Ligand Designs. PhD Dissertation. University of Montana, Missoula, MT, 2006.
67. Walker, M. A. Serotonin Transporter Inhibitors: Studies of 2'-substituted-6-nitroquipazine Agents. Masters Thesis. Central Washington University, Ellensburg, WA, 2001.
68. Rondu, F.; Le Bihan, G.; Wang, X.; Lamouri, A.; Touboul, E.; Dive, G.; Bellahsene, T.; Pfeiffer, B.; Renard, P.; Guardiola-Lemaitre, B.; Manechez, D.; Penicaud, L.; Ktorza, A.; Godfroid, J. J., Design and synthesis of imidazoline derivatives active on glucose homeostasis in a rat model of type II diabetes. 1.

Synthesis and biological activities of N-benzyl-N'-(arylalkyl)-2-(4',5'-dihydro-1'H-imidazol-2'-yl)piperazines. *J Med Chem* **1997**, *40*, (23), 3793-803.

69. Gilman, H.; Crouse, N. N.; Massie Jr., S. P.; Benkeser, R. A.; Spatz, S. M., Rearrangement in the Reaction of alpha-Halogenonaphthalenes with Lithium Diethyl-amide. *J Am Chem Soc* **1945**, *67*, 2106-2108.
70. Bolstad, D. B.; Chandler-Ferguson, D.; Davis, E. S.; DeFina, S. C.; Gerdes, J. M.; Walker, M. A.; Weller, M. L.; Wilson, P. A.; Ono, M. Y.; Taylor, S. E., Serotonin Transporter Inhibitor Ligands: Synthesis and Biochemical Studies of 2'-Methoxymethyl-6-nitroquipazine. In *The 221st American Chemical Society National Meeting*, Chicago, IL, 2001.
71. Lee, B. S.; Chu, S.; Lee, B. C.; Chi, D. Y.; Choe, Y. S.; Jeong, K. J.; Jin, C., Syntheses and binding affinities of 6-nitroquipazine analogues for serotonin transporter. Part 1. *Bioorg Med Chem Lett* **2000**, *10*, (14), 1559-62.
72. Se Lee, B.; Chu, S.; Lee, B. S.; Yoon Chi, D.; Song, Y. S.; Jin, C., Syntheses and binding affinities of 6-nitroquipazine analogues for serotonin transporter. Part 2: 4-substituted 6-nitroquipazines. *Bioorg Med Chem Lett* **2002**, *12*, (5), 811-5.
73. Moon, B. S.; Lee, B. S.; Chi, D. Y., Syntheses and binding affinities of 6-nitroquipazine analogues for serotonin transporter. Part 4: 3-Alkyl-4-halo-6-nitroquipazines. *Bioorg Med Chem* **2005**, *13*, (16), 4952-9.
74. Kusche, B. R. Serotonin Transporter Inhibitor Ligands: Synthesis of 2-(2-alkyl-piperazin-1-yl)-6-nitroquipazine Analogs as Potential Positron Emission Tomography Imaging Agents. PhD Dissertation. University of Montana, Missoula, MT, 2006.
75. Olah, G. A.; Narang, S. C., Iodotrimethylsilane - A versatile synthetic reagent. *Tetrahedron* **1982**, *38*, (15), 2225-2277.
76. Jung, M. E.; Lyster, M. A., Quantitative Dealkylation of Alkyl Ethers via Treatment with Trimethylsilyl Iodide. A New Method for Ether Hydrolysis. *J Org Chem* **1977**, *42*, (23), 3761-3764.
77. Olah, G. A.; Narang, S. C.; Balarma Gupta, B. G.; Malhotra, R., Synthetic Methods and Reactions. 62. Transformations with Chlorotrimethylsilane/Sodium Iodide, a Convenient in Situ Iodotrimethylsilane Reagent. *J Org Chem* **1979**, *44*, (8), 1247-1251.
78. McOmie, J. F. W.; Watts, M. L.; West, D. E., Demethylation of Aryl Methyl Ethers by Boron Tribromide. *Tetrahedron* **1968**, *24*, 2289-2292.
79. Greene, T. W.; Wuts, P. G. M., *Protective groups in Organic Synthesis*. 3rd ed.; John Wiley & Sons, Inc.: New York, 1999; p 779.
80. Demuynek, M.; De Clercq, P.; Vandewalle, M., (+/-)-Hysterin: Revised Structure and Total Synthesis. *J Org Chem* **1979**, *44*, (26), 4863-4866.

81. Personal communication (E-mail) with Dr. Hong Fan, 2001.
82. Jacobsen, E. J.; Stelzer, L. S.; TenBrink, R. E.; Belonga, K. L.; Carter, D. B.; Im, H. K.; Im, W. B.; Sethy, V. H.; Tang, A. H.; VonVoigtlander, P. F.; Petke, J. D.; Zhong, W. Z.; Mickelson, J. W., Piperazine imidazo[1,5-a]quinoxaline ureas as high-affinity GABAA ligands of dual functionality. *J Med Chem* **1999**, *42*, (7), 1123-44.
83. Le Bail, M.; Aitken, D. J.; Vergne, F.; Husson, H.-P., Alkylation of chiral 2-(aminomethyl)oxazolines. *J Chem Soc Perk T 1* **1997**, *11*, 1681-1689.
84. Green, T. W.; Wuts, P. G. M., *Protective Groups in Organic Synthesis*. 3rd ed.; John Wiley & Sons: New York, 1999; p 779.
85. Frank, R.; Schutkowski, M., Extremely mild reagent for Boc deprotection applicable to the synthesis of peptides with thioamide linkages. *Chem. Commun.* **1996**, (22), 2501-2510.
86. Kaiser, E.; Picart, F.; Kubiak, T.; Tam, J. P.; Merrifield, R. B., Selective Deprotection of the N-tert-Butyloxycarbonyl Group in Solid Phase Peptide Synthesis with Chlorotrimethylsilane and Phenol. *J Org Chem* **1993**, *58*, 5167-5175.
87. Brown, H. C.; Knights, E. F.; Scouten, C. G., Hydroboration. XXXVI. A Direct Route to 9-Borabicyclo[3.3.1]nonane *via* the Cyclic Hydroboration of 1,5-Cyclooctadiene. 9-Borabicyclo[3.3.1]nonane as a Uniquely Selective Reagent for the Hydroboration of Olefins. *J Am Chem Soc* **1974**, *96*, (25), 7765-7770.
88. Cox, D. P.; Terpinski, J.; Lawrynowicz, W., "Anhydrous" Tetrabutylammonium Fluoride: A Mild but Highly Efficient Source of Nucleophilic Fluoride Ion. *J Org Chem* **1984**, *49*, (17), 3216-3219.
89. Bishop, J. E.; Mathis, C. A.; Gerdes, J. M.; Whitney, J. M.; Eaton, A. M.; Mailman, R. B., Synthesis and in vitro evaluation of 2,3-dimethoxy-5-(fluoroalkyl)-substituted benzamides: high-affinity ligands for CNS dopamine D2 receptors. *J Med Chem* **1991**, *34*, (5), 1612-24.
90. Le Bihan, G.; Rondu, F.; Pele-Tounian, A.; Wang, X.; Lidy, S.; Touboul, E.; Lamouri, A.; Dive, G.; Huet, J.; Pfeiffer, B.; Renard, P.; Guardiola-Lemaitre, B.; Manechez, D.; Penicaud, L.; Ktorza, A.; Godfroid, J. J., Design and synthesis of imidazoline derivatives active on glucose homeostasis in a rat model of type II diabetes. 2. Syntheses and biological activities of 1,4-dialkyl-, 1,4-dibenzyl, and 1-benzyl-4-alkyl-2-(4',5'-dihydro-1'H-imidazol-2'-yl)piperazines and isosteric analogues of imidazoline. *J Med Chem* **1999**, *42*, (9), 1587-603.
91. Bunnett, J. F.; Happer, D. A. R.; Patsch, M.; Pyun, C.; Takayama, H., Orientation, Reactivity, and Mechanism in the Addition of Methanol to 4-Chlorobenzene. *J Am Chem Soc* **1966**, *88*, (22), 5250-5254.

92. Carey, F. C.; Sundberg, R. J., *Advanced Organic Chemistry Part A: Structure and Mechanism*. 4th ed.; Kluwer Academic / Plenum Publishers: New York, 2000; p 823.
93. Roberts, J. D.; Semenow, D. A.; Simmons, H. E.; Carlsmith, J. L. A., The Mechanism of Aminations of Halobenzenes. *J Am Chem Soc* **1956**, *78*, (3), 601-611.
94. Biehl, E. R.; Nieh, E.; Hsu, K. C., Substituent effects on the reactivity of arynes. Product distributions as an index of relative reactivities of arynes in methylamine and dimethylamine solvents. *J Org Chem* **1969**, *34*, (11), 3595-3599.
95. Cannon, S. J.; Hegarty, A. F., Diels-Alder cycloadditions of stabilised 2,3-pyridynes. *Tet Lett* **2001**, *42*, (4), 735-737.
96. Mock, B. H.; Vavrek, M. T.; Mulholland, G. K., Solid-phase reversible trap for [¹¹C]carbon dioxide using carbon molecular sieves. *Nucl Med Biol* **1995**, *22*, (5), 667-70.
97. Langstrom, B.; Lundquist, H., *Int. J. Appl. Radiat. Isot.* **1976**, *27*, 357.
98. Kretzschmar, M.; Brust, P.; Zessin, J.; Cumming, P.; Bergmann, R.; Johannsen, B., Autoradiographic imaging of the serotonin transporter in the brain of rats and pigs using S-([¹⁸F]fluoromethyl)-(+)-McN5652. *Eur Neuropsychopharmacol* **2003**, *13*, (5), 387-97.
99. Jones, F. N.; Velasquez, V., Effect of repeated discriminations on the identifiability of the enantiomers of carvone. *Percept Mot Skills* **1974**, *38*, (3), 1001-2.
100. Matthews, S. J.; McCoy, C., Thalidomide: a review of approved and investigational uses. *Clin Ther* **2003**, *25*, (2), 342-95.
101. Manning, B. H.; Mao, J.; Frenk, H.; Price, D. D.; Mayer, D. J., Continuous co-administration of dextromethorphan or MK-801 with morphine: attenuation of morphine dependence and naloxone-reversible attenuation of morphine tolerance. *Pain* **1996**, *67*, (1), 79-88.
102. Stinson, S. C., Chiral Pharmaceuticals. *Chemical & Engineering News* **2001**, *79*, (40), 79-97.
103. Davis, E. S.; Gerdes, J. M.; Walker, M. A.; Weller, M. L.; Wilson, P. A.; DeVietti, T. L.; Renk, K. J.; Ono, M. Y.; Taylor, S. E., Studies of the Serotonin Transporter: Synthetic, Pharmacological and Whole Animal Investigations of Inhibitor 2'-Methyl-6-nitroquipazine. In *The 221st American Chemical Society National Meeting*, Chicago, IL, 2001.
104. Wu, G.; Zhao, H.; Luo, R. G.; Wei, D.; Malhotra, S. V., Chiral synthesis and enzymatic resolution of (S)-(-)piperazine-2-carboxylic acid using enzyme alcalase. *Enantiomer* **2001**, *6*, (6), 343-5.

105. Binisti, C.; Assogba, L.; Touboul, E.; Mounier, C.; Huet, J.; Ombetta, J. E.; Dong, C. Z.; Redeuilh, C.; Heymans, F.; Godfroid, J. J., Structure-activity relationships in platelet-activating factor (PAF). 11-From PAF-antagonism to phospholipase A(2) inhibition: syntheses and structure-activity relationships in 1-arylsulfamido-2-alkylpiperazines. *Eur J Med Chem* **2001**, *36*, (10), 809-28.
106. Weigl, M.; Wunsch, B., Synthesis of 6,8-diazabicyclo[3.2.2]nonanes: Conformationally Restricted Piperazine Derivatives. *Org Lett* **2000**, *2*, (9), 1177-9.
107. Dinsmore, C. J.; Bergman, J. M.; Bogusky, M. J.; Culberson, J. C.; Hamilton, K. A.; Graham, S. L., 3,8-Diazabicyclo[3.2.1]octan-2-one peptide mimetics: synthesis of a conformationally restricted inhibitor of farnesyltransferase. *Org Lett* **2001**, *3*, (6), 865-8.
108. Dinsmore, C. J.; Zartman, C. B., Efficient synthesis of substituted piperazinones via tandem reductive amination-cyclization. *Tet Lett* **2000**, *41*, 6309-6312.
109. Soukara, S.; Wunsch, B., A Facile Synthesis of Enantiomerically Pure 1-(Piperazin-2-yl)ethan-1-ol Derivatives from (2S,3R)-Threonine. *Synthesis* **1999**, *1999*, (10), 1739-1746.
110. Bedurftig, S.; Wunsch, B., Synthesis and receptor binding studies of 3-substituted piperazine derivatives. *Eur J Med Chem* **2006**, *41*, (3), 387-396.
111. Naylor, A.; Judd, D. B.; Lloyd, J. E.; Scopes, D. I.; Hayes, A. G.; Birch, P. J., A potent new class of kappa-receptor agonist: 4-substituted 1-(arylacetyl)-2-[(dialkylamino)methyl]piperazines. *J Med Chem* **1993**, *36*, (15), 2075-83.
112. Velluz, L.; Amiard, G.; Heymes, R., Utilization of N-benzyl intermediates in peptide synthesis. 1. Benzylamino acid chlorides. *Bull Soc Chim Fr* **1954**, 1012-1015.
113. Andurkar, S. V.; Stables, J. P.; Kohn, H., Synthesis and anticonvulsant activities of (R)-(O)-methylserine derivatives. *Tet Asym* **1998**, *9*, 3841-3854.
114. Sheehan, J. C.; Yang, D.-D. H., The Use of N-Formylamino Acids in Peptide Synthesis. *J Am Chem Soc* **1958**, *80*, 1154-1158.
115. Ghosh, S.; Santulli, R. J.; Kinney, W. A.; Decorte, B. L.; Liu, L.; Lewis, J. M.; Proost, J. C.; Leo, G. C.; Masucci, J.; Hageman, W. E.; Thompson, A. S.; Chen, I.; Kawahama, R.; Tuman, R. W.; Galemno, R. A., Jr.; Johnson, D. L.; Damiano, B. P.; Maryanoff, B. E., 1,2,3,4-Tetrahydroquinoline-containing alphaVbeta3 integrin antagonists with enhanced oral bioavailability. *Bioorg Med Chem Lett* **2004**, *14*, (23), 5937-41.
116. Olofson, R. A.; Martz, J. T.; Senet, J.-P.; Piteau, M.; Malfroot, T., A New Reagent for the Selective, High-Yield N-Dealkylation of Tertiary Amines: Improved Synthesis of Naltrexone and Nalbuphine. *J Org Chem* **1984**, *49*, 2081-2082.

117. Gubert, S.; Braojos, C.; Sacristan, A.; Ortiz, J. A., A Convenient Synthesis of Parent and 2-Substituted Octahydro-2H-pyrazino[1,2- α]-pyrazines. *Synthesis* **1991**, 1991, (4), 318-320.
118. Kudzma, L. V.; Severnak, S. A.; Benvenga, M. J.; Ezell, E. F.; Ossipov, M. H.; Knight, V. V.; Rudo, F. G.; Spencer, H. K.; Spaulding, T. C., 4-Phenyl- and 4-heteroaryl-4-anilidopiperidines. A novel class of analgesic and anesthetic agents. *J Med Chem* **1989**, 32, (12), 2534-42.
119. Bernady, K. F.; Brawner Floyd, M.; Poletto, J. F.; Weiss, M. J., Prostaglandins and Congeners. 20. Synthesis of Prostaglandins via Conjugate Addition of Lithium trans-1-Alkenyltrialkylalanate reagents. A Novel reagent for Conjugate 1,4-Additions. *J Org Chem* **1979**, 44, (9), 1438-1447.
120. Middleton, W. J., New Fluorinating Reagents. Dialkylaminosulfur Fluorides. *J Org Chem* **1975**, 40, (5), 574-578.
121. Strazzolini, P.; Giumanini, A. G.; Runcio, A., Nitric acid in dichloromethane solution. Facile preparation from potassium nitrate and sulfuric acid. *Tet Lett* **2001**, 42, 1387-1389.
122. Dale, J. A.; Mosher, H. S., Nuclear Magnetic Resonance Enantiomer Reagents. Configurational Correlations via Nuclear Magnetic Resonance Chemical Shifts of Diastereomeric Mandelate, O-Methylmandelate, and α -Methoxy- α -trifluoromethylphenylacetate (MTPA) Esters. *J Am Chem Soc* **1973**, 95, 512-519.
123. Plenge, P.; Mellerup, E. T., Antidepressive drugs can change the affinity of [3H]imipramine and [3H]paroxetine binding to platelet and neuronal membranes. *Eur J Pharmacol* **1985**, 119, (1-2), 1-8.
124. Plenge, P.; Mellerup, E. T.; Laursen, H., Affinity modulation of [3H]imipramine, [3H]paroxetine and [3H]citalopram binding to the 5-HT transporter from brain and platelets. *Eur J Pharmacol* **1991**, 206, (3), 243-50.
125. Plenge, P.; Mellerup, E. T., An affinity-modulating site on neuronal monoamine transport proteins. *Pharmacol Toxicol* **1997**, 80, (4), 197-201.
126. Chang, A. S.; Chang, S. M., Nongenomic steroidal modulation of high-affinity serotonin transport. *Biochim Biophys Acta* **1999**, 1417, (1), 157-66.
127. Weller, M. L.; Gerdes, J. M., Neurosteroids and Bioflavonoid Steroid Mimics as SSRI Binding Affinity Modulators for the Serotonin Transporter. In *32nd Society for Neuroscience National Meeting*, Orlando, FL, 2002.
128. Katzenellenbogen, J. A., The structural pervasiveness of estrogenic activity. *Environ Health Perspect* **1995**, 103 Suppl 7, 99-101.
129. Griffin, L. D.; Mellon, S. H., Selective serotonin reuptake inhibitors directly alter activity of neurosteroidogenic enzymes. *Proc Natl Acad Sci U S A* **1999**, 96, (23), 13512-7.

130. Woodrum, S. T.; Brown, C. S., Management of SSRI-induced sexual dysfunction. *Ann Pharmacother* **1998**, *32*, (11), 1209-15.
131. Rosen, R. C.; Lane, R. M.; Menza, M., Effects of SSRIs on sexual function: a critical review. *J Clin Psychopharmacol* **1999**, *19*, (1), 67-85.
132. Morrell, M. J.; Flynn, K. L.; Done, S.; Flaster, E.; Kalayjian, L.; Pack, A. M., Sexual dysfunction, sex steroid hormone abnormalities, and depression in women with epilepsy treated with antiepileptic drugs. *Epilepsy Behav* **2005**, *6*, (3), 360-5.
133. Gardner, E. A.; Johnston, J. A., Bupropion--an antidepressant without sexual pathophysiological action. *J Clin Psychopharmacol* **1985**, *5*, (1), 24-9.
134. Waldinger, M. D.; van De Plas, A.; Pattij, T.; van Oorschot, R.; Coolen, L. M.; Veening, J. G.; Olivier, B., The selective serotonin re-uptake inhibitors fluvoxamine and paroxetine differ in sexual inhibitory effects after chronic treatment. *Psychopharmacology (Berl)* **2002**, *160*, (3), 283-9.
135. Modell, J. G.; Katholi, C. R.; Modell, J. D.; DePalma, R. L., Comparative sexual side effects of bupropion, fluoxetine, paroxetine, and sertraline. *Clin Pharmacol Ther* **1997**, *61*, (4), 476-87.
136. Roderick, W. R.; Platte, H. J.; Pollard, C. B., Derivatives of Piperazine. XXXV. Synthesis of 2-Phenylpiperazine and Some Derivatives. *J Med Chem* **1966**, *9*, (2), 181-185.
137. Blythin, D. J.; Chen, X.; Piwinski, J. J.; Shih, N. Y.; Shue, H. J.; Anthes, J. C.; McPhail, A. T., Synthesis and NK(1)/NK(2) binding activities of a series of diacyl-substituted 2-arylpiperazines. *Bioorg Med Chem Lett* **2002**, *12*, (21), 3161-5.
138. Epstein, J. W.; Brabander, H. J.; Fanshawe, W. J.; Hofmann, C. M.; McKenzie, T. C.; Safir, S. R.; Osterberg, A. C.; Cosulich, D. B.; Lovell, F. M., 1-Aryl-3-azabicyclo[3.1.0]hexanes, a New Series of Nonnarcotic Analgesic Agents. *J Med Chem* **1981**, *24*, 481-490.
139. Se Lee, B.; Chul Lee, B.; Jun, J.-G.; Yoon Chi, D., A New Efficient Synthesis of 6-Nitroquipazine. *Heterocycles* **1998**, *48*, (12), 2637-2641.
140. Meyers, A. I.; Williams, D. R.; Erickson, G. W.; White, S.; Druelinger, M., Enantioselective Alkylation of Ketones via Chiral, Nonracemic Lithioenamines. An Asymmetric Synthesis of alpha-Alkyl and alpha,alpha'-Dialkyl Cyclic Ketones. *J Am Chem Soc* **1981**, *103*, 3081-3087.
141. Fujino, T.; Morii, S.; H., S. Preparation of 1-substituted 2-alkylpiperazines. JP 2003342264, 2003.
142. Habert, E.; Graham, D.; Tahraoui, L.; Claustre, Y.; Langer, S. Z., Characterization of [3H]paroxetine binding to rat cortical membranes. *Eur J Pharmacol* **1985**, *118*, (1-2), 107-14.

143. Mathis, C. A.; Gerdes, J. M.; Enas, J. D.; Whitney, J. M.; Taylor, S. E.; Zhang, Y.; McKenna, D. J.; Havlik, S.; Peroutka, S. J., Binding potency of paroxetine analogues for the 5-hydroxytryptamine uptake complex. *J Pharm Pharmacol* **1992**, *44*, (10), 801-5.
144. Cheng, Y.; Prusoff, W. H., Relationship between the inhibition constant (K₁) and the concentration of inhibitor which causes 50 per cent inhibition (I₅₀) of an enzymatic reaction. *Biochem Pharmacol* **1973**, *22*, (23), 3099-108.
145. Gerdes, J. M.; Bolstad, D. B.; Davis, E. S.; Kusche, B. R.; Weller, M. L.; Wilson, P. A., Serotonin Transporter Inhibitor Probes: Synthesis and Pharmacological Profile of (rac)-[3H]2'-propyl-6-nitroquipazine. In *33rd National Meeting of the Society for Neuroscience*, New Orleans, LA, 2003.
146. Armarego, W. L. F.; Chai, C., *Purification of Laboratory Chemicals*. 5th ed.; Butterworth-Heinemann: London, 2003; p 608.
147. Kofron, W. G.; Baclawski, L. M., A Convenient Method for Estimation of Alkyl lithium Concentrations. *J Org Chem* **1976**, *41*, (10), 1879-80.
148. McCortney, B. A.; Jacobson, B. M.; Vreeke, M.; Lewis, E. S., Methyl Transfers. 14. Nucleophilic Catalysis of Nucleophilic Substitution. *J Am Chem Soc* **1990**, *112*, 3554-3559.